Cranfield University

Cian Harrington

Definition and Verification of a Set of Reusable Reference Architectures for Hybrid Vehicle Development

School of Engineering

PhD Thesis

Cranfield University

School of Engineering

PhD Thesis

Academic Year 2011-2012

Cian Harrington

Definition and Verification of a Set of Reusable Reference Architectures for Hybrid Vehicle Development

Supervisors: Dr. James Marco, Prof. Nicholas D. Vaughan,

This Thesis is submitted in partial fulfilment of the requirements for the degree of PhD

Abstract

Current concerns regarding climate change and energy security have resulted in an increasing demand for low carbon vehicles, including: more efficient internal combustion engine vehicles, alternative fuel vehicles, electric vehicles and hybrid vehicles. Unlike traditional internal combustion engine vehicles and electric vehicles, hybrid vehicles contain a minimum of two energy storage systems. These are required to deliver power through a complex powertrain which must combine these power flows electrically or mechanically (or both), before torque can be delivered to the wheel. Three distinct types of hybrid vehicles exist, series hybrids, parallel hybrids and compound hybrids.

Each type of hybrid presents a unique engineering challenge. Also, within each hybrid type there exists a wide range of configurations of components, in size and type. The emergence of this new family of hybrid vehicles has necessitated a new component to vehicle development, the Vehicle Supervisory Controller (VSC). The VSC must determine and deliver driver torque demand, dividing the delivery of that demand from the multiple energy storage systems as a function of efficiencies and capacities. This control component is not commonly a standalone entity in traditional internal combustion vehicles and therefore presents an opportunity to apply a systems engineering approach to hybrid vehicle systems and VSC control system development.

A key non-functional requirement in systems engineering is reusability. A common method for maximising system reusability is a Reference Architecture (RA). This is an abstraction of the minimum set of shared system features (structure, functions, interactions and behaviour) that can be applied to a number of similar but distinct system deployments. It is argued that the employment of RAs in hybrid vehicle development would reduce VSC development time and cost. This Thesis expands this research to determine if one RA is extendable to all hybrid vehicle types and combines the scientific method with the scenario testing method to verify the reusability of RAs by demonstration.

A set of hypotheses are posed: *Can one RA represent all hybrid types? If not, can a minimum number of RAs be defined which represents all hybrid types?* These hypotheses are tested by a set of scenarios. The RA is used as a template for a vehicle deployment (a scenario), which is then tested numerically, thereby verifying that the RA is valid for this type of vehicle.

This Thesis determines that two RAs are required to represent the three hybrid vehicle types. One RA is needed for series hybrids, and the second RA covers parallel and compound hybrids. This is done at a level of abstraction which is high enough to avoid system specific features but low enough to incorporate detailed control functionality.

One series hybrid is deployed using the series RA into simulation, hardware and onto a vehicle for testing. This verifies that the series RA is valid for this type of vehicle. The parallel RA is used to develop two sub-types of parallel hybrids and one compound hybrid. This research has been conducted with industrial partners who value, and are employing, the findings of this research in their hybrid vehicle development programs.

Acknowledgements

This Thesis represents the culmination of a significant period of work and time in my life and it would not have been possible without the support of many people. Nick and James presented this opportunity to me and supported me throughout this process. James, my supervisor, has also been the world's best editor. For that I thank him. Others in our department have also supported me in many other ways, thanks to you all.

My parents have been a constant source of support and encouragement throughout my academic career, and I'm sure they will be glad it is finished. Tanya and Kevin have also provided valuable advice and support throughout this endeavour

Siobhán has been an evolving constant with me on this Thesis journey. She started as girlfriend, moved onto fiancée and finally wife. Your love and support are immeasurable, without which this Thesis would never have been completed. I could not have got this far without the SeanyGen.

Finally, my baby girl, Maya Rose, far too young to remember that she completed this Thesis. I dedicate this to you.

Table of Contents

Table of Figures

Table of Tables

Acronyms & Terms

Acronym	Definition
2WD	2 Wheel Drive
4WD	4 Wheel Drive
A-ECMS	Adaptive Equivalent Consumption Minimisation Strategy
ABS	Anti Blockier System
AC/DC	Alternating Current/Direct Current
AD	Architectural Description
ATAM	Architecture Trade-off Analysis Method
BCU	Brakes Control Unit
BiCon	Bi-directional Converter
BLDC	BrushLess DC (electric machine topology)
BMS	Battery Management System
BoCon	Boost Converter
BSFC	Brake Specific Fuel Consumption
Cap	Capacitor
CARB	California Air Resources Board
CASE	Computer Aided Software Engineering
CD	Charge Depleting
Chgr	Charger
CIMG	Crank Integrated Motor Generator
CO	Carbon Monoxide
CPP	Change Propagation Probability
CPS	Continuous Power Source
CR	Charge Recovery

CS	Charge Sustaining
CVT	Continuously Variable Transmission
CVT	Continuously Variable Transmissions
DC/DC	Direct Current/Direct Current
DD	Driver Demand
DP	Dynamic Programming
Drv	Drive system (Compound HVs)
DSM	Design Structure Matrix
ECE	United Nations Economic Commission for Europe, ECE-15
ECMS	Equivalent Consumption Minimisation Strategy
EM	Energy Management
ESC	Energy Systems Controller
EUDC	Extra Urban Drive Cycle
EV	Electric Vehicle
FC	Fuel Cell
FE	Fuel Economy
FLC	Fuzzy Logic Control
Gen	Generator system (Compound HVs)
GenSet	Generator Set (electric machine & inverter combination)
GPS	Global Positioning System
HC's	Hydrocarbons
HIL	Hardware In the Loop
HV	Hybrid Vehicle
HVAC	Heating Ventilation and Air Conditioning
ICBM	Inter-Continental Ballistic Missile
ICE	Internal Combustion Engine
IEEE	Institute of Electrical and Electronic Engineers

INCOSE	International Council On Systems Engineering
INV	Inverter
IPCC	Intergovernmental Panel on Climate Change
LCVTP	Low Carbon Vehicle Technology Project
LUT	Look Up Table
M	electric Machine
MC	Motion Control
NAIGT	New Automotive Innovation and Growth Team
NEDC	New European Drive Cycle
NiMH	Nickel Metal Hydride
NN	Neural Networks
NOx	Oxides of Nitrogen
NREL	National Renewable Energy Laboratory
OMG	Object Management Group
PF	Power Following
PPS	Peak Power Source
RA	Reference Architecture
SAAM	Software Architecture Analysis Method
SE	Systems Engineering
SOC	State Of Charge
SysML	Systems Modelling Language
TCU	Transmission Control Unit
TPS	Tertiary Power System
Trn	Transmission
TTR	Through The Road (a form of hybridisation)
UC	Ultra Capacitor
UML	Unified Modelling Language

VEM	Vehicle Energy Management
VMC	Vehicle Motion Control
VSC	Vehicle Supervisory Controller

Term	**Definition**	**Units**
$\dot{m}_{f\_CPS}$	CPS fuel flow	g/s
$\dot{m}_{f\_PPS}$	PPS fuel flow	g/s
Cp_{fuel}	Heating value of fuel	kJ/kg
Eff_{CPS}	CPS efficiency	-
Eff_{PPS}	PPS efficiency	-
P_{Drv}	Drive Power	W
P_{Gen}	Generator Power	W
f_{pen}	Penalty Function	-
J	Equivalent Fuel Consumption	g/s
P_{CPS}	Continuous Power System Power	W
P_d	Demand Power	W
P_{PPS}	Peak Power System Power	W
P_{TPS}	Tertiary Power System Power	W
u	Split	-

1. Introduction

1.1. Background

The Intergovernmental Panel on Climate Change (IPCC) has gathered and presented a significant body of evidence demonstrably linking human activity to increased CO_2 emissions which is causing climate change. This evidence was initially presented in 1990 in their first assessment report, and additional evidence was presented in three subsequent reports up to 2007, [1, 2]. Whilst detailing the evidence of anthropomorphic climate change, the assessment reports also presented scenarios of degrees of impact on global temperatures. These impacts were modelled against a variety of mitigation strategies. The IPCC claim that maximum mitigation could result in minimal impact to global temperatures while no mitigation strategies or 'business as usual' could result in a global rise of 5 degrees Celsius by 2050 [2].

As a response to these findings, the UK government commissioned the Stern Review assessing the economic impacts of climate change mitigation, specifically comparing the cost versus benefit for various mitigation strategies [3]. One of several recommendations of the Stern Review was to increase government support for advancing low carbon technology in the transport sector.

As a follow up to the Stern Review, the King Review focused on passenger and light commercial vehicles which emit 45% of UK transport CO_2, itself 14% of the total UK equivalent CO_2 emissions [4]. The King Review highlighted three areas i) cleaner fuels, ii) smart driver choices and iii) more efficient vehicles. The King Review states that *cleaner fuels* or bio-fuels can play a small part in reducing transport emissions in the short term but may impact food supply on a disproportionally large scale. *Driver choice* includes creating increased demand for more efficient vehicles or smaller vehicles, but also increasing car sharing or public transport usage. Finally, the King Review focuses on the technology required to increase *vehicle efficiency* and the associated cost barriers. Primarily the King Review supports vehicle electrification (both hybrids and battery only vehicles) as the strongest candidate for the mid to long-term in to reduced transport emissions [4]. There are also several policies being employed across different jurisdictions to encourage efficient transport [5]. In the UK for example, London's congestion charging was initially established to reduce pollutant emissions [6]. A direct consequence of this charge was increased public usage of alternate forms of transport, such as public transport or cycling [7, 8]. In the context of either CO_2 emissions or energy security (reducing dependency of fossil fuels) this change of behaviour is deemed to be broadly beneficial.

Clearly not every location has the advantage of London with a high population density and an integrated, high capacity public transport network. Also, many transport functions cannot be done on a bicycle or by mass transit. Rail, flight, shipping and heavy goods transport modes are already highly fuel efficient, as these industries are very sensitive to fuel price and are relatively optimised [9]. Since passenger and light goods vehicles make up nearly half of transport emissions they will be the focus of this Thesis [3, 4]. Technological advancements to the vehicle powertrain are the third possible

avenue to improving passenger vehicle efficiency presented in the King Review. This can include high efficiency engines, alternative fuels, Electric Vehicles (EV) and multiple power sources or Hybrid Vehicles (HV[1]). This approach concurs with the conclusion of the UK government report by the New Automotive Innovation and Growth Team (NAIGT) [10]. This research will constrain its scope to the overlap between HV technology and passenger and light commercial sized vehicles.

1.2. Context

Appendix A presents a historical review of automotive technology, highlighting alternate powertrains. Automotive development took hold towards the end of the 19th century. Due to decreased fuel and manufacturing cost the Internal Combustion Engine (ICE) became the dominant powertrain by the 1920s. Several other technologies including electric and hybrids had been demonstrated but only reappeared from the 1960s and commercially from the 1990s. The review also highlights that electronic control of distinct sub-systems appeared on vehicles in the early 1970s. Powertrain systems have been historically integrated as per deployment, mainly between engine management and transmission (automatic) [11]. It is argued that modern HVs present a step-change in system complexity due to the combination of complex powertrains and integrated electronic control.

Traditional ICE based vehicles can be described as single power source vehicle. This continuity of system structure ensured that system control architectures remained largely similar over time. The control architecture interfaces for this type of vehicle is normally driven by the component supplier [12]. These issues ensure that vehicle architectures include legacy constraints and supplier dependencies. As a result, the automotive industry has inertia to change. As discussed earlier, factors outside the control of the industry have created a drive for a step change in automotive powertrain complexity. This presents an opportunity to reduce legacy and supplier constraints.

HVs can have several configurations comprising many permutations of components. HV can be divided into three sub-groups, series, parallel and compound. A full review of the configurations and HV components will be addressed in Chapter 2. However, traditional vehicles (single power source) transfer fuel energy from a tank to motive torque at the wheels via a power converter (normally an ICE) and usually a transmission. This architecture is the same for gasoline and diesel ICEs, two and four wheel drive, manual and automatic transmissions. HVs can have two 'tanks' (one being a battery for example) with a variety of power converters, transmission (including none) and methods of hybridisation. Therefore automotive companies must transition from a single architecture for all vehicles to having a variety of architectures for a variety of vehicles.

[1] A common term is HEV meaning Hybrid Electric Vehicle. However, a Hybrid may comprise an engine and a mechanical flywheel or hydraulic power source, whereby the term 'Electric' is redundant. The term HV is more generic and will be used throughout this thesis.

Cloutier and Verma state that system complexity can increase development cost [13]. This cost is compounded by the fact that systems are not only complex but differ significantly between vehicles. Therefore a systematic approach to the development of HVs is required. It is argued that this must be a top-down systems approach to reduce legacy and supplier constraints. The inherit learning from successive applications of this approach must be book-shelved to reduce the cost of future HV development programs.

1.3. Problem statement

Legislative and commercial pressures are increasing automotive powertrain system complexity. Purchase cost of HVs has been noted as a significant barrier to success [4, 10]. Battery cost presents a significant barrier however there is evidence that significant cost reduction can be generated in lithium technologies [14]. System development and integration cost is and will remain significant unless approached systematically with a view to future reusability [15, 16].

A holistic approach to development, including functional and non-functional requirements, has been described as 'systems engineering' [17]. A subset of the systems engineering process is upstream system definition capture which generates artefacts which describe the system architecture. This subset of systems engineering is commonly referred to as systems architecting [18]. A key tool of systems architecting is capturing the lessons learnt from one development exercise and book-shelving it as an abstracted Reference Architecture (RA). This can then be reused to reduce cost in future system developments [15, 19]. Appendix B gives a detailed presentation of the origins and development of systems engineering, systems architecting and the RA. Their applications and implication for this research are presented in detail in Chapter 2.

The problem addressed by this Thesis is the increasing cost of system development in the context of HV powertrains in general and the Vehicle Supervisory Controller (VSC) specifically. Systems engineering is not new to the automotive industry. As in-vehicle systems became more complex and coupled, systems engineering became a necessary tool for the automotive industry [20]. More recently, infotainment, chassis and body system complexity has grown and systems engineering has been applied successfully in these domains [12, 21]. Powertrain, however, is only experiencing this step change in complexity as a result of the introduction of HV technologies [20]. An important difficulty facing the automotive industry is how to minimise HV system development cost.

To summarise, purchase cost is a significant barrier to HV deployment. It is believed that reused learning from previous developments can reduce future development costs. This can be achieved by defining reusable RAs through a systems engineering and system architecting process.

1.4. Area of research

Project Wren was tasked with defining a generic control RA for HVs which would support easy integration of different HV powertrain configurations. An overview of the Wren project is presented in Appendix C. The first of two key outcomes of Wren are a systems engineering based methodology for capturing and analysing HV system

architectures. The second key outcome is a RA derived from the analysis of three fuel cell HVs [22]. The analysis methodology and the RA are presented in Chapter 3. The RA was derived from the three fuel cell HVs and does not account for other HV configurations and real world considerations such as hybrid braking, mechanical transmissions and 12V systems. This defines the starting point of this research. In that context, this Thesis represents a continuation of the Wren project.

The aim of this research is to derive and present the minimum number of RAs which capture the full scope of feasible HV configurations including real world considerations.

The rationale for this aim is discussed by Cloutier and Verma; reusable patterns or RAs can significantly reduce development time and hence cost [15].

Methodology: scenario & scientific approach

Methodologies for assessing the validity (reusability, modularity etc) of an Architectural Description (AD[2]) are often subjective [23]. Whereas the applicability of these methodologies to a RA (a higher level of abstraction again) is wholly questionable [24]. The methodology for assessing the validity of the RAs derived in this Thesis is outline by Alexander, Del Rosso, Maier and Rechtin [18, 19, 24, 25]. They combine a scenario analysis with the scientific method.

Scenario analysis

The validity of an AD may be tested by means of a series of scenarios. By declaring a set of ADs as scenarios from an RA perspective, the same methodology can apply. The key is careful definition of the scope of ADs and by inference the scope of HV configurations. This will be discussed in detail in Section 2.4.2. Figure 1-1 shows an overview of how this scenario based approach will be applied through two levels of abstraction. ADs will be validated by a series of deployment scenarios and the RA will be validated by the ADs.

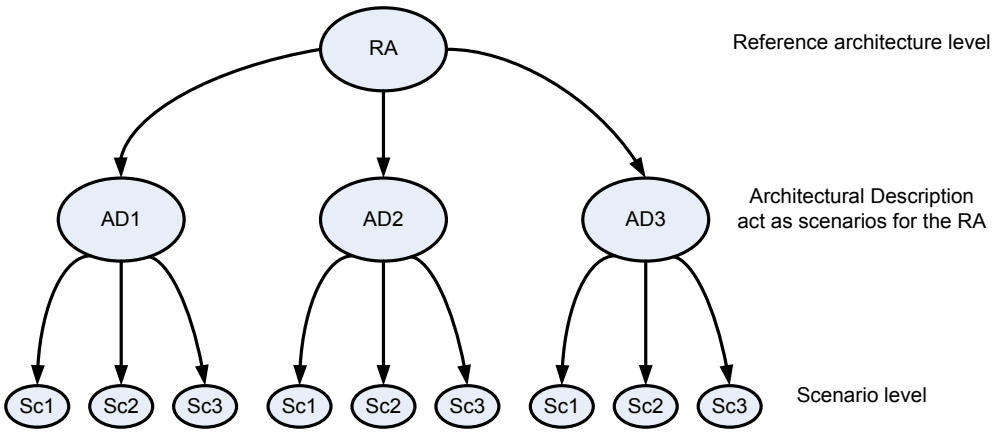

Figure 1-1: Scenario approach applied through two levels of abstraction

[2] AD will be defined in Section 2.2.2.

The scientific method

The stages of the scientific method are the problem statement, the hypothesis declaration and the experimental testing of the hypothesis. [26]. If the hypothesis continually tests positive (against discrete scenarios) confidence is built up that the hypothesis is valid. One failed test and the hypothesis is declared invalid.

By combining scenario analysis and the scientific method, the aim of the Thesis can be addressed by means of testing a set of hypotheses. The experiments that test the hypotheses examine the RA by testing scenarios of the RA. These scenarios are implementations of HV configurations represented as ADs. These implementations are tested numerically. The tests can take place in several environments, architectural systems analysis, numerical simulation, Hardware In the Loop (HIL) and vehicle deployment.

Therefore the objectives or research questions take the form of hypotheses:

1. The RA defined in Wren can be applied to ICE based (and other) series HVs
   1.1. If not, the RA can be extended to encompass ICE based series HVs
   1.2. The RA can be extended for other system and real-world consideration
2. The extended RA can be applied to parallel HVs
   2.1. If not, a new RA can be defined reusing structure and content of the first
3. One of the two RAs defined above can be applied to compound HVs.

The resulting research structure is presented in two parts in Figure 1-2 and Figure 1-3. In Figure 1-2, the first scenario for the Series RA comprises the three fuel cell vehicles analysed in Wren. These scenarios were in turn tested by systems analysis (Sys) and numerically in simulation (Sim), in HIL and on a vehicle (Veh). The next RA scenario is the ICE based series HV. The systems analysis, simulation, HIL and in-vehicle test work for this scenario was conducted in conjunction with a UK and EU funded project called the Low Carbon Vehicle Technology Project (LCVTP). An overview of LCVTP is presented in Appendix C. Other series HV configurations are similar to the first two scenarios and their applicability is demonstrated by systems analysis. In this case a series HV with a gas turbine and also a series HV with an electrically mounted flywheel.

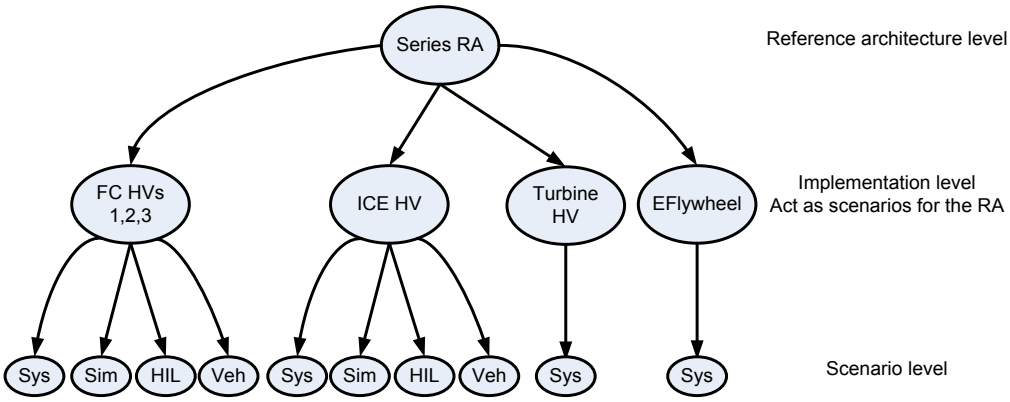

Figure 1-2: Research Structure for Series RA

Figure 1-3 presents a similar research structure for the Parallel RA. The key scenarios for the RA are pre-transmission (including mechanically connected flywheel variants) or post transmission parallel HVs. To test the RA to its limit, a Continuously Variable Transmission (CVT) has been included in the post-transmission variant. The power split and Through The Road (TTR) compound HVs are included to demonstrate as they fall under the Parallel RA. A full definition of all HV configurations and component permutations is presented in Section 2.4.2.

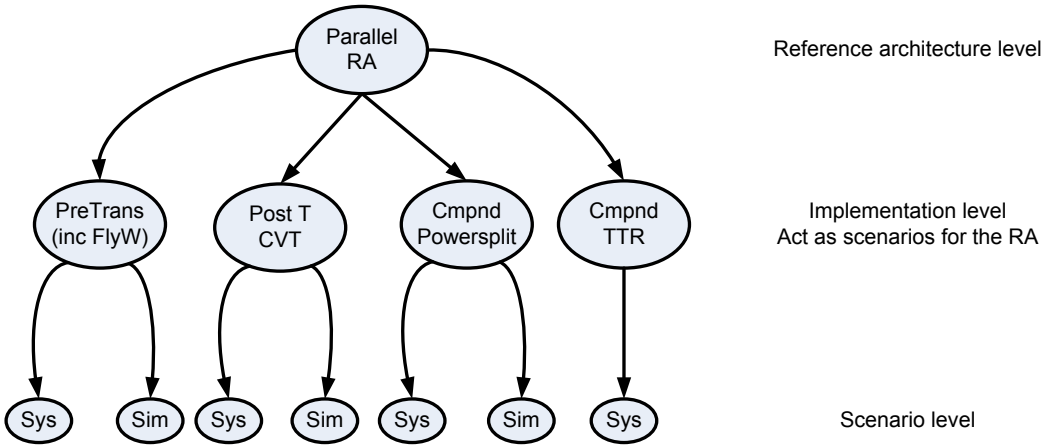

Figure 1-3: Research structure for Parallel RA

A key attribute of a RA is its level of abstraction. Harrington et al, set the level of abstraction of the RA to match the highest level requirement of a HV VSC *"deliver driver demand efficiently"* [23]. This implies three key functional tasks, Driver Demand (DD) determination, Energy Management (EM) and Motion Control (MC). These will be referred to throughout this Thesis

This Thesis presents a set of RAs which are generic enough to include all feasible HV configurations yet detailed enough to incorporate key requirements which must be met by all VSCs, and usable as a template for HV system and control VSC development. The scope of HVs will be clearly grouped to align with fundamental differences between RAs. Future developers can use the RAs as templates to initiate their VSC control architecture.

These reusable RAs are the main novel aspect of this research. Chapter 2 will show that RAs exist for HVs however they are too closely aligned with the particular HV deployment they were distilled from. Therefore they are not reusable in the context of other HV deployments. Another aspect of novelty is to be found in the application of a particular EM strategy in the series VSC, which is presented and noted in Chapter 5.

1.5. Thesis outline

The following chapter presents the literature review pertaining to the key facets of this research. Firstly, systems engineering and architecting focusing on reference architecture is reviewed including the methodologies for assessing non-functional attributes of ADs and RAs. Secondly the scope of EM control strategies is presented. This

will be used to inform the choice of strategy to be used in numerical simulation. Finally the scope of feasible HV configurations is presented.

Chapter 3 introduces the architecture analysis methodology as defined in Wren. The resultant Wren RA is presented and reviewed. The first hypothesis is assessed. That the Wren RA as defined is extendable to ICE based series hybrids, and is it extendible to cover real word considerations is addressed.

Chapter 4 addresses the two remaining hypotheses, that a second Parallel RA is required. Finally the Parallel RA is shown to encompass compound HVs.

Chapter 5 presents the theory and implementation methodologies of the EM control strategy selected in Chapter 2. The core requirements and interfaces are discussed in the context of the HV configurations presented in Section 2.4.2.

Chapter 6 presents the first of three case studies, on an ICE based series HV. The architectural analysis of the HV is presented. The vehicle plant and VSC are modelled in simulation and tested for basic functionality, performance and against the scenarios. The system controller is deployed onto a HIL experimental environment and onto a vehicle demonstrator and the key scenarios repeated.

The second case study addresses the second hypothesis, the architecture of the parallel HV in Chapter 7. The vehicle presented is a pre-transmission ICE battery HV, with an complex transmission and clutched driveline. A second parallel post-CVT transmission diesel ICE battery plug-in HV is also analysed architecturally and deployed into simulation, and a sensitivity analysis of the EM strategy discussed in Chapter 5 is presented.

Chapter 8 presents the final case study addressing the third hypothesis, which analyses the extendibility of the Parallel RA to the compound HV configuration. The Toyota Prius architecture is analysed and then modelled. A VSC derived from the extended Parallel RA is developed in simulation. A second through-the-road compound HV is defined and analysed. Alternate compound configurations are also discussed.

Chapter 9 concludes by discussing the lessons learnt from the case-studies and other architectural analysis within the HV scope set out in Chapter 2. Limitations of this research are discussed and future research is outlined.

2. Literature review

2.1. Overview

As stated in the introduction the aim of this Thesis is to define and present the minimum number of RAs required to act as development templates for the VSCs of a defined scope of HVs. Both the background rationale for this aim and the process required to achieve this aim are multifaceted in nature. Therefore this review covers a wide range of topics, however they all converge to make the case for the validity of the research questions and the methodologies proposed to answer them.

To support the research objectives presented in Chapter 1, a critical evaluation of the following topics is required:

1. Systems Engineering, Systems Architecting, Reference Architectures
    - Methods for assessing non-functional attributes of architectures
2. Energy management control strategies
3. Feasible HV configurations
    - HV enabling component technologies

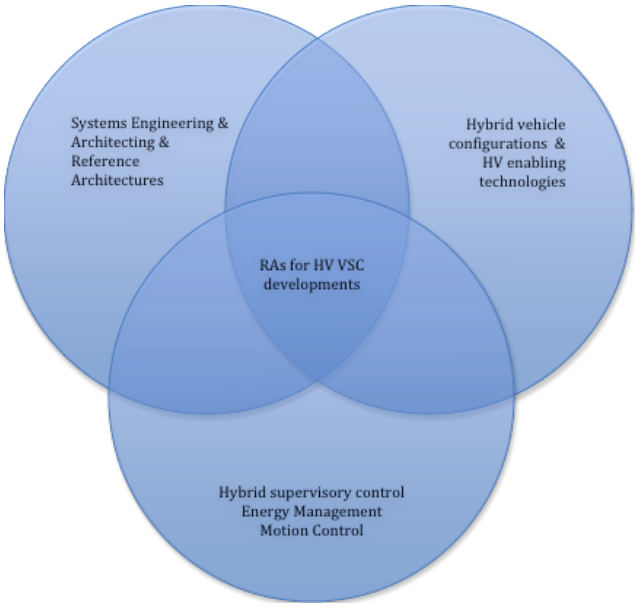

Figure 2-1: Intersection of research areas defining research gap

Figure 2-1 presents a diagram showing the overlap of the three areas reviewed showing the key research gap being addressed by this Thesis. Section 2.2 explains the rationale and growth of systems engineering architecting and the concept of RAs. This will be referenced to industry wide applications, the automotive industry and more pertinently HV applications. A key point from this is the assertion that ADs and RAs are beneficial in terms of non-functional requirements (reusability, modularity etc). This review addresses the published methodologies for measuring the non-functional attributes and the complexity of applying these methodologies to RAs. From this a proposed methodology of assessing the reusability of the RAs defined in this Thesis.

This methodology requires numerical deployments of ADs in the simulation environment. This requires a choice of EM strategy. The EM function is specific to HVs and, as will be shown in review, can impact system architecture. Therefore the available EM strategies will be discussed in Section 2.3 and an appropriate strategy chosen for continuity throughout all deployments in this Thesis. The full scope of feasible HV configuration and enabling technologies are defined and discussed in Section 2.4.

2.2. Systems engineering & architecting

2.2.1. Systems engineering

An overview of the origins of Systems Engineering (SE) is presented in Appendix B which addresses the various industries which employ SE. Therefore this section will present a definition of and a rationale for SE to support HV development. A significant outcome of SE with regards to this research is the concept of standardising and unifying the modelling tools. This will be presented in detail.

What is Systems Engineering?

The International Council On Systems Engineering (INCOSE) defines Systems Engineering as:

"an interdisciplinary approach and means to enable the realization of successful systems. It focuses on defining customer needs and required functionality early in the development cycle, documenting requirements, then proceeding with design synthesis and system validation while considering the complete problem" [27].

This is not the only definition of a broad engineering discipline. A more comprehensive list of SE definitions is presented in Appendix C. Many publications refer to the four pillars of SE as being structure, behaviour, requirements and parametric relationships [17, 27]. This multifaceted approach is reflected in the modelling methodology defined by Wren and will be discussed in detail in Chapter 3.

A rationale for Systems Engineering.

As the capability and application of software and software dependent systems has developed over time, the deficiencies inherent in ad hoc or organic development become more apparent. Some examples are listed below.

- The number of individuals interacting with systems grew in accordance with system size and complexity, often in different geographical locations [28] [29].
- Multi-developer and multi-user systems showed clear difficulties born out of the diversity of stakeholder understanding of the system itself [30] [31].
- Poor communication and differing levels of understanding between developer and user often resulted in poor functionality [32, 33].
- Systems straddling several domains often required development and maintenance practitioners with very different technical backgrounds [34, 35].
- Future system problems became difficult to diagnose in the absence of co-ordinated documentation or the key developers [33, 36].

A methodology which could capture the essence of a system so it could be viewed and discussed by different types of users is required.

Systems Engineering Modelling

Initially for the software domain, an international computer software consortium was formed called Object Management Group (OMG), who developed and released the Unified Modelling Language (UML) in 1995 [36]. Since then, Grobshtein et al point out that the UML has become the SE tool of choice across the software development industry [37]. The UML captures the essence of a system into two broad categories of models: behavioural and structural. Each category contains a set of prescribed diagram formats, (containing system elements) each reflecting one particular facet of the system. Bennett et al state that within the software industry, the UML can be fully integrated with Computer Aided Software Engineering (CASE) tools [28]. For example Fernandes and Lilus show how to form a computationally complete programming language, which enables the UML to be integrated with CASE automatic code generation [38].

By design, the UML is domain non-specific, therefore applicable to systems outside the software industry; examples include business process [39] and engineering modelling [40]. Vanderperren et al further state that in these industries the UML remained a system documentation exercise, and is not necessarily directly coupled with the system design tools [40]. A drawback of this universal applicability is the lack of sufficient semantics to reflect the key characteristics of some engineering disciplines. In conjunction with INCOSE, OMG created the Systems Modelling Language (SysML), an extension of the UML, which provides extended capabilities to systems engineers [41]. The SysML removes extraneous diagrams from the UML which have no great use in Systems Engineering, such as the Communication Diagram [40]. The SysML advances the capability of the structure diagrams by introducing the concept of a Block, the basic unit of structure, a stereotyped class used to describe system entities such as hardware, software and stakeholders. Further to that, The Block Definition Diagram is used to define the features of and relationships between blocks. The Internal Block Diagram is used to support information flows between blocks and show the relationships of parts of the system. In the Behaviour Diagrams, the SysML introduces (amongst other improvements) Control Operators, which output a control command which enables the execution of other actions within the system, a clear description of this is presented by Hause et al [42, 43].

The most significant enhancement is a new diagram (set at the level of the structure and behaviour diagrams), called the Requirement Diagram. In the UML, requirements were only informally integrated and only linked with Use Cases, a subset of the Behavioural Diagram, as discussed by Grobshtein and Dori [44]. The SysML formally integrates requirements, including design rationale information in design blocks and providing links between design rationale and requirements. This enables stakeholders to assess the consequences of requirement changes through a requirement verification method which links requirements with appropriate test cases. As per Marco and Vaughan [16], requirements diagrams will not be included in the RAs due to the level of abstraction, however they should be used for formal deployment. A final extension of the UML to the

SysML is Allocation, discussed by Guo and Jones [45]. Allocation extends the ideal of linking across the whole model or cross-cutting, by providing a generalised capability to allocate one model element to another. This allows stakeholders to navigate vertically between levels of abstraction or laterally between different diagrams, or both. This idea of abstraction is a defining characteristic of the SysML allowing significant system detail to be removed with only the 'big picture' remaining. The main advantage of abstraction is the dislocation from implementation specific detail thereby retaining only the core information required for system understanding. Marco and Vaughan state that if this core information can be captured and ported to other applications then a key non-functional requirement of reusability can be realised [46]. This idea is central to the work being presented here, and is discussed further towards the end of this section. It should also be noted that the SysML semantics prove difficult for the uninitiated to easily understand, as discussed by Marco and Vaughan and Vanderperren [47, 48]. When presenting this research to an external audience simplified models were used as shown in Harrington et al [23].

This has direct implications for this research as Guo and Jones state that development of automotive powertrain and control systems, and more specifically HV systems, lend themselves to SE [45]. A key aspect of SE is the initial system definition referred to as architecture by Rechtin and Maier [18, 19]. The following section addresses system architecting in the context of system design as applied throughout industry.

2.2.2. Systems architecting & architecture

Depending on the literature source, systems architecting is either an integral part of the systems engineering process [33] or a standalone discipline in its own right [19]. In either case, the activity of capturing the essence of a system in a collection of views, models or documents is integral to this research. Hence systems architecting and system architecture is addressed separately here. As in the previous section, an overview of the history of system architecting has been given in Appendix B for reference.

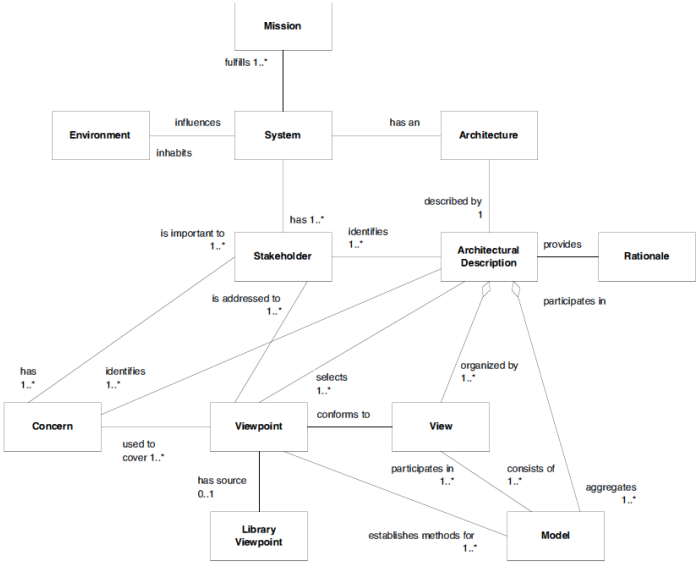

Figure 2-2: IEEE conceptual model showing the Architectural Description [49]

The Institute of Electrical and Electronic Engineers (IEEE) published a recommended practice in 2007, IEEE 1471-2000 [49]. This document defines a recommended practice for an architectural description of a software intensive system. Each system, by definition of its existence, has an architecture whereas an AD is a set of artefacts (diagrams etc) which describe or in some way document facets of the architecture of that system. The relationships between the system, the stakeholders, their concerns, the context of their concerns (viewpoint) and a method by which this viewpoint can be represented (view, which consists of models) are defined. The number of views will be dependent on the number of stakeholders and associated concerns. The views (and specific models contained therein) when collected together form the AD. In the same year, Richards et al presented their architecture framework paper to INCOSE which addressed many of the same concerns as the IEEE guidelines [50]. They identified the key relationship between key stakeholders and the format of the artefact with which they communicate. Each stakeholder has concerns. A viewpoint is used to cover the concerns of a stakeholder. A view, which is the IEEE definition of an artefact, conforms to a viewpoint. These relationships are directly drawn from Figure 2-2. This collection of artefacts or views is referred to as the AD of the system and will be referred to as such from here.

Designing and communicating systems using ADs became standard practice in the software industry, as demonstrated by van Gurp et al [51]. Termeer et al use 3D visualisation, (data store metrics showing the relative 'size' of AD components) to improve understandability of the system [52]. Other industries which now use ADs are aviation [53], manufacturing (to design in adaptability to production facilities) [54], robotics [55], business management [56] and automotive [57]. The application of ADs in the automotive industry will be addressed later in this section. The application of ADs in robotics however has produced some interesting findings which are applicable to this research.

The area of autonomous robotics presents challenges for control architectures. They must manage a dynamic environment, use multiple sensor and actuators, realise multiple goals and do all this in a robust and reliable manner [58]. Yunho et al define key non-functional requirements which allow system developers to meet these challenges: flexibility, modularity and expandability [58]. Ridao et al and Rosenblatt and Hendler both survey the range of system architectures applied to robotics and both show the benefit of distributed and hierarchical control [59, 60]. One of the main benefits of this is the ability to encapsulate and layer functional groups as described by Yunho et al and Li and Jiang [58, 61]. The high level functional groups address global goals while the lower layer directly manages one particular feature, behaviour or sub-system. The key to this encapsulation is the interfaces between layers, the aim of which is to minimise dependency. The concept of supervisory control to generate reusability through encapsulation and modularity is further described by Yavuz and Bradshaw [62]. Encapsulation is a key theme of this research and is used throughout to maximise reusability.

The automotive industry has experienced an increase in system complexity and customer demand for individualisation (leading to variant complexity) [63]. Reichart

and Haneberg state that this is a core driver for the introduction of systems architecting to the automotive industry. They speculate that avoidable complexity (a result of organic bottom-up systems development, proprietary solutions, and ill-defined standardisation) will be highlighted through formal and coordinated architectural description. Santos et al show how an architectural approach can be used to integrate safety critical x-by-wire systems into an electric vehicle [64]. Ibarra et al employ systems engineering to conduct safety analysis in an automotive context [65]. Wild et al, state that automotive system complexity can only be captured in formalised AD languages [66]; they describe a proprietary language, CAR-DL. Ahrens et al point out that UML based AD languages are not executable outside the software industry and they describe a method to convert from UML to an executable ASCET modelling tool [57]. The AD language used in this Thesis is a combination of the UML/SysML and the IEEE 1471 guidelines, as defined by Marco and Vaughan [22]. This Thesis uses this AD language to analyse the architectures of HV powertrain systems.

Rosario et al present a modular EM structure for what they call an EV [67]. The vehicle in question has two bi-directional converters to actively control the battery power and capacitor power. They break the EM function into three sub-functions: Energy management, power management and power electronics. The Energy sub-function defines the system limits. Power sub-function determines the appropriate split between the battery and capacitor in the form of two power set points. Power electronics converts the two power setpoints into the required pulse width modulated signal. This Thesis defines the first sub-function as *Power_Available* and the second as *Instantaneous_Optimisation*[3]. The third sub-function is a local plant control function and would not be encapsulated in the VSC as to do so would generate significant plant specific dependency in the VSC. Also, Rosario et al do not address MC functions or their relationship with EM. Baher and Werthschulte conducted another study on energy management, [68], which also failed to address the interface between EM and MC. However, they confirm that abstract and generic interfaces increases modularity and reusability. Generic interfaces are an important feature of the RAs defined in this Thesis.

Philips concurs with Beher and Werthschulte regarding the need for generic interfaces [69]. However he includes MC functions in his study on hybrid control functional decomposition of a pre-transmission parallel mild hybrid. He lists sub-functions and allocates them to EM and MC functional groups. However, the confluence of high level vehicle and driver interface functions (cruise control, transmission etc) in the MC functional group, suggests that this is an organic extension of a traditional ICE powered vehicle control architecture. More importantly the AD presented could not be reused on other HVs, such as post-transmission parallel HV or a series HV. Ceraolo et al show that series and parallel HV require fundamentally distinct architectures [70]. However the architecture they present omits some key features. Firstly they lump the EM and MC functional groups which will reduce reusability. Also in their series architecture there is

[3] The terms *Power_Available* and *Instantaneous_Optimisation* refer to functional blocks and will be discussed in detail in Chapter 3. Also these functional blocks are indicated by *Capitalised_Italics.*

no link between EM/MC functionality and the driver demand to the electric drive which would enable the system to exceed available system limits, as will be discussed in Chapter 3. Reusable RAs should contain this necessary feature and should demarcate the high level Driver Demand, Energy Management and Motion Control functional groups with the generic interfaces between them and the external systems; thereby designing in reusability.

2.2.3. Reference Architecture

A review of the origins of RAs and patterns is presented in Appendix B for reference. Therefore this section presents the rationale for RAs. The form and content of RAs are presented in the context of the broadest interpretations in literature. Several industrial applications of RAs are also presented, culminating in two examples from the automotive industry, including an application of an RA to a hybrid vehicle.

A rationale for Reference Architectures

Cloutier an Verma confirms the assertion of Alexander et al, that lessons learnt from analyses of systems can be documented and retained in the form of a "Reference Architecture" or "design pattern" [15, 25]. This is done to reduce the risk, cost and time for subsequent developments. An RA is an abstraction of a system or an aspect of a system. According to Maier and Rechtin, the level of abstraction is important; too abstract and the RA loses usefulness, too low and the RA is too system specific. Gamma et al cite several benefits of using RAs which include reuse and design for change but mainly the ability to employ captured knowledge and avoid reinventing the wheel for every development [71].

Cloutier and Verma also state that using a RA is one means of reducing development time and cost, and can improve communications between engineering groups [15]. Coplien demonstrated this extensively in the software industry, especially in the context of Object-Orientated system development [72]. One of the greatest benefit of RAs, in the view of Coplien, is its ability to unveil whole system structure to practitioners used to operating at the implementation end of software development [72]. Cloutier et al [13] collate industry rationale for employing RAs and their benefits as:

- reuse and commonality,
- risk reduction,
- interoperability,
- knowledge repository

The form of Reference Architectures

The form of an RA varies with literature source. [73]. Alexander states that each "design pattern" describes a problem that repeatably occurs and then describes the core of the solution to that problem in such a way that the solution can be repeatably implemented [25]. Avgeriou and Zdun highlight a group of 'architecture styles' which address semantics of components and connectors only [74]. Unlike Alexandrian patterns, these 'architecture styles' do not address the problem, solution or context. Avgeriou and Zdun

collate the existing literature on 'Pattern Language', a set of semantics closely related to the structure of views defined by the IEEE 1471 guidelines [49, 74]. As mentioned, the concept of patterns or RAs has been most comprehensively adopted by the Object-Orientated software industry, captured in the seminal text by Gamma et al, [71]. Gamma et al, present the definition of and rationale for patterns in software, followed by a worked example. Then they present a catalogue of the common patterns in object-orientated software development.

Examples of applied Reference Architectures

Reference architectures have been successfully applied within several industries, such as aviation [75], software [71], telecommunications [72] and control engineering [76]. Maier and Rechtin provide a critical review of the use of a RA within the different areas of systems architecture (including, nuclear, military, business enterprise and manufacturing) all demonstrating an improved system development time based on the formal capture of previous learning [18]. Howard et al describe, in detail, the application of RAs to manufacturing enterprises showing an improvement in flexible manufacturing practices [77].

Boulanger and Overland address 'reconfigurability in real-time' in the context of aerospace life-support systems [78]. Boulanger and Overland state that it is only through the employment of RAs that this can be achieved in the context of a distributed system with many engineering groups and suppliers with proprietary concerns. While maintenance in real-time is not currently a concern for the automotive industry, managing a wide range of suppliers and engineering disciplines is. Therefore, this supports the application of RAs to novel and complex aspects of automotive development.

Sanz and Zalewski examine the application of an RA to the control engineering environment and use automotive cruise control function as a case study [76]. They declare that one of the main advantages of using RAs is their ability to capture non-functional requirements including software implementation, human issues and engineering process. RAs also ensure that knowledge is transferred horizontally across enterprises. Sanz and Zalewski also state that *"pattern-based architectural design is considered the most effective and safe method for defining architectures"*. The author concurs; as will be discussed in detail many published examples of hybrid control systems are developed organically and from a control solution point of view. It is argued that a by-product of this approach is limited reusability.

Larsen et al derive an RA for a HV application [79]. They correctly identify the benefit of an RA in terms of modularity, i.e. the ability to replace one component without excessive system dependency resulting in excessive modification to accommodate the new component. However, as with Phillips, Larsen et al have derived their RA from an architecture which is an organic extension of an ICE based control architecture [69, 79]. This can result in designing in legacy constraints. This Thesis will approach the RA definition with a view to minimising legacy constraints. Larsen et al correctly identify the high level requirements of a HV: driver demand, energy management and motion

control. They also identify ancillary load control as a fourth high-level requirement, which this research allocates to EM. However they fail to encapsulate EM and MC functional groups from each other in the RA. They use two parallel HV implementations to show that their RA holds true for both applications. They do not attempt to apply this RA to a series HV configuration.

In summary, RAs are a widely used and effective method for designing complex systems, especially for including non-functional requirements such as reusability. They have been applied to the automotive industry and an example of a RA for HVs shows promise but have deficiencies which are addressed by this research.

2.2.4. Methods of assessing architectures

This section critically reviews the different methods that may be employed to assess the effectiveness of a system architecture. Based on this, the most appropriate method for assessing a RA will be identified. Firstly however, the metrics used to assess the effectiveness of the Systems Engineering process are reviewed by Vanek et al [80]. They state that metrics for SE generally focus on nonfinancial measurements in the process such as requirements raised versus requirements satisfied against the project time line. Vanek et al confirm that industry feels that applying SE shows benefits. However they also point out that some defined metrics have been "gamed" by suppliers for their own benefit; the opportunity for which they suggest arises from inherent subjectivity of the metrics [80]. This subjectivity is a pattern throughout the various methods of measuring the effectiveness of architectures. The RA assessment methodology selected for this research independent of this subjectivity.

Numerical based methods

The software industry has pioneered the use of metrics to assess the effectiveness of system architectures. Muskens et al propose a method to combine standard coupling metrics, such as fan-in or fan-out[4], through relating the standard views of an AD [81]. The main concern with this approach, in the opinion of Muskens et al, is that most systems are rarely 'finished' and often only a subset of the key AD views are used. This renders this approach specific to the AD language defined and must be completed late in the development process. Also, this approach is only applicable to ADs and not RAs.

Lung and Kalaichelvan highlight the subjectivity of metrics by stating that due to their arbitrary nature, they can only be used to assess ADs by comparison [82]. This point is illustrated well by Ahrens et al, who compare a legacy AD with the same AD re-factored for non-functional requirements using an in-house developed metric system [83]. The paper does not address the possibility of bias in the development of the metric method or the architecture re-factoring process.

There exist methods of creating an executable model of a UML based architecture, through the use of Petri Nets [84, 85]. However both Bai et al and Wagenhals et al state

[4] Fan-in and Fan-out refer to a node centric view of coupling throughout a system, Fan-in relates to related input nodes and Fan out refers to related output nodes.

that this requires a mature AD and therefore would be an inappropriate method for assessing RAs. A more common method for measuring architectures is called the Design Structure Matrix (DSM). It identifies the interfaces (or interactions) of the sub-system elements of the architecture. An example DSM is presented in Figure 2-3, based on a simple interconnected system. A numerical value of 1 within any cell indicates that a relationship exists between two sub-systems. Clearly such a binary evaluation provides no indication of the level, quality or importance of this interrelationship only that it exists [86]. This method is good at identifying sub-system interactions which can be used for optimising partitioning, [87]. However several methods have been tried to include the relative value of the interactions. Sharman and Yassine use the visibility calculation (node X can 'see' node Y via Z intermediate nodes) [88] and Browning and Eppinger use a probability of interaction as a means of assessing the 'value' of a dependency [89].

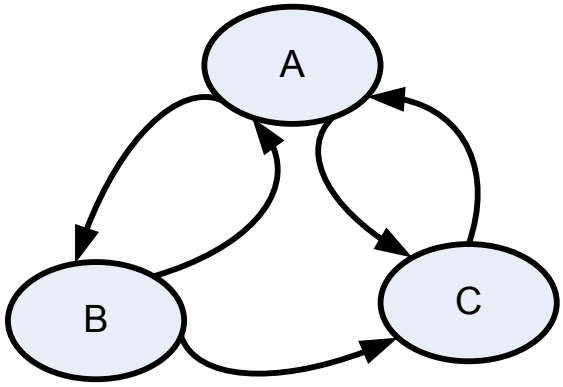

	A	B	C
A		1	1
B	1		1
C	1	0	

Figure 2-3: Simple interconnected system with binary DSM

Several publications explore the value of further defining these architectural dependencies. For example, Engle and Browning attempt to assess the future cost of adding functionality to a system [75]. To do this they employ a finance industry tool used to determine the future cost of a commodity or stock. Engel and Browning apply this method to the likely future cost of adapting the functionality of a system, and then populate the DSM with this figure [75]. Sharman and Yassine again employ a DSM to explore the functional clustering of a simple system to demonstrate that clustering can be easily misinterpreted without having a deep systems knowledge and appropriate domain experience [88].

Stochastic methods for determining architecture robustness or change and error are also common. Abdelmoez et al demonstrate change propagation probability on software architectures [90] while Popic et al demonstrate error propagation probability [91]. A concern with these stochastic methods is the increased uncertainty when being applied to a higher level of abstraction of an AD, for example a RA. Finally, Shaik et al proposes a stochastic method for assessing the system dependencies for determining the impact of future changes, called Change Propagation Probability (CPP). [92, 93]. The authors compare this method to three other commonly used architecture assessment methods. The papers show that only their method could detect an "improvement" between the

two systems. Their CPP relies on the use estimates of probabilities of the likelihood of change in one function driving change in another.

The weakness of all the above methods is the requirement to define an arbitrary value to non-functional attributes of ADs. This introduces a level of subjectivity which depends on the system, enterprise or architect and may not be repeatable. This weakness is further compounded in the context of an RA. In principle this is not necessarily a problem and relative numerical assessment is an accepted means of assessing architectures. However it requires a body of consistent assessments against which to measure. This data is not available to this research. Therefore an assessment method is required which is independent to this subjectivity.

Scenario based methods

Muskens et al state that the scenario based techniques of Software Architecture Analysis Method (SAAM) and Architecture Trade-off Analysis Method (ATAM) are the most common architecture assessment methods in the software industry [94]. Both ATAM, and its precursor SAAM, require a set of scenarios against which the system architecture will be tested. Ideally the list of scenarios will be exhaustive however this is often impractical. Therefore a bound of expected scenarios must be defined and grouped so a limited set of tests can cover the scenarios most completely. The scenarios must be derived from the concerns of key stakeholders. Del Rosso compares scenario analysis with software performance (memory usage) and experienced based analysis [24]. Del Rosso concludes that the three methods are complimentary however, with regards to this research, software performance is implementation specific. Also, the lack of experienced based analysis data can be overcome by carefully defining a given scope of HV configuration. Therefore scenario based analysis is of interest to this research. Eriksson et al demonstrate use-case scenario analysis of a system's architecture [95], this is the approach applied to assessing the applicability of an AD. Also Lung et al clearly highlight the importance of scoping carefully the bound of scenarios which will validate the AD in question. This bounding of the scope of scenarios is a key facet of the RA assessment methodology of this research.

Low level metrics, such as 'lines of code' are not applicable to ADs and RAs may affect software with no quantifiable effect on 'lines of code' [82]. Metric and DSM values can be arbitrary and often contain probability based data. Therefore the previous discussion highlights the challenges associated with assessing the architecture of a system based on an abstraction of its implementation [96]. This fact is further compounded when trying to assess an RA, which by definition represents a further level of abstraction of the system design [13].

The literature on RAs shows that claims are demonstrated by means of a scenario analysis. Howard et al field test their manufacturing planning RA [77], Cloutier and Verma demonstrate their format for documenting patterns by means of an example [15]. This applies to the automotive RA discussions also, Sanz and Zalewski continuously return to the case study on Cruise Control throughout their article on pattern based control engineering [76]. Finally Larson et al demonstrate the reusability of their HV

control system RA by demonstrating it on two distinct HV configurations [79]. However, it is argued that the two HV configurations in question are not truly distinct, but variants in the same base structure.

Based on this section it is argued that scenario based analysis is the most appropriate methodology for assessing RAs. The following section will detail further the proposed methodology.

2.2.5. Proposed methodology for validation of RA

It has been shown that RAs are a specific application of systems architecting, itself a subset of the systems engineering process. SE, AD and RAs have been shown, with example, to be applicable to HV development. If an RA is defined, its universal reusability over the scope of HVs must be demonstrated. A range of numerical and subjective methods of measuring the SE process, ADs and RAs have been presented, with scenario analysis being the most appropriate for the high level of abstraction inherent in RAs. This method is compatible with the scientific method. Hickey describes in detail how the scientific method and the systems engineering process align [26]. Hickey defines the stages of the scientific method as the problem statement, the hypothesis declaration and the experimental testing of hypothesis. If the hypothesis continually tests positive (against discrete scenarios) confidence is built that the hypothesis is valid. One single failed test and the hypothesis is declared conclusively invalid.

The problem statement, 'that repeated development from first principles or reworking of legacy increase future HV VSC system development costs' is highlighted repeatedly in literature; by Cloutier and Verma, Marco and Vaughan, Sage and Armstrong and Beher and Werthschulte [15, 16, 33, 68]. This was distilled into a set of hypotheses to be tested in Section 1.4.

Therefore the final stage must be a definition of a set of experiments (or scenarios) which can be used to generated confidence in (or disprove) the hypotheses. This will be achieved by using the two level scenario based analysis presented in Figure 1-1. An RA will be tested against a set of ADs which have been shown by inspection to be derived from that RA. Therefore the ADs become the testable scenarios of the RAs. The ADs are subsequently tested numerically, i.e. particular events or activity sequences of the system. Therefore the use-cases become the testable scenarios of the ADs. This can be completed in three ways:

- Architectural analysis; structure and behaviour diagrams defined in Wren [46].
- Simulation; an executable deployment of the AD.
- Hardware-In-the-Loop; a real- world VSC deployment testing.
- In-vehicle testing of the deployed VSC

This approach draws together the Alexandrian methodology of repeated application [18, 25] and the confidence of scenario-based analysis [24]. However, there are still gaps in the argument. In order to deploy an AD into the simulation, HIL or in-vehicle environment, control strategies must be chosen. The correct strategy will allow flexibility to be applied to all HV configurations. Also the architectural analysis used

throughout the research must be presented in conjunction with a clear definition of the starting point of this research. Confidence in the hypotheses can be generated by testing them against a defined scope of HV configurations. This requires a definition of the possible scope of HVs and by inference the key HV technologies that may need to be modelled as part of the simulation or HIL experiments. The following two sections address these points.

2.3. Energy management strategies

This section has two aims. The first is to determine the most appropriate HV control strategies for deployment into the experiments conducted as part of this research. The second aim is to assess the existing literature on HV control strategies in terms of architectural considerations.

The key and distinct algorithm for HVs is the EM function. EM may at some stage govern some or all of the vehicle plant directly or indirectly and therefore may have an impact on the system architecture. Many HV control strategies reviewed combined the EM and MC functions thereby minimising reusability opportunities. Moreover, as will be shown, system architecture and general non-functional requirements are rarely addressed.

HV energy management control strategies can be divided broadly into two groups, Heuristic and Optimisation. Heuristic based control comprises deterministic methods such as thermostat, rule-based power-following, power-split, and intelligent control such as fuzzy logic and neural networks. Optimisation based control methods comprise global optimal methods, such as genetic algorithms and dynamic programming and other off-line methods and real-time optimisation such as the equivalent fuel consumption method. Global optimisation methods cannot be implemented in real-time, are usually used for benchmarking and calibration and therefore will not be addressed in detail here [97, 98]. The following sections will discuss a selection of publications pertaining to each set of control methods mentioned.

2.3.1. Heuristic control

Deterministic control

Thermostat control is the most basic form of EM strategy and is discussed in the context of a parallel HV by Ehsani et al, [99]. Simply, when State Of Charge (SOC) reaches a minimum level, the ICE is set to its maximum efficiency point (for that given speed) and the excess power is absorbed by the battery until the SOC has reached a maximum level. This is a complex torque management task in parallel HVs which is avoided by applying the thermostat strategy to a series HV as described by Ross and Wu and Mohammadian and Bathaee [100, 101]. However both also note issues which need to be addressed. Ross and Wu note that the high power point of the ICE will generate a high recharge power value, therefore the battery has to be sized correctly; otherwise the recharge current will be high, reducing the life of the battery. They have avoided this issue by setting the study vehicle as a high power HV, with a 0.5kWh capacity as the energy buffer. Repeated starting and stopping of the ICE will cause discomfort for the driver and other occupants, Mohammadian and Banthaee address this by forcing hysteresis by means of time restrictions between ICE on/off events.

The Power Following[5] (PF) EM strategy is very common and intuitive, and is described as applied to a parallel HV in detail by Bumby and Forster [102]. Normally, low demand conditions are met by the electrical system and mid to high demand is achieved by setting the ICE to a defined operating point or line with excess power delivered or absorbed by battery. Jalil et al compare the thermostat and PF strategies on a series HV, showing that both can be used together, but the combined system is better than the thermostat alone [103]. Effectively the VSC control the HV as a normal PF until the SOC reaches some minimum then the thermostat initiates and any demand higher that the defined thermostat level will operate as PF.

Rahman further compares thermostat to PF for consumption and emissions on three parallel HVs: one pre-transmission and two post-transmission (discrete and Continuously Variable Transmissions - CVT) [104][6]. The results show some conflicting information. In the cases of the pre and post transmissions, reductions in fuel consumption and pollutant emissions figures were shown (power-split versus thermostat). However in the case of the pre-transmission configuration, the NOx emissions was shown to increase slightly for the power-split strategy. Also, in the case of the CVT configuration for mild hybridisation, the thermostat strategy showed an improvement in Fuel Economy (FE) over the power-split strategy.

The PF strategy was being used by Buntin and Howse as far back as 1995 [105]. In this paper the control system is designed to optimise only one goal; keep SOC at maximum. Today the PF EM strategy is the most common used in production HVs such as the Toyota Prius, [106]. PF has also been demonstrated by Wu et al on hydraulic HVs [107]. The paper presents a process of comparing an intuitive PF strategy with a second PF strategy, the rules of which have been derived from a Dynamic Programming (DP) exercise. This is an optimal control design strategy that cannot be deployed in real-time, but may be used to calibrate real-time systems. Against a benchmark mechanical only vehicle, the basic strategy generates a 32% improvement in Fuel FE. The second PF strategy generates a 47% FE improvement. However the fully DP optimised run demonstrated that this configuration could generate 77% FE improvement over the same drive cycle, [107]. Whereas Lin et al also analyse their PF strategy for a hydraulic truck HV with DP which shows a significant improvement [108, 109].

Intelligent control

Fuzzy Logic Control (FLC) is a natural extension to deterministic rule-based control, with the added benefits of robustness to imprecise measurements and relative ease of calibration [110]. The capability of FLC is demonstrated by Lee and Sul, incorporating emissions management on a parallel hybrid bus [111]. This was a very early application of FLC which had no SOC sustaining functionality; the battery was sized for the bus route. Lee and Sul address this with a speed based SOC weighting in a later paper [112].

---

[5] Sometimes referred to as load following or power split strategies

[6] The terms pre-transmission and post-transmission will be defined in Chapter 4 in the context of parallel HVs.

Bathaee et al and Li et al address the power split and ICE on/off functions distinctly by architectural demarcation [113, 114]. Bathaee et al implement the ICE mode functionality as a state machine and the power split as a FLC. They constrain the function of the state machine to determining the binary state of the engine. Whereas Li et al allow the state machine to determine the relative power of the ICE to the electrical system, such as ICE only, charging or boosting.

Glenn et al and Baumann et al demonstrated that FLCs can effectively constrain the engine near to or on the best Brake Specific Fuel Consumption (BSFC) line, [115, 116]. They also demonstrate FLCs on parallel HVs managing driver demand, driveability, SOC maintenance all while minimising fuel consumption. Salmasi and et al and Schouten et al extended the FLC and best BSFC methods to other powertrain components such as the electric machine(s), power electronics and the battery [110, 117].

A series of papers on adaptive control presented by Langari and Won describes a FLC whose rule-base can be altered depending on road and driving condition [118-121]. Using information collected from the driver and vehicle the FLC can discern a range of roadway type, driver style, driving trend and driving mode. Depending on the outputs from these four interpreters, the system will alter the rule base of the FLC based torque-split to one of nine pre-calibrated options. Ichikawa et al introduce the idea of using Global Positioning System (GPS) data to determine some of this information, namely the planned route, including incline and some information on likely traffic condition such as transitions from motorway to urban [122]. This information can be used to change the parameters of the control system to utilise stored electrical energy more efficiently.

The use and advantages of GPS and other navigation data, in an adaptive FLC, for improving HV performance is outlined in detail by Rajagopalan et al from the National Renewable Energy Laboratory (NREL) [123]. If a transition from highway mode to urban mode is detected the target SOC will be increase similarly if a future incline is detected the same SOC increase will occur. The opposite will happen in the converse conditions. To further extend the capability of control systems studies have been conducted which combine FLC's with Neural Networks (NN). Baumann et al provide a concise and clear overview of NN's in relation to FLC's [116]. Liu et al propose a complex combination of FLC with NN control in the context of a proposed parallel hybrid motorcycle [124].

The strategies discussed so far show that energy management is achievable in a computationally light heuristic or fuzzy format. The risk associated with these algorithms is the requirement for excessive calibration. The control system must be calibrated for each vehicle, and either calibrated to be near optimal for one particular drive cycle or calibrated generally for a variety of cycle; non optimal for most cycles and in extreme drive cycle cases not charge sustaining without additional SOC protection functionality.

2.3.2. Real-time optimal control

Real-time or sub-optimal optimisation refers to an approach derived from standard optimal cost function minimisation. However, in the absence of *a priori* knowledge the

minimisation is reduced to an instantaneous minimum. This means that the instantaneous optimum may not lead to the global optimum for a given mission; however this is more than offset by the flexibility offered by real-time systems. The story of Equivalent Consumption Minimisation Strategy (ECMS) begins in 2000, with the publication of a PhD derived paper by Paganelli et al, [125]. Serrao and Rizzoni, and Serraro et al, present a classical and full derivation of Pontryagin's minimisation principle and how it related and compares to ECMS [98, 126]. A detailed procedural step by step description of the minimisation loop is given by Huang et al [127]. Guzzella and Sciarretta also present a detailed theoretical review of the ECMS [128].

Paganelli et al introduce a penalty weighting for stored energy to the ECMS algorithm which assures minimum SOC [129-132]. They also simplify the mean efficiency calculations based on Willans line models developed by Rizzoni [133, 134]. In Paganelli et al [131] they present the same analysis, however this time the cost function includes a weighed emissions component. They show a 3% reduction in FC can generate a 12% reduction on NOx; they consider this to be an acceptable trade off. The ECMS was demonstrated successfully on a test vehicle described in detail by Hopka et al [135].

A series of studies conducted under Giorgio Rizzoni expand the capabilities of ECMS on series HVs with compound storage [136-140], while Pisu and Rizzoni extended the work onto parallel HVs [141]. Koprunasi et al show how ECMS can incorporate modes, for example electrical pull away to clutch engagement to hybrid mode, with the associate driveability issues involved [142]. Tulpule et al demonstrating the applicability of ECMS to Plug-in HVs and through-the-road HVs [143]. Finally Liu and Peng and Cipollone and Sciarretta demonstrate ECMS as applied to a compound HV, such as the Prius [144, 145].

ECMS lends itself to adaptive and predictive functionality. Sciarretta et al adapt the SOC maintenance functionality by determining charge and discharge equivalency factors on a drive cycle basis [146]. Rodatz et al present the same strategy as applied to a series Fuel Cell electric vehicle with super capacitor [147]. Musardo et al take advantage of the potential for adaptability of the equivalence factor [148, 149]. They use an algorithm to assess past driving conditions and combine this with future navigation data (such as road type and altitude) to predicted horizon driving conditions. They refer to this as Adaptive Equivalent Consumption Minimisation Strategy (A-ECMS). A-ECMS is compared to DP and to Sciarretta's ECMS and shows very positive results over a range of drive cycles remaining within 2% of the optimal DP results and 1% of the original ECMS [148, 149].

Guzzella and Zhang et al demonstrate the modularity of ECMS by inclusion of GPS terrain data to alter, in real-time, the SOC penalty function to minimise consumption [128, 150]. Chen and Salman propose a driving condition adaptive SOC management solution [151]. They describe a methodology that "learns" the most appropriate equivalency factor to maintain the SOC between acceptable bounds.

The benefits of some of these adaptive strategies are contingent on accurate third-party map data or assumptions on future driving patterns. However, there is clearly an industrial interest in adaptive EM strategies, especially for plug-in HVs. Any RA should

be modular enough to interface with future adaptive strategies. The RAs proposed in this Thesis address this. The following section summarises the EM strategies presented and explains the selection for this Thesis.

2.3.3. Comparison and selection rationale

Sciarretta and Guzzella published an article in the IEEE Control Systems Magazine discussing the qualitative pros and cons of the full spectrum of control systems in detail [152]. Offline solutions are mainly used to demonstrate full capability and to compare online solutions, but cannot themselves by used in a real-time application. Heuristic control systems are very light on computational power, but when based on Look Up Tables (LUT) may require extensive calibration from vehicle to vehicle. In the authors' consideration, this inflexibility can be overcome by ECMS including the potential of future prediction algorithms.

As part of the extensive research conducted under Rizzoni, Pisu and Rizzoni published a paper specifically addressing the comparisons between various hybrid control systems [141]. The paper presents a comparison between a heuristic controller, an A-ECMS, a H_∞ controller and a DP comparator. The particular A-ECMS in question has the navigation supplied altitude data along with a future horizon estimation of speed. In terms of fuel consumption this paper shows that the A-ECMS is the best controller when compared to the DP analysis. PF, A-ECMS and the H_∞ controllers are qualitatively compared. The discussions dominated by difficulties presented by the preparation of the H_∞ controller, its lack of portability to other applications (needs to be totally re-derived) and its requirement for tuning a potentially high number of parameters.

Papers by Wu et al and Gao et al compare real-time controllers in terms of fuel consumption. Wu et al present a comparison between ECMS and PF control, while Gao et al include a thermostat controller in the comparison [153, 154] Wu et al conclude that ECMS generates improved fuel consumption for a fuel cell hybrid electric vehicle. While Gao et al give the same conclusion for a series hybrid electric bus, showing that both the PF and ECMS strategies are better than the thermostat strategy.

It is arguable that a RA derived around ECMS only may not be robust[7] to other EM strategies. However, all real-time EM strategies carry out the same task. Many EM strategies presented, especially the Heuristic methods, convert this split into two set-points, e.g. a LUT with driver demand and SOC as inputs and two torque set-point outputs [112]. This drives vehicle specific dependency into the EM strategy. Therefore if the heuristic algorithms were constrained to determining split (power or torque) only then they would be interchangeable with ECMS. ECMS has been shown to be nearer optimal, real-time compatible, is easily reconfigured for different HV configurations, and

[7] It should be noted that the term 'robust' is used in two contexts in this thesis. The first refers to the flexibility of the RAs to a variety of functionality (hence ECMS or other EM strategies) and components, for example the RAs are valid for ICEs or fuel cells. The second use of the term 'robust' refers to the ability of the RAs to respond smoothly to variance in component capabilities, such as decreasing energy levels (SOC), or component degradation over time.

can interface easily with a variety of adaptive algorithms without altering the architecture of the VSC. Therefore ECMS is the EM strategy use throughout this research.

Research addressing EM focus on functionality and almost exclusively ignores control architectural consideration. When architecture is touched upon, it is only in an implementation level context. This section has determined that an ECMS implementation is the preferred energy management solution. This will aid architectural analysis as ECMS has demonstrated its applicability to key features such as adaptability and reusability to the full set of HV configurations.

2.4. HV configuration scope definition

This section defines the scope of HV configuration under examination. In order to do this the scope of HV technology enablers, or sub-system components must be discussed.

2.4.1. Key HV enabling technologies

The vehicles analysed by Marco and Vaughan were electric drive series HVs with Fuel Cells (FC) and either battery and or supercapacitors as the energy storage. The FC electrical power was passed through a boost converter and depending on the vehicle the storage (battery or capacitor, or a combination of both) was either passively connected or in a controlled manner through a Bi-directional converter. The electrical drive comprised four electric machines with four associated AC/DC Inverters. The above list is a subset of HV enabling technologies. A fuller list of feasible HV enabling technologies is presented below.

Energy storage

Hydrocarbon fuels are the present day dominant energy storage media, primarily gasoline and diesel [6, 9]. Alternative or bio-fuels (ethanol, bio-oils, etc.) are also available. In some cases their production is net energy positive and in some cases not [155, 156]. Hydrogen fuel is included (the natural extension of the hydrocarbon chain with zero carbon atoms) for completeness, however production infrastructure and storage concerns suggests that H_2 fuel will remain a long-term goal [157].

Batteries are a common form of mobile energy storage. Lead Acid, Nickel Metal Hydride (NiMH) and Lithium chemistries are the most common. Lead Acid is considered too heavy [158]. NiMH has been used for production vehicles such as the Prius and the Insight [159, 160]. However it is widely accepted that the cost of Lithium technologies (known for best power and energy density) will decrease [14]. Other battery technologies include Nickel-Chloride, Metal-Air, and REDOX, but are widely deemed unfeasible [14, 159, 161]. However any RA defined should be technology neutral therefore any reference to battery from here should be considered to mean any chemistry.

The systems outlined above can be considered energy dense storage media, whereas the following is considered power dense [162]. Supercapacitors, or ultracapacitors are electrostatic forms of energy storage. They benefit from very high power density, ideal for capturing full regenerative braking power, as confirmed by Marco and Vaughan [14, 163]. A flywheel is a mechanical storage medium, with energy and power density figures

comparable to supercapacitors [164]. The flywheel can be mechanically connected to a drive shaft or through an electric machine and is used to buffer the electrical power. Hydraulic accumulators have been demonstrated in bus and municipal truck applications [107, 165]. The technology is low cost, but requires high pressure to store enough energy to accelerate the vehicle up to operating speed once (100-350 bar) which results in a containment system which is both heavy and difficult to package in a passenger vehicle [14]. Pneumatic accumulators are not considered for this research as the compressors involved are relatively bulky [14].

Power converters

Power converters convert power form one domain to another. The EU state that ICEs will remain as a significant feature of road transport for the foreseeable future in HVs [10, 166]. Kalhammer et al and Bossel concur [157, 160]. An example of an engine designed for HV applications is the Lotus range extender [167]. This engine forms the basis of numerical analysis in the first case study, presented in Chapter 6. This is a gasoline engine, which was first designed for one efficient operating point in a series hybrid. However driver acceptance requires the ICE to cycle through the speed range, hence the engine has been recalibrated for a best BSFC line, between 17kW and 35kW.

FC are commonly used to convert stored H_2 (and O_2 from the environment) to electrical power, although other hydrocarbons and alcohols can be used [161, 168]. However the transient response is quite slow [163], therefore FCs are usually used as a continuous power source for series HVs. Gas turbines, like ICEs convert hydrocarbon fuel to mechanical power, however like FCs, they have poor transient response and therefore are also reserved for series HV applications [169].

The above power converters can be classed as nonreversible, whereas electric machines are classed as reversible. They are becoming a very common feature in the automotive industry and come in a variety of topologies [170, 171]. The most common topology for vehicle traction applications is the permanent magnet Brushless type DC (BLDC) [172]. However other topologies being used for traction applications are the induction motor and the switched reluctance motor [173]. However each topology can be described by its dynamic response, its sub-system limits (power, torque or speed) and efficiency. This will be the extent of electrical machine discussion for this research, as a full analysis on all electrical machine topologies is outside the scope of this research. For completeness, hydraulic pumps and pneumatic compressors are included here, however as mentioned above lie outside the scope of this research.

Power transformers

Power transformers convert the relationship of power within a given domain, e.g. a mechanical transmission will change the speed and torque by a given ratio. However (ignoring losses) the power will be equal. Discrete transmissions dominate automotive applications, however, for the purposes of this research only controllable transmission will be considered (automatic and automated manual) [11]. The CVT is very common in light weight vehicle applications [174] and can be useful for ICE parallel hybrids giving the ICE an extra degree of freedom by decoupling it from vehicle speed [79]. The

powersplit, planetary or epicyclic transmission is the basis of the Toyota Prius, but was first developed in the 1960s [175, 176]. This is the common method for compound HV configurations, such as the Chevrolet Volt [177]. So far, mechanical power converters have been discussed. Remaining mechanical components required for HV realisation include clutches (to separate the ICE and the electrical machine in parallel HVs) and differentials (to direct electrical machine torque in electric drive series HVs).

The electrical converters include DC/DC converters (buck and boost) as describe by Marco and Vaughan [46], which step voltage up or down. As with the mechanical converters, the power is maintained (ignoring losses) by alternately stepping up or down the current and the voltage. AC/DC Inverters convert DC electrical power to AC electrical power [178]. As with electrical machines these power electronic components will be treated as simple systems for the purposes of this research. All of the above components can be combined in many permutations to form different HV configurations. The feasible HV configurations, based on complexity or efficiency, are grouped and listed in the next section.

2.4.2. The scope of HV configurations

This section groups and lists powertrain configurations. For completeness, traditional powertains, (with a single power source) will be included.

Single source powertrain configurations

This includes traditional ICE only vehicles. However it also includes EVs [179], assuming there is no power buffering. In principle, it is possible to define other single source configurations, such as FC or gas turbine based vehicles, as long as there is no power buffering, the absence of which would limit the performance of such vehicles.

Figure 2-4 and Figure 2-5 present two variants of the single source configurations, the conventional ICE powertrain, including a transmission (Trn), and the EV. In this form of diagram, the powerflow is generally from left to right and it finally flows into a 'wheel' which represents the vehicle or chassis. Note the notation in the battery EV diagram, the battery is connected to an earth on one side and the inverter (INV) on the other, clearly this is not a correct circuit diagram. This indicates that, normally the power (positive tractive power) flows from the battery to the vehicle via the INV and the electric Machine (M). This notation will reoccur throughout this Thesis.

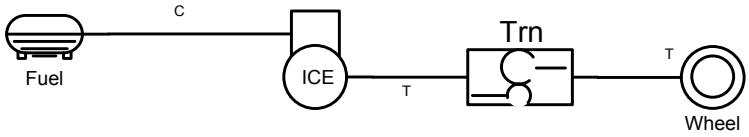

Figure 2-4: Conventional ICE powertrain with transmission

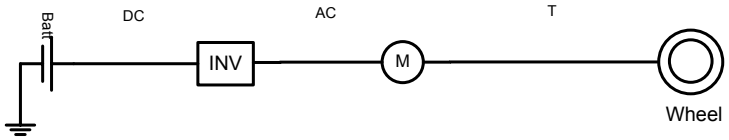

Figure 2-5: Battery electric vehicle powertrain

Series configuration HV

This HV group can be defined as having two (or more) power sources which are hybridised electrically (by means of a DC bus). Series HVs have dedicated electric drive(s) which draws electrical power from the DC bus. Ordinarily one of the power sources is reversible and the other is not. In the Wren project, Marco and Vaughan refers to the two power sources as the Continuous Power Source (CPS), and the reversible power source as the Peak Power Source (PPS) based on their relative response rates [163]. The CPS is most often the non-reversible power source, but not exclusively so. These terms and Wren in general will be discussed in more detail in Chapter 3, but the definitions of PPS and CPS will be utilised here. The CPS generally defined as a system which converts stored fuel into electrical DC power [23]. With this definition, the CPS comprises a fuel tank, an ICE, an electric machine and an inverter (sometimes referred to as a Generator Set - GenSet). Taking the fuel tank and DC bus as the system boundaries, it can be seen that a gas turbine can be interchanged without difficulty. The whole CPS can also be a H_2 tank with a fuel cell, which already outputs DC power. This configuration may include a converter to match the FC output voltage to the bus voltage as in Marco et al [163].

The PPS (sometimes referred to as the buffer) is commonly a battery or a supercapacitor. Depending on voltage matching or ability of the DC bus voltage to fluctuate, supercapacitors may require a bi-directional converter, which makes the power source controllable. Battery based PPS are often passive as the voltage is relatively stable compared to supercapacitors. The buffer can also be a compound of battery and supercapacitor as described by Marco and Vaughan [16]. The PPS can also be a mechanical flywheel drive by an electric machine [180]. In an unusual case Rosario et al describe a series HV where the CPS is a battery and the PPS is a supercapacitor [67]. This would be an unusual but valid series HV configuration.

Production series HVs are not common, other than the Volvo EEC [181] and the development Series HV from the LCVTP project, which contains a transmission, on which the first case study is based [23].

Figure 2-6, Figure 2-7 and Figure 2-8 show a representation of the three vehicles analysed as part of the Wren project. The vehicle powertrains can be divided into two groups, upstream of the DC bus and downstream of the DC bus. The CPS and the PPS are upstream systems and the drive system is downstream. The CPS in each case comprises a H_2 tank, a fuel cell and a DC/DC Boost Converter (BoCon). The drive systems for each vehicle are identical and are structurally the same as the drive system of the battery EV. The drive system may have more than one instance of these components, i.e. two or four motor drive systems, however the architecture remains the same.

The PPS changes for each vehicle. In Figure 2-6 the PPS is a passive capacitor (Cap), in other words the DC bus voltage will float up and down with the voltage of the capacitor. The vehicle in Figure 2-7 uses a DC/DC Bidirectional Converter (BiCon) to fix the DC bus voltage. Figure 2-8 shows a compound PPS with a capacitor and a battery.

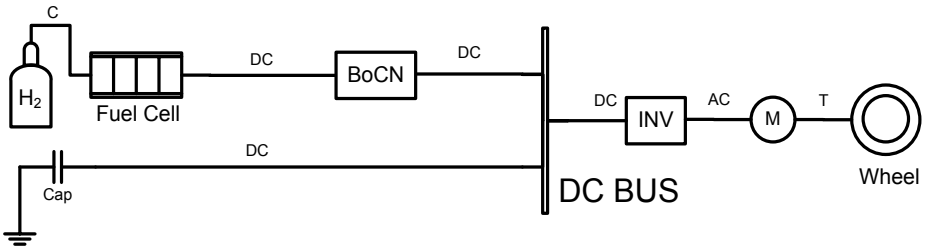

Figure 2-6: Floating bus FC UC series HV

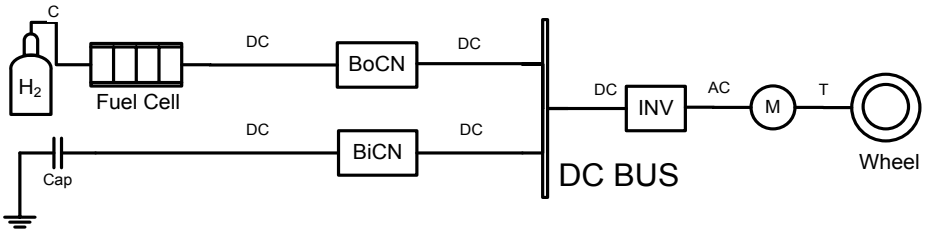

Figure 2-7: Fixed Bus FC UC series HV

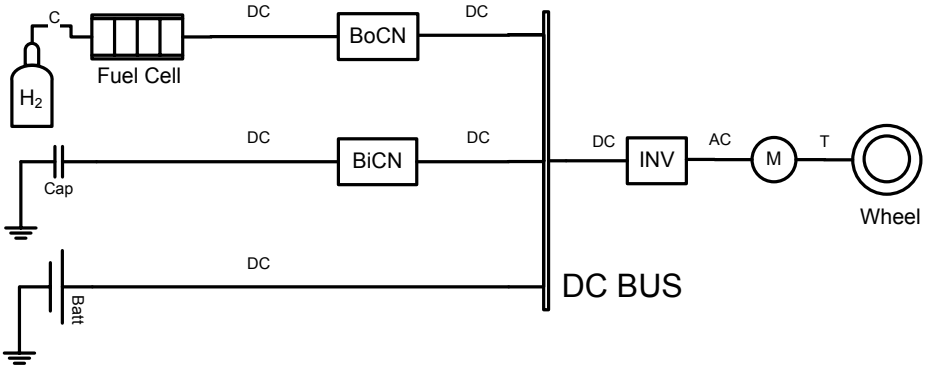

Figure 2-8: FC Compound storage (UC & Battery) series HV

Figure 2-9 and Figure 2-10 show two representations of the same vehicle, an ICE based series HV. The first diagram is the classical representation of a series HV, with the ICE driving a GenSet, which supplies electrical power to a battery. The drive system can draw power from the battery to generate motive torque. It is this sequential representation that gave this configuration its name, series hybrid. Figure 2-10 on the other hand shows that the CPS and the PPS are in fact electrically in parallel, and a true circuit diagram of the high voltage system would confirm this. However it is useful to show this configuration in this way as it separates out the PPS and CPS an also separates upstream from downstream. The vehicle in Figure 2-9 and Figure 2-10 also includes a transmission. This is an optional component, but may be required for high-speed applications and the RAs should be flexible enough to incorporate this. The battery is interchangeable with or compoundable with supercapacitors

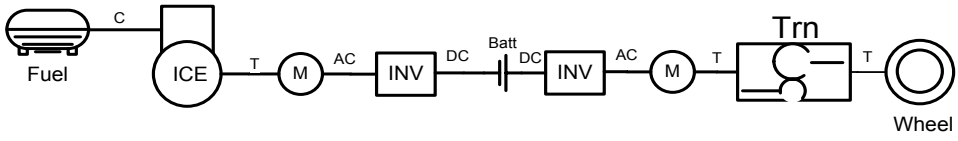

Figure 2-9: The common (mis)representation of a series HV

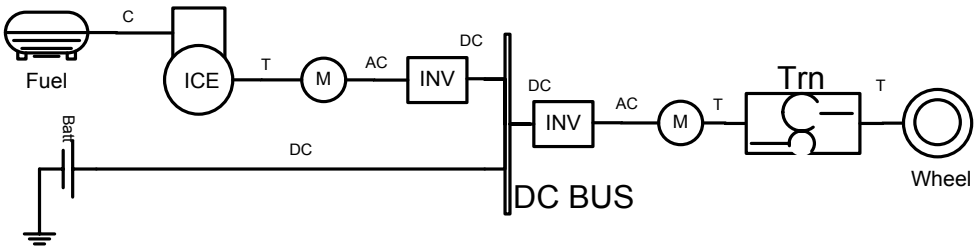

Figure 2-10: An ICE Battery series HV with discrete transmission

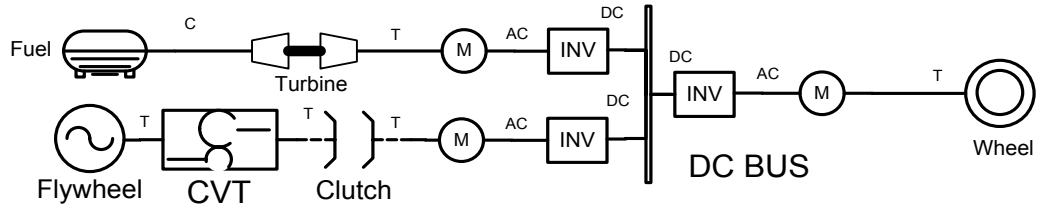

Figure 2-11: Turbine e-flywheel series HV with no transmission

Figure 2-11 completes the extension of the series HV configuration by removing the transmission, with a gas turbine CPS and an clutched electrically driven flywheel PPS (the CVT maximises flywheel speed). It has been shown already that the ICE EM and inverter are interchangeable with the FC and BoCon. This completes the scope of the series configuration. A RA should be applicable to all variants of the series configuration.

Parallel configuration HV

The most common parallel configuration is comprises an ICE with an electric machine mounted to the output shaft (directly, toothed gear or belt) which draws power from a battery via an inverter. The combined torque is normally passed through a transmission to keep the ICE in the optimal speed range. This is referred to as a pre-transmission parallel HV [104], and is shown in Figure 2-12. An example of this type of vehicle is the Honda Insight [182]. The joining of the two torque sources indicates the defining attribute of this type of HV. The two power sources are hybridised mechanically, via a 'torque bus', analogous to the DC bus in the series configuration [23]. One or more clutches are commonly required to implement this type of vehicle. If the vehicle is in EV mode, the ICE should be off and disconnected from the torque bus (an open clutch between the ICE and electric machine, upstream of the electric machine). If the vehicle is at rest and the ICE is charging the battery the transmission must be disconnected from the torque bus (open clutch downstream of the electric machine). Other variants of this configuration can replace the battery and electric machine with a mechanical flywheel (usually through a CVT shown in Figure 2-13) [180] or a hydraulic pump and accumulator [165]. The battery can also be replaced or integrated with a supercapacitor.

In post transmission parallel configurations the electric machine (drawing power from a battery) is mounted downstream of the transmission which is connected directly to the ICE. The transmission is commonly a CVT, shown in Figure 2-14 [23, 183]. This can be used to maintain the ICE along the best BSFC line. This configuration may require a set of clutches to generate distinct operating modes as before. Also the battery may be

replaced or compounded with supercapacitors, and the battery electric machine system may be replaced with a mechanical flywheel.

Figure 2-15 shows the final version of the parallel HV configurations is the 'Through the Road' HV. In this case the ICE drives one axle and a battery powered electrical machine drives the other axle [158]. It is possible to charge the battery by applying negative torque to the EM to 'brake' the vehicle while applying positive torque to the ICE driven axle.

The same substitutions described above apply here. Therefore it is suggested that demonstrating the RA to be extendible to these substitutions once will negate the need to repeat the exercise for every HV configuration, assuming the interfaces are the same.

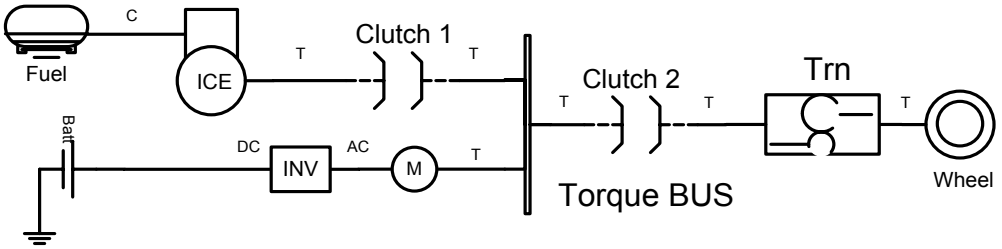

Figure 2-12: ICE Battery Pre transmission parallel HV

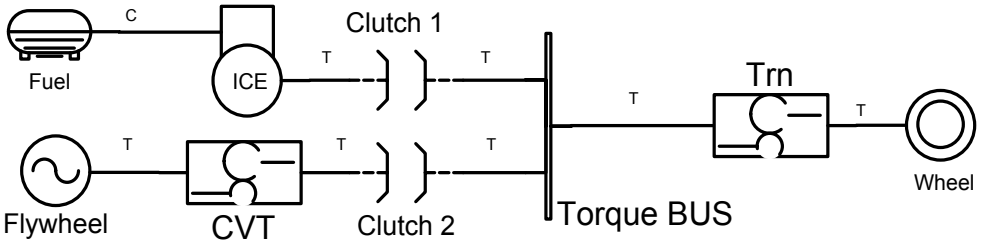

Figure 2-13: ICE flywheel pre transmission parallel HV

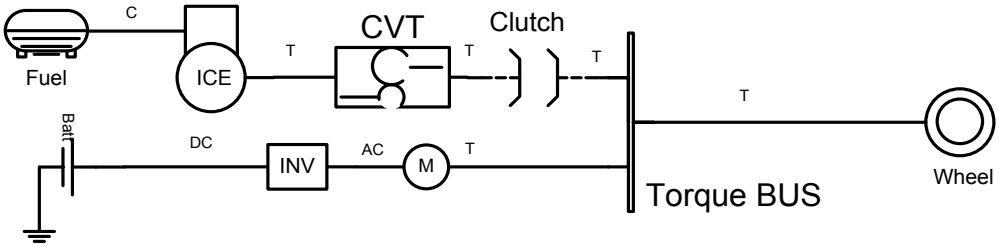

Figure 2-14: ICE CVT Battery Post transmission parallel HV

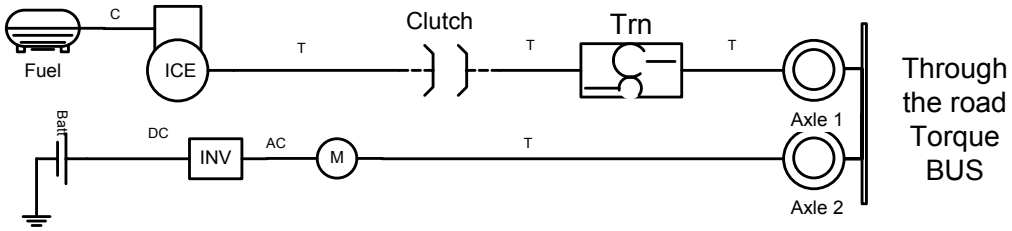

Figure 2-15: ICE Battery through-the-road parallel HV

Compound configuration HV

The compound hybrids often referred to as a series-parallel, as it can emulate both. A more correct definition is that the two (or more) power sources are hybridised mechanically and electrically. In most instances there are two torque busses and one DC bus. The most famous example of this configuration is the Toyota Prius [144], but more recently the Chevrolet Volt [177]. The core of the system comprises a planetary gearset, which has three input-output shafts. The ICE is connected to one, and an electric machine (acting like a generator by directing ICE power into the battery) is connected to a second shaft. The final shaft is connected to the wheels, as is a second electrical machine (the motor, which propels the vehicle, drawing power from the battery). This configuration is presented in Figure 2-16, the Torque bus on the left represents the power split device. In high demand scenarios both electrical machines can generate positive drive torque.

A through the road compound HV configuration exists, where the ICE is connected to an electric machine in a parallel configuration, driving one axle, and a second electrical machine is directly mounted to the second axle, see Figure 2-17. This vehicle is defined and modelled in detail by a Morbitzer et al and Koprubasi et al, a team under the direction of Rizzoni [138-140]. Finally, Algrain and Bumby et al describe a system comprising a small electrical machine integrated onto the shaft of a turbocharger which can draw some power form the ICE to charge the battery [184, 185], see Figure 2-18. An alternate version of this type of compound HV variant which includes exhaust gas energy recovery system as described by Stobart [186] and presented in Figure 2-19.

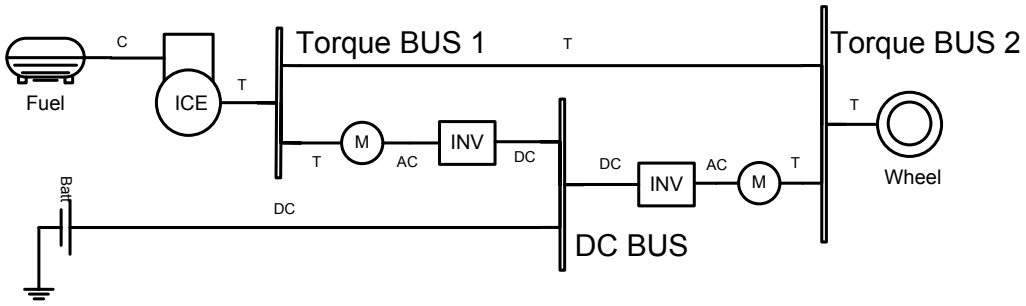

Figure 2-16: Power-split compound HV

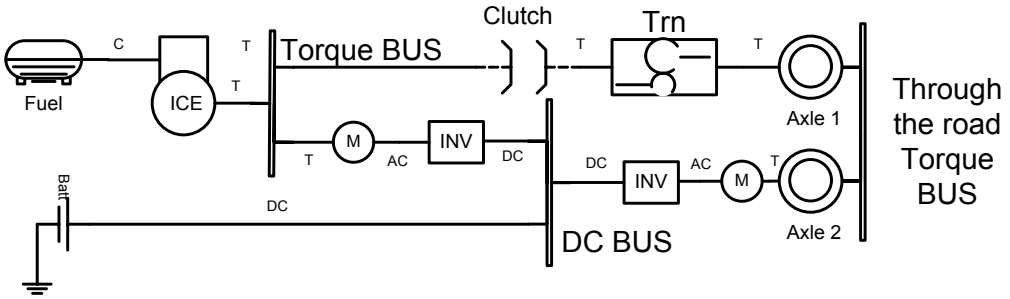

Figure 2-17: Through-the-road compound HV

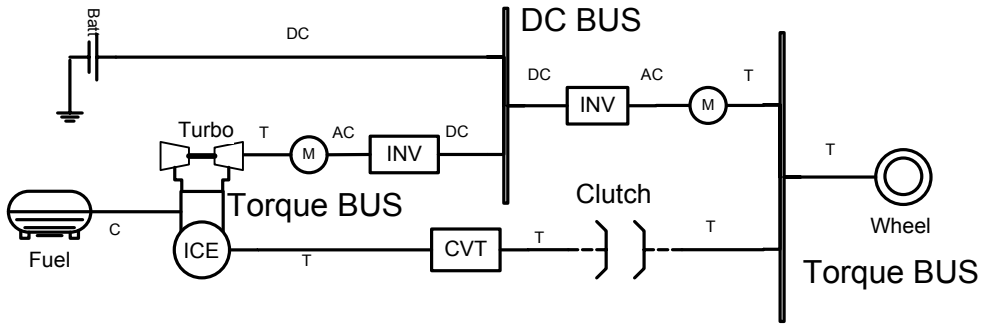

Figure 2-18: Turbo generator compound HV

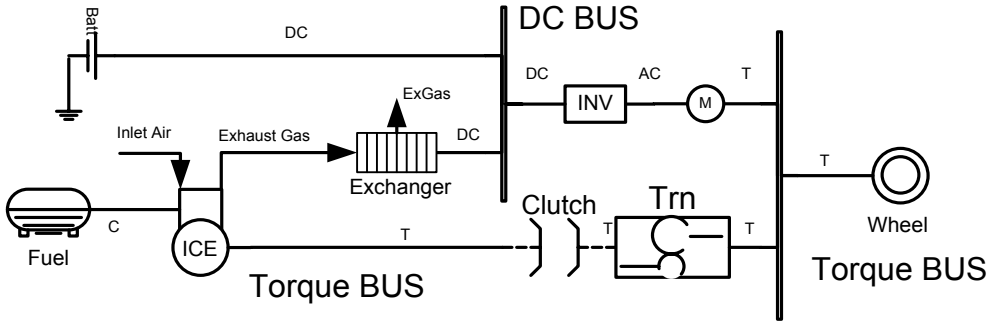

Figure 2-19: Thermo generator compound HV

It is on this scope of HV configuration that this research will be conducted. There may exist other configuration, but these are either too complex (expensive) or will not generated a fuel consumption benefit. It should also be noted that this form of representation is independent of level of hybridisation (mild, full, plug-in etc), as should any RA defined in this Thesis. The plug-in HVs will require inclusion of an on-board charger, however the key powerflows remain the same for all configurations. On-board chargers will be addressed as a real world consideration in the next chapter.

2.5. Summary

This review set out to define the context, aim, objectives, methodology and rationale for this research, in terms of systems engineering, energy management and HV technology and configurations. A HV powertrain is a complex system comprising multiple domains. Therefore it is argued that SE is the most appropriate process to analyse and develop such systems. The system architectural description is the industry standard method for capturing and analysing the structure, content and interfaces of complex systems such as HV powertrains. Patterns or RAs are a common way to reduce cost and risk. From a critical review of the literature, there is very little evidence of this being applied to HVs. This elicits the research aim: define and present the minimum number of RAs required to act as development templates for the VSCs of the defined scope of HV.

The methods and techniques of assessing architectures and RAs was reviewed and it was concluded that scenario based analysis in conjunction with the scientific method is appropriate for this research. In turn, this conclusion elicits the objectives of this Thesis in the form of a set of hypothesis to prove (for a given scope) or disprove. The testing of

these hypotheses requires the definition of a set of experiments. The experiments require a definition of the scope of HV configurations which will act as scenarios for the RA. The key HV technology enablers have been defined and an overview on how they may be combined to form permutations of HV configurations.

Chapter 3 presents the Wren methodology, and resulting RA. This is followed with a critique of the Wren RA and resulting extension to the Series RA. Chapter 4 presents a critique of the Series RA, and the resultant, distinct Parallel RA. The ability of the Parallel RA to be extended to compound HVs is then shown as an Extended Parallel RA.

3. Chapter 3

3.1. Overview

This chapter presents the key inputs to this research, the systems engineering analysis methodology and architectural description language defined in the Wren project. A key output of Wren was an RA distilled from three series HVs. A key hypothesis of this research is to determine if this RA is applicable to a wider range of series HVs. The methodology is reviewed and the RA presented in Section 3.2. In Section 3.3 the RA is critically reviewed in the context of functional demarcation, reusable interfaces and real world considerations. Based on this the Wren RA is extended and presented in Section 3.4, accounting for the full scope of series HVs defined in Section 2.4.2. This Series RA is presented at a systems level and a control level, and incorporates real world considerations. The two levels of abstraction address the concerns of systems integration stakeholders and control system development stakeholders.

3.2. Wren methodology and RA

3.2.1. Overview of Wren Methodology

Members of this research team, led by Marco and Vaughan, have been working on Wren, which aims to develop a generic control RA for HVs, [187]. To do this the team defined an architectural analysis methodology. This was done by combining the SysML and IEEE 1471-2000, by using SysML diagram structures and a notation to guide the structure of views, which form the architectural description [46]. This approach was applied to a fuel cell capacitor series electric hybrid vehicle. In the context of control development for hybrid energy management, the view employed is referred to as the Control View. The Control View comprises four SysML derived models; Decomposition Model, Context and Causality Model, Strategy Model, and Interaction Model, as described by Marco and Vaughan [46]. A summary is provided below for reference.

The *Decomposition Model* shows the principle elements of the system and their hierarchy, with no reference to structure or behaviour.

The *Context and Causality Model* is a structural model which defines those elements (from the Decomposition Model) that interact and how they do so, in a causal sense. This also give the architect the ability to partition the global system into bounded subsystems; an essential feature of architectural analysis of a multi-domain, multi-stakeholder system.

The *Strategy Model* is an extension of the Context and Causality Model. The model shows the control functional integration and dependencies, between all units of functionality whether or not they physically exist on the same ECU.

The *Interaction Model* is a behaviour orientated model. The interaction models show how the system should respond to actor triggers, or scenarios.

This system engineering analysis methodology and architectural description language will be utilised throughout this research. A full description of the semantics employed

can be found in the SysML documentation and the series of papers by Marco and Vaughan and will not be repeated here [22, 41, 46, 48]. As discussed in Section 2.2.1, a requirements diagram is not included here due to the level of abstraction, as system requirement would necessarily be system specific.

3.2.2. The Wren RA

Marco and Vaughan applied the above methodology to the fuel cell based series HV as described in 2.4.2. From this, an abstract *'Reference Architecture'*, was distilled [22, 187]. With a view to non-functional requirements of modularity and extendibility, this high level abstracted RA provides a framework which will enable an architect to design other hybrid architectures. This is a common approach to distil implicit knowledge and to reduce system complexity, as discussed by Cloutier and Verma, and Howard et al, and Grady [15, 77, 188]. This work has proposed that EM can be dislocated from MC, with minimal interfaces, *power_available*[8] and *vehicle_speed*, see Figure 3-1. As stated in Section 2.4.2, the EM functionality is divided into the CPS and PPS sub-systems. In the context of the vehicle studied, CPS refers to the fuel cell and BoCN and PPS refers to a set of reversible storage system options. It is proposed that this RA can contain the key reusable functionality for all hybrid energy management applications.

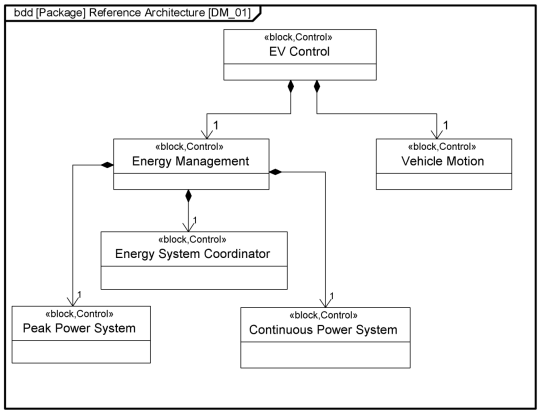

Figure 3-1: Decomposition of RA as defined by Marco and Vaughan [48]

However there are some areas for expansion. This RA has not been tested on an ICE based series HV. In most HVs there will be an integrated braking system and there may be a transmission, and an on-board charger. This research extends this RA to include these features. This RA assumes that the PPS and CPS will remain exclusively within the EM domain. As will be discussed in Chapter 4, this does not apply to parallel or compound HVs. Looking closer at Figure 3-2, it can be seen that the RA models presented it can be seen that the PPS receives an *esc_soc_dmd*[9] for a target SOC from the energy systems coordinator. The PPS responds with a *pps_pwr_req* to the coordinator. This means the calculation of the power required to achieve the desired SOC is encapsulated in the PPS control feature. As discussed in the previous section, the ECMS

[8] Throughout this Thesis, SysML signal flows representing control signals will be in *uncapitalised_italics*

[9] SysML model naming abbreviations and acronyms is this Thesis are presented in Appendix E.

controller, as with many others, define a *split*, which is a function of demand and the SOC state. This represents a reversal of this encapsulation, and the RAs will be amended to address this.

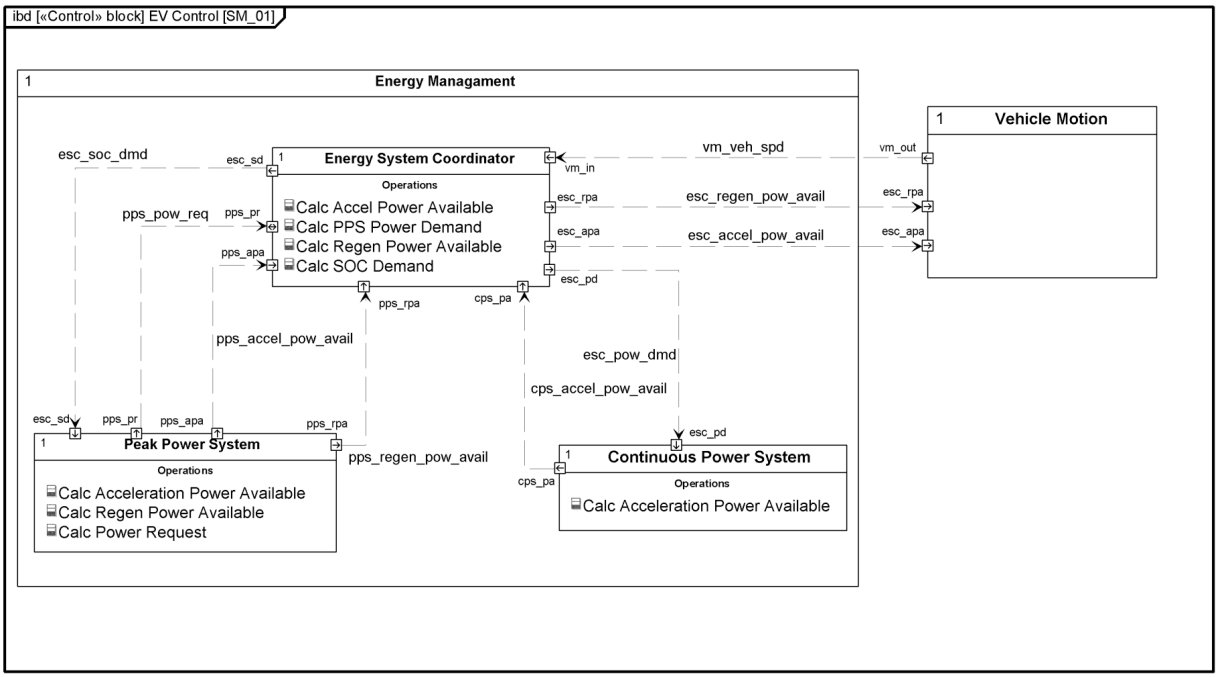

Figure 3-2: Strategy Model of RA as defined by Marco and Vaughan [48]

Figure 3-2 shows the key interfaces between the coordinator and the PPS and CPS: of *pow_dmd* from the coordinator and *pow_avail* to the coordinator. This research will add to these as necessary, and this will be discussed in detail in Section 3.4.

This architectural analysis methodology, RA and the vehicles it has been applied to comprise the inputs to this research. From this point the scope of HV variants and configurations will be expanded and the RA extended where necessary.

3.3. Critical review of the Wren RA

As presented in Section 2.4.2 the vehicles initially analysed under the Wren project have been grouped as series HVs. Therefore the next logical step is to apply this RA onto other series HVs, for example with an ICE as opposed to a FC. However a critical assessment of the RA from Wren is required to enable this.

3.3.1. Energy Management versus Motion Control

Figure 3-1 and Figure 3-2 show the decomposition and, strategy models of the RA as developed by Marco and Vaughan. The first feature of the RA is the clear demarcation of EM and MC. This is a key feature for increasing VSC reusability across HV deployments and will be retained in the extended RAs.

3.3.2. Driver Demand

There is no clear indication in the interface to the driver in the RA. Marco and Vaughan include the drive in their ADs, where it communicates directly with the Motion Control block, but this feature was omitted through the abstraction to the RA [22]. It is reasonable to assume that a driver will be required to interface with the vehicle and this entity is included in the RAs presented in this Thesis. In addition, functions such as route data, driver interpreter and drive mode select (such as EV mode) may not directly interact with Motion Control. Torque demand (potentially arbitrated between pedal and cruise functionality) is a function which will be available on both series and parallel vehicles, so it is sensible to remove this from the MC functional group. The extended RA will include a Driver Demand functional group in the VSC, the output of which will be torque demand for MC and mode select for EM.

3.3.3. Reusable interfaces

Figure 3-2 shows the key interfaces of the RA. Between MC and EM, there is *vehicle_speed* and two *power_available* signals (positive and negative). In the case of the HVs analysed, the EM strategy was a vehicle speed weighted PF strategy. Also, in legacy architectures, vehicle speed is commonly broadcast from the brakes module. It is also unsigned, which creates difficulties for electric drive vehicles as will be discussed in Section 3.4.3.

The interfaces between the Energy Systems Controller (ESC) and the CPS are *power_available* and *power_command*. These interfaces are employed in the RAs presented in this Thesis. The same interfaces are used between the ESC and the PPS, however two extra interfaces are employed, *esc_soc_dmd* and *pps_pwr_req*. This is a feature of a vehicle speed weighted power following EM strategy. The ESC generates a target SOC and based on a difference between this and the actual SOC the PPS will generate a power required to correct this error. This power request is passed on to the CPS. This form of EM strategy is ideal for HV with a high power, low capacity storage system such as a supercapacitor or flywheel. In essence, the energy storage level is inversely proportional to vehicle speed, i.e. full at zero speed for maximum acceleration and low at high speed to capture maximum regenerative braking energy. While this EM strategy is appropriate for this HV type, it is not universally applicable.

The architectural idea behind this functional partitioning is to encapsulate the storage system reducing dependency on the ESC. However to determine the appropriate *pps_pwr_req* the PPS must be aware of the CPS power limits, thereby creating a dependency between the PPS and CPS. This dependency is avoidable as will be demonstrated by the RA presented in the next section.

3.3.4. Real world considerations

It is common for HVs to have integrated braking. There are different levels of integrated braking. Category A braking is defined by the brake pedal having no interaction with the secondary braking system (regenerative braking), and is commonly referred to as throttle off braking. Category B braking blends the primary and secondary braking systems (hydraulic and electrical) as a function of brake pedal position [189]. The architecture presented will incorporate legacy and ideal braking interfaces. Also, electric

drive series HVs may include a transmission, in order to keep the electric machine in its high efficiency zone at high speed. The interface between transmission and ICE drive is mature with the shift control in the transmission controller [11]. Therefore the RA incorporates three transmission variants; no transmission, simple transmission governed by the VSC and a complex transmission governing its own shift strategy. The RA will include an on-board charger for plug-in HV variants.

Common to all vehicles is a continuous ancillary load, to run controllers, air conditioning, heating and other body and infotainment loads. In traditional vehicles, this power is provided by the alternator absorbing mechanical power from the ICE. In series HVs there is commonly a DC/DC converter. Not only does this provide a continuous power draw which the EM strategy must account for, but in some cases the power can be decreased or increased in high positive power (acceleration) or high negative power (regenerative braking events). It is also conceivable that this system could generate power if a solar cell is integrated to the vehicle. This system is included in the RA.

3.3.5. Summary

The RA presented by Marco and Vaughn is valid for the vehicles analysed. The clear demarcation between EM and MC is beneficial as are the key interfaces of *power available* and *power command.* The RA will be extended to show how a defined set of four generic interfaces, including *available* and *command*, results in architectural robustness and reusability. The encapsulation of EM functionality in the PPS will be reversed and this will solely be encapsulated into the ESC. The real world considerations above strengthen the RA. How the RA can be deployed on to the variety of series HVs and real world variants. As the RAs are developed and deployed in the example chapters (Chapters 6 through 8), a common language of notation and semantics will emerge. The convergence of which indicates that the RAs are at the right level and are reusable across many deployments.

3.4. The extended Series RA

This section presents the RA of the series HV configuration. A high level abstraction of a generic series HV in the form of a system schematic (in the format shown in section 2.4.2) is presented first. Subsequent models are grouped into system domain and control domain to address the level of abstraction required for either systems integration or control development. The system domain addresses the highest level relationship between the VSC and the rest of the system. The control domain models present a more detailed view of the internal architecture of the VSC.

The system domain is presented by a decomposition model of the HV powertrain system shows the key subsystems. A context and causality model is also used to show the key functional groups, their operation and interfaces. Finally an interaction model is used to assist in the understanding of the system.

The control domain is presented by the control domain view and contains one decomposition model, two strategy models and one interaction model focusing on the control architecture of the Series RA. This presents functional detail within the VEM and

VMC functional blocks. Another strategy model, used to describe in detail the torque available functional block, is also presented.

Throughout this section, and the following chapter, the RAs are presented in the SysML format devised by Marco and Vaughan. However one of the noted advantages of model based system analysis is that there is no longer a need for unwieldy and documents [43, 45]. Clearly the models are being presented in document format in this Thesis. This creates an unusual constraint on the models. They must be readable in document format.

In the progress of the LCVTP project introduced in Chapter 1, it was discovered that most parties either did not have access to a SysML tool or exposure to the semantics. Therefore to aid understanding and communication simplified versions of the models have been rendered, as in Harrington et al [23]. Also Appendix F contains tabulated summaries of all the architecture information. The aim of these tables is to aid the uninitiated to understand the SysML models. They also allow for limited qualitative description of the models and hence should be used for reference when reading the models presented. This limitation of readability based on access to tools and or experience is observed by Marco and Vaughan and Vanderperren [47, 48]

3.4.1. System Schematic

Figure 3-3 presents the highest abstraction of a series HV configuration which retains the minimum detail to characterise the system. The schematic comprises a DC bus and six sub-systems and a 'wheel' representing the vehicle chassis. The CPS, as defined by Marco and Vaughan, represents the generic set of continuous power sources, outlined in Table 3-1. Four variants of interest are listed, FC with or without a BoCon, an ICE with a GenSet, a gas turbine and a GenSet or a battery with a charger (Chgr) with or without a BiCon. If a battery was to be used as a CPS it is expected that a charger would also be necessary [67].

Similarly the PPS permutations are listed below, a battery with or without a BiCon, an Ultra-Capacitor (UC) with or without a BiCon and a flywheel with a GenSet. In keeping with the nomenclature from Wren, the ancillary sub-systems shall be grouped as the Tertiary Power Source (TPS). The TPS creates a placeholder for all other vehicle loads such as Heating Ventilation and Air Conditioning (HVAC). The TPS can also incorporate dedicated loads such as "power dump resistors" or sources such as solar cells. The RA must be robust to this potential use.

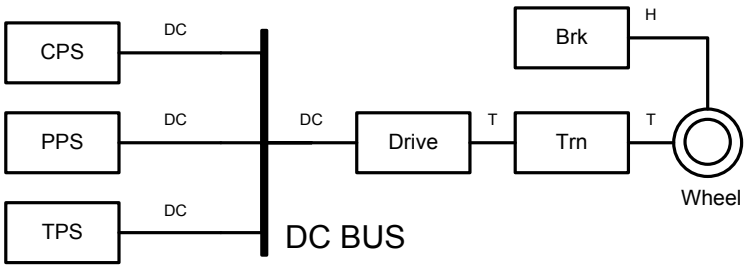

Figure 3-3: System schematic of Generic Series HV

The drive system can be two wheel drive (2WD) or four wheel drive (4WD). These drive modes can be achieved by various permutations of electric machines and differentials. Series HV transmission are divided into three groups; single ratio transmissions, i.e. no transmission; simple transmissions i.e. few ration and controlled by the VSC; complex transmissions i.e. many ratio and dedicated transmission control. The brake torque apportionment functionality may reside in a typical brakes controller or the VSC. For the purposes of this research, the legacy constraint case of this function residing in the Brakes controller will be noted but the RA presented will incorporate the ideal case where it resides in the VSC.

Therefore it can be seen that there exists a wide range of Series HV configuration permutations which can be generated by combining the subsystem variants listed in Table 3-1, into the structure presented in Figure 3-3. This confirms that the level of abstraction for systems integration is valid. It is high enough to incorporate all Series HV configurations while detailed enough to express the key sub-system functional characteristics. Moreover, if the subsystem encapsulation and generic interfaces are defined correctly (in the following section) then it should not be necessary to test the validity of the RA each individual permutation of Series HV.

CPS	FC (+ BoCon) ICE + GenSet Turbine + Genset Battery + Chgr (+ BiCon)	PPS	Battery (+BiCon + Chgr) UC (+BiCon + Chgr) Flywheel + GenSet	TPS	12V loads HVAC Power Dump PV Source
Drive	2WD 1M + Diff 2WD 2M Inboard 2WD 2M Hub 4WD 1M +TC+2Diff 4WD 2M + 2Diff 4WD 4M Inboard 4WD 4M Hub	Trn	1 ratio (no trn) 2 to 3 ratio simple 5-8 ratio complex	Brk	Category A or Category B VSC = Master or Brk = Master

Table 3-1: Series HV sub-system permutations

3.4.2. System Domain Models

The system domain models present the RA at a level of abstraction applicable to systems integration.

3.4.2.1. System Decomposition Model

As initially stated in Chapter 1 the key attribute of a RA is the level of abstraction. Harrington et al, set the level of abstraction required of the RA for systems integration purposes to match the highest level requirement of a HV *"deliver driver demand efficiently"* [23]. Therefore the VSC will contain three high level functional blocks, referred to previously as VEM, VMC and DD. DD can be used as a placeholder for vehicle specific functions such as cruise control and GPS navigation interfaces.

Figure 3-4 presents the RA decomposition model of the series HV powertrain system architecture. The series HV powertrain is shown to comprise (direct composition: solid line with arrowhead and solid diamond) the six sub-systems presented in Figure 3-3 and the vehicle chassis and the DC Bus. The VSC is also shown to be a part of the HV powertrain as it should not be encapsulated into any of the other sub-systems. It is

assumed at this stage that each sub-system contains a local control function, and these are shown (Transmission Control Unit-TCU, Brakes Control Unit-BCU, PPS-PPS Manager). The VSC high-level functional groups of DD, Vehicle Energy Management (VEM[10]) and Vehicle Motion Control (VMC) are shown. The connection between the driver and DD is shown (association: red line).

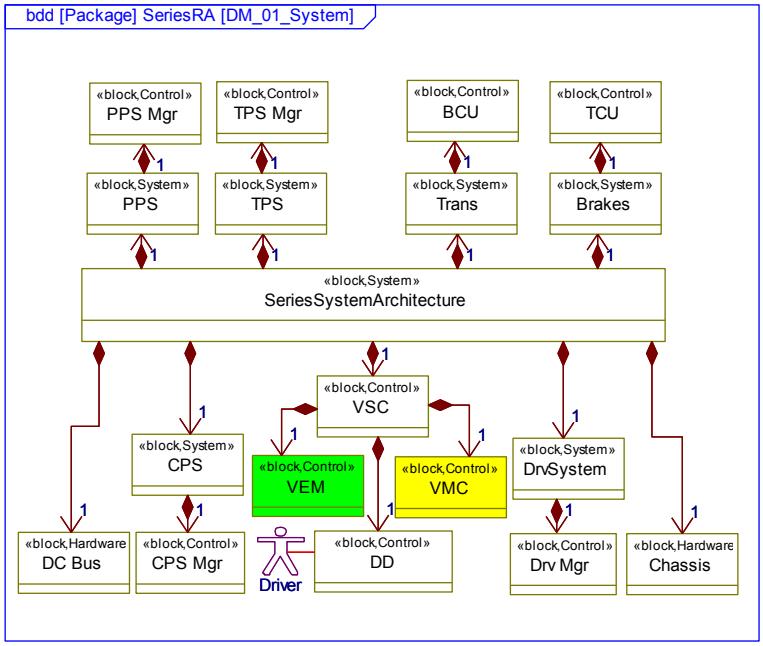

Figure 3-4: Series RA decomposition model of HV powertrain system

3.4.2.2. System Context and Causality Model

Figure 3-5 shows a context and causality model of the series HV powertrain system architecture. This expands upon the decomposition model in Figure 3-4. All the blocks shown in the context and causality model make up the series system architecture through direct decomposition. The main block in the context and causality model is the VSC. This is shown to comprise the DD, the VEM (shaded green) and the VMC (shaded yellow)[11]. The key operations of these blocks are shown. The key generic interfaces between the VSC and the external systems are shown (as item flows: solid line with arrowhead). The key VSC functions and interfaces will be described in summary below, however the Series RA tables shown in Appendix F should be referenced throughout.

VSC functional blocks, Driver Demand

The key operation of the DD is to determine the *torque_demand* as a function of accelerator and brake pedal positions. In this configuration the VSC is the master and the brakes is the slave. This is the ideal configuration but the legacy configuration will

[10] Note that VEM is equivalent to the ESC in the Wren RA. Also the term Vehicle (V) is added to EM and MC to differentiate a functional control block from the Energy Management and Motion Control domains, see Section 3.4.3

[11] The green and yellow shading will be used throughout all SysML models in this Thesis to easily identify the VEM and the VMC.

remain for the foreseeable future. The alternate architecture (brakes is master) in which the brake pedal position interfaces directly with the brakes controller and the brakes communicates *regen_torque_command* to the VSC within a known *regen_torque_available* range from the VSC - is presented in Appendix F Figure F-1. All architectural discussion in this chapter will assume this ideal configuration is in place. Chapter 6 will critically review the implications of a deployment with the legacy brakes integration constraint. An important learning point from this is the impact of legacy or supplier constraints on system design. It is argued that the relationship between driver demand and the BCU shown in Appendix F Figure F-1 is not optimal, but is a sensible compromise. The RA does however empower vehicle manufactures in their discussion with their suppliers regarding who should have supervisory control. In this situation, the RA can be used as force for change on the relationship between manufacturers and their suppliers.

VSC functional blocks: Vehicle Energy Management & Vehicle Motion Control

The role of the VEM is to determine the total system *power_available* (positive and negative), from the CPS and the PPS minus the power being consumed by the TPS, and to efficiently apportion *power_demand* between the PPS and the CPS. The role of the VMC is to determine the *torque_available* to propel the vehicle. The *torque_demand* from the DD is limited by this *torque_available* signal. Based on the driver *torque_demand*, the VMC will command the drive transmission and brakes system, confident that the energy and power limits of the PPS or the CPS will not be exceeded. Both the VEM and the VMC functions will continuously verify that their subordinate systems do not exceed their broadcasted limits (*availables*).

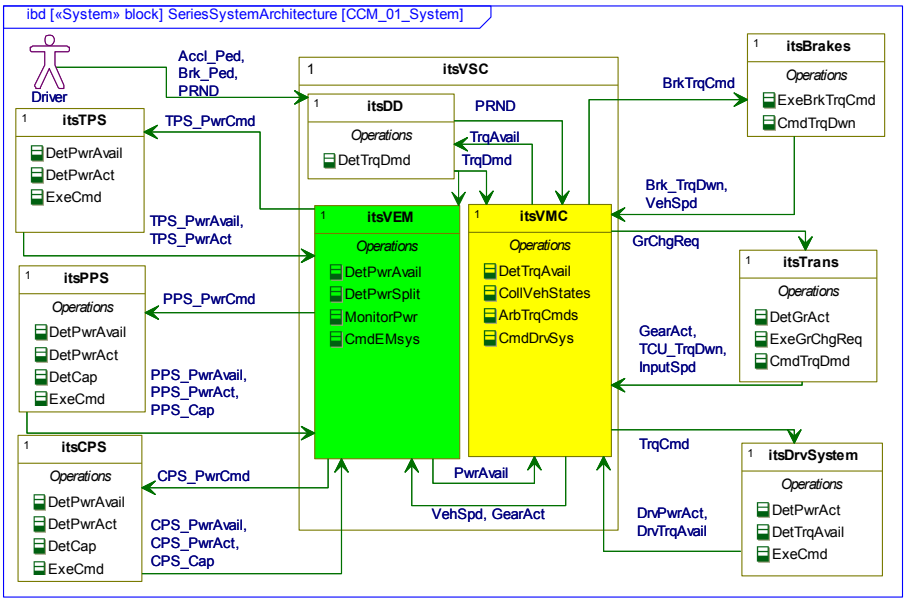

Figure 3-5: Series RA context and causality model of HV powertrain system

Generic & Reusable Interfaces

The research has identified that with a few exceptions [23, 79], the key control interfaces within the architecture can be generically defined as; *available, actual,*

capacity or *command*. The interfaces between the VEM or the VMC and their respective external systems will contain a subset or all of these interfaces. Within the VEM, the *available*, *command* and *actual* interfaces are in *power*. However within the VMC the generic interfaces are in *torque*. The *capacity* interfaces are dedicated to systems which can store energy (the PPS and the CPS) and is commonly represents as a SOC or fuel level. The TPS, drive and brakes systems cannot store energy hence this interface is absent. The transmission in this case represents a placeholder for both simple and complex variants. Therefore the generic interfaces comprise *gear_change_request* from the VMC and *torque_down_request* from transmission. The first is the key setpoint for a simple transmission and the latter is the key interface for the complex transmission allowing the TCU to interrupt torque command during gear change. In the case of a series HV with no transmission, this block and its interfaces can be removed. The *command* interfaces represent set-point control signals. Finally, as in the Wren RA, the VMC communicates *vehicle_speed* to the VEM but also *gear_actual*. The DD broadcasts *torque_demand* to both the VEM and the VMC.

3.4.2.3. System Interaction Model

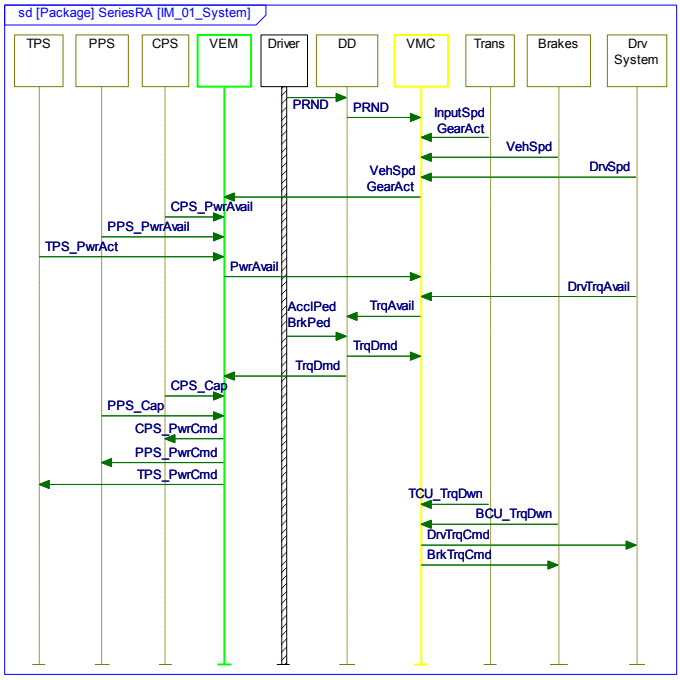

Figure 3-6: Series RA interaction model of the HV powertrain system

The previous two models show how the system is composed and how they interact however it is always necessary to present a model with a temporal aspect to get a deeper understanding of system behaviour. The example interaction model presented in Figure 3-6 shows how the key systems interact. Each system is represented as an instance line, with the driver highlighted. Systems interface by means of a message (solid line with arrow). The vertical order of the messages is significant. Is defines a functional dependency on information. For example the VEM cannot determine *power_available* until it has received *power_available* from the CPS and the PPS, *power_actual* from the TPS and *vehicle_speed* and *gear_actual* from the VMC.

The series of messages presented in Figure 3-6 relates to the basic scenario of responding to driver demand for motive torque. The key sequence of necessary events is shown. As discussed earlier VEM *power_available* must be determined. Then the VMC functional block can determine *torque_available* based on *power_available*, *torque_available* and Park Reverse Neutral Drive (PRND). This *torque_available* term constrains the driver demand ensuring that none of the vehicle system limits can be breached.

Based on the *torque_demand, vehicle_speed* and *gear_actual,* the VEM can determine the appropriate ratio to which to generate the *power_command* for the PPS and the CPS. In extreme demand scenarios the VEM may alter the TPS *power_command.* Finally in torque_demand is converted into a Drive and Brakes *torque_command* (assuming no torque intervention from Transmission or Brakes). Should Brakes or Transmission broadcast a *torque_down* command then the total *torque_command* is altered accordingly.

Although this *torque_command* sequence appears 'after' the VEM *power_command* sequence, it should be noted that they occur in parallel. It is a limit of the SysML behavioural models that events are single instances of discrete events and no two events can occur at the same moment in time. It is also a limit that the behavioural diagram cannot truly represent continuously broadcast communication, commonly found in vehicles [16].

3.4.3. Control Domain Models

The control domain models present the RA at a lower level of abstraction. This is a more appropriate level of abstraction for VSC control development.

3.4.3.1. Control Decomposition Model

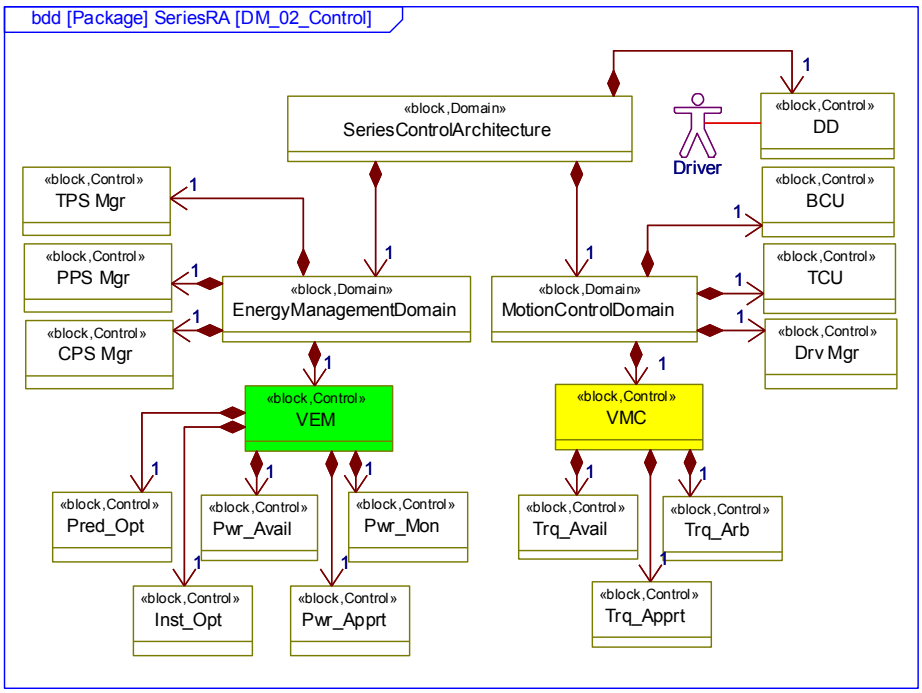

Figure 3-7: Series RA decomposition models of HV control domain

Figure 3-7 shows a RA decomposition model of the Series HV control architecture. The control architecture is divided between the Energy Management Domain and the Motion Control Domain, with the DD as the outlier. The local controllers for the PPS, CPS and TPS and the VEM are all lie within the Energy Management Domain. The VMC, BCU, TCU and the Drive Manager lie within the Motion Control Domain. The VEM comprises *Predictive_Optimisaiton, Power_Available, Instantaneous_Optimisation Power_Monitor* and *Power_Apportionment*. The VMC comprises *Torque_Available, Torque_Arbitration* and *Torque_Manager*. Each block represents core or significant secondary functions which a VSC developer should encounter. Table F-2 in Appendix F presents the VSC sub-functions in tabular form with inputs, operations and outputs.

3.4.3.2. Control Strategy Models

Figure 3-8 and Figure 3-9 show strategy models of the Energy Management and Motion Control domains respectively. These models present a detailed view of the interactions between the VSC and the sub-system controllers and within the VSC. As before, the VEM is shaded green and the VMC is shaded yellow. The driver is shown interfacing to the DD. The key interfaces between the DD, the VEM and the VMC presented in Figure 3-5 are retained. The newly introduced interface, *future_data,* represents a generic interface for data required by the *Predictive_Optimisation* functional block, such as GPS data.

VEM sub-functions

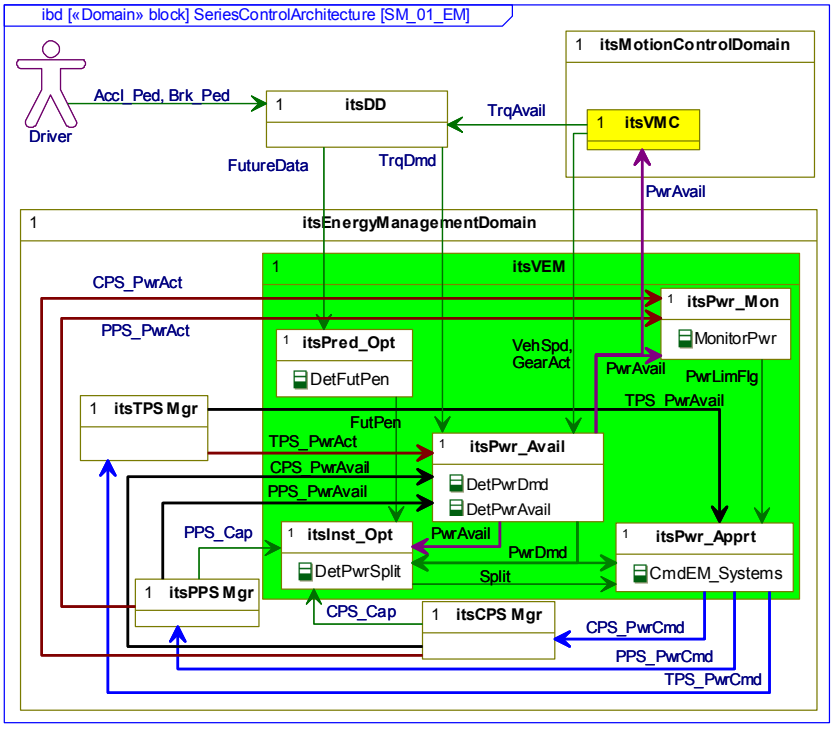

Figure 3-8: Series RA strategy model of energy management domain

The core functions of the VEM are *Power_Available*, *Instantaneous_Optimisation* and *Power_Apportionment*. The first function determines the system wide power available, namely power available upstream of the DC bus. Based on this information and

power_demand (a function of *torque_demand*) the *Instantaneous_Optimisation* function must determine the appropriate *power_split*. The *Power_Apportionment* function commands the CPS and the PPS systems as a function of *power_demand* and *power_split*. Under conditions of a low *power_available*, relative to *power_demand*, *Power_Apportionment* can reduce or increase the power consumption of the TPS in order to meet driver demand and to maximise the efficiency of key vehicle subsystems[12]. The *Power_Apportionment* block will also include real world functionality. In the case of an ICE based CPS this may include cold start protection, and a strategy which would protect against CPS on off hunting, as shown in Section 6.2.3. This encapsulates this variance, which may be vehicle dependent, from the *Instantaneous_Optimisation* block.

The secondary functions of the VEM are *Predicitive_Optimisation* and *Power_Monitor*. *Predictive_Optimisaiton* is an optional function which should be represented in the RA based on the research [148]. The RA shows this as a distinct function, encapsulated from *Instantaneous_Optimisation*. This minimises the dependency between the two functions. *Power_Monitor* is required to ensure that total system and sub-system limits are not breached. Given two or more power sources it is trivial to point out that the total system power available exceeds the individual sub-system power *availables*. This is particularly an issue for a passive battery (assuming no control electronics), which will deliver whatever power is demanded at the Drive system less the power supplied by the CPS. The *Power_Monitor* can instruct *Power_Apportionment* to alter the *power_command* to the TPS. This introduces the concept of functional diagnostics, which is outside the research scope and is discussed in future work in Section 9.2.5.

VMC sub-functions

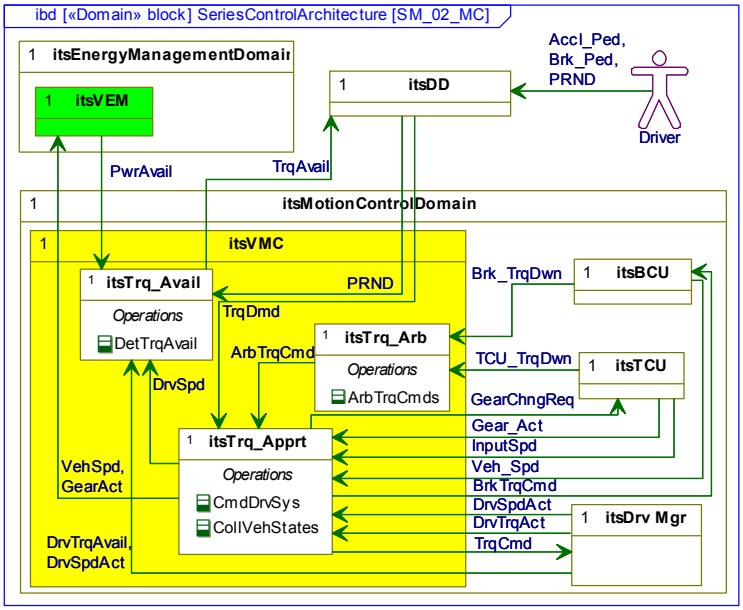

Figure 3-9: Series RA strategy model of motion control domain

[12] Common scenarios would include reducing power to HVAC under maximum demand or maximising HVAC under regenerative braking when the battery capacity is high.

The core functions of the VMC are *Torque_Available*, *Torque_Arbitration* and *Torque_Apportionment*. The role of *Torque_Available* is to determine the total torque available to constrain DD. This is a function of the Drive *torque_available* and VEM *power_available*. This is important as a torque demand within the limits of the Drive system may exceed the limits of the PPS or CPS. This is even more complex in the context of four quadrant motors delivering positive torque while rolling backwards in effect generating. This means that the relevant limits must be a function of the sign of the torque and speed. This is a key issue for electric drive vehicle and will be discussed in detail later in this section. *Torque_Arbitraiton*, detects the real-world signals such as torque interrupt from brakes (in the event of a stability event) or transmission (in the event of a gear change) and alters the total torque demand accordingly. An *arbitrated_torque_command* is sent to *Torque_Apportionment* which adds or subtracts it from the main *torque_demand*. *Torque_Apportionment* acts as the dynamic torque controller for the drive system and may be required to control more than one machine.

3.4.3.3. Torque Available functional block: detail

The *torque_available* signal is required to constrain the *torque_demand* from the DD. As previously mentioned the *torque_available* signal is calculated in the *Torque_Available* functional block. This is a function of *torque_available* from Drive and *power_available* from the VEM. In the context of an electrical drive system this function deals with two key considerations; signed speed and signed torque. An electrical machine may apply positive and negative torque while spinning in both directions. The operational torque speed map of an ICE normally occupies the northeast quadrant with engine braking the southeast quadrant. An electric machine may operate fully in all four quadrants, see Figure 3-10.

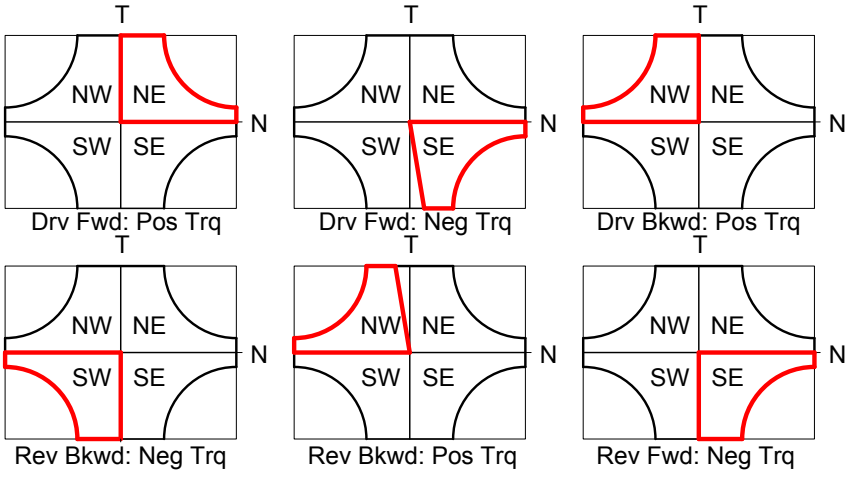

Figure 3-10: Six modes of operation of electrical drive

Under normal operation, accelerating forward, while moving forward (in drive) the electric machine operates in the northeast quadrant. In this case the *torque_available* must be constrained by the positive *power_available* from VEM. However, the vehicle may be rolling backwards (downhill) while positive torque for pull away is being demanded (in drive). In this case the electrical machine will be retarding rollback for a time, generating negative power, i.e. the northwest quadrant. In this case the positive

torque_available must be constrained by negative *power_available* from VEM. Therefore the *Torque_Available* block determines the maximum and minimum *torque_available* for DD and *regenerative_torque_available* for the BCU. Reverse operation is the southwest quadrant where negative *torque_available* must be constrained by positive *power_available* from VEM. This is presented in detail as a strategy model in Figure 3-11.

This relatively low level structure is included as part of the RA because it is common requirement for all electric drive vehicles. This includes both series HVs and EVs.

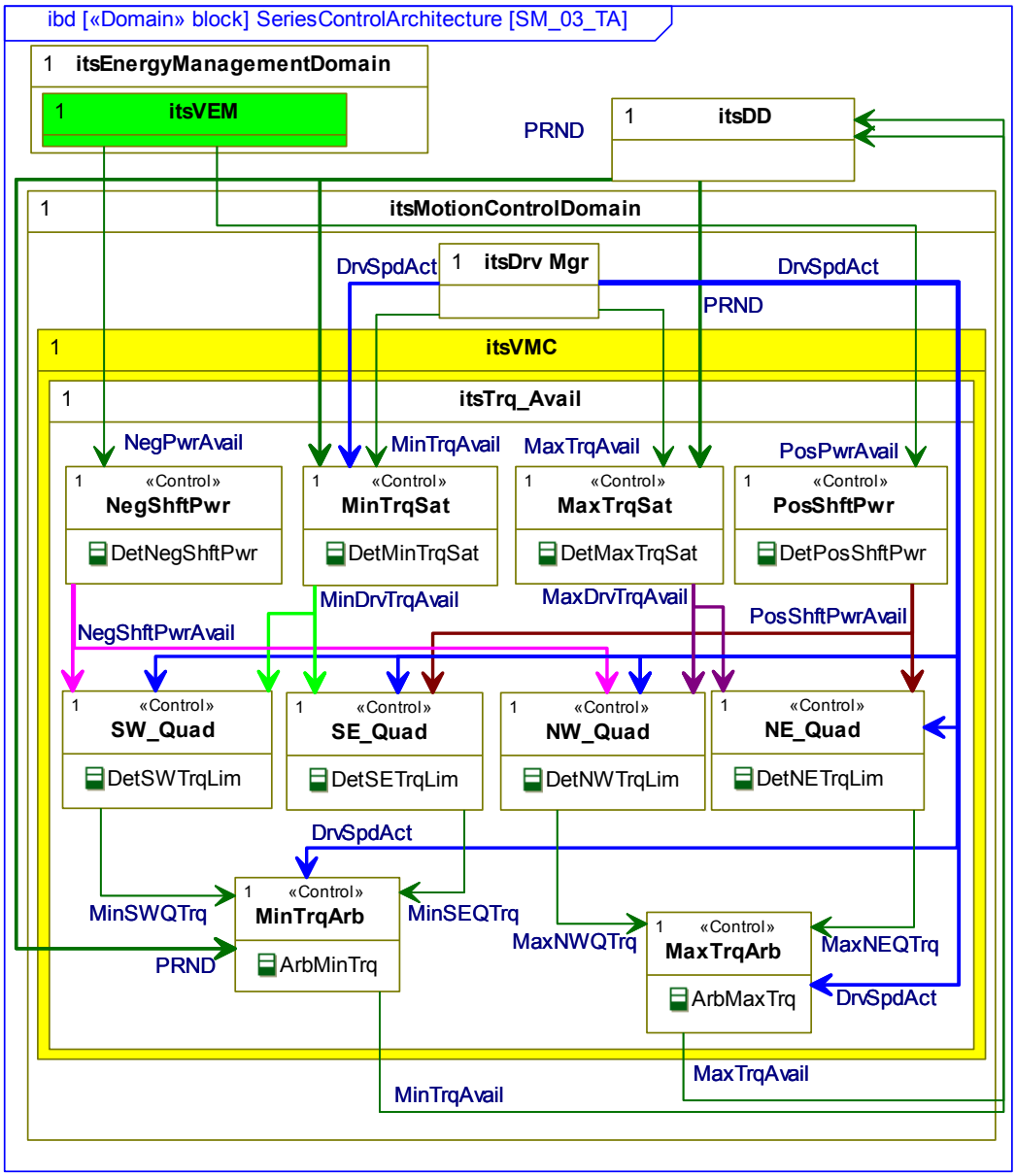

Figure 3-11: Series RA strategy model of *Torque_Available*

3.4.3.4. Control Interaction Model

For completeness an interaction model for the control domain is presented in Figure 3-12. When comapring this to
Figure 3-6, it can be seen tha the VEM and the VMC block have been split into their composite parts. The secondary fucntions of the VEM have been omitted for clarity. The

internal VEM and VMC messagers are highlighted in red. Several key sequences are highlighted by this diagram. As has been discussed in the last section the *Torque_Available* funcitonal block requires *drive_speed_act* to determine *torque_available*. However the sequence required to generate the correct CPS and PPS *power_command* signals should be noted.

The *Power_Available* funcitonal block requires the CPS and the PPS *power_available* signals, the TPS *power_actual* signal. The *power_demand* signal is calculated by *Power_Available* using the *torque_demand* from DD and *vehicle_speed* and *gear_actual.* The system *power_availables* (and the PPS and CPS *capacity* signals) are required by the *Instantaneous_Optimisation* block to calculate the *split*. It is this *split* that that *Power_Apportionment* uses to distribue the *power_demand* between the CPS and the PPS. Given that the *torque_demand* from the DD has been constrained by *power_available* it can be seen that this architecture inherently protects the sub-systems from over-demand.

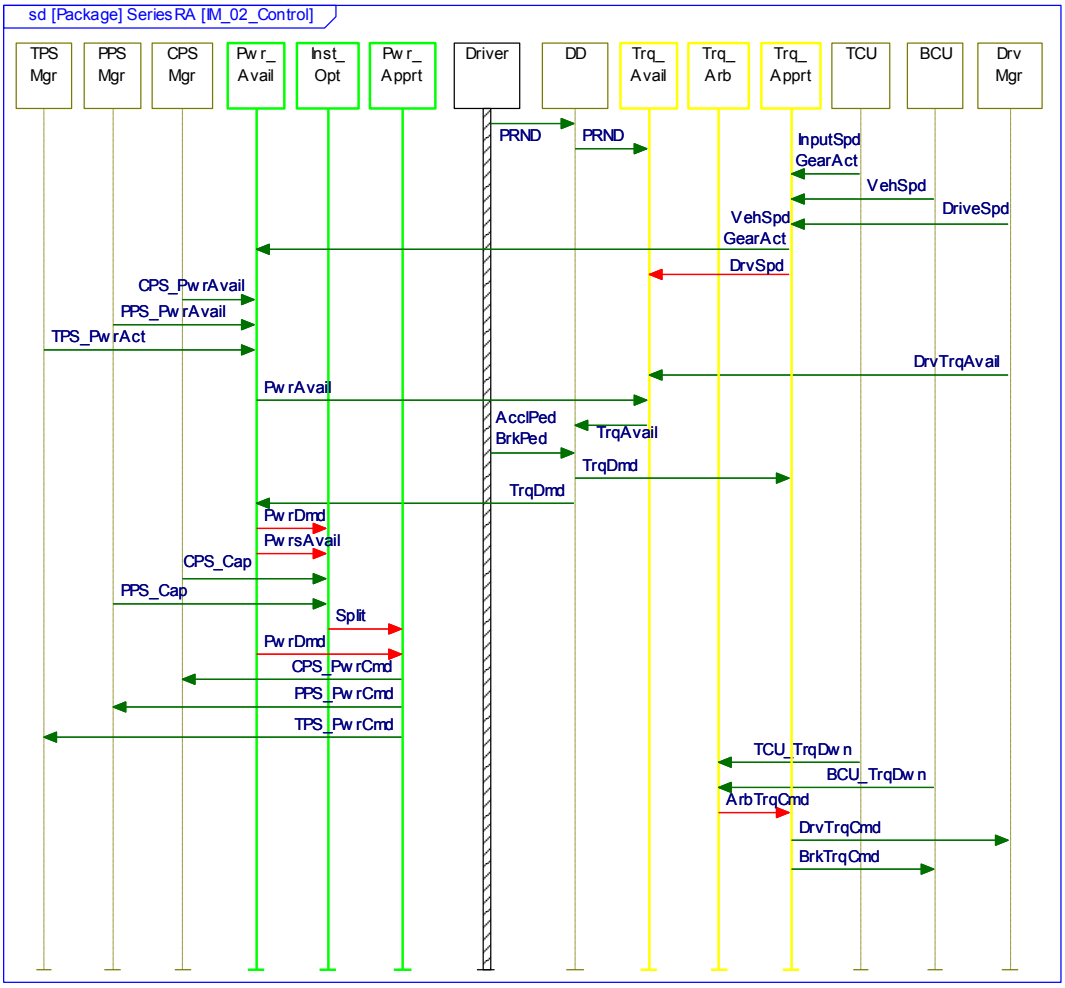

Figure 3-12: Series RA interaction model of HV control domain

3.5. Summary

The hypothesis being tested in this Chapter is whether or not the Wren RA is applicable to a wider set of series HVs. Based on the architectural analysis presented here, it can be

stated that the hypothesis holds true for most facets of the Wren RA. The key structure of demarcating EM from MC with *power_available* and *vehicle_speed* interfacing is retained. The generic interfaces between the VSC and the sub-systems of *available* and *command* are also retained.

The Wren RA is extended to include the generic interfaces of *actual* and *capacity*. A DD block, at the same level as VEM and VMC is introduced to contain functions which should not be encapsulated into either VEM or VMC such as driver demand, cruise control, GPS interface, and vehicle mode management.

The RA is further extended to incorporate real world systems such as brakes, transmission, 12V system and an on board charger. The charger function is encapsulated into the PPS (or CPS if appropriate) while the brakes, transmission and 12V system become sub-systems in their own right. The 12V system is generically defined as the TPS and included into the energy management domain and utilises the generic interfaces with the exception of capacity.

The brakes interface defined here presents the ideal configuration. The legacy constrained configuration, which will be encountered in the near to midterm, is presented in Appendix F. The transmission system is a placeholder which may be removed if the particular deployment requires no transmission. It also defines a simple transmission controlled by the VSC or a complex transmission which controls gear shifting itself.

The medium through which the RA has been presented, the SysML and IEEE 1471 guideline derived methodology presented in Wren, has limitations. Grobstien and Dori, Linhares et al and Marco and Vaughan [34, 44, 46] all discuss the benefits of model-based systems engineering analysis, however, it has been presented here in documentation format. In essence this Thesis is attempting to present a benefit of model-based SE in a sub-optimal format. This has resulted in poor acceptance of the format of the RA within the on-going research project, LCVTP. The RA has received wide acceptance when it has been presented in the simple format shown in Harrington et al [23] and the tables presented in Appendix E.

This lack of acceptance is largely due to lack of access to tools or experience with the semantics of the SysML. Therefore for the purposes of this Thesis the Wren methodology will be retained as SysML presents a more formal and accurate representation of the RA than other media.

The next chapter assess the hypothesis that this extended RA is applicable to parallel and compound HVs.

4. Parallel hybrid reference architecture

4.1. Overview

This chapter address two hypotheses. The first is that the Series RA is applicable to Parallel HV configurations. This hypothesis is shown to be false therefore a Parallel RA is defined which represents all Parallel configurations. The concept of pre and post transmission HVs is introduced. The second hypothesis is that the Compound HV can be described by either the Series or Parallel RA, if not a third RA must be developed. It is shown that the Parallel RA is extendible to represent the key characteristics of the compound HVs

The hypotheses are addressed in the same manner as outlined in Chapter 3. Each configuration is distilled into a generic system schematic which captures the key characteristics of each configuration. Then they are analysed at a systems level and a control level. The system level analysis presents a decomposition model followed by a context and causality model and an interaction model. The control domain analysis presents a second decomposition model, two strategy models, one for the energy management domain and the other for motion control domain, and an interaction model.

4.2. Critical review of series RA

This section will assess the applicability of the extended series RA to the parallel HV configuration.

4.2.1. Energy Management versus Motion Control

Reviewing the series HV variants presented in Section 2.4.2 and the system schematic of the generic series HV in the last section, some similarities can be seen. Each has a dedicated drive system for delivering require tractive torque, separated from the CPS and PPS by a DC bus. Both Series RAs show a clear demarcation between the systems which interact with the VEM and the VMC. This point is clearly presented in Figure 3-7 Figure 3-8 and Figure 3-9 and as the energy management and motion control domains. The TPS, PPS and CPS reside entirely within the energy management domain and the Drive, Brakes and Transmission systems reside entirely within the motion control domain.

Parallel HVs have no dedicated drive system. In all the parallel variants presented in section 2.4.2 the two main systems[13] directly deliver the tractive torque required for vehicle motion via the torque bus. In the case of series HVs these systems have been generically defines as the CPS and the PPS. In all series HV instances discussed to date the VEM directly controls both these systems and the VMC controls the drive system. This structure is not applicable to parallel HV configurations. An alternate architecture must therefore be defied.

[13] In the case of Figure 2-12 an ICE and an electrical machine drawing power from a battery

4.2.2. Real world considerations

Another aspect of parallel HVs is that both power source systems are mechanically coupled to each other and the vehicle. There may be instances where it is desirable to decouple one or both systems. This will require clutches to be introduced to the drivetrain. The location of the clutches will be depended on the parallel HV variant.

Parallel HVs presented in literature are divided into two groups, pre-transmission and post-transmission. This refers to the positioning of the transmission relative to the torque bus (see section 2.4.2). Some post-transmission parallel HV variants include a CVT. This decouples the engine speed form the vehicle speed. The RA needs to be robust to the position of the transmission. Transmissions come in two forms, discrete or continuous. Continuous transmissions introduce an extra degree of freedom, and can be placed upstream or downstream of the torque bus.

4.3. The Parallel RA

This section presents the Parallel RA. Two high level abstractions of generic parallel HV system schematics are presented first. A decomposition model of the HV powertrain system shows the key subsystems. A context and causality model is used to show the key functional groups, their operation and interfaces. An interaction model presents an iteration of the behavioural facet of the control view. Then decomposition, strategy and interaction models focusing on the control architecture of the Parallel RA are presented. This presents a lower level of abstraction.

4.3.1. System Schematics

Figure 4-1 and Figure 4-2 presents the highest level of abstraction of the Parallel HV configuration. The pre-transmission variant is shown in Figure 4-1, including the TPS being fed from an electrical PPS via a DC bus. Figure 4-2 shows the post-transmission variant. Figure F-2 in Appendix F also shows how the TPS would be configured for a mechanical PPS, in this case the TPS would be fed from the CPS via a torque bus. It should be noted that the TPS may be powered by the CPS even if there is an electrical PPS or in pre-transmission configuration. Figure 4-1 and Figure 4-2 present a superset of parallel VH variants. Any RA defined for parallel HVs must be robust to all structure variants presented in Figure 4-1 and Figure 4-2. The key systems are the CPS and PPS which are mechanically joined by the torque bus which drives the vehicle. The torque bus can manifest as gear or belt coupling or direct shaft mounting or through-the-road.

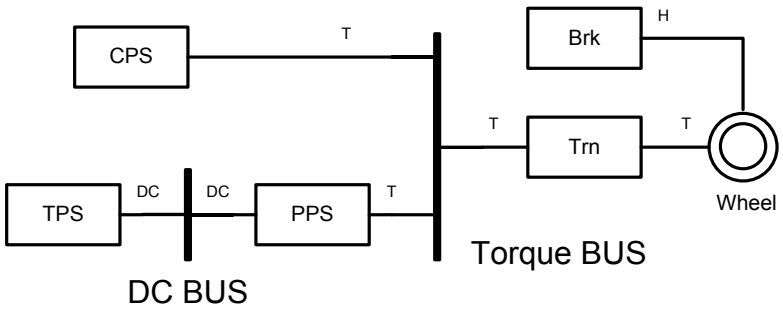

Figure 4-1: System schematic of generic pre-transmission parallel HV

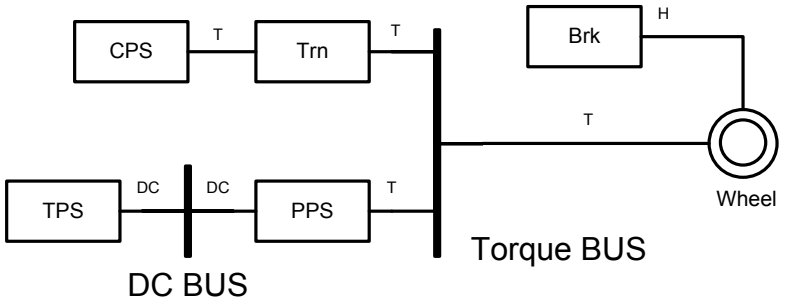

Figure 4-2: System schematic of generic post-transmission parallel HV

Table 4-1 presents the sub-system options for the parallel HV configuraiton. In all literature reviewed, parallel HVs have contained an ICE. In the case of post-transmission HVs, the inclusion of a continusous tranmsission would enable the engine speed to be decoupled from the speed of the vehicle and the PPS. Therefore including this into the CPS system boundary enables the whole CPS to be treated as a power source, see Figure F-3 in Appendix F. While this may be an unusual instance any RA should be robust to that structure.

CPS	ICE (+cont trn)	PPS	Battery + GenSet (+ Chgr) UC + GenSet Flywheel + CVT Hyd Accumulator + Pump	TPS	12V loads HVAC Power Dump PV Source
Drive	Absent	DriveLine	Discrete transmission Continuous transmission Clutch1 Clutch 2 Clutch n	Brk	Category A or Category B VSC = Master or Brk = Master

Table 4-1: Parallel HV sub-system permutations

The PPS can comprise the components described in Section 2.4.1. The most common in literature are the battery with GenSet and the hydraulic accumulator with pump. If the battery PPS is used, the vehicle may have an on-board charger. Mechanical flywheels have also been used, but normally in conjuction with a CVT. Since flywheels act as a high power low energy form of storage, then in principle an ultracapacitor with GenSet could also be used. However it is highly unlikely that an onboar charger would be included.

The parallel TPS comprises the same components listed in the Chapter 3. The TPS may be powered directly from an electrical PPS via a DC/DC converter or mechancially via an alternator. The electrical connection is used normaly for powering the TPS but the TPS may be required to start the CPS, such as an alternator linked to the ICE.

The braking system remains the same and there is no drive system. The driveline system is an extension of the tranmission system defined in the Series RA. It will contain the tranmsission and the driveline clutches required to define key vehicle modes such as the electric only mode. As the driveline configuration is deployment specific it is beneficial to encapsulate this to protect the wider system from driveline variations.

4.3.2. System Domain Models

As per Chapter 3, Appendix E contains a set of tables which can be used as aids for following the RA description presented here.

System Decomposition Model

Figure 4-3 presents an RA decomposition model of the Parallel HV powertrain system architectrue. The Parallel RA is shown to comprise the five sub-systems defined above, the VSC, the vehicle chassis, the torque bus and a DC bus. As with the Series RA each system is shown with its local controller. The VSC has the same decompostion as shown in the Series RA. The CPS is shown to potentially comprise a continuous transmission, as per the encapsulation discussed earlier. The driveline system comprises a number of clutches and local clutch controllers and an instance of a transmission. The two transmissions are mutually exclusive. The inclusion of a Driveline Manager enables the driveline system to be standalone, and this encapulates the functionality from the rest of the systems. This Driveline Manager my be deployed onto a VSC but the demarcation should remain.

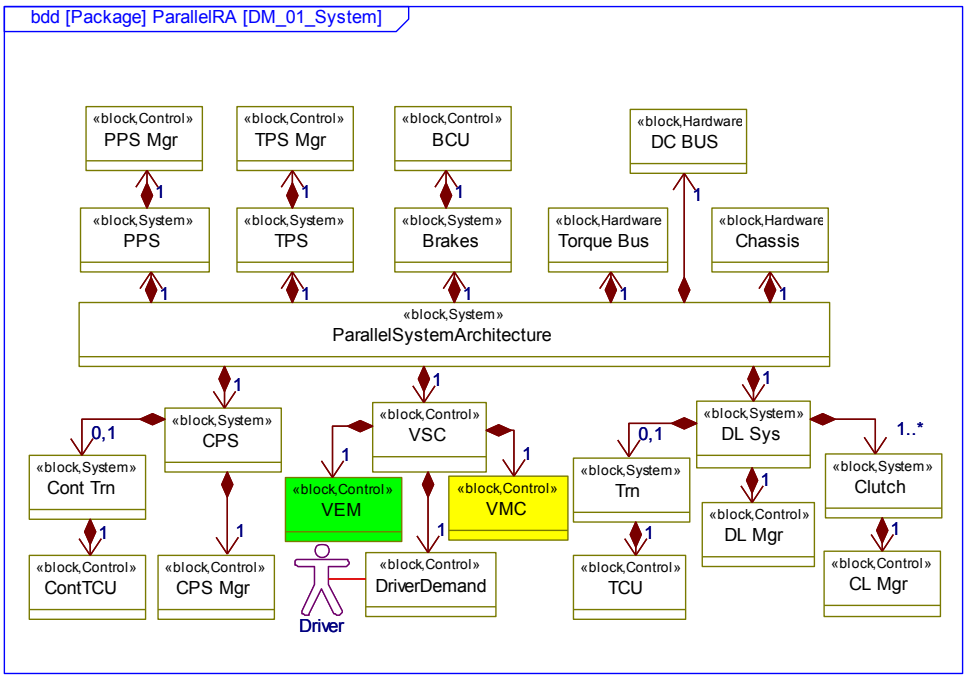

Figure 4-3: Parallel RA decomposition model of HV powertrain system

System Context and Causality Model

Figure 4-4 shows a context and causality model of the parallel HV powertrain system architecture. This expands upon the decomposition model in Figure 4-3. All the blocks shown in the context and causality model make up the Parallel System Architecture presented in the decomposition model. As per the series RA the VSC comprises the DD, the VEM (shaded green) and the VMC (shaded yellow). The key operations of these blocks are shown, as are the key generic interfaces between the VSC and the external systems. The key operation of the DD is to determine the *torque_demand* as a function of accelerator pedal position and regenerative brake torque command from the brakes

system. As per the series RA the brakes interface represents the VSC-master, brakes-slave configuration.

The Parallel RA VEM differs from the Series RA VEM in that it no longer directly commands the CPS and the PPS. The VEM can only now command the TPS. The VEM still determines the *power_available*, and monitors the power flows. In addition, the VEM must now broadcast the *torque_split* term to the VMC. This is an internal signal in the Series RA VEM. In conjunction with determining *power_available*, the VEM must also determine *torque_available*, previously a VMC function. This function has been moved because the VEM still requires the *available* signals from the PPS and CPS. These can manifest as power or torque in the context of vehicle speed and ratio, but both power and torque available must be determined on a system wide basis by the VEM.

The VMC now directly controls the PPS and CPS. The *torque_demand* is combined with the *torque_split* generating *pps_torque_command* and *cps_torque_command*. The VMC still must arbitrate conflicting torque commands and must collate vehicle informaiton such as *vehicle_speed*. The existence of a number of clutches in the driveline requires that the VMC must manage the discrete driveline modes and transitions between them. This is referred to as *driveline_mode* (*DL_Mode* in Figure 4-4). For example there will be distinct EV only and hybrid modes, which are defined by the clutch states. During transitions between states the clutch slip must be controlled. This requires a closed loop speed control function and this will be discussed further in the next section.

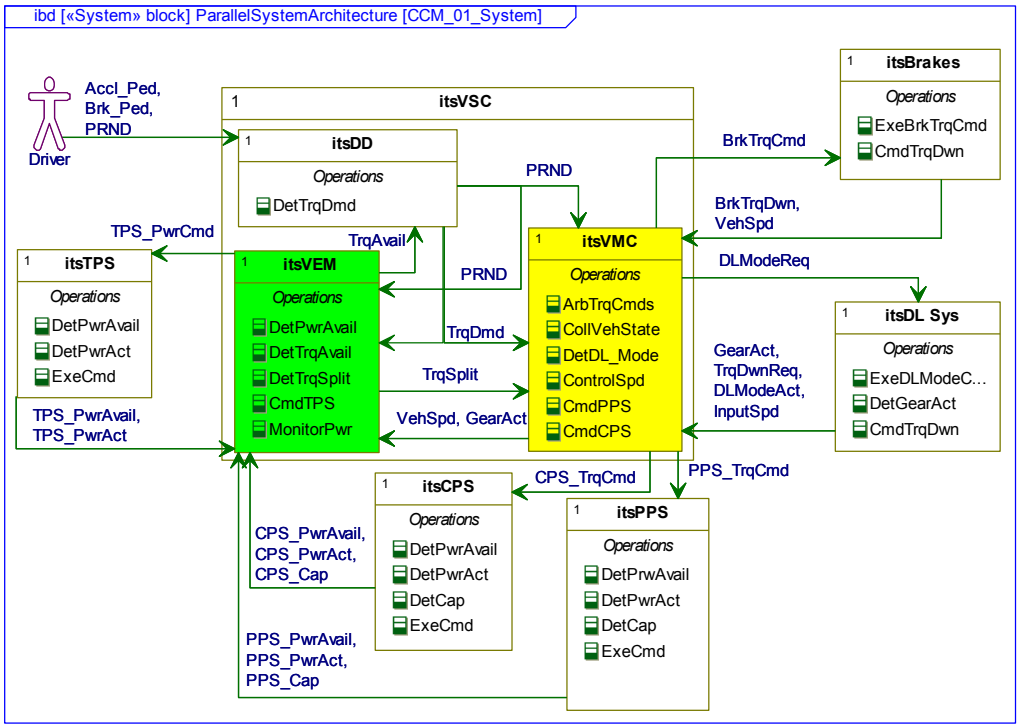

Figure 4-4: Parallel RA context and causality model of HV powertrain system

The interfaces between VEM and VMC in the Series RA were *vehicle-speed* and *gear-actual* from the VMC and *power_available* from the VEM. The Parallel RA replaces the *power_available* signal with *torque_split.* This is the key characteristic of the Parallel RA

and what differentiates it from the Series RA. As discussed above, many of the VSC functions are the same or similar, and in some cases reallocated. Also, the generic interfaces of *available*, *actual*, *capacity* and *command* are retained. Therefore even though this is a distinct RA, there is significant reusability. The key differences and similarities will be presented in detail in Section 4.3.3.

System Interaction Model

The interaction model follows the semantics described in Chapter 3. As per the Series RA the interaction model is describing an example scenario of responding to driver pedal demand, see Figure 4-5. The vertical sequence of the messages is key and indicates the information required before the next step can take place. The key differences to the Series RA is the source of *torque_available*, which is from the VEM in this RA, while it was the VMC in the Series RA. Also, in the Series RA, the VEM directly controls the PPS and the CPS, whereas in the Parallel RA they are directly controlled by the VMC, as a function of *torque_demand* and *split.*

Otherwise, this interaction model is very similar to the one presented in the last chapter, indicating confidence in some level of reusability between the RAs.

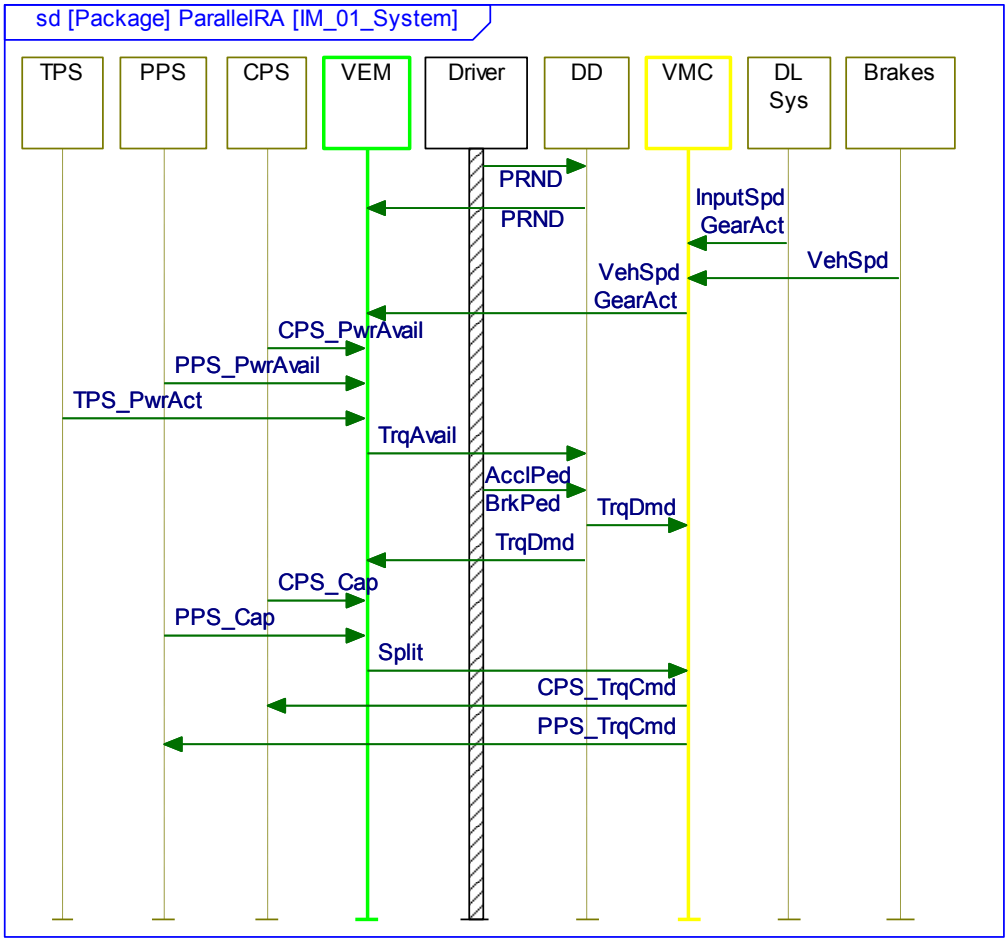

Figure 4-5: Parallel RA interaction model of HV powertrain system

4.3.3. Control Domain Models

Control Decomposition Model

Figure 4-6 shows a decomposition model of the Parallel RA control domain. As before the control architecure is divided between the Energy Management Domain and the motion control domain with DD being the exception. VEM and the TPS manager reside in the energy management domain as per the Series RA. The instance of the CPS encapsulated continuous transmission is shown. The VMC, BCU and TCU reside in the motion control domain, as does the the Driveline Manager and the local clutch controllers. The fundemental difference between the Series RA and the Parallel RA is that the PPS and CPS Managers reside in both domains. This potential overlap is managaged by the fact that the VEM handles the *available, actual* and *capacity* signals while the VMC broadcasts the *command* signal.

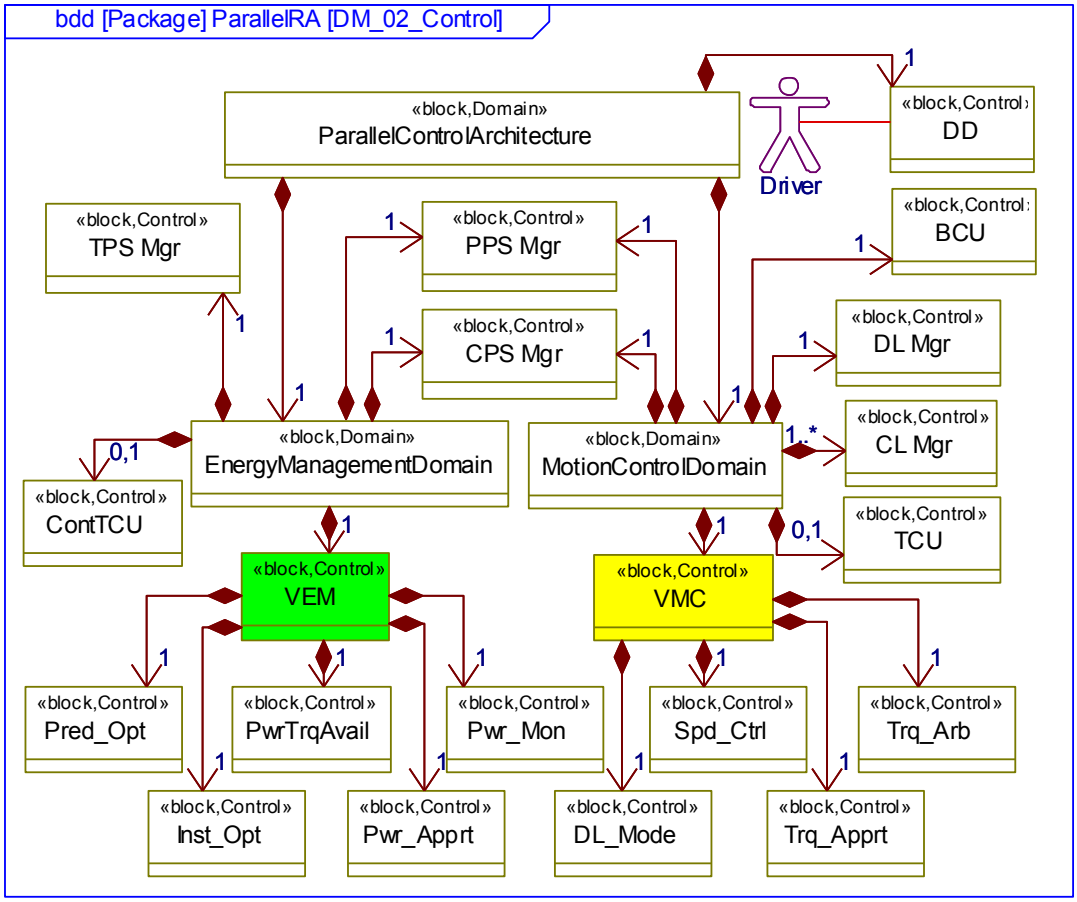

Figure 4-6: Parallel RA decomposition model of HV control domain

The sub-functions of the VEM remain the same or similar to those presented in the Series RA. However the *Power_Available* function block has become the *PowerTorque_Available* function block, determining *power_available* and *torque_available*. The *Power_Apportionment* block is reduced to only commanding the TPS. The sub-functions of the VEM on the other hand show significant change from the Series RA. The *Torque_Available* block has been transferred to the VEM. The *Torque_Arbitration* block remains the same. The *Torque_Apportionment* block

complexity is significantly increased relative to the *Torque_Apportionment* block in the Series RA. It now must control the *torque_command* signals to the PPS and the CPS in the context of their system dynamics. The *Driveline_Mode* and *Speed_Control* blocks are novel to the Parallel RA. The first triggers a driveline mode shift and the second controls the PPS and the CPS during this transition.

Control Strategy Models

Figure 4-7 and Figure 4-8 show strategy models of the energy management domain and the motion control domain respectively. The strategy models show a detailed view of the VEM and the VMC sub-functions and their interactions, internally and to the external sub-systems. Figure 4-7 is very similar to Figure 3-8, the equivalent strategy model for the Series RA. However the key difference is immediately apparent. The *Instantaneous_Optimisation* block broadcasts the *torque_split* to the VMC and not *Power_Apportionment*. This reduces the *Power_Apportionment* block to managing the power consumption of the TPS in limit demand events. The PPS *power_command* and the CPS *power_command* signals from *Power_Apportionment* no longer exist, however all other interfaces are retained. The new interface is the *PRND* from the DD to *PowerTorque_Available*, which replicates the interface between the DD and *Torque_Available* in the motion control domain of the Series RA in Figure 3-9.

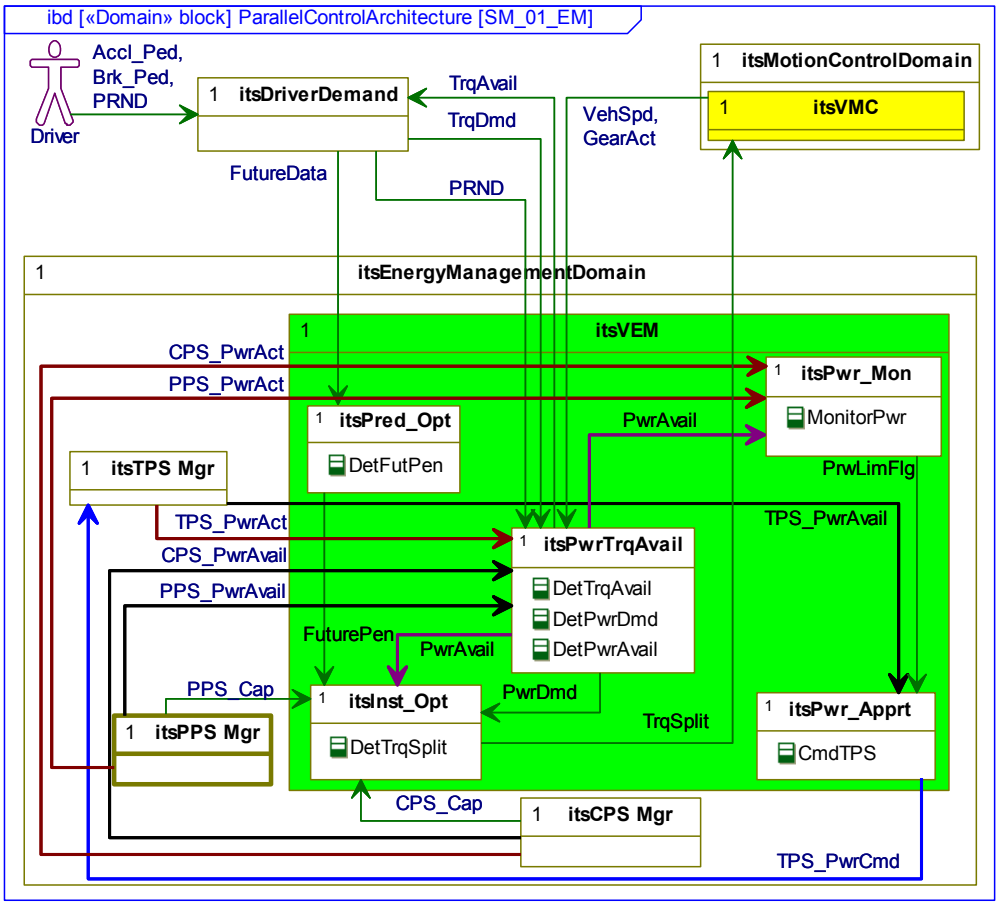

Figure 4-7: Parallel RA strategy model of energy management domain

The Parallel RA strategy model of the motion control domain (Figure 4-8), shows clear differences with the corresponding model from the Series RA, (Figure 3-9). Firstly, the *Torque_Available* block has been moved to the VEM. Secondly, the PPS and the CPS Managers are also within the motion control domain and receive *torque_command* from *Torque_Apportionment*. Finally two new functional blocks are introduced, *Speed_Control* and *Driveline_Mode*. Depending on *PRND*, *torque_demand* and *torque_split*. The *Driveline_Mode* block will determine the most appropriate mode to transition to. For example, a high demand scenario my require a transition from EV only mode to hybrid mode. During the transition some of the subsystem must be controlled by speed in order to match clutch plate speeds. This is the role of the *Speed_Control* block.

The *Torque_Apportionment* block is important in the context of Parallel HVs (and as will be discussed in Seciton 4.5 for compond HVs). This block determines two *torque_commands*, which are funcitons of total driver *torque_demand* and *split*. This implies that the block has an awareness of the relative dynamics of the PPS and the CPS. There exists many methods for torque management. The value of this RA is that this funcitonality will always be encapsulated within the *Torque_Apportionment* block, hence increasing its reusability. It is assumed that detailed local control remains the responsibility of the local controller which the VSC will govern, for example, current control for an electric machine. By inference this will guide the decision making for the capability of the communicaitons bus between the VSC and the local controllers. But the relationship between the two torque setpoints remains the responsibility of the VSC.

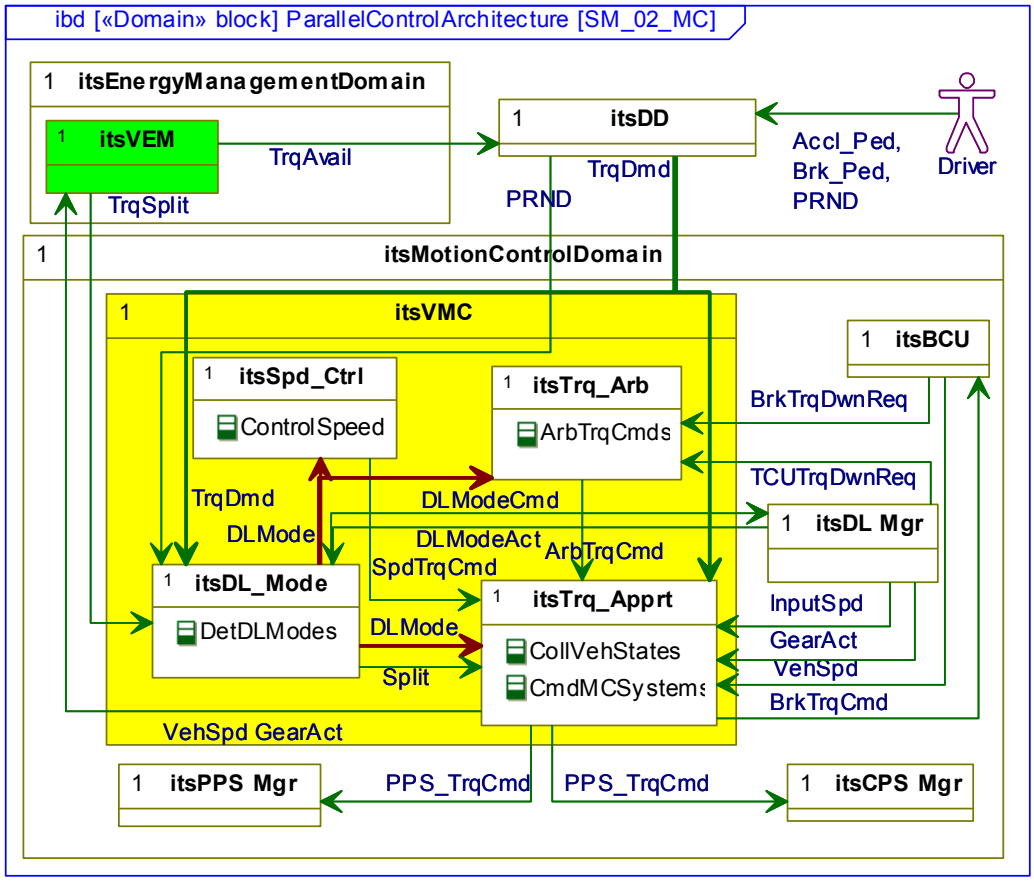

Figure 4-8: Parallel RA strategy model of motion control domain

While this section of the RA is different from the Series RA, many functions and interfaces are similar or the same. There will be reusability across the two RAs but given the *torque_split* versus *power_available* interface between VEM and VMC and the interfaces between VMC and the PPS and CPS sub-systems, it can be said that the two RAs are distinct.

Control Interaction Model

As per the last chapter, a control interaction model is included. In effect Figure 4-9 is an extension of Figure 4-5 with some of the key VEM and VMC functional blocks expanded to show the internal behaviour of the VSC. The internal VEM or VMC messages are highlighted in red. The example scenario presented in Figure 4-9 is a transition from torque control to speed control and back, for example when the CPS is required to deliver non zero power based on a change in *split*. This means initiating the CPS activity in order to transition from EV mode to hybrid mode.

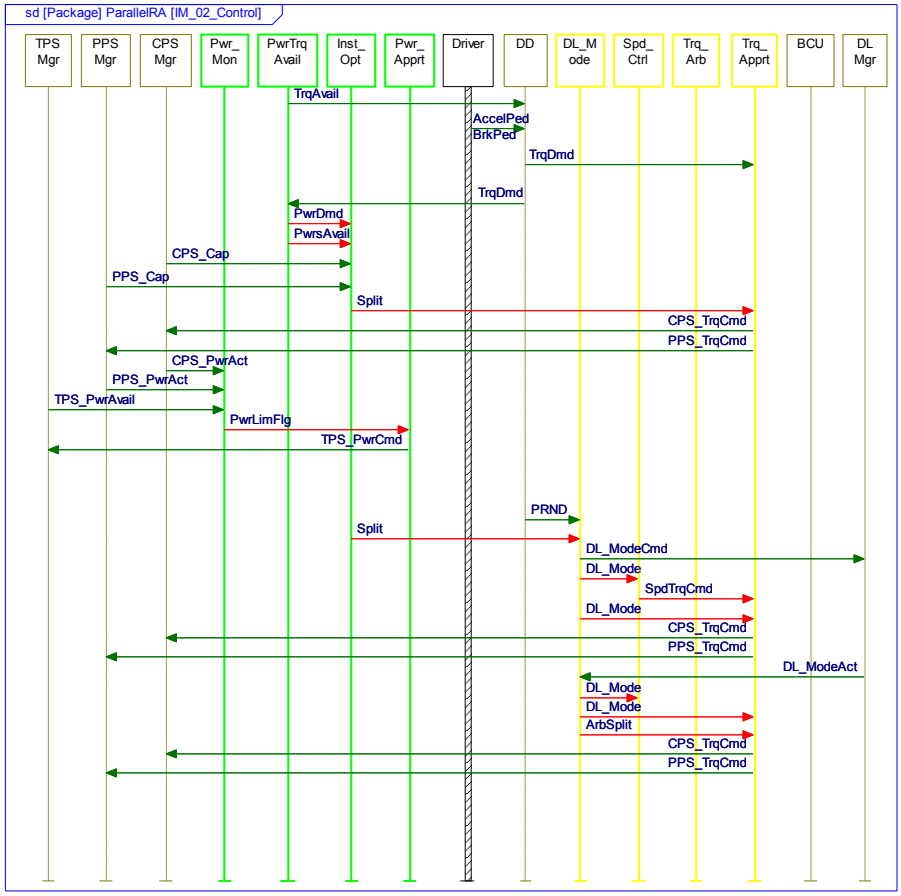

Figure 4-9: Parallel RA interaction model of control domain

The first half of the model shows normal EV torque control operation, with split set to zero. This sequence shows the situation in which a power limit is being reached, resulting in a TPS *power_command* to reduce load demand. If this is unsuccessful, the system alters the *split* to source increased power from the CPS. This triggers a sequence to start and engage the CPS. The *DL_Mode* block manages the mode change from EV to hybrid. Firstly the DriveLine system receives a *mode_command* which initiates any clutch activations necessary. Then the *DL_Mode* block instigates *Speed_Control* to match

speeds. As the speeds converge and the DrivLine reports engagement, the *DL_Mode* will re-establish torque control where the *Torque_Arbitraiton* reverts to command the PPC and the CPS based on *torque_demand* and *split*.

4.4. Critical review of RA in the context of compound HVs

This section assess the applicability of either RA to the compound HV configurations, and presents the Extended Parallel RA.

4.4.1. Energy Management versus Motion Control

Compound HVs are often referred to as series-parallel HVs, which can present characteristics of each depending on the situation. The Series and Parallel RAs are differentiated by the existence of a drive system. Series HVs have CPS and PPS systems whose sole responsibility is to deliver power required by the drive system in a ratio set out by the VEM. The Parallel RA CPS and PPS systems directly deliver the traction torque in a ratio defined by the VEM. The compound HVs presented in Section 2.4.2 contain systems which are directly involved in delivering tractive torque, as per the Parallel HVs. However there are also systems which are not directly involved in delivering torque.

Figure 2-16 presents the simplest form of compound HV, the power split which is based on the Toyota Prius and GM Volt. The epicyclic gear is represented by the 'torque bus' directly downstream of the ICE. The output, which leads to the second 'torque bus', is a conduit for the ICE tractive torque. The electrical machine is connected to this output by means of the second torque bus, this manifests as a shaft mounted 'Drive' machine. The torque from the ICE and the electric machine nearest the wheel directly propel the vehicle. The second electrical machine connecting the third output of the epicyclic to the DC bus acts like a 'Generator'. This draws power from the ICE to replenish the SOC of the battery.

In the context of compound HVs, it is not clear where the subsystem boundaries lie with respect to the CPS and the PPS. This must be answered before the subsystems can be allocated to the energy management or motion control domains, thereby assigning the compound HVs to either the Series or Parallel RAs.

All the previous definitions of the subsystems have been single input single output, i.e. fuel in, electrical power out or electrical energy in, mechanical power out. Each definition previously used either the DC or torque bus as the system boundaries. Therefore the fuel tank and ICE is a standalone system, as is the battery. The Generator machine and its INV, is a third system (Gen) and the Drive machine and its INV, is a fourth system (Drv). Clearly the ICE system and the Drv system fall within the motion control domain. As the Gen system is not fully decoupled from the output of the ICE it can be considered that it also should be part of the motion control domain.

The key differentials between the Series and Parallel RAs are the interface between VEM and VMC and the source of the command signals for the subsystems. The Series RA VEM broadcasts *power_available* to VMC whereas the Parallel RA VEM broadcasts *torque_split*. Based on this *torque_split* the VEM commands the key subsystems. In

compound HVs, there are three controllable subsystems. Therefore it should be controllable using two *toraue_split* values. The *torque_split* signals are determined by the *Instantaneous_Optimisaiton* functional block, within the VEM. Some or all the controllable subsystems will be controlled by the VMC as they can directly or indirectly impart torque to the vehicle chassis. Therefore it is argued that the Parallel RA is most appropriate to describe compound HVs. This section assesses the validity of this assertion.

4.4.2. Real world considerations

The real-world considerations from Chapter 3 regarding the TPS and braking system are carried over. As shown in Figure 2-17 and Figure 2-18, some compound HVs may have transmission and clutches, therefore the concept of the DriveLine subsystem is carried over from the Parallel RA presented in the last section. This includes the possibility of encapsulating a continuous transmission within the CPS.

4.5. The extended Parallel RA

This section presents an extension of the Parallel RA. It shows that the Parallel RA is applicable to the compound HV configurations. A high level abstraction of a generic compound HV system schematic is presented first. A decomposition model of the HV powertrain system shows the key subsystems. A context and causality model is used to show the key functional groups, their operation and interfaces. Then decomposition and strategy models focusing on the control architecture are presented.

4.5.1. System Schematic

Figure 4-10 presents the highest level abstraction of the compound HVs presented in Section 2.4.2. The key characteristics of the compound HV configuration are the multiple hybridisation bus points. Each of the variants presented in Section 2.4.2. contains two torque busses and one DC bus. In the powersplit variant the torque bus furthest from the wheel represents the epicyclic transmission. Non-powersplit variants may have traditional (discrete or continuous) transmissions which (in theory) may be located anywhere between the ICE and the wheel. Figure 4-10 represents this as transmission instances, a through c, which are mutually exclusive and all are absent in the powersplit variant.

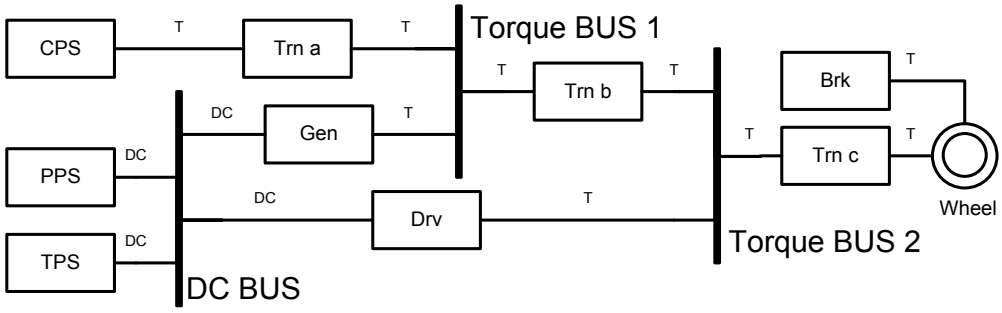

Figure 4-10: System schematic of a generic compound HV

Table 4-2 presents the full permutations of subsystems. The CPS in this configuration is exclusively an ICE (and by inference a fuel tank). The PPS in this case has been exclusively a battery. There is no reason why a capacitor set cannot be used, but there is

no record of this being implemented. The TPS and the brakes system are as per the Series and Parallel RAs. However, in this instance the Driveline subsystem as defined in the Parallel RA, is optional and would be omitted for power split variants.

The Drv system and Gen system, in all instances have manifested as a GenSet, defined earlier an electrical machine and an inverter. Depending on the compound HV variant, the Drv may be mounted to the output shaft of the epicyclic, the output shaft of the CPS (or transmission) or it may independently drive a separate axle, as in the through-the-road variant. The Gen can also be mounted to one of the outputs of the epicyclic, but is used to draw power from the CPS to the DC bus. It may also be used to deliver assist torque in high demand events. The Gen may also be directly mounted to the output shaft of the CPS as in the through-the-road variant. In the Turbo Generator variant, see Figure 2-18, the Gen is used to draw power from the exhaust air path of the CPS. In theory this decouples the Gen from the torque delivery function. However there is a link between power drawn from the turbocharger and the power (and hence torque) output at the crankshaft. This reasoning also applies to any exhaust gas thermal energy capture system, presented in Figure 2-19.

It should be noted that the drive system presented here (Drv) and the Drive system presented in the Series RA are not equivalent. The Drive system in the Series RA has the exclusive responsibility for delivering tractive torque. This is not the case for the Drv system in the compound configuration.

CPS	ICE (+CVT)	PPS	Battery	TPS	12V loads HVAC Power Dump PV Source
Drv	GenSet Epicyclic coupled to ICE OR ICE shaft mounted OR Independent drive of Axle 2)	Gen	GenSet (Epicyclic coupled to ICE OR ICE shaft mounted OR turbocharger mounted) Thermal energy capture system	Brk	Category A or Category B VSC = Master or Brk = Master
Drive Line	Discrete transmission Continuous trn Clutch1 Clutch n				

Table 4-2: Compound HV sub-system permutations

4.5.2. System Domain Models

System Decomposition Model

Figure 4-11 presents the decomposition model of the Extended Parallel RA for the Compound HVs. For simplicity this will be referred to as the Compound RA but it remains the hypothesis of this section that this is a subset or extension of the Parallel RA.

The Compound RA consists of the seven subsystems defined above and the VSC, two torque busses, the DC bus and the vehicle chassis. The VSC has the same decomposition as per the Series and Parallel RAs. The key subsystems are shown with their respective local controllers and the instance of an encapsulated continuous transmission within the CPS is shown. The DriveLine system is as per the Parallel RA but its multiplicity is zero or one, indicating that it is not required for some deployments of the RA, namely the powersplit variants. As before the driver is shown to interact with the DD and the BCU.

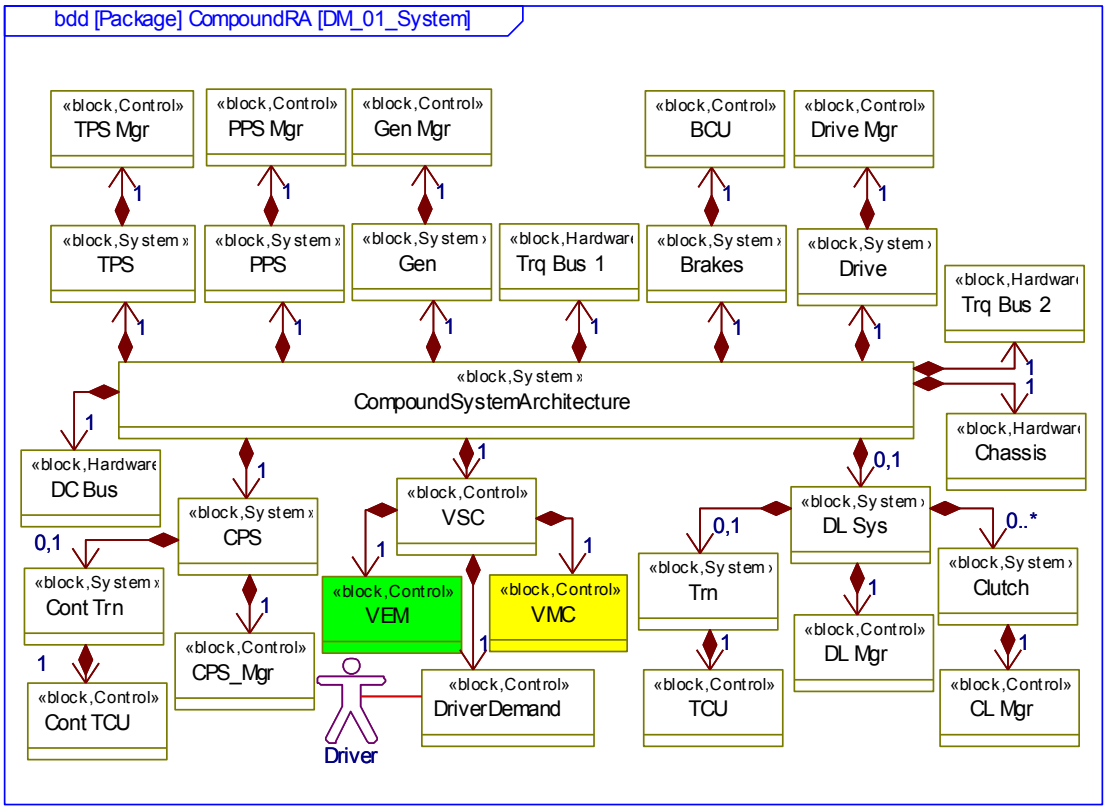

Figure 4-11: Compound RA decomposition model of HV powertrain system

System Context & Causality Model

Figure 4-12 presents the context and causality model of the Compound RA system architecture. As per the Series and Parallel RAs the VSC comprises the DD, the VEM and the VMC (shaded green and yellow respectively). The key funcitons of the VEM and the VMC are presented as are the key interfaces. The VEM determines *power_available* and *torque_available*, the first for internal fucntionality and the latter to be broadcast to the DD. The VEM also determines two *torque_split* values. This is broadcast to the VMC which distrtibutes the *torque_demand* to the controllable sub-systems in the proportion of the splits. The subsystems communicate their *actuals*, *availables*, and if appropriate, their *capacity* to the VEM. It is this configuraiton which defines the Compound RA as a subset of the Parallel RA.

The exception presented in Figure 4-12 is the PPS system. It is shown to communicate its *power_available*, *power_actual* and *capacity* to the VEM and the VEM is shown to generate the *pps_power_command* signal. This does not seem to fit within the Parallel RA

format. Looking back at Figure 2-16, Figure 2-17 and Figure 2-18 it can be seen that the PPS in all cases was a passive battery. If so the *pps_power_command* will be redundent and it will seem that the Parallel RA fits compound HV configurations better.

However a more robust explaination is required. In the context of the generic compound HV in Figure 4-10 the PPS is isolated from the torque domain by the DC bus and the powerflow in or out of the PPS is an arithmetic sum of the Drv power, Gen power and TPS power. Therfore if the PPS was controllable, its command can be calcualted by the VEM. Hence the PPS should be encapsulated within the VEM and the VMC should remain PPS independent. Otherwise the key interfaces are retained from the Parallel RA. The VMC commands the the CPS, the Drv and Gen systems. The Driveline system is exactly as per the Parallel RA, however this may be removed as per the deployment requirements. The Brakes system configuration is per the Parallel and Series RA configuration with the VSC acting as master and Brakes as slave.

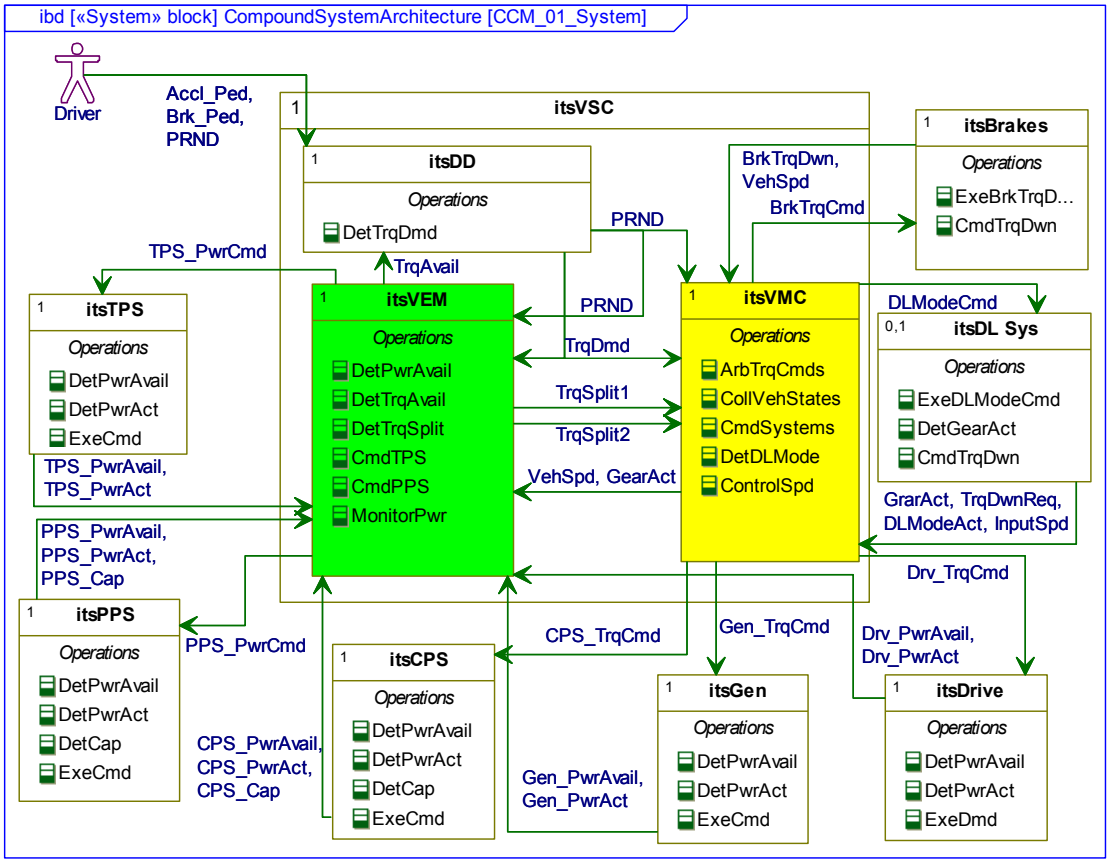

Figure 4-12: Compound RA context and causality model of HV powertrain system

System Interaction Model

As before a system interaction model is presented to incorporate the behaviour of the Compound RA. Figure 4-13 presents the interaction model which is a natural extension of Figure 4-5, namely the the original Parallel RA interaction model. In keeping with the definition of the Parallel RA some systems are under the shared control of the VEM and VMC, in this case the Drv, Gen and CPS systems. The example scenario presented is a simple demand following case. This model shows that the VEM contains the

power/torque available functionality, shown to output *torque_available*. The key VEM function, to determine split, can now be conducted based on demand and capacity, producing two split commands. Based on this, the VEM can command the CPS, the Gen and Drive systems.

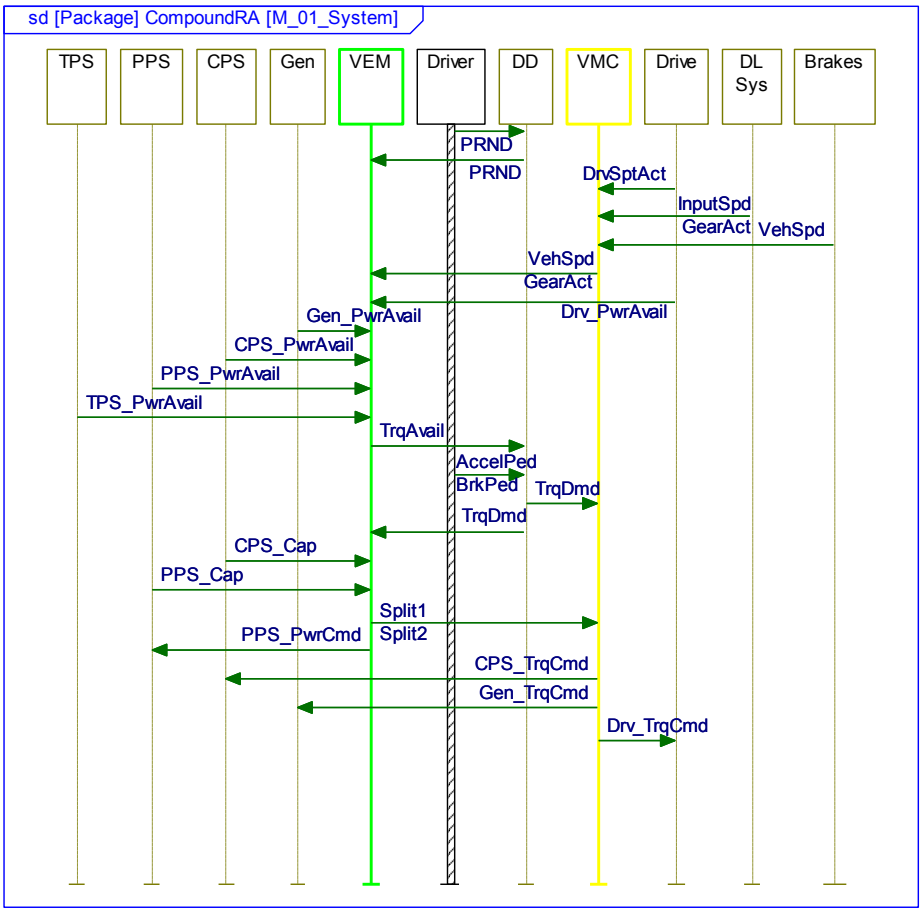

Figure 4-13: Compound RA interaction model of powertrain system

4.5.3. Control Domain Models

Control Decomposition Model

Figure 4-14 presents the control domain decomposition model of the Compound RA. The energy management and motion control domains are shows with DD being the outlier. The model is almost identical to that of the Parallel RA control domain model, in Figure 4-6. The key difference is the inclusion of the two new subsystem local controllers, Drive Manager, and Gen Manager. As per the CPS these subsystem reside in both the energy management and motion control domains. The PPS only resides in the energy management domain.

Other minor differences exist between the Parallel and Compound RAs regarding multiplicity. In the context of the powersplit variant, it is possible to have zero clutches. This extends to the *Speed_Control* and *DL_Mode* functional blocks within the VMC. In the absence of any clutches, speed synchronisation is not required nor is a function to manage the transition between clutch states.

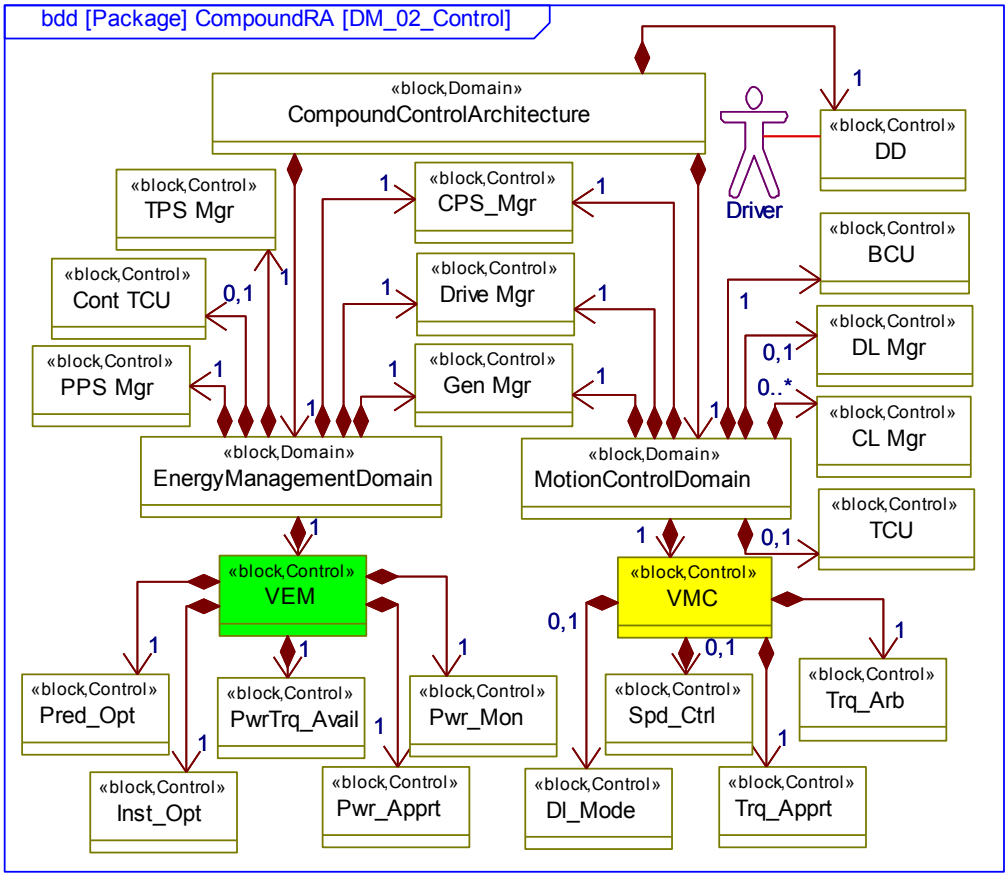

Figure 4-14: Compound RA decomposition model of HV control domain

Control Strategy Models

Figure 4-15 and Figure 4-16 present the Strategy Models of the Energy Management and Motion Control Domains respectively. Figure 4-15 shows that the internal structure of the VEM is identical to that of the Parallel RA in Figure 4-7. There are some internal interface differences. The *power_available*, *power_demand* and *split* signals are broadcast to *Power_Apportionment*. This enables *Power_Apportionment* to calculate PPS *power_command*. The *Power_Monitor* and *Power_Available* blocks must now include the *actuals* and *availables* of the two extra systems, Drv and Gen. Other than these differences the VEM internal structure and external interfaces are identical.

Figure 4-16 shows the similarity of the two RAs when compared to Figure 4-8. The Compound RA VMC now commands the CPS the Drv and the Gen, instead of the CPS and PPS only as in the Parallel RA. This is based on a *torque_demand* from the DD and *torque_split1* and *torque_split2* from the VEM. Other than the multiplicity of the *Speed_Control* and *DL_Mode* blocks, this VEM is structurally identical to that if the Parallel RA.

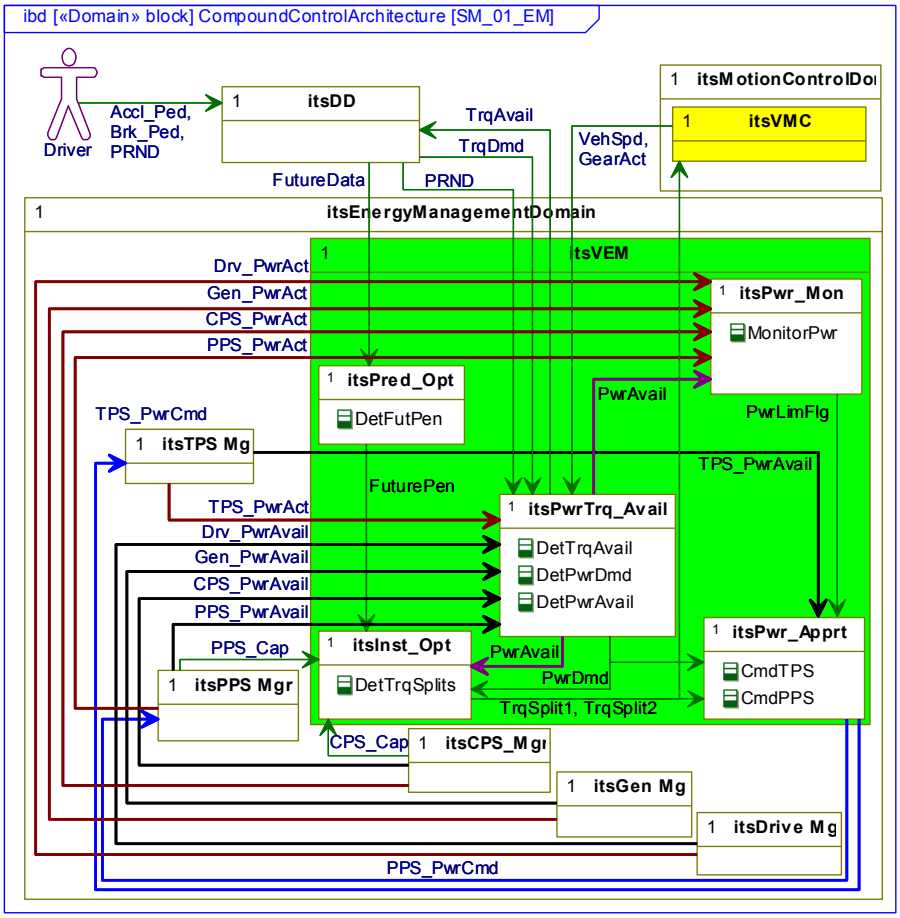

Figure 4-15: Compound RA strategy model of energy management domain

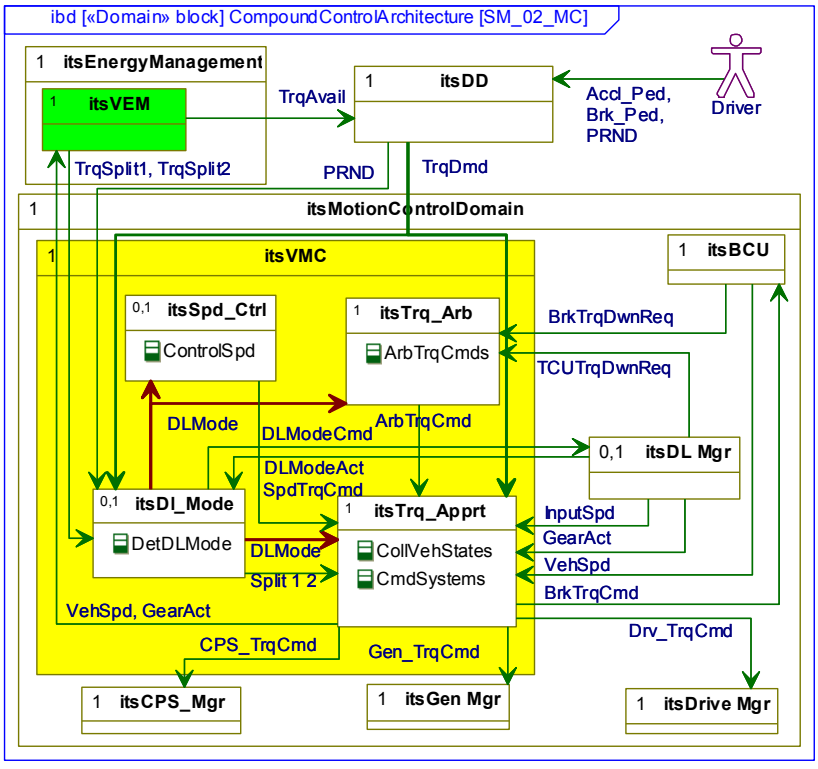

Figure 4-16: Compound RA strategy model of motion control domain

It would be expected to include a control interaction model but this would be an extension of
Figure 4-9 and Figure 4-13 and would present no new information and would be very hard to read in document format. This point will be discussed in the conclusion of this Thesis.

4.6. Summary

The goal of this chapter is to test two hypotheses. The first declares that the Series RA from Chapter 3 is applicable to other HV configurations, such as parallel HVs. Having shown this not to be true, a Parallel RA was developed which addressed Parallel HVs. The second hypothesis was that one of the two RAs are applicable to compound HVs. The Parallel RA was shown to be most applicable, and an Extended Parallel RA was defined, and termed the Compound RA. However it should be reinforced that the Compound RA is an extension of the Parallel RA and not a distinct RA in its own right.

The Series RA discussed in Chapter 3 is an abstraction of the minimum set of functions, interface and structure which describe the full set of Series HV variants. This includes the fuel cell variants analysed by Marco and Vaughan, and the ICE and flywheel variants outlined in Section 2.4.2. The key defining attribute of all these variants is a distinct and dedicated Drive System, which is isolated from the rest of the system by a DC bus. This means that the VEM described in Chapter 3 could no longer directly control the PPS and the CPS of Parallel HV configurations. This is because the PPS and the CPS in the parallel variants have a direct torque coupling to the vehicle chassis.

To remedy this, the *split* signal, which used to be an internal signal within the Series RA VEM, is now broadcast to the VMC. The VMC distributes the *torque_demand* between the PPS and the CPS as a function of this split. This is the defining characteristic of the Parallel RA.

The system schematic of the Compound HV configuration describes two new systems, Drv and Gen. The model shows a torque coupling between the CPS, Drv and Gen to the vehicle chassis. Therefore based on the definition set out in the Parallel RA, these systems should be directly controlled by the VMC, by distributing the *torque_demand* between them by a function of *split* information determined by the VEM. As there are three controllable systems, there is the need for two *split* signals. The PPS is treated much like it is in the Series RA, under the total control of the VEM, if it is not a passive system.

There exists a range of hybrid vehicle configurations and variants thereof. These have been distilled into the minimum set of three configurations series, parallel and compound, which can be described by two distinct RAs. This means that future HV variants can be developed expediently by defining which RA to use as a development template. In order to validate this statement one variant from each configuration will be analysed and simulated to show that the RAs are applicable in a realworld context. In order to do this a consistent choice of *split* determinations or EM function must be defined. The following chapter presents this definition and guidelines for ECMS deployment in the context of the range of configurations and variants of HVs.

5. Application of Equivalent Consumption Minimisation Strategy

This chapter presents an overview of the theory governing ECMS, and a step by step description of the implementation of ECMS onto the series, parallel and compound HV deployments.

5.1. Cost function control algorithm theory

As discussed in Chapter 2 there exist a variety of control strategies that can manage the power split (or torque split) of HVs. Of the strategies that can be run in real time, ECMS often achieves nearer optimum fuel consumption when compared to other real-time options [141, 152]. In the case of optimised heuristic or fuzzy methodologies, there can be a significant lack of adaptability when used over different drive cycles or different driving styles. ECMS has been demonstrated with adaptability, and in some cases predictability when utilised with GPS route gradient prediction algorithms [141, 148].

The purpose of the ECMS algorithm is to determine the appropriate split value (u), between main power sources of the HV, the PPS and the CPS. For a given driver demand power (P_d), the power delivered by the PPS (P_{PPS}) and the CPS (P_{CPS}) sums to exactly P_d, (1)[14]. The relative magnitude of P_{PPS} and P_{CPS} is determined by u, (2) & (3). The limits of u are described in equations (4) & (5).

$$P_d = P_{PPS} + P_{CPS} \tag{1}$$

$$P_{PPS} = (1-u)P_d \qquad \mathbb{B}[P_{PPS,min}, P_{PPS,max}] \tag{2}$$

$$P_{CPS} = uP_d, \qquad \mathbb{B}[P_{CPS,min}, P_{CPS,max}] \tag{3}$$

$$u_{min} = \max\left(1 - {P_{PPS,max}}/{P_d}, {P_{CPS,min}}/{P_d}\right) \tag{4}$$

$$u_{max} = \min\left(1 - {P_{PPS,min}}/{P_d}, {P_{CPS,max}}/{P_d}\right) \tag{5}$$

The limits of u depend on the relative powers of the PPS and CPS. Usually in literature, a split of zero indicates 100% of power being met by the PPS. The PPS is commonly a reversible energy store, such as a battery (via an electrical machine in the case of a parallel HV). A split of one indicates the CPS is matching the demand power. A split greater than one indicates the CPS is delivering excess power which is being captured by the PPS.

To determine the most appropriate value for u, the control system calculates the equivalent fuel consumption (J) (7) comprising the fuel flow through the CPS ($\dot{m}_{f\_CPS}$) in addition to a weighted equivalent fuel flow through the PPS ($\dot{m}_{f\_PPS}$), (6). The

[14]Assumes P_{TPS} is zero

appropriate value of u is determined by the minimum value of the cost function J (7), bounded by the constraints defined in (2), (3), (4) & (5).

$$J = \dot{m}_{f\_equi} = \dot{m}_{f\_CPS} + f_{pen} \cdot \dot{m}_{f\_PPS} \tag{6}$$

$$\min_{P_{PPS}(t),P_{CPS}(t)} \sum_{u=min}^{u=max} J(u) \tag{7}$$

The $\dot{m}_{f\_PPS}$ weighting (f_{pen}) is an essential feature of the ECMS approach. The f_{pen} is a penalty function which weights the PPS equivalent fuel consumption as a function of the PPS capacity [84], see Figure 5-1.

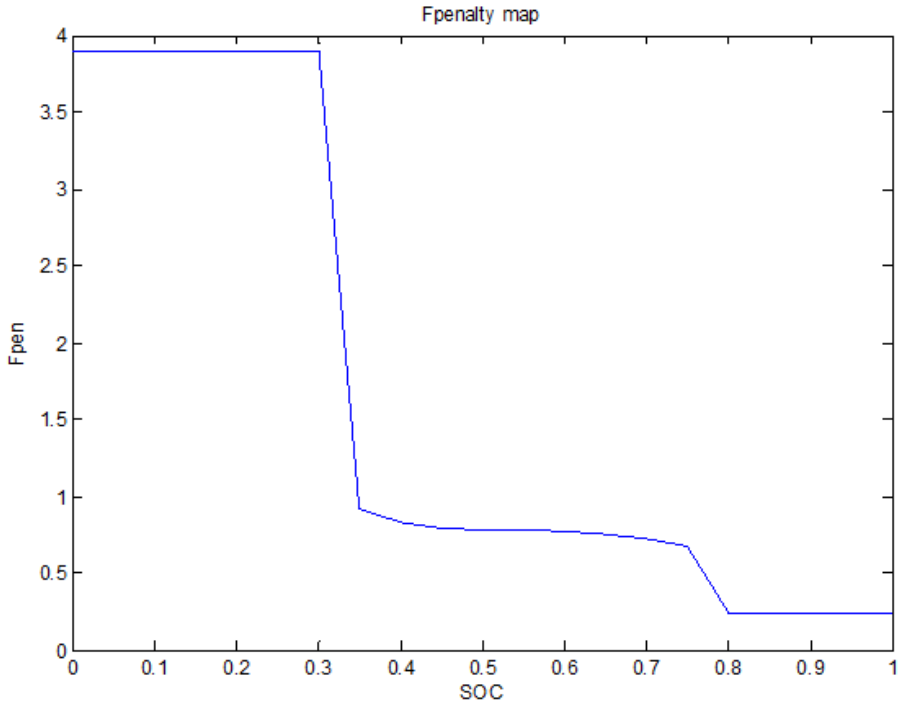

Figure 5-1: Example of ECMS penalty function map for battery HV, PPS SOC [146, 190]

Within this study, the penalty function is a calibratable LUT. Section 7.4.2 presents a detailed analysis of the implications of the shape of LUT. The purpose of this map is to alter the equivalent cost of PPS energy to ensure charge sustainability. As stated by Yassine [84], without this penalty function an ECMS algorithm will always favour the reversible storage over the fuel source i.e. exclusive EV operation uses no fuel. If the PPS capacity[15] is high, the cost of using PPS energy should be relatively low, i.e. the penalty function should be low. As SOC decreases, there should come a point when electrical energy becomes prohibitively expensive, i.e. the penalty function should increase dramatically, as shown in Figure 5-1.

[15] Referred to as SOC in the context of this chapter.

The equivalent fuel cost of electrical energy, $\dot{m}_{f\_PPS}$, is measured as the fuel cost of replacing the PPS energy consumed with the CPS incorporating the efficiencies within the CPS and PPS (electric machines, power inverters). Firstly, $\dot{m}_{f\_CPS}$, is determined in g/kWh (or g/s) and in implementation can be read from a pre-calibrated LUT (8). This is a deficiency, as the future cost of replacing used PPS energy is determined by the present running conditions of the CPS. However, as discussed in Chapter 2, this deficiency can be circumvented through the use of future drive cycle knowledge or the statistical probability of future conditions. However, these approaches are deemed to be impossible without integrated GPS technology and contain statistical errors which result in no significant improvement over the method presented here [148, 149, 152].

To calculate the real time consumption required to replace the PPS energy, the equivalent fuel flow for the PPS is determined as per equation (9), which normally alters as a function of P_{PPS} sign (batteries have different charge and discharge efficiencies). The efficiency chain components are usually implemented as calibratable LUTs as indicated in equations (10) & (11).

$$\dot{m}_{f\_CPS} = f(CPS\ parmetrised\ data) \tag{8}$$

$$\dot{m}_{f\_PPS} = \begin{cases} \dfrac{P_{PPS}}{Cp_{fuel} \cdot Eff_{CPS} \cdot Eff_{PPS}} & \text{if } P_{PPS} \geq 0 \\ \dfrac{P_{PPS} \cdot Eff_{PPS}}{Cp_{fuel} \cdot Eff_{CPS}} & \text{if } P_{PPS} < 0 \end{cases} \tag{9}$$

$$Eff_{CPS} = f(CPS\ parmetrised\ data) \tag{10}$$

$$Eff_{PPS} = f(PPS\ parmetrised\ data) \tag{11}$$

5.2. Deployment of ECMS into the Series HV

This section presents how it is implemented in a real world deployment of a series HV. As discussed in Section 1.4 the first case study was conducted as part of the LCVTP and was based on an ICE and battery based Series HV as described in Figure 3-3. This section presents a step by step guide of the implementation of the ECMS in the Series HV deployment. This deployment was conducted in connection with the case study presented in Chapter 6.

5.2.1. Algorithm overview

First, the steps of the algorithm will be described and secondly some detailed discussion will be presented on the key steps of the algorithm. Figure 5-2 presents a flow diagram of the ECMS algorithm, and Table 5-1 presents its interfaces. The goal of the ECMS is to define a split (or ratio) between the two main power sources.

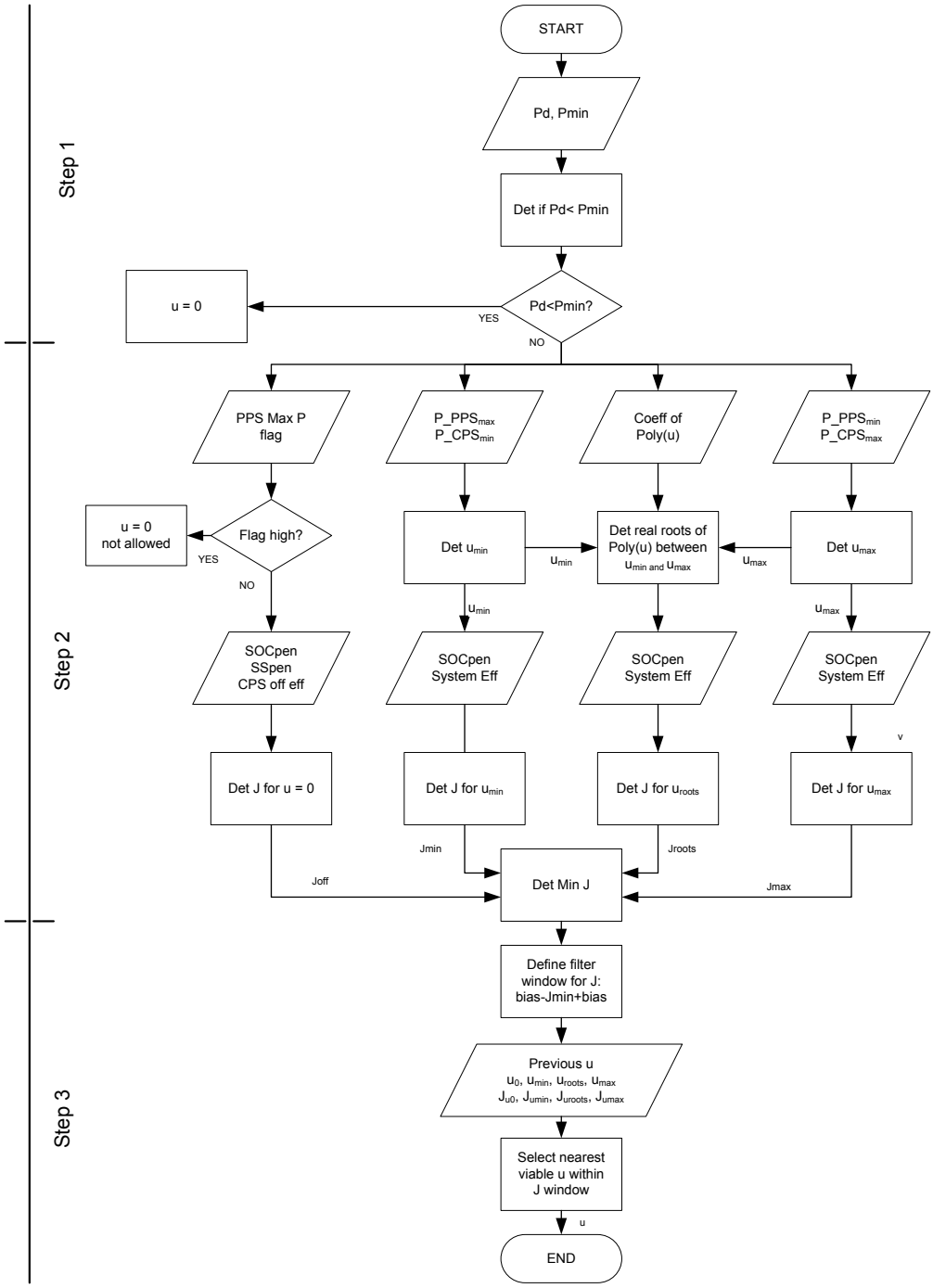

Figure 5-2: ECMS algorithm as deployed in the Series HV

In the first step P_d is compared to a pre-set minimum power (P_{min}). P_{min} is a function of the minimum power capability of the CPS. This function ensures only EV operation for very low power demands[16]. If P_d is less than P_{min} then the split value is forced to zero. Otherwise the algorithm continues.

[16] As discussed in Chapter 3, this may be overridden by the *Power_Apportionment* block.

The second step determines the minimum equivalent fuel consumption (J) for a set of allowed split values (u). Therefore the second step is divided into a set of parallel subroutines. The first subroutine determines J for u equals zero (u_0), if the PPS is operating below a predefined maximum power level (90% of maximum in the case study in Chapter 6). This subroutine uses the inputs of PPS maximum power flag to determine if u_0 is allowed. If so, it uses the PPS SOC penalty, a Start_Stop penalty and an assumed value of future CPS efficiency. The CPS Start_Stop penalty is added to the J_{off}[17] term in order to prevent frequent stop starting. These terms are used to calculate J using Equation (6). A limitation of the ECMS approach is the need to use an assumed CPS operating point to determine the equivalent consumption for EV operation. Several options are presented in the literature and discussed in Section 2.3.2. For the purposes of this Case Study, the minimum CPS power of 15kW was used as defined by the CPS supplier, Lotus [167].

The second and fourth subroutines determine J for u_{min} and u_{max} respectively. The terms u_{min} and u_{max} are determined as per equations (4) & (5) and shown graphically in Figure 5-3. The methodology for determining u_{min} and u_{max} will be discussed later in this section. J_{min} and J_{max} are calculated based on u_{min} and u_{max}, the PPS SOC penalty and the system efficiencies,[18] as per Equation (6).

The third subroutine determines the J for any local minima of u between u_{min} and u_{max}. (shown in Figure 5-2 as J_{roots}). This routine uses a polynomial equation which represents the engine power to efficiency map for the Lotus engine as described by Turner [167]. This map and set of polynomial fits are shown in Figure 5-4. This map will be discussed in more detail later in this section. Any real roots of the polynomial between u_{min} and u_{max} are used to calculate a corresponding J using the PPS SOC penalty function and the system efficiencies using Equation (6). The second step ends by selecting the minimum J and the corresponding u as per Equation (7). Figure 5-5 presents the minimum J options across the range of u, and will be discussed in detail later in this section.

Inputs	Outputs
1. Power demand 2. PPS maximum power flag 3. CPS maximum power 4. CPS minimum power 5. PPS maximum charge power 6. PPS maximum discharge power 7. Electric equivalent fuel consumption penalty 8. PPS charge/discharge efficiency 9. StartStopPenalty 10. Previous split	1. Power split (u)

Table 5-1: Series ECMS interfaces

[17] J_{off} refers to the assumed J to be used when in EV mode.

[18] It is possible for the ECMS to receive system efficiencies as live signals or as calibratable maps

The third and final step creates hysteresis around u preventing chattering. It is included to prevent oscillations between remote minima. In effect a filter is created which minimises the rate of change of u, based on a window of viable J values around J_{min}. The code is aimed to find the ideal power split that delivers a low equivalent consumption, taking into account of real-time system limits and requirements. Normally ideal u gives the lowest J. However, the continuity of u becomes more important when there is not so much difference in equivalent consumption, hence the use of this hysteresis.

5.2.2. Split boundary determination.

To define a continuous u_{max}, u_{min} the system assesses the feasible splits for a given demand as per Equations (4) & (5). Figure 5-3 presents the split limits for an CPS with maximum and minimum limits of 15kW and 35kW respectively [167] and a PPS with a maximum power of 75kW and a minimum of -25kW, i.e. charging. For a given demand the u range is constrained by two of the four boundaries. In the case study in Chapter 6 CPS is the limiting factor for both u_{min} and u_{max}. At high power demands the maximum PPS power overrides minimum CPS power for u_{min}. At low power demand (high split), the minimum PPS power line becomes the constraint after it crosses the maximum CPS line.

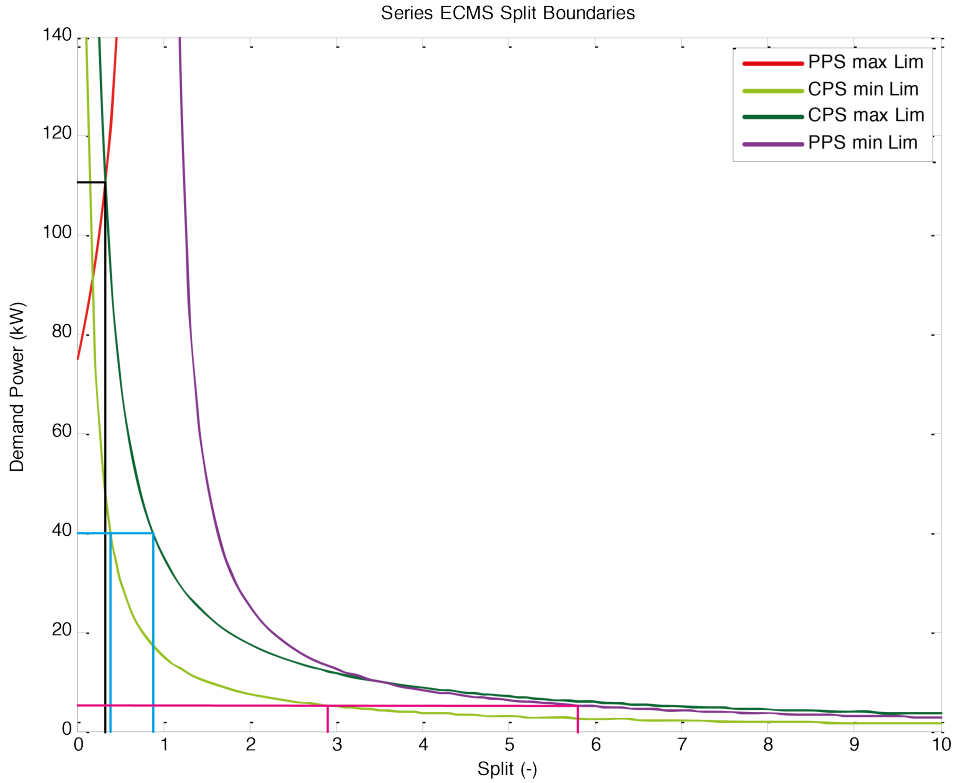

Figure 5-3: Series split boundary limits showing u limits for 110kW, 40kW and 5.3kW

Three P_d scenarios are presented in Figure 5-3, at 110kW (black), 40kW (blue) and 5kW (pink). These scenarios are shown as horizontal lines from the power axis and vertical drop lines when they cross the power limit lines. The 110kW line represents maximum power, and this is indicated by the intersection of the PPS maximum limit (u_{min}) and the

CPS maximum limit (u_{max}). In this case there is only one viable value for u, 0.32. Using Equations (4) & (5) it can be shown that a demand of 110kW, and a split of 0.32 results in maximum CPS and PPS power being demanded.

The 40kW scenario represents a reasonably high demand such as motorway cruise speed cruise (for the vehicle analysed in Chapter 6). In this case, the demanded power is higher than CPS maximum, therefore the PPS will always be delivering some power and u will be less than one. This calls into question the initial sizing of the CPS, however this is outside the scope if this research and, more importantly, creates no difficulty for ECMS or the architecture. At the 40kW power line, the limitations are CPS minimum and maximum (u_{min} and u_{max} respectively). Equations (4) & (5) generate a u_{min} of 0.4 and a u_{max} of 0.9. The algorithm will therefore determine J for both these values of u, and for any local minima of the polynomial between these two values.

The final scenario is a relatively low power demand, 5.3kW. The Equations (4) & (5) give values of u_{min} and u_{max} of 2.8 and 5.7 respectively. Interestingly the u_{min} min value will result in a CPS power of 15kW, which is the minimum power available. However u_{max} results in a CPS power of 30.3kW which is less than CPS maximum power. Closely examining Figure 5-3 shows that the limiting power line at this point is the PPS minimum power limit. The minimum PPS power is -25k (charging), therefore running the CPS at 30.3kW at a demand of 5.3kW results in maximum PPS charge power. ECMS will still evaluate J for these two split values and any local minima of the polynomial between these two values as per Equation (6). Hence ECMS does not need a mode change function to change from CPS power assist to charge while in drive mode.

5.2.3. BSFC line fitting

The polynomial in Figure 5-4 is a fitted curve of the best efficiency line of the Lotus Range Extender [167]. Due to the twin efficiency peaks at 27kW and 34kW the 6th order polynomial was required. Fourth and fifth order polynomials (also shown) give norm of residual values many times higher than the sixth order polynomial fit [19].

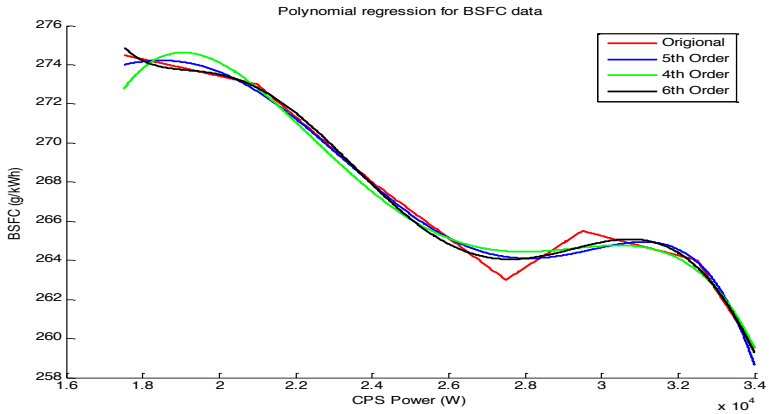

Figure 5-4: Polynomial fit of best consumption line of the Lotus Range Extender [167]

[19] Norms of residual: 4th order = 1.5, 5th order = 1.1, 6th order = 1.6e-09

Different engines may be solved by a lower order polynomial as they normally have a single local minimum unlike the data from the Lotus engine. This particular engine was originally optimised for 27kW, for the purposes of a single power level CPS. However customer acceptance required that the CPS is free to move up and down its speed range. Therefore this BSFC line is unusual and most engines would have a smoother line [191]. The implication if this is that ECMS would be simpler to implement for different engines.

5.2.4. Scope of minimum consumption values

ECMS solves the polynomial between the bounds of u_{min} and u_{max}. A real root indicates a local minimum for equivalent consumption J. ECMS must also solve for u_{min} and u_{max} on the assumption that no real minimum exists for the polynomial between these bounds. As mentioned earlier the scenario for u_0 must also be evaluated.

The set of local minima available is presented in Figure 5-5 a) u_{root}, b) u_{max}, c) u_{min}, d) u_0 as read from left to right. Figure 5-5 a) shows one real polynomial root which is the minimum of four options highlighted in red. It is possible for more than one real root to exist between u_{max} and u_{min}. In this case each real root must be evaluated for J and stored for later minimisation. Figure 5-5 b) and c) show the u_{max} and u_{min} being selected as the minimum j. Figure 5-5 c) u_0, indicates that EV operation is most beneficial.

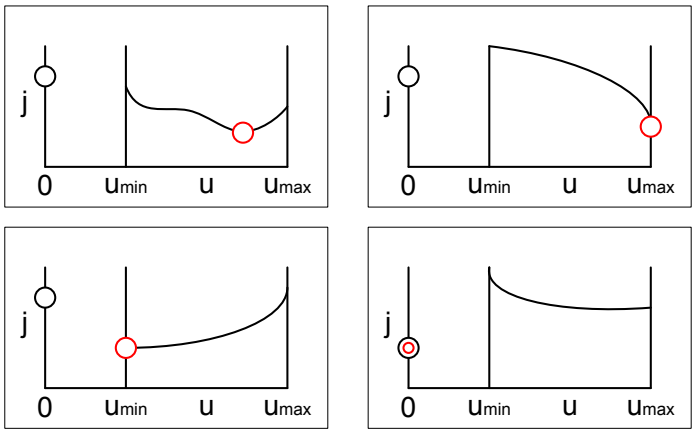

Figure 5-5: Set of local minima for equivalent consumption: a) u_{root}, b) u_{max}, c) u_{min}, d) u_0

5.2.5. Summary

This section has presented a step by step description of the key points for implementing ECMS in a Series HV. With regards to the Series RA, this function resides within the *Instantaneous_Optimisation* block. The key considerations are the determination of the split boundary, deriving a polynomial of engine BSFC and the idea of multiple minima including the special condition of CPS off, or EV mode.

The minimisation of a polynomial function of efficiency presented here is novel in the context published ECMS approaches discussed in Section 2.3.2. The published descriptions of ECMS deployments discuss evaluating J for a predefined set of values for u between the maximum and minimum values for u. This presents two deficiencies. Firstly, the resultant u (which generated the minimum J) will be broadcast stepwise as per the predefined steps of u. It could be possible to filter this signal. However this may

present a problem if a CPS off event is required, such as a braking event. Secondly, employing the polynomial function results in a continuous u signal.

Another consideration not presented here is the dynamic limitations of the CPS. If maximum CPS power is assumed to be reachable within the next time step then it may be possible to deviate from ideal split during transients. However the methodology to mitigate against this issue resides within the *Power_Available* and *Torque_Available* functional blocks. For a given CPS power a maximum CPS power within a given timeframe is calibratable and communicated to *Power_Available*. Based on the dynamic *power_available*, the *torque_available* for DD will be constrained. Therefore the *power_demand* signal into ECMS is correspondingly constrained to ensure CPS dynamics and PPS power limits are respected. This may occur outside of the ECMS but is an essential point to be aware of when developing this energy management functionality.

Section 6.2 presents simulation, and experimentation results of this ECMS being deployed into the Series HV selected as part of LCVTP. The next section presents how to deploy ECMS in a parallel HV, which will be utilised in the case study in Chapter 7.

5.3. Deployment of ECMS into the Parallel HV

As per the series application, this section takes the theory from Section 5.1 and presents an example of how it is implemented in a real world deployment of a parallel HV. The second case study is also based on a vehicle analysed as part of the LCVTP project, the results of which are presented in Section 7.2. For the purposes of this deployment the CPS is an ICE and the PPS comprises of a battery, inverter and electrical machine. The electrical machine is mounted to the output shaft of the ICE hence it is a pre-transmission Parallel HV as indicated by Figure 4-1.

5.3.1. Algorithm overview

The process for determining best split for a parallel application is very similar to the series deployment. However the key difference is that the speed of the engine is coupled to the speed of the vehicle thereby losing one degree of freedom. Therefore it is impossible to maintain the engine on the best BSFC line. This means that the band of J between the minimum and maximum u must be a function of engine speed. In principle this process flow presented in Figure 5-2 could be applied. However the polynomial function of power against consumption would be insufficient in the context of the coupled engine and vehicle speed. Therefore that step of the third subroutine is replaced with a polynomial equation of a surface which is a function of torque and speed against consumption.

This polynomial function of a surface was attempted but in the simulation environment at hand (Matlab/Simulink) it resulted in long simulation times. This does not preclude the implementation of the polynomial surface method in a realtime environment. Therefore a traditional stepwise implementation of ECMS was employed, to segment the window between u_{min} and u_{max} and determine J for each u before determining the minimum J. This will be discussed in more detail in Section 5.3.3. Figure 5-6 presents the altered algorithm for the parallel HV deployment.

Figure 5-6: ECMS algorithm as deployed in the Parallel HV

Table 5-2 presents the key interfaces for the parallel implementation of the ECMS. The key difference between these interfaces and those of the Series ECMS are the input torque bus shaft and output torque split. As mentioned the CPS speed is coupled to the vehicle speed, therefore the consumption map must be in terms of torque and speed. Therefore a continuous speed signal must be incorporated into the ECMS.

Inputs	Outputs
1. Power demand 2. PPS maximum power flag 3. CPS maximum power 4. CPS minimum power 5. PPS maximum power 6. PPS minimum power 7. Torque bus/shaft speed 8. PPS efficiency 9. Electric equivalent fuel consumption penalty 10. StartStopPenalty 11. Previous split	1. Torque split 'u'

Table 5-2: Parallel ECMS interfaces

The torque split set-point can be used in the case of a pre-transmission parallel HV as the CPS and PPS electric machine are mounted directly together. Therefore both speeds are identical. If a single ratio exists between the electric machine and the shaft, then the PPS torque must be defined at the mounting at the CPS shaft and not the output of the PPS electric machine. In this case the torque split is directly proportional to an equivalent power split.

The first step is exactly as per the series algorithm. The system demanding a power higher than a predefined minimum before the CPS can be started. The second step still comprises a set of subroutines for determining an appropriate set of u to determine J. The first subroutine is as per the series algorithm. The split value u_0 is still required to compare hybrid u values with EV operation equivalent consumption. The parallel ECMS presents the same problem regarding the assumption of a future CPS operating point to determine CPS off consumption. A mean value for CPS efficiency is used in this case.

Initially, the second and fourth subroutines are identical to the series algorithm, the determination of u_{min} and u_{max}. This step of the subroutines is determined as per Equations (4) & (5). At this point the second and fourth subroutines merge into an equivalent of the third subroutine. In this step, the surface is cut along the fixed speed line and the resulting line is solved for a predefined set of u values. This set of u values is determined by segmenting the band between u_{min} and u_{max}. This will be discussed in Section 5.3.3.

Therefore the end of the second step remains the same, a set of equivalent consumption values are minimised to define the corresponding split set-point. The third step is exactly as per the series algorithm.

5.3.2. Split boundary determination

As per the Series deployment, the u_{min} and u_{max} terms are calculated using Equations (4) & (5). However, the P_{PPS_max}, P_{PPS_min} and P_{CPS_max} terms are functions of speed which is coupled to the road speed. Figure 5-7 presents three of the four boundary conditions for the parallel system, (P_{CPS_min} is assumed to be zero). The red surface is P_{PPS_max} and the green surface is P_{PPS_min}. both are limited to 35kW for the purposes of the vehicle

analysed as in Section 7.2. The blended surface is P_{CPS_max}, (corresponds to ICE power) reaches 120kW at 2000rpm. Comparing this to Figure 5-3 it can be seen that it contains an extra dimension, engine speed. Given a real-time value of speed the surfaces can be converted to lines as per Figure 5-3 and u_{min} and u_{max} determined accordingly. The units on the z axis of Figure 5-7 should be noted carefully. The P_{CPS_max} surface indicates a demand power of up to 1.5MW. This is a mathematical representation of the leveraging of demand power using Equation (3), as u decreases, P_d must increase to give P_{CPS_max}. This region is excluded from analysis by the P_{PPS_max} boundary, shown as a red surface.

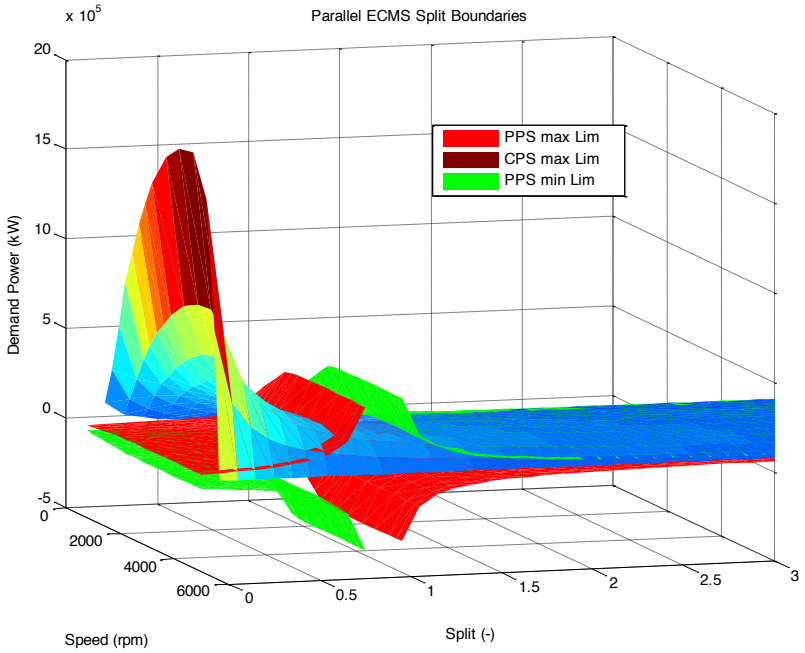

Figure 5-7: Parallel ECMS split boundary surfaces with an extra speed dimension

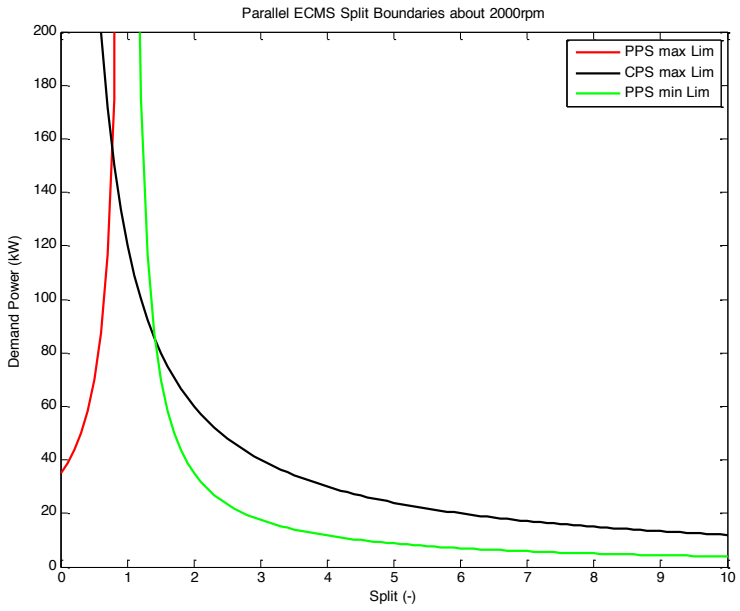

Figure 5-8: Parallel ECMS split boundaries about 2000rpm

Figure 5-8 presents the resultant boundary lines derived from Figure 5-7 along the 2000rpm speed line. The black line represents the blended surface from Figure 5-7. This line crosses 120kW at u equals one, indicating the CPS is exclusively following the driver demand for power. The P_{PPS_max} line (shown in red and corresponding to the P_{Batt_max} line from Figure 5-3) shows that at u equals zero, the maximum demand power available is 35kW. As P_{CPS_min} is always zero, u_{min} is always bounded by P_{PPS_max}, whereas u_{max} is bounded by either P_{CPS_max}, or P_{PPS_min} as per Equation (5).

5.3.3. BSFC surface fitting

The third subroutine of the series algorithm solved for the roots of a polynomial expression of consumption against power. This was possible as the series CPS was not coupled to the vehicle speed. This is not the case for the Parallel HV deployment. The power term must be broken into its speed and torque terms, resulting in a 2D map against consumption.

Figure 5-9 presents a surface of the fuel flow data points in light blue (grams per second) against speed and torque. Figure 5-9 also presents a 6th order surface expression of the same data in dark blue. Fuel flow was chosen as it can be represented as a fairly smooth surface requiring a lower order equation, whereas a contour of BSFC (a more complex surface) would require a much higher order equation to express, which resulted in long simulations times on the desk PC based simulation environment.

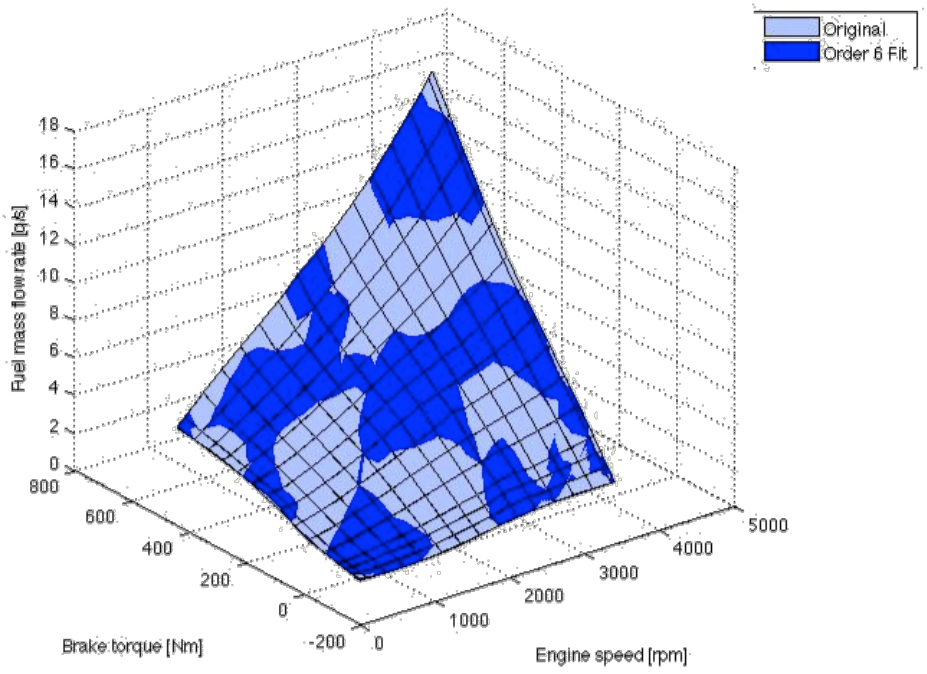

Figure 5-9: surface fit of ICE fuel map

Therefore, as the ECMS is being used as a tool to test the RAs presented in Chapters 3 & 4, a compromise has been deployed. For a fixed speed, the surface equation is solved for a defined array of u between u_{max} and u_{min}. In this deployment, a vector of 20 (points from u_{min} to u_{max} inclusive) is selected for every time-step to find 20 values for J. A 21st

point is added reflecting the ICE off state and the minimum of the 21 J values is determined. From that point on the ECMS behaves as per the series deployment.

The simulation results for this deployment are presented in Section 7.2. For reference previous analysis on a post-transmission parallel HV with a CVT is presented in Section 7.4. This configuration allows the ICE to be decoupled from the vehicle speed. Therefore the same type equation of power versus BSFC deployed in the series ECMS is possible instead of the surface expression.

5.4. Deployment of ECMS onto a Compound HV

This section presents the application of ECMS to a compound HV. Both series and parallel HVs have two power systems from which the drive torque must be delivered, which require one split signal. In a compound HV there are four power sub-systems, the CPS, the PPS (commonly an ICE and a battery respectively), the Gen and the Drv. Only three of these, the ICE, Gen and Drv, are mechanically connected to the drive wheels. Hence for ECMS purposes, two split signals are required. Therefore the theory presented in Section 5.1 must be adapted. This adaption will be discussed in the next section. Subsequently the algorithm overview and the splits' boundaries are discussed.

5.4.1. Adaption of theory

In Section 5.1, equations (1) to (3) represent the key relationships between the demand, CPS and PPS powers. Figure 5-10 presents a simplified version of the generic compound HV previously shown in Figure 5-10. In this case the transmission placeholders, the brakes system and the TPS have been removed for clarity. What remains is a clear representation of the demand power and the required CPS, Gen and Drv powers required to deliver it. The PPS power is a direct summation of the Gen and Drv powers as transmitted through the DC bus.

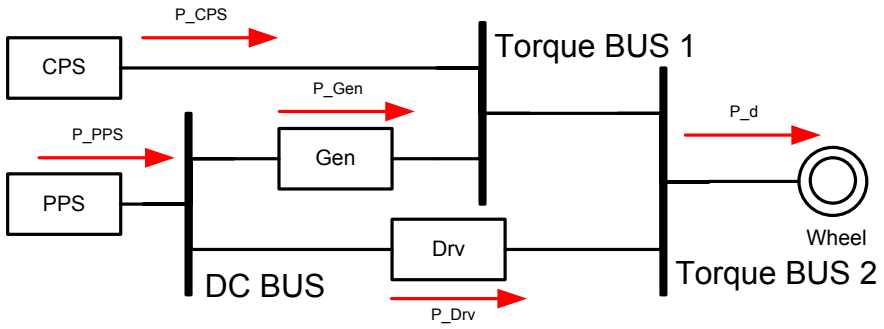

Figure 5-10: Generic compound HV showing key power flows

The aim of this adaption is to determine an allocation of two splits which can relate all powers to the demand powers. Cipollone and Sciarretta allocate the two splits to the Gen and Drv power paths, and determine the CPS and PPS powers accordingly [145]. This allocation will be used here, but others are possible. Equation (12) declares that the total demand power is a direct summation of the CPS, Gen and Drv powers. Equations (13) and (14) show how the Gen and Drv powers are related to the demand power by split 1 (u_1) and split 2 (u_2) respectively. Equation (15) shows that the CPS power is determined by the demand power minus the Gen and Drv powers. CPS power is shown

as a function of u_1 and u_2. The PPS power is also a function of demand power, u_1 and u_2 as shown in Equation (16). It should be noted that system efficiencies (a function of the sign of the power flow) should be accounted for, especially the transition from mechanical to electrical, but these are omitted for clarity.

$$P_d = P_{CPS} + P_{Gen} + P_{Drv} \tag{12}$$

$$P_{Gen} = u_1 P_d \qquad \mathbb{B}\left[P_{Gen,min}, P_{Gen,max}\right] \tag{13}$$

$$P_{Drv} = u_2 P_d \qquad \mathbb{B}\left[P_{Drv,min}, P_{Drv,max}\right] \tag{14}$$

$$P_{CPS} = (1 - u_1 - u_2) P_d \qquad \mathbb{B}\left[P_{CPS,min}, P_{CPS,max}\right] \tag{15}$$

$$P_{PPS} = (u_1 + u_2) P_d, \qquad \mathbb{B}\left[P_{PPS,min}, P_{PPS,max}\right] \tag{16}$$

Since the core of the ECMS function still equates actual CPS fuel flow with equivalent PPS fuel flow, then Equations (6) through (11) still apply. Also as the CPS speed is decoupled from the vehicle speed, the engine power to efficiency polynomial fit methodology used in Section 5.2.3 can be applied here.

5.4.2. Algorithm overview

The methodology for determining the minimum equivalent consumption (J) in a compound HV differs from the series and parallel application. Previously the max and minimum of a single split (u) was defined and minimum J was determined either along the continuum of valid u or stepwise. The boundary conditions, u_o u_{min} and u_{max} were determined separately and the full set of resultant J values were minimised again. However in the case of a compound HV, there are two splits, u_1 and u_2. This results in a matrix of valid split coordinates in the form (u_1,u_2), as determined by the subsystem power limits (to be discussed in detail in Section 5.4.3).

Hence the boundary conditions become part of the matrix to be minimised. Figure 5-11 presents the compound HV ECMS algorithm. First the ECMS determines if the demand power is lower than a predetermined minimum and if the PPS limit is not being approached. This will result in EV operation. This function is optional but exists on production vehicles [144]. The use of the PPS flag ensures that both power and capacity limitations are being accounted for, as a reduced capacity will manifest as a reduced *power_available* also.

Then the system determines the allowable split matrix from demand power and the PPS, CPS, Gen and Drv limits. As discussed previously these limits are in real-time and communicate degradation, such as reduced capacity, or due to temperature or wear over life. This matrix of split in u_1 and u_2 is used to calculate a matrix of J. This matrix is then minimised to determine J_{min}. The coordinate (u_1,u_2) for that J_{min} is converted into torque splits for the given system speeds. The steps to prevent hunting described in the series and parallel ECMS algorithms are omitted here for brevity, but would be required in a real world application. The key interfaces are presented in Table 5-3.

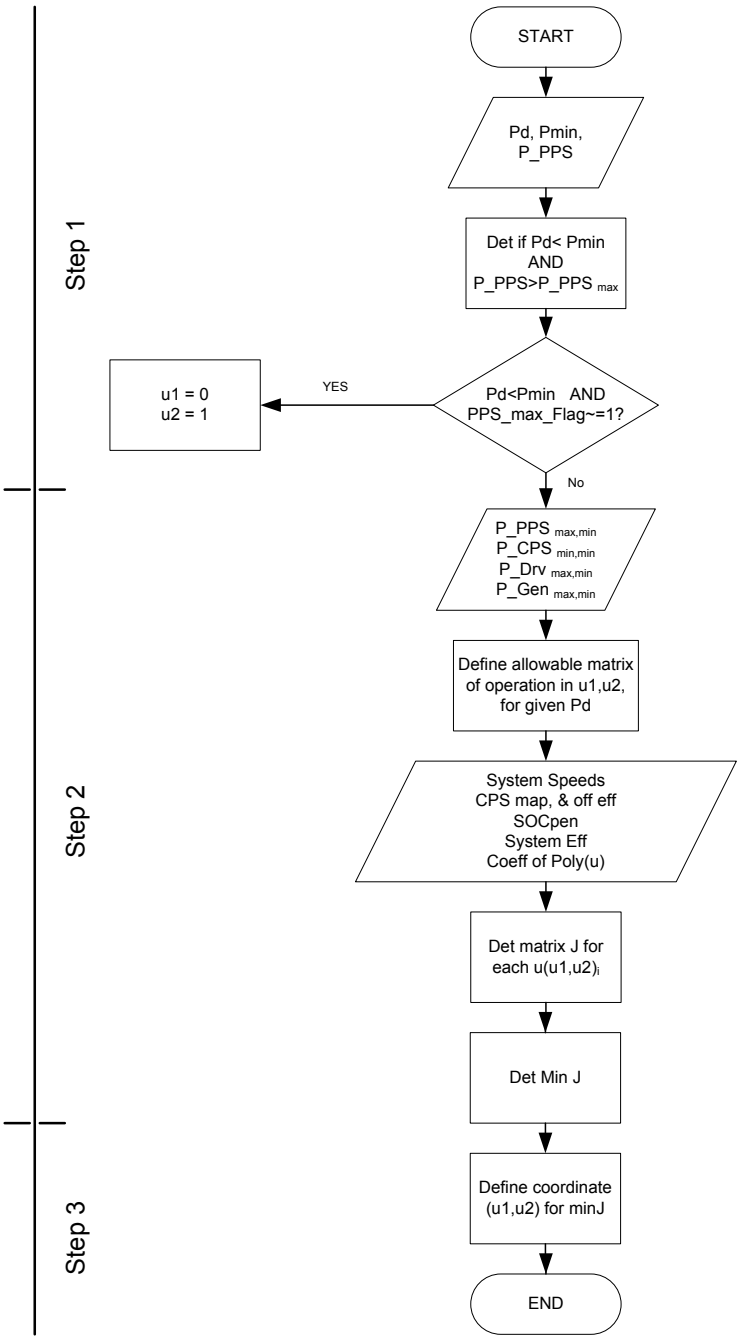

Figure 5-11: ECMS algorithm as deployed in the compound HV

For the calculation of J for each (u_1,u_2), the same process discussed earlier was used. The energy drawn from the PPS is calculated as CPS energy which would be required to replace it via the Gen system at a later time, accounting for system efficiencies. If (u_1,u_2) resulted in a negative PPS power flow (into the PPS), the system would calculate that is CPS energy saved for use at a future time, also accounting for the efficiencies, noting the sigh of the power. As previously discussed a polynomial function of the CPS power versus efficiency is used from a pre-calibrated map. The algorithm used for Section 8.2 was calibrated based on the Toyota Prius, as described by Manssour and Clodic and Ayers et al [192, 193].

Inputs	Outputs
1. Power demand 2. PPS maximum power flag 3. Gen minimum power 4. Gen maximum power 5. Drive minimum power 6. Drive maximum power 7. CPS maximum power 8. CPS minimum power 9. PPS maximum power 10. PPS minimum power 11. System speeds 12. PPS efficiency 13. Electric equivalent fuel consumption penalty	1. Torque split 1 'u1' 2. Torque split 2 'u2'

Table 5-3: Compound ECMS interfaces

As mentioned the splits' boundaries are defined by the limits of four systems, the PPS, CPS, Gen and Drv. The following section presents how this is formulated.

5.4.3. Splits' boundaries determination

In the series application, the CPS speed was decoupled from the vehicle speed, therefore the limits of split could be expressed on a graph of demand power versus split. The parallel application required a third axes, CPS speed, as this was coupled to the vehicle speed. In the compound application the CPS is also decoupled from vehicle speed, but there is still a third axes, namely the second split term.

Each of the sub systems (Gen, Drv, CPS and PPS) presents a maximum and minimum power limit. On any given axes, the minimum of the relevant minima will apply. This means that for a given use case, the limiting system may change. An example of this is regenerative braking, initially the PPS limit will normally apply (assuming battery PPS low negative power limit), however as the speed decreases, the Drv system limits may reduce. Therefore the ECMS must account for all sub-system limits at all times.

The following figures build up a picture of the limit boundaries in three axes matrix of P_d, u_1 and u_2. Beginning with the Gen sub-system, using Equation (13) and the minimum value for P_{Gen}, a surface can be described in the P_d, u_1 and u_2 space. Figure 5-12a presents the boundary surface for $P_{Gen,Min}$. Figure 5-12b presents the boundary surface for $P_{Gen,Max}$. These surfaces are a function of P_d and u_1 only, and do not change along the u_2 axis, as per Equation (13). This shape is representative of those found in Figure 5-3 for the CPS limits. However, as this is a more complex driveline, the splits are shown over four quadrants as opposed to one in the case of the series ECMS.

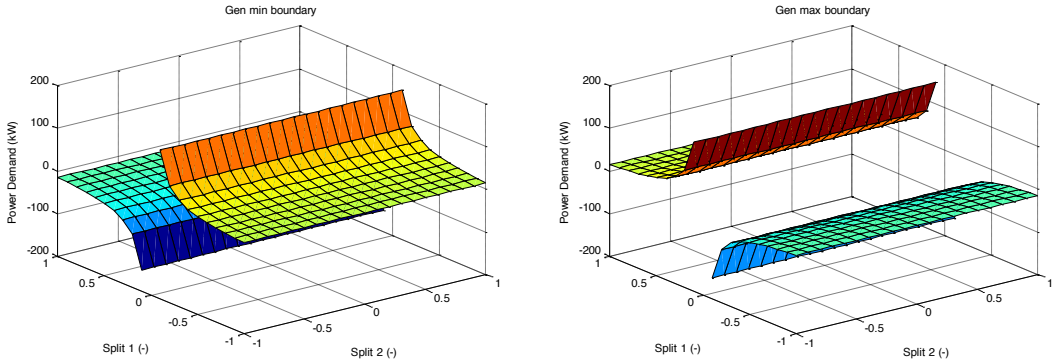

Figure 5-12: a) Gen minimum power boundary, b) Gen maximum power boundary

Figure 5-13a show how these two boundaries are combined together. The valid volume of operation lies within the confines of these surfaces. Figure 5-13b presents the same minimum and maximum boundaries for the drive system, as defined by Equation (14). The axes for both figures are in the same orientation, but as the P_{Drv} is a function of u_2, the surfaces are unchanged along the u_1 axis. This results in a 90 degree offset in the surfaces. Figure 5-14 shows how the Gen and Drv boundary surfaces are combined. The altered scale is a reflection of the relatively higher power of the Drv system. It is clear how the set of surfaces are used to constrain a volume of valid split coordinates, in P_d, u_1 and u_2.

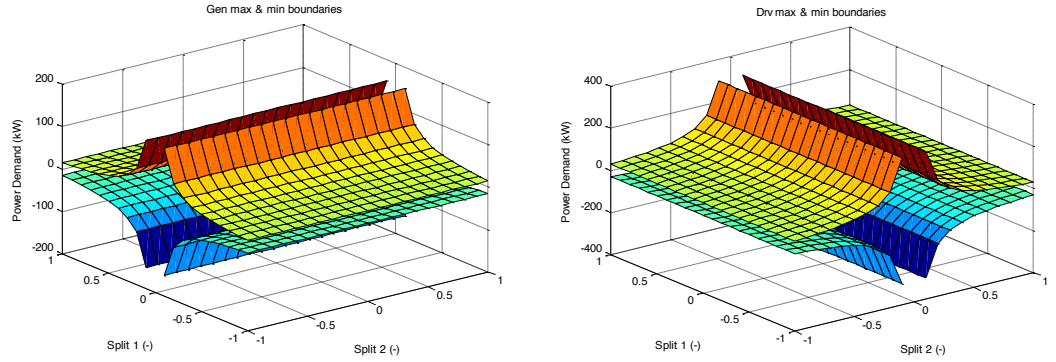

Figure 5-13: a) Gen min & max boundaries, b) Drv max & min boundaries

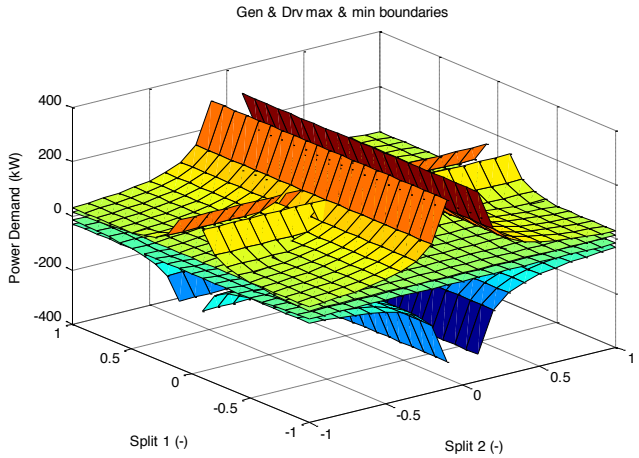

Figure 5-14: Gen and Drv max and min boundaries

Figure 5-15a presents the maximum and minimum boundaries for the CPS system. Note the axes have been rotated 90 degrees relative to the previous figures, and the u_1 and u_2 axes are reversed. These surfaces are defined by equation (15). There is an offset and diagonal singularity which represents the CPS off state. This includes the u_1, u_2 coordinate (0,1) which equates to EV operation.

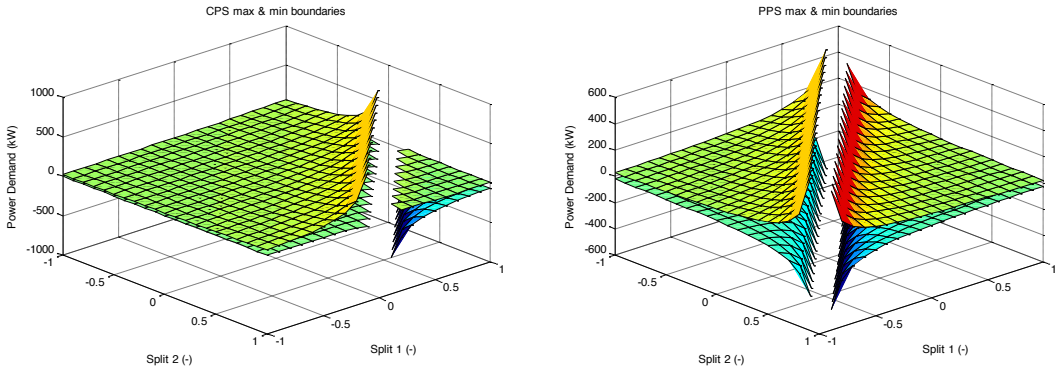

Figure 5-15: a) CPS max & min boundaries, b) PPS max & min boundaries

Figure 5-15b presents the limits for the PPS as derived from Equation (16). The singularity in this case equates to points of operation where u_1 equals u_2, hence no power will flow in or out of the PPS. This is also a function of system efficiencies but that is not shown here for clarity.

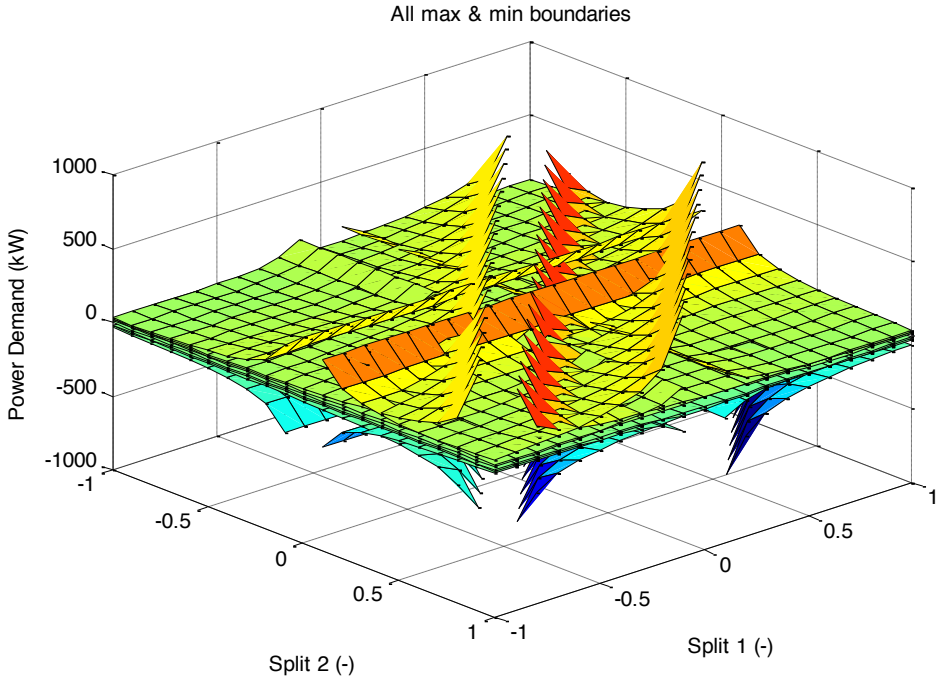

Figure 5-16: All sub-system boundaries

Figure 5-16 finally shows all the sub-system boundaries together. This is a complex bounded volume of valid operation coordinates (P_d, u_1, u_2). However, the ECMS reduces this complexity by creating a two axes matrix in u_1 and u_2 by slicing the volume horizontally across the P_d axis, based on the current P_d.

Figure 5-17 presents the u_1, u_2 matrix for a P_d of 10kW. For a given slice of the volume perpendicular to the P_d Axis, the various boundary surfaces appear as lines. The Drv maximum and minimum limits are shown in dashed and solid orange lines respectively. The Gen limits are shown in green, the CPS in blue and the PPS in red. At each time step the ECMS must determine a J value for each coordinate (u_1,u_2) which lies within all the boundary lines shown. At this power demand the u_1 is limited by $P_{Gen,max}$ and $P_{Gen,min}$, shown as horizontal lines. Whereas u_2 is limited by $P_{Drv,max}$ and $P_{Drv,min}$ which is represented by vertical lines. The CPS and PPS limits affect both u_1 and u_2 which is indicated by diagonal lines.

The blue dashed line represents $P_{CPS,min}$ which in the deployment in Section 8.2 refers to ICE off. In this case u_1 plus u_2 must equal one. The previously mentioned EV operation point of (0,1) satisfies this requirement, but there exists a continuum of this type of coordinate. For example (0.5,0.5) would also suffice. However this manifests as the Drive delivering 50% of the demanded power, and the Gen system delivering the other 50%. In the case of the deployment in Section 8.2, this would mean delivering this power through an epicyclic. Even if the motion of the third part of the epicyclinc could be constrained, then this would still result in an efficiency loss on that 50% of the power. Therefore if EV operation is desired, it is normal for the ECMS to select (0,1) as will become apparent in Section 8.2. This EV point of operation is highlighted as a red point in Figure 5-17.

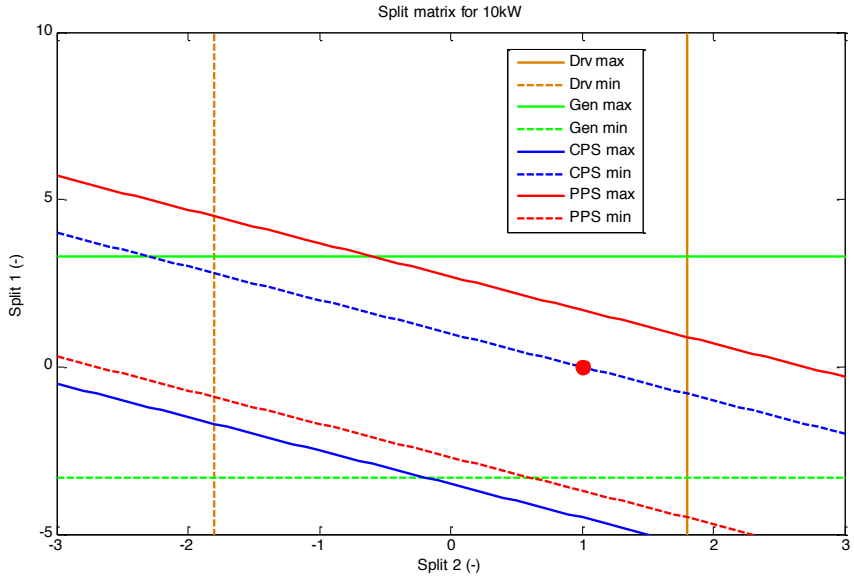

Figure 5-17: split matrix of valid operation for a 10kW demand power

The rest of the matrix is constrained by Drv limits on the left and right hand sides. The bottom of the matrix is constrained by the PPS minimum limit for lower levels of u_2, and Gen minimum limit for high levels of u_2. As mentioned previously this matrix of (u_1,u_2) is determined for each P_d and a resultant J for each is calculated. From there it is a simple minimisation process to determine the best coordinate in u_1 and u_2. These become the setpoints for the Motion Control functional blocks.

The algorithm described here is the basis of the energy management function used to numerically test the compound AD in Section 8.2.

5.5. Summary

This chapter has presented the theory behind the ECMS energy management methodology. How the ECMS is deployed onto each HV type is also presented. These algorithms form the basis for the numerical scenario testing for each of the ADs presented in Chapters 6, 7 and 8. It was necessary to present this control algorithm in detail as the energy management function can have a significant effect on the system architecture. A badly designed EM function, with bespoke interfaces, will render the architecture unusable. Therefore it is essential to show in detail how one EM methodology can be applied across all HV variants using the same architecture interfaces.

It could be argued that the same applies to the Motion Control functionality. However it is clear that Motion Control, or more specifically *Torque_Apportionment,* is deployment specific. Therefore in the context of this research, a sensible encapsulation of *Torque_Apportionment* from the rest of the architecture ensures variant robustness. The EM functionality is a novel function of a HV VSC, whereas *Torque_Apportionment* is a common and understood problem which exists in traditional ICE vehicles. Therefore it is sensible that this level of detail is presented for EM functionality in this Thesis. Hence, as described in Chapter2, ECMS is a well understood EM strategy. ECMS also has the advantages of simplicity (enough to run in real time) and good fuel economy over blind duty cycles when compared with rule based methods which have been optimised using off-line methods, as discussed in 2.3.3.

The following three chapters use these algorithms to numerically test the ADs deployed from the RAs presented in Chapters 3 and 4. The ADs act as scenarios for the RAs, thereby testing the hypotheses presented at the outset of this Thesis, whereas the numerical deployments act as scenario tests for the ADs. Chapter 6 presents the deployment of the Series RA to a series deployment, conducted in conjunction with the LCVTP project. This deployment is numerically tested in simulation, HIL and on a running vehicle. Further to this, other series HV considerations are discussed.

Chapter 7 presents the deployment of the Parallel RA into two distinct parallel variants, pre-transmission and post-transmission. These deployments are numerically tested in simulation. Finally Chapter 8 presents the deployment of the Extended Parallel RA or Compound RA onto a power-split and one through-the-road compound HVs. The power-split compound HV is numerically tested using the algorithms presented in this chapter.

6. Deployment of Series RA

This chapter presents a case study undertaken as part of the LCVTP project. The vehicle is a traditional series HV with an ICE and GenSet CPS and a passive battery based PPS, as per the definitions set out in Section 2.4.2. Based on this vehicle an AD has been derived using the RA set out in Chapter 3 as a template. This case study of the LCVTP series AD acts as a scenario for the Series RA. Lower level scenario tests are achieved by developing and testing the resulting VSC in simulation, HIL and in-vehicle environments. These scenarios will add confidence to the hypothesis that the Series RA represents a wider set of series HVs than those tested in the Wren project.

Section 6.1 presents the deployment of a series AD using the Series RA as a template. This AD acts as a scenario test for the RA. The main deployment is described in architectural terms, focusing on changes between the AD and the RA, including real world considerations, such as brakes integration and CPS encapsulation. Lessons learnt are presented in Section 6.1.4. Section 6.2 presents the numerical deployment of the series AD. This includes simulation, HIL and in-vehicle testing. The various tests presented here represent scenarios for the AD. Section 6.3 presents architectural analysis on the extendibility of series HV variants not analysed in Sections 6.1 and 6.2. This includes gas turbine and electrically integrated flywheel series HV variants.

6.1. Case Study 1: Deployment of an AD from Series RA

This section presents the physical and system domain models of the series AD. The control domain models show little difference to the RA and therefore are presented in Appendix G. This section concludes will an analysis of sub-system encapsulation. This is a crucial feature for reusability when extending the RA to alternate series HVs.

6.1.1. System schematic

Leading up to the LCVTP project Jaguar Landrover built a Series HV demonstrator based on their XJ model, named LimoGreen, see Figure 6-1. The LCVTP was tasked with improving the development process of this type of vehicle to generate a system integration which is more readily productionable.

Figure 6-1: Jaguar XJ, LimoGreen series HV demonstrator (supplied by JLR).

The series AD system schematic is presented in Figure 6-2. Relating this back to Figure 2-10 in Section 2.4.2, it can be seen that several real-world subsystems are additionally present. The DC/DC converter represented the gateway to the TPS. The on-board charger and hydraulic brake systems are also represented. In the Series RA presented in Chapter 3, the brakes system is a standalone system, but the on-board charger is encapsulated within the battery system under the umbrella of the PPS.

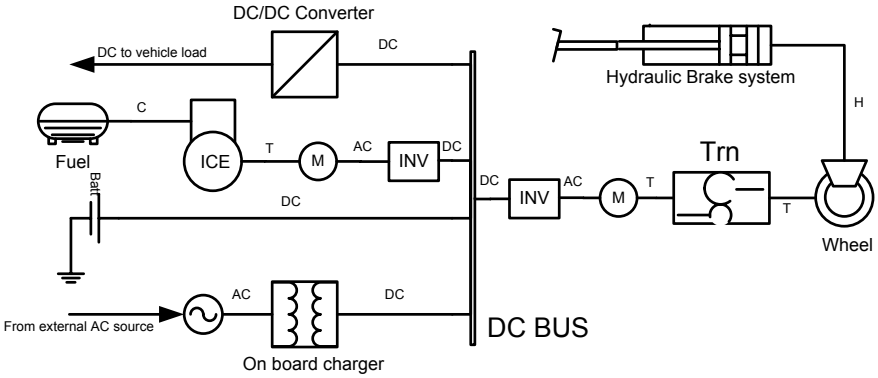

Figure 6-2: System schematic of LCVTP series deployment

6.1.2. System domain models

A key constraint in the project was to retain the legacy brakes configuraiton described in Figure F-1 in Appendix F. Figure 6-3 presentes the system decomposition model for the series AD clearly showing the association between the driver and the BCU. As discussed in Chapter 3 this is not an ideal solution but is expected to be realistic for the forseeable future due to component supplier constraints and legislation which states that any hybrid braking solution (including brake-by-wire) can be implemented as long as it is controlled by the brakes controller [189].

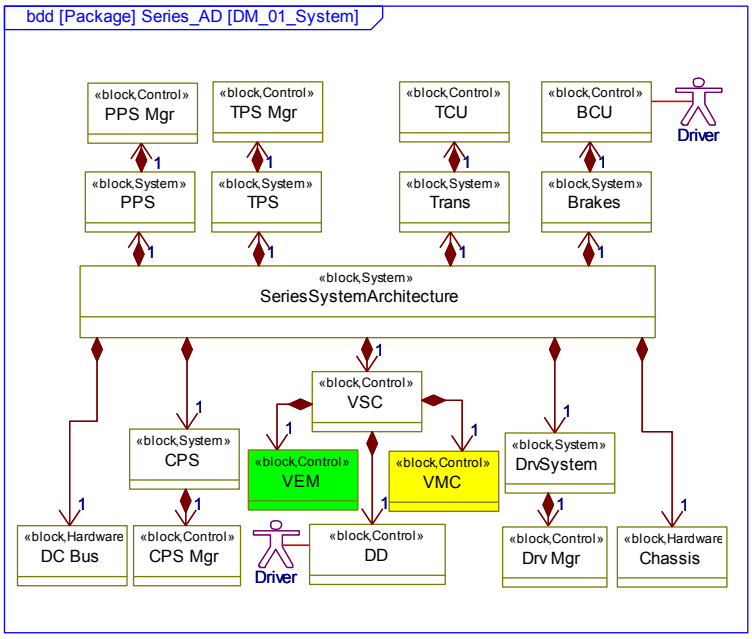

Figure 6-3: AD decomposition model of series powertrain system

The PPS represents the battery system, and the local PPS Manager which is commonly referred to as a Battery Management System (BMS). The CPS represents the ICE and a GenSet and includes with its own local controller the CPS Manager. The impact of correctly encapsulating the CPS is addressed in detail later in this section.

Figure 6-4 presents the context and causality model of the powertrain system of the series AD. As can be seen it is very similar to Figure 3-5. The key difference is the relationship between the VSC and the Brakes. In short, the brake pedal interfaces directly with the brakes system which in turn passes a *regen_torque_demand* to DD. In keeping with the ideal RA this *regen_torque_demand* is constrained by *regen_torque_available* from the VMC to ensure system linits can not be breached. It is beneficial that the DD retains the role of determining total *torque_demand* for both positive and negative demands. That this future proofs the RA ensuring it is applicable to both brakes configurations with minimal change.

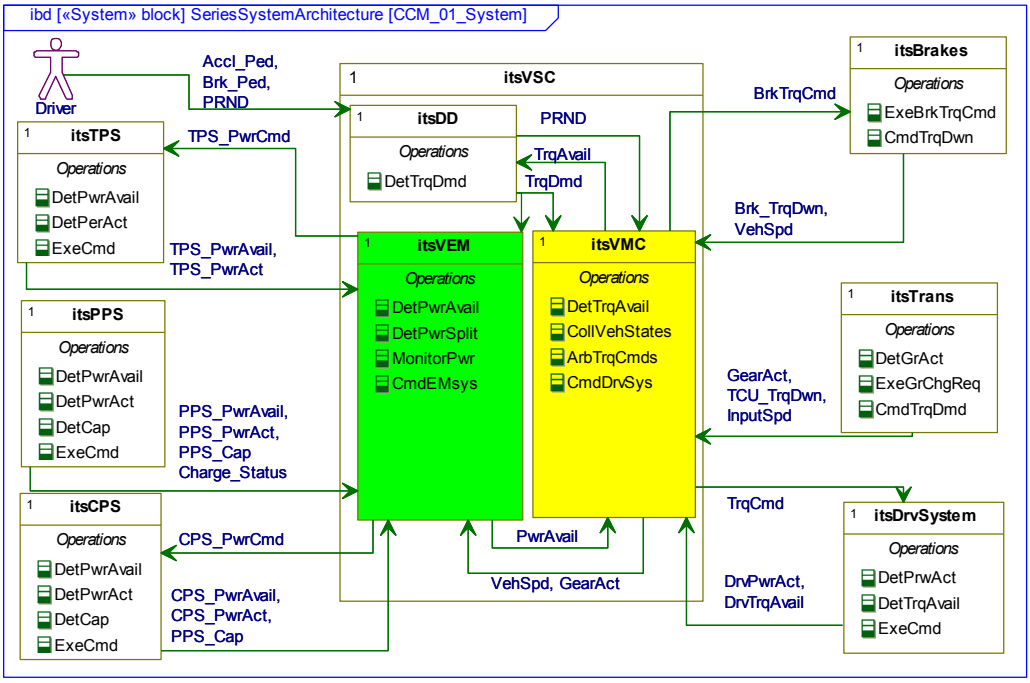

Figure 6-4: AD context and causality model of series powertrain system

Other notable differences between the RA and the AD at the systems level are the absence of a PPS *power_command* and a transmission *gear_change_request*. Also a *charge_status* flag is included. This is used to prevent vehicle motion during charging. The RA presented in Chapter 3 needs to be robust to a controllable PPS or a simple transmission which is controlled by the VSC. In this deployment the PPS is a passive battery system whose power is a function of the Drive, the CPS and the TPS powers. The transmission is controlled by functionality outside the VSC.

It is important to note that this altering of details of the RA to initiate a deployment AD is both expected and necessary. The Series RA has been developed to represent a superset of series HVs therefore it will contain features not deployed on every series HV variant. In principle this goes against the ethos of object oriented development, resulting in functional overload at the RA level. However omission is the opposite of addition and

is necessary in the search for a universal RA representing a broad range of HV variants. A controllable PPS is a good example. Battery based PPS systems are commonly passive, resulting in the *power_comand* interface being redundant, whereas an electrically mounted flywheel would require this interface. Omitting this interface does not invalidate the RA rather it demonstrates its inherent robustness.

Figure 6-5 presents one example of an interaction model of the series powertrain system. It should be noted that many interaction models will exist, one for each path through every use case associated with the functional requirements of the AD. Again, this is largely similar to the RA interaction model in Chapter 3, Figure 3-6. VEM still requires CPS and PPS *power_available* and TPS *power_actual* to determine system *power_available*. VMC still requires this and Drive *torque_available* to determine total *torque_available*. However a key difference between the Series RA and the series AD is that the negative limit of *torque_available* is broadcast to brakes as *regen_torque_available*. The brake pedal is shown as interfacing with the brakes system. Importantly, the value of *regen_torque_demand* cannot be determined until brakes receives both *brake_pedal* and *regen_torque_available* signals. Also the PPS *power_command* and the CPS *capacity* signals are omitted. CPS *capacity* would indicate fuel level, which would need to be indicated to the driver but is not required to calculate the EM *split* and therefore is not shown here. As discussed, the AD control domain models correlate well with the RA, therefore are presented in Appendix G for brevity.

A key novelty in this deployment is the requirement of the VEM to be aware of the *charge_status* before it will broadcast a nonzero *power_available.* This ensures that *torque_available* will be zero when the vehicle is being charged. This was formulated throught an ISO 26262 process from with in the LCVTP project, [194]. This is a functional safety feature which can manifest is several ways which is why it is not captured in the RA. A second manifestation will be presented in the next chapter.

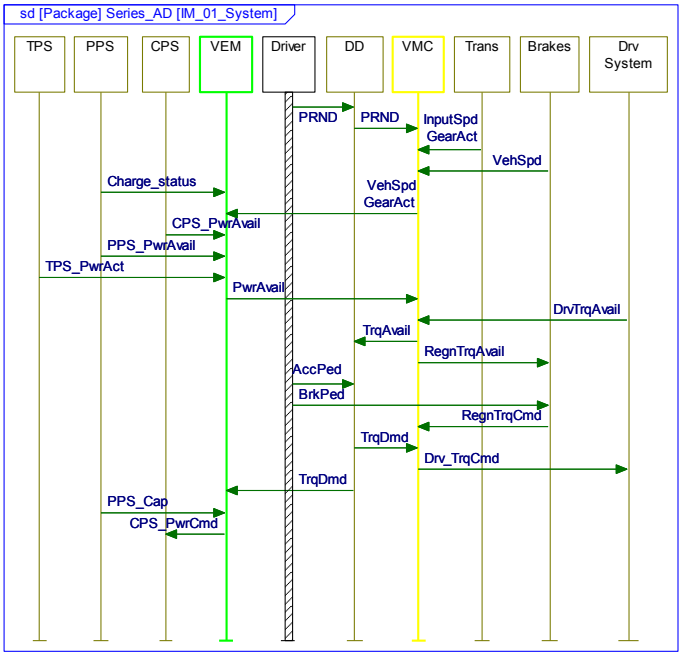

Figure 6-5: AD interaction model of series powertrain system

6.1.3. Series CPS encapsulation discussion

A controversial point from LCVTP was the idea of encapsulation, specifically pertaining to the CPS. Figure 6-6 shows a decomposition model of an ideal CPS. It is shown to comprise an ICE and a GenSet (electrical machine and inverter) as described in Chapter3. For completeness a fuel tank is also shown. Each sub-system group has its own local controller, ICE and Gen manager, which are in turn governed by a local CPS manager.

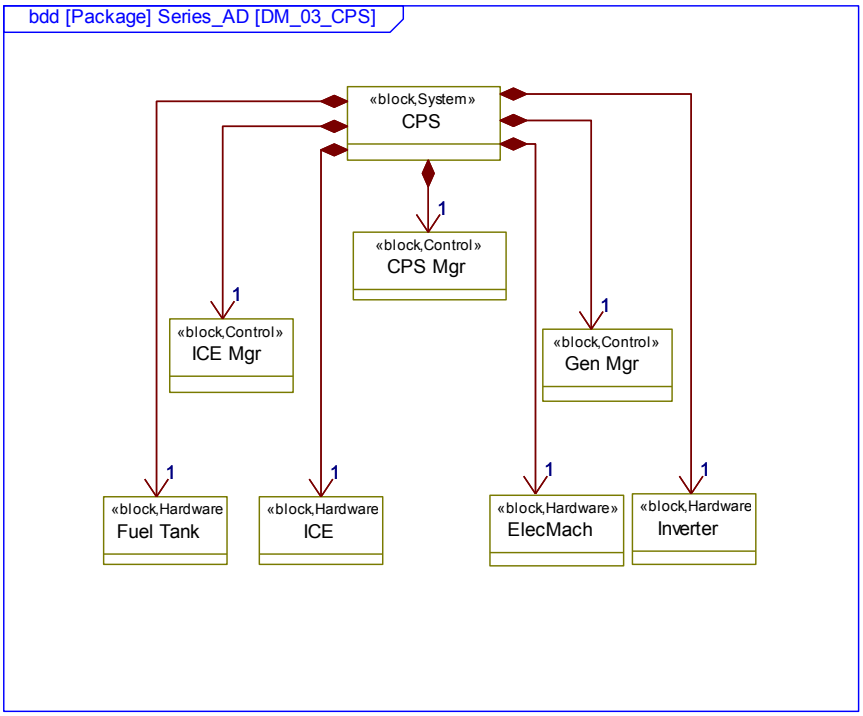

Figure 6-6: AD decomposition model of ideal series CPS

Figure 6-7 shows a context and causality model of the ideal CPS. It shows how the CPS manager shields the VSC from sub-system specific interfaces. The interfaces to the CPS manager include ICE and Gen specific information such as throttle position (an inference of torque command) and system temperatures. Therefore the VSC interfaces remain the *available, actual, capacity* and *command* interfaces defined as part of the RA.

The source of the controversy was that partners within LCVTP asserted that this should consist of two distinct systems, ICE and GenSet, as shown in Figure 6-8. It was suggested that integration should take place at the VSC level. This would contravene the multi-disciplinary principle of systems engineering. CPS integration at the VSC level would significantly increase VSC interfaces. As discussed by Ridao et al and Rosenplatt this enhanced centralisation can increase hierarchical dependency [59, 60]. This would ensure that the VEM would be deployment specific.

A compromise was agreed with the project partners, that the CPS Manager should be retained but deployed onto the VSC, thereby retaining the reusability of the VEM. Figure 6-9 shows how this decision affected the decomposition model of the Series AD. It includes two new systems at this highest level of abstraction. Also the VSC now contains the CPS manager. Figure 6-10 shows the effect on the context and causality model. The

inclusion of the CPS manager into the VSC increases the number of interfaces. Table 6-1 shows an interaction matrix of how this would look. Comparing this to the matrix in Appendix F, it can be seen that the inclusion of the CPS manager into the VSC increases the number of interfaces which cross the VSC boundary from 21 to 31.

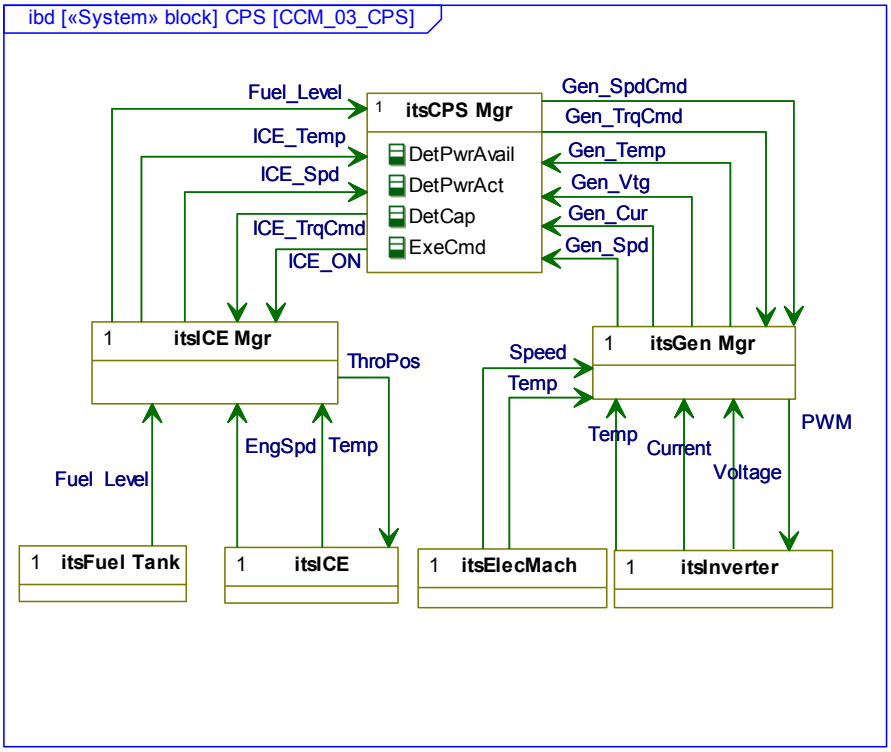

Figure 6-7: AD Context and Causality model of ideal series CPS

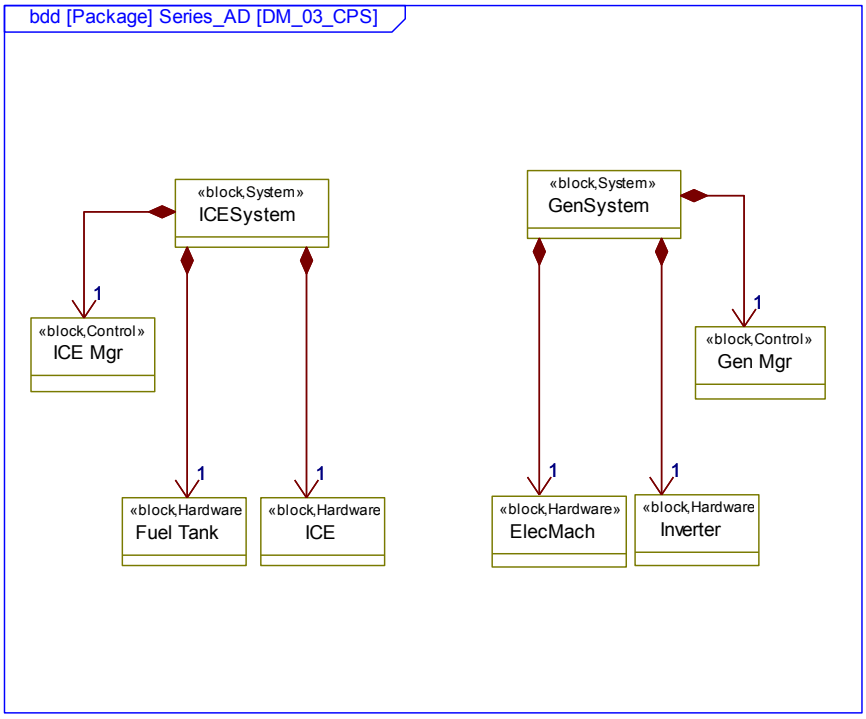

Figure 6-8: AD decomposition model of partitioned series CPS

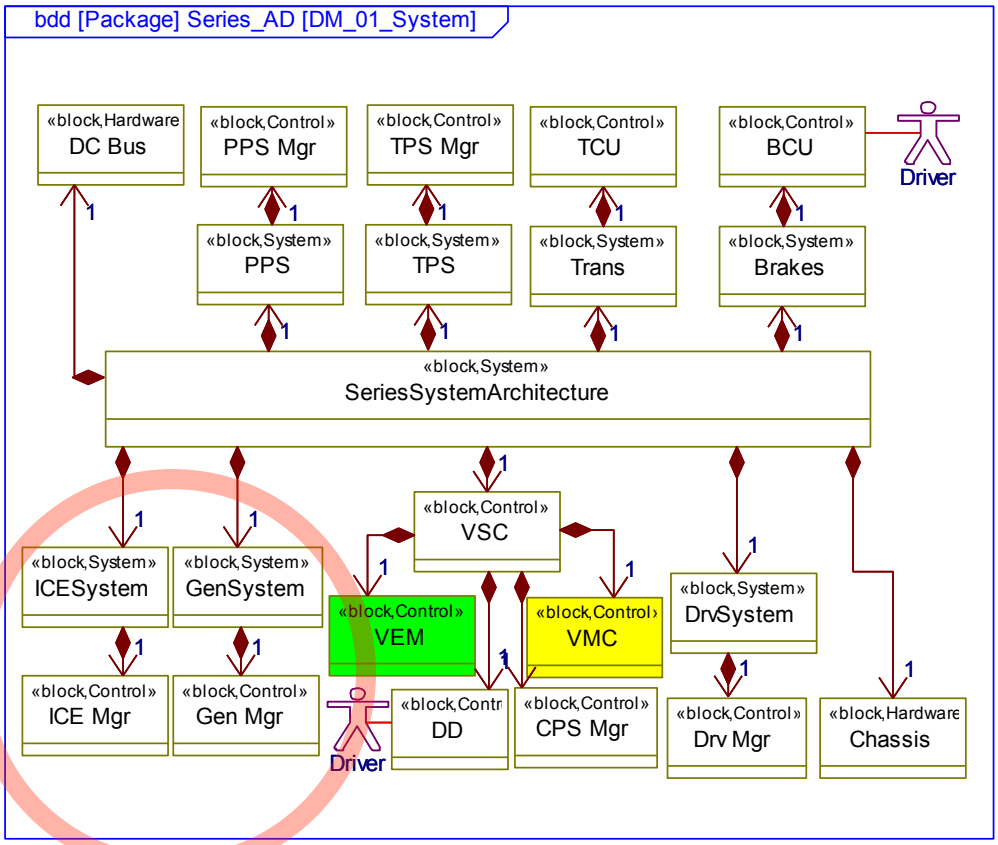

Figure 6-9: AD Decomposition model of series system domain with altered CPS

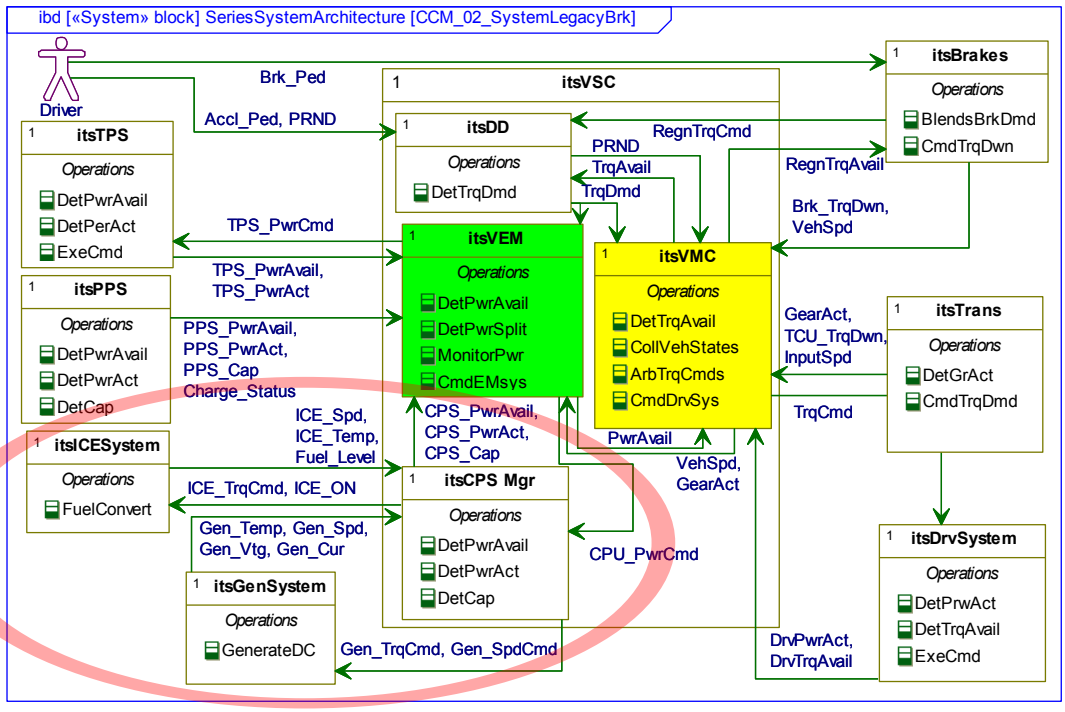

Figure 6-10: AD context and causality model of series system domain with altered CPS

Table 6-1: Interaction matrix for series AD showing CPS manager deployed into VSC

Drive System, Drive Manager	BrakesSystem, BCU	Transmission System, TCU	VSC, CPS Manager	VSC, Vehicle Motion Control	VSC, Vehicle Energy Management	VSC, Driver Demand	Driver	TPS Manager	Gen Manager	ICE Manager	PPS Mgr	
												PPS Mgr
			ICETrqCmd ICE_ON									ICE Manager
			GenTrqCmd GenSpdCmd									Gen Manager
					TPS PwrCmd							TPS, TPS Manager
												Driver
				TrqAvail			PRND AcclPed BrkPed					VSC, Driver Demand
			CPSPwrAvail CPSPwrAct CPSCap	VehSpd GearAct		TrqDmd		TPS PwrAvail TPSPwrAct			PPSPwrAvail PPSPwrAct PPSCap, ChrgStatus	VSC, Vehicle Energy Managem
DrvPwrAct DrvTrqAvail	BrkTrqDwn VehicleSpeed	GearAct TrnTrqDwn InputSpeed			PwrAvail	TrqDmd PRND						VSC, Vehicle Motion Control
					CPSPwr Cmd				GenVtg GenCur GenTemp GenSpd	FuelLevl ICETemp ICESpeed		VSC, CPS Manager
				Gear ChgReq								Transmission System, TCU
				BrkTrqCmd								Brakes System, BCU
				TrqCmd								Drive System, Drive

Clearly the decision to partition the CPS has significantly altered the architecture. The compromise of retaining the CPS manager and deploying it onto the VSC has preserved the integrity of the VEM. However it is argued that this may limit CPS functionality.

Cacciatori et al state that there exist three bandwidths of control can exist when integrating an electrical machine to and the ICE [195]. These have been defined by as slow medium and fast but not directly quantified. Specifically slow bandwidth control means gross torque set point or pseudo-steady-state control. The medium bandwidth control allows the electrical machine to compensate for the natural ICE lag during transitions from one torque set-point to another. The bandwith of this control was defined by the air path dynamics of the ICE analysed by Cacciatori et al. The high bandwidth control is used to offset ICE cylinder–to-cylinder event torque oscillations, which is a function of the combustion events in the ICE. All the analysis conducted by Cacciatori et al was at low engine speeds, below 2,500 rpm, and hence the frequencies concerned were relatively low, significantly lower than the control bandwith of an electric machine via its power electronics. However the bandwith requirement for an engine operating at 3,500 rpm or higher would be increased, as is the case in the vehicle analysed in the Section 6.2 [167].

It is argued that this functionality would be difficult to achieve over a traditional non-deterministic communications bus such as CAN. A deterministic bus, such a FlexRey may be able to achieve this, but it is argued that this seems a high cost penalty only to avoid a more considered sub-system boundary definition. This level of integration can only be done locally to ensure that all such functionality be retained. Also it is impossible to see how this deployment could be easily altered to include a fuel cell CPS as opposed to an ICE and GenSet CPS without significant development cost. If the RA in Chapter 3 had represented this un-encapsulated CPS then it would be immediately non-reusable for other series HV variants.

A common concern in the automotive industry is the prevalent culture of silo based enterprise structure, with minimal interaction between ICE departments and other departments [63]. Enforcing encapsulation is a widely accepted method of minimising system dependency and alleviating the effect discussed above [46, 58, 61, 62]. It was accepted by LCVPT partners on this evidence that CPS encapsulation presents an improvement over the traditional sub-system centric approach to systems integration. This is a key contribution from this research. It is interesting to note that the partners who initially resisted encapsulation of the CPS had distinct responsibilities for ICE development and GenSet respectively.

The encapsulated of the on-board charger within the PPS system should be presented here. However, for brevity and balance, this will be presented n the context of a plug-in parallel HV, with associated model, in Section 7.1.3.

6.1.4. Lessons learnt

This section distils the lessons learnt from the deployment of the series AD from the Series RA. Three main points can be taken from this AD deployment. Firstly, the concept of a superset RA containing enough functionality to represent all series HV variants is

most applicable to this research question being addressed by this Thesis. Secondly, The RA must be robust to real-world considerations such as braking integration, transmission variants and on-board chargers. Finally the concept of encapsulation ensures reusability, but may face acceptance inertia within traditional component based engineering design environments commonly found within the automotive sector

Traditionally, patterns or RAs contain the minimum commonality between similar systems, and reusable deployment is achieved by means of extension [18, 71]. In the case of the AD described in this section, some features of the Series RA have been omitted, for example the PPS power command. This runs counter to prevailing practice, but it is argued that omission is equal and opposite to extension. Therefore presenting an RA, which contains a superset of functionality and interfaces, is valid for the research question being addressed by this Thesis. More importantly, reducing the RA to the absolute minimum set of shared functionality across all series HV variants may limit the efficacy of the RA itself in terms of reduced development time and cost. If the RA is too generic, it becomes meaningless.

The real world issues encountered within this deployment included brakes integration, transmission variance and the existence of an on-board charger. Some HVs will have an on-board charger, and some will not. Therefore the charger system is encapsulated within the PPS. The benefits from this decision are twofold. Firstly, this masks the charger variance from the rest of the system. If a charger exists in a deployment, its functionality may be dependent on the grid interface, which will change over time. Secondly, as a charger is designed and controlled with a battery chemistry in mind, it is sensible to encapsulate this within the PPS. Brakes and transmission exist as systems unto themselves in the RA which therefore must be robust to integration variance. A key difference between the AD and the RA is the employment of the legacy brakes integration. Also in this case a self-controlling transmission exists and the RA is designed for this, but a transmission controlled by the VSC (or none) is also derivable from the same RA.

It is common in automotive enterprises to demarcate operations along component-based lines. The RA presented in Chapters 3 and 4 defines sub-system boundaries which may contain several different component types. A typical example of this is the ICE and GenSet CPS in a series HV. Traditionally these components are developed by separate departments within the enterprise. Their understandable assumption is that the VSC should coordinate the interaction between the ICE and the GenSet. However it has been shown that this may reduce the functionality of the CPS and would certainly render the Series RA not reusable to other HV variants such as one with a fuel cell based CPS. The main function of the CPS is to irreversibly convert stored fuel to DC power. How this is managed locally is the responsibility of the CPS sub-system, and not the VSC. Hence the minimum set of interfaces between the VSC and the CPS (*available, actual, capacity* and *command*) can be retained which ensures cross variant reusability.

6.2. Case Study 1: Numerical validation of deployed series AD

This section presents the deployment of the series VSC in simulation, HIL and on vehicle. For the purposes of this research the LCVTP deployment is used as a scenario to test the

series AD. The first section presents the simulation activity, which was conducted as part of the LCVTP. This is followed by the HIL and in-vehicle test results. The input from this research is exclusively the VSC control software. The simulation environment, the HIL system and test vehicle were built and prepared by the other LCVTP partners. Deploying the VSC control software within these externally developed environments demonstrates the advantages of an architected design process.

6.2.1. Simulation

This section presents the simulation deployment and results for the series VSC. The deployment choices are presented and discussed. This is followed by a validation section which compares the simulated VSC and vehicle models with data captured from the LimoGreen vehicle. Finally the series VSC functionality is deployed into the LimoGreen vehicle itself and small number of tests were conducted and the results are presented here.

6.2.1.1. Deployment

As part of the LCVTP the other partners developed a simulation environment. This simulation environment was used to demonstrate the series VSC (developed as part of this research) as derived from the Series RA. Figure 6-11 shows the highest level view of the LCVTP simulation environment, with all control systems in Simulink, and plant models in Dymola. The LCVTP partners used the term Alternate Power Unit (APU) to represent the CPS, as indicated in Figure 6-11. The term CPS will be used throughout the rest of this Thesis for consistency.

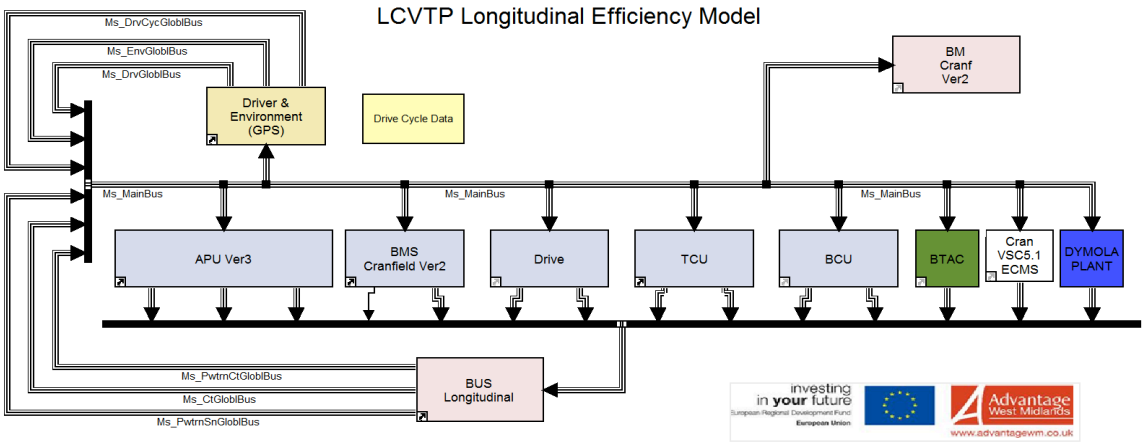

Figure 6-11: Highest level view of LCVTP simulation environment

Figure 6-12 shows the VSC as deployed in the Simulink envoronment. Figure 6-12a shaws the layer immidiately below the block VSC block indicated in Figure 6-11. This shows the VSC core with input-output wrappers. Figure 6-12b shows the layer immediately below the VSC core. This shows five high level funcitonal blocks:

- Driver Demand
- Vehicle Energy Management
- Vehicle Motion Contorl
- CPS Manager
- Thermal Manager

The first three have been discussed in detail in Chapter 3. The CPS manager functional block exists within the VSC, at this level, due to the inital requirement of LCVTP research partners to partition the CPS subsystems as discussed in Section 6.1.3. Based on this, Figure 6-12b represents a funcitonal deployment of the series AD context and causality model presented in Figure 6-10. This includes the CPS Manager within the boundary of the VSC, but this does not interfeer with the architecture of the VEM and VMC, which is essential to ensure reusability. In principle the CPS Manager functionality can be depoyed within the VSC as described in Figure 6-12b or external to the VSC as described in Figure 6-11. The decision to include a separate CPS Manager within the Dymola simulation was based on evidence provided from this research. Therefore as the simulation and experimental activity continued, the CPS Manager functionality was redeployed from within the VSC to the external CPS Manager. The CPS Manager place holder shown in Figure 6-12b has been retained to demonstrate the flexibility of the RA and the essential requirement to protect the boundary definition of the VEM.

The Thermal Manager represents the wishes of some LCVTP partners to locate the HVAC control on the VSC. Other than to create the TPS *power_actual* and *power_available* signals, this funcitonal block does not interact with the rest of the VSC. This could be deployed anywhere on the vehicle and, for this reason, is not represented in the Series RA presented in Chapter 3, nor is it discussed further in this Thesis.

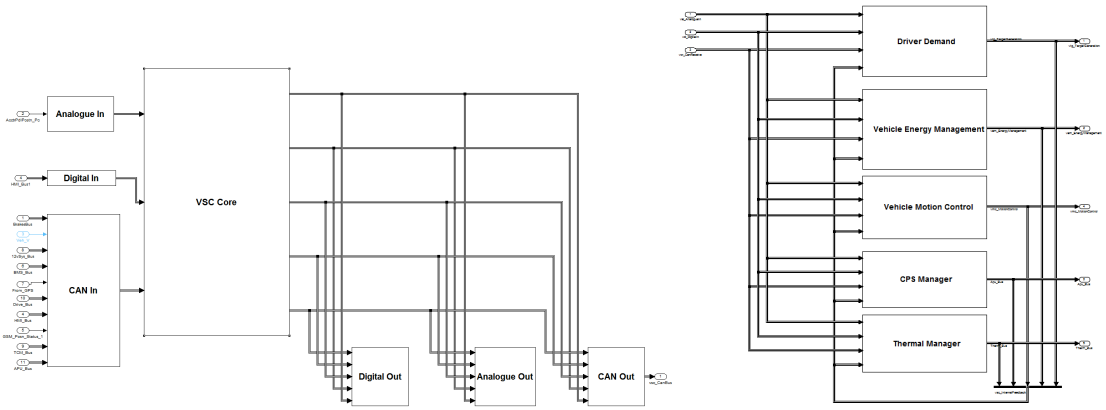

Figure 6-12: Series VSC deployment in Simulink

Figure 6-13 and Figure 6-14 show the internal structure of the VEM and VMC blocks respectively. The VEM funcitonal blocks are clealy displayed.

- Power Available
- Predictive Optimisaiton
- Instantenous Optimisaiton
- Power Apportionemnt
- Power Monitor
- VEM Mode

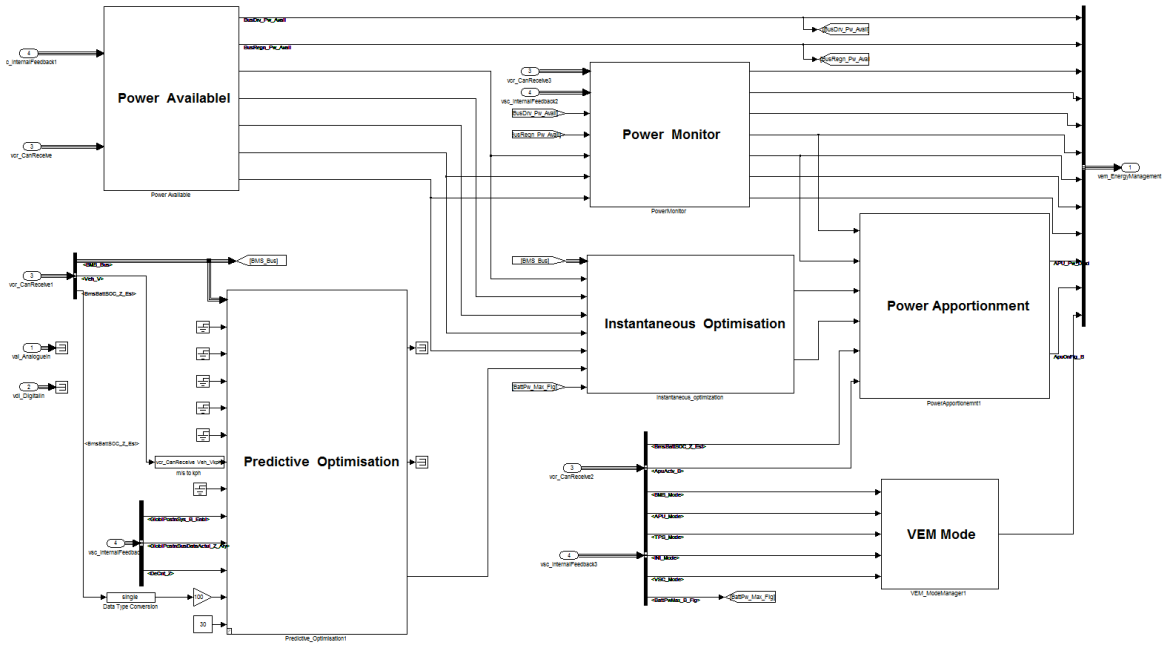

Figure 6-13: Deployment of series VEM

The *VEM_Mode* block is an addition, not represented in the Series RA. This block coordinates system initialisation with other mode management blocks. There is a similar *VMC_mode* block in Figure 6-14. This mode management structure is specific to this deployment, hence it is not part of the Series RA. Figure 6-14 shows the *Torque_Available* and *Torque_Apportionment* blocks along with the *VMC_Mode* block. The *Torque_Arbitraiton* block is omitted in this deployment. The reason for this is twofold. Firstly, it was not envisiged to develop a transmission and brake system with the ability to override the VSC torque command, therfore the *Torque_Apportionment* block is redundent. Secondly, this funcitonalty is not novel to hybrid applications, well understood and therfore it was deemed unnecessary for LCVTP and by extension this research.

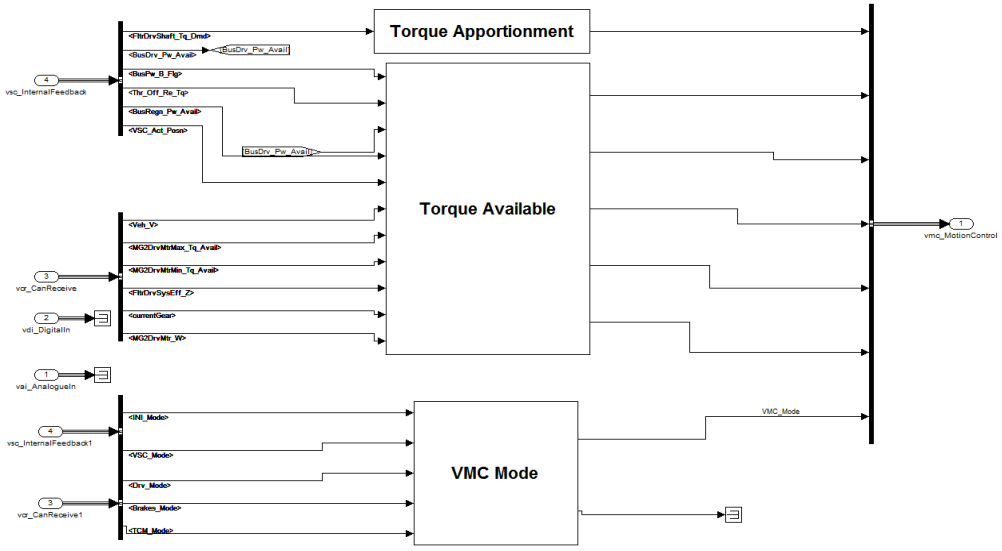

Figure 6-14: Deployment of series VMC

6.2.1.2. Validation

Initial validation was conducted against recorded data from the LimoGreen vehicle at the MIRA Ltd test track[20] . Figure 6-15 presents a subset of the validation results. The top trace is CPS Power, the middle is the SOC trace (PPS capacity) and the bottom graph is vehicle speed. The green traces represent the empirical LimoGreen data, taken over the Artimus Urban drive cycle. The test was conducted at a charge sustaining level of 25% SOC.

The blue traces represent the simulation using the VSC as described in this Thesis. However this energy management functionality is heavily constrained. On examination it can be seen that the LimoGreen CPS is limited to 8kW. Also the decision to activate or deactivate the CPS was derived from a rule based EM algorithm, based on driver demand and vehicle speed. In order to emulate this, the on and off CPS *power_command* was analysed and emulated. This resulted in an artificial CPS power profile, shown in blue. Therefore it can be stated that, given the constraint on the VEM, the VMC and plant models correlate as shown by the SOC, vehicle speed traces and consumption values.

The red traces represent the same cycle, with the same initial conditions (25% SOC, charge sustaining) with no restriction on the VEM. Clearly the red CPS power trace is different. The resultant SOC trace is also different but the final SOC is comparable and the consumption figure is significantly better. Again it should be noted that this test does not prove that ECMS is better than the rule-based EM algorithm as this was constrained to 8kW which is an operating point with poor efficiency. It does, however, confirm that the VEM and VMC as architected perform well and in a coordinated manner, giving strength to the assertion that the Series RA holds for this deployment.

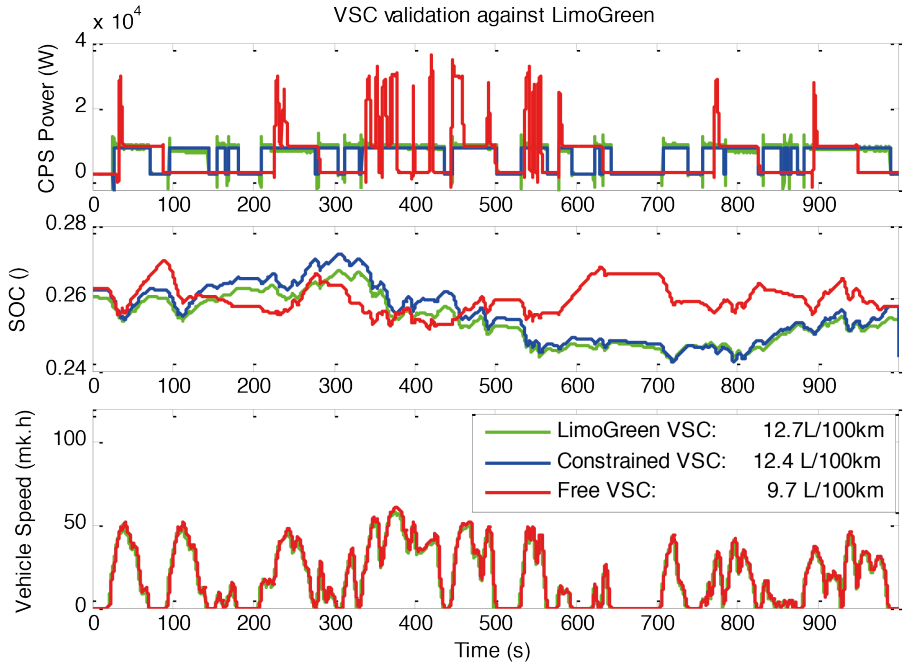

Figure 6-15: Validation data against LimoGreen over Artimus Urban showing correlation

[20] MIRA Ltd was an LCVTP partner.

6.2.1.3. Testing

It is not envisiged that a full spectrum of funcitonal tests will be presented here. This would be required to demonstrate the produciton readieness of any VSC. However to show that the Series RA and derived AD are valid it is sufficient to demonstrate key funcitonality, especially funcitonlaity which crosses the DD, VEM and VMC boundaries. In this context two funcitons will be tested, ECMS sensitivity and its effect on the rest of the system and the ability of *torque_available* to constrain torque demand in the event of a sub-system saturaturaiton or degredation.

The test was conducted twice over the New European Drive Cycle (NEDC[21]) as this cycle shows up algorithmic functionality well. This initial condition of interest is SOC, which was set at 50% in both tests. The ECMS SOC penalty weighting was calibrated to firstly generate a target SOC of 20% and in the second instance 55%. The selection of these target SOC values shows how the system operates in charge depletion to 20% SOC and charge recovery and charge sustaining modes to 55% SOC. The key outcome of the test is to show that the VEM responds differently with no effect on the vehicle motion.

Regarding *torque_available*, the maximum torque of the drive system at high speed was artifically reduced. This limits the vehicles ability to accelerate at higher speeds. Drive *torque_available* is processed by the *Torque_Available* funcitonal block in VMC, using *power_available* from the VEM. *Torque_Available* broadcasts a total *torque_available* to DD. This parameter was identical for both tests, therefore the test should show how the VSC copes with this issue in either charge sustaining or depletion modes.

Figure 6-16 and Figure 6-17 present the results for the two tests. The results are laid out as follows. The top graph shows the target (green) and actual (blue) vehicle speed traces with SOC overlaid in red. The middle graph shows the accelerator demand (blue) and brake (green) pedal position in a scale of zero to one with ECMS split command overlaid in red. As described in Chapter 5, the ECMS *split* can range from 0 to 10 but is scaled down here by a factor of 10. The final graph shows the three key power traces, PPS power (blue), CPS power (green) and Drive power (red).

Figure 6-16 shows the system in charge depletion mode. The SOC trace can clearly be seen to decrease. The ECMS split command is constant at zero and hence the CPS power is also zero. Therefore the PPS and drive power are identical (the sign convention is as per the diagrams set out in Seciton 2.4.2: from storage to vehicle inertia is positive). Figure 6-17 shows the same test with the SOC penalty fucntion offset to affect a target SOC of 55%. The response from EMCS *Instantaneous_Optimisaiton* block is clearly different. The split comand varies dramatically form zero to 10, as a fucntion of demand and SOC. Also the CPS power is evidently higher than the demand, with the resultant charging the PPS, shown as negative power. The result of which is an increasing and

[21] It is widely accepted that NEDC does not reflect the severity of real world driving conditions and would be a poor choice of drive cycle to objectively test the performance of a control system in terms of fuel consumption or torque delivery. However due to its simplistic nature it is ideal to show how different subsystems operate under constant acceleration, cruise or deceleration.

then stabalising SOC. Both sets of results show an anomoly after 1100 seconds. It can be seen that the accelerator pedal position ramps to maximum while the speed traces diverge slightly. On closer examination, it can be seen that the vehicle can not accelerate with the target speed. This is based on the limited drive *torque_available* at high speed. To underline that this is not an energy management domain power limitaiton Figure 6-17 shows how the VEM system responds. The *accel_pos* is 1 but neither the CPS or PPS are running at their respective limit conditions. Therefore it can only be the Drive torque limitaiton, and the VEM is largely unaffected by this.

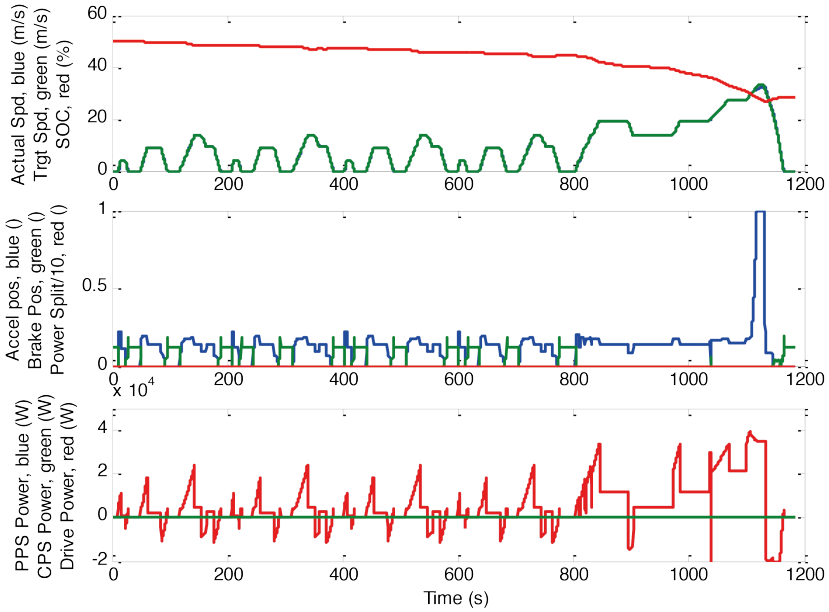

Figure 6-16: Series simulation in Charge Depletion over NEDC

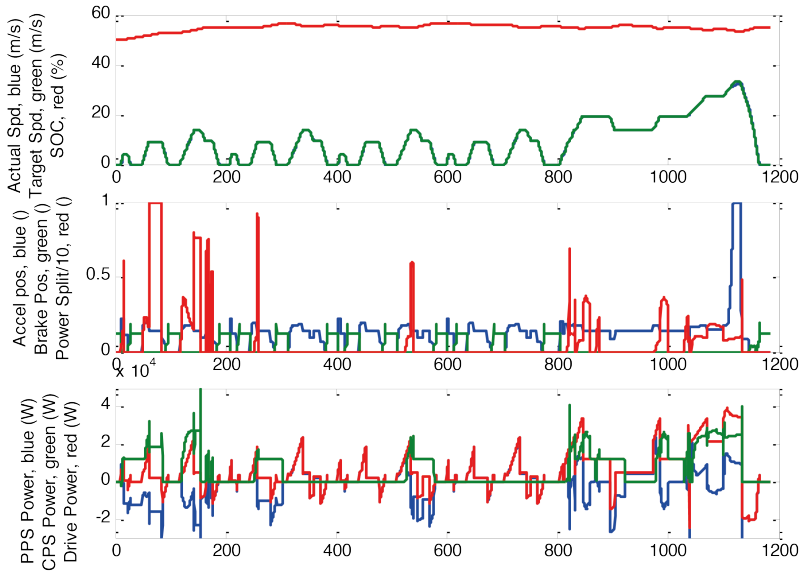

Figure 6-17: Series simulation in Charge Sustaining over NEDC

As stated, these tests do not amount to a full functional validation of the VSC. These tests were selected as scenarios that highlight key functionality which may be affected by the architectural decisions. Based on this it can be stated with confidence that the VSC architected using the Series RA defined in Chapter 3, is functionally sound.

6.2.2. Hardware In the Loop

Following the simulation activity, the VSC was deployed onto a rapid prototype controller and tested in the HIL environment. The LCVTP HIL environment, based at Warwick University, is presented in Figure 6-18. It shows the IPG[22] HIL stack on the right hand side of the picture, with four DSpace micro-Autoboxes on top. The screens to the left show the IPG Carmaker front-end which manages vehicle, environment and simulation configuration control and also the IPG trace viewer.

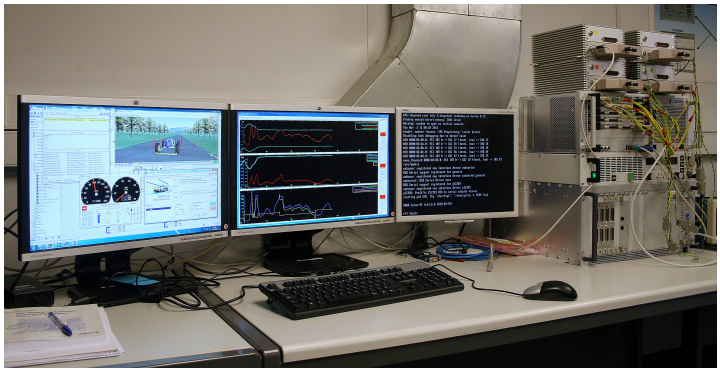

Figure 6-18: LCVTP HIL platform

Figure 6-19 shows how the HIL system is configured. The tool set is as follows. The host PC manages the IPG Carmaker front-end, including the vehicle, environment and simulation configuration. The HIL platform houses the full simulation presented in the last section minus three controllers: Brakes, Drive and the VSC which are deployed onto DSpace MicroAutoBoxes. These communicate over a CAN Bus, and the Brakes and Drive controllers also communicate over HW signals. These represent the local actuation of plant, such as hydraulic valves and power electronics. The fourth box shown in Figure 6-18 is a spare. The rational for deploying these three controllers relates to testing requirements for integrated hybrid braking in dynamic slip conditions, which is beyond the scope of this research.

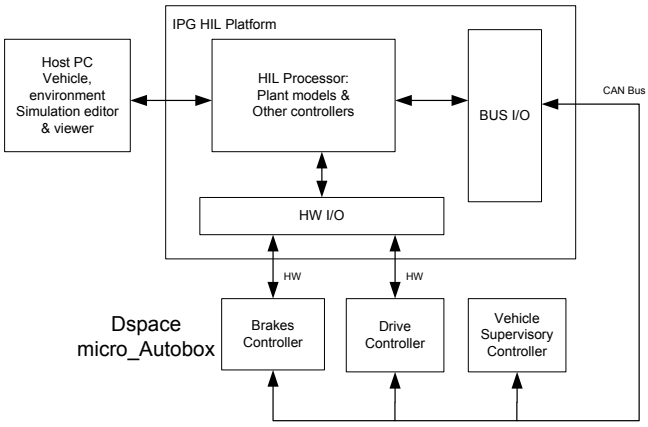

Figure 6-19: HIL platform layout

[22] IPG is a company which produces HIL systems and proprietary software such as IPG Carmaker.

Successfully deploying the VSC into the HIL environment confirms two things automatically, that the VSC runs in realtime, and the key control functions operate over a CAN Bus. Taking these outcomes as a given, the opportunity was taken to further test the functionality of the VSC. Specifically, the sensitivity of the system to ECMS SOC penalty weighting alterations in the context of varying demand was tested.

IPG Carmaker can be used to predefine the environment and driver parameters, which is different to generating a predefined drive cycle, as in NEDC or Artimus urban. A section of road can be defined and drive aggressiveness can be set. The tests defined below were conducted over a 5km section of the Nurburg Ring. The tests can be divided in two groups, high demand and low demand. The high demand driver is allowed to accelerate up to 5m/s^2 and a top speed of 50m/s. The low demand driver is allowed to accelerate at no more than 1m/s^2 and a top speed of 30m/s. This resulted in two distinct velocity profiles over the same course (including inclines).

Then the tests were run with four ECMS SOC penalty function offsets, zero, 0.5, 0.1, and 2. The results are presented in Figure 6-20, Figure 6-21, Figure 6-22 and Figure 6-23. Each figure is divided into high demand results in the left and low demand results on the right. The top graphs show the three key power traces, CPS, PPS and Drive, and the bottom graph shows vehicle speed, SOC and distance. The high demand is over a shorter time stamp as the average velocity is higher while the maximum distance reached for all tests is the same. These tests were chosen to demonstrate the cooperation of the VEM and the VMC as architected.

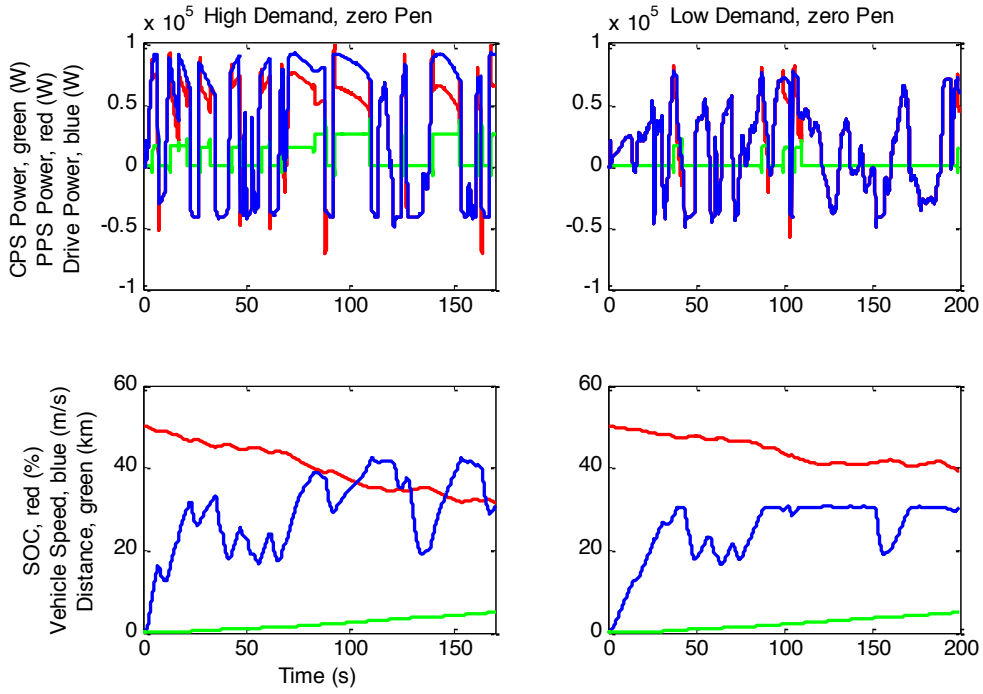

Figure 6-20: HIL test 1: zero penalty uplift

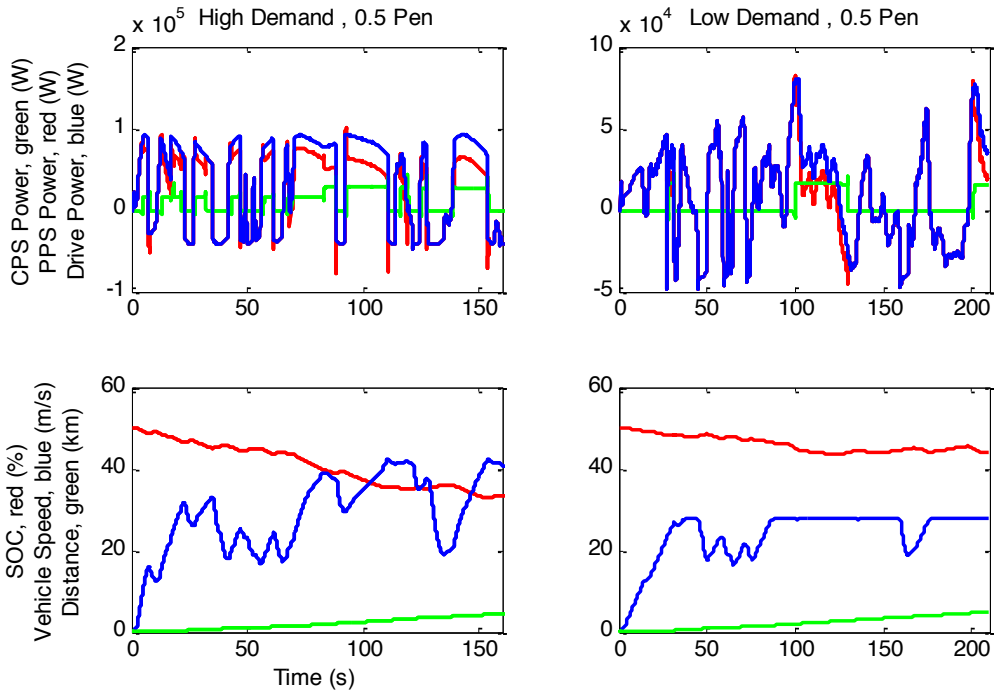

Figure 6-21: HIL test 2: 0.5 penalty uplift

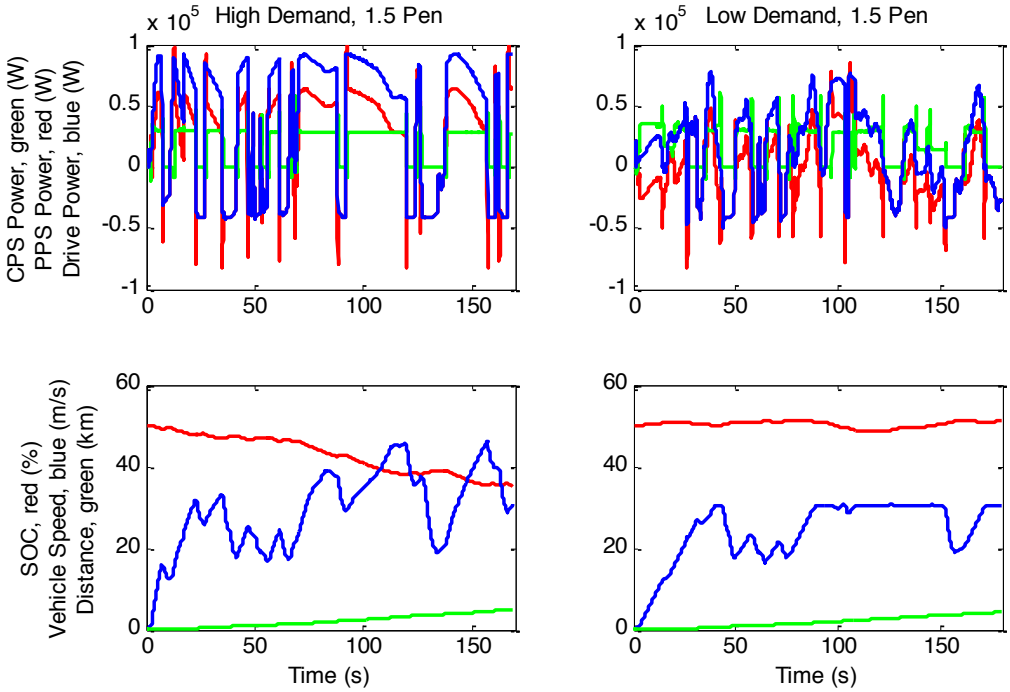

Figure 6-22: HIL test 3: 1.5 penalty uplift

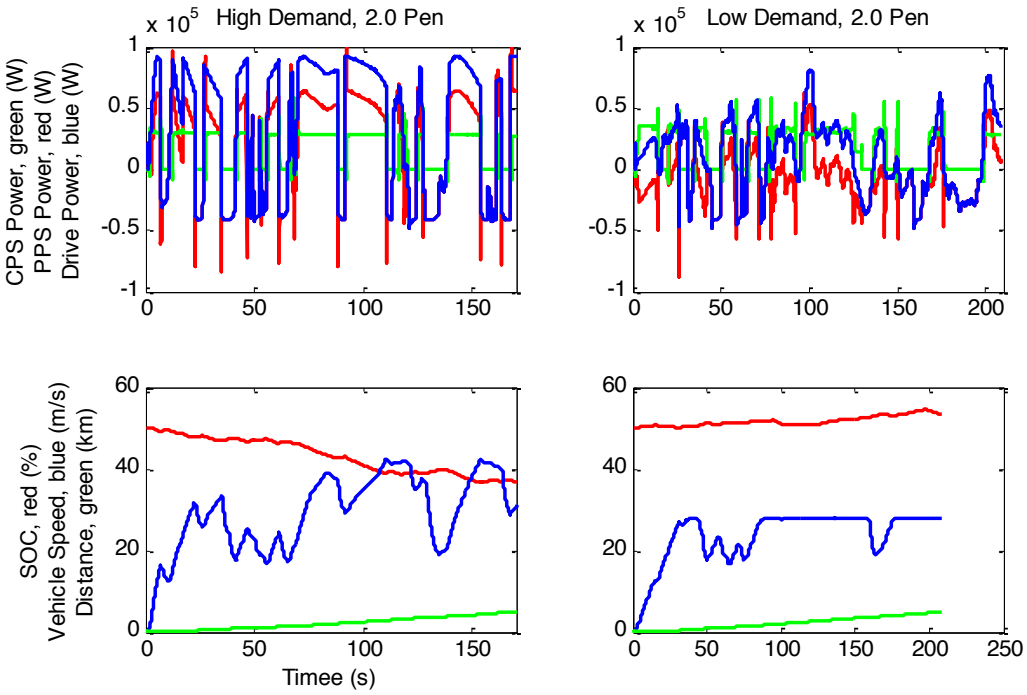

Figure 6-23: HIL test 4: 2.0 penalty uplift

The test showed some interesting results. Looking a the low demand results only it can be seen that a small offset on penalty can alter the system from charge depleting to recovery. This is interesting as the penalty function is the key interface between *Predictive_Optimisaiton* and *Instantaneous_Optimisation*[23]. This test is required to calibrate the output of the *Predictive_Optimisaiton* funcitonal block. Architecturally it can be seen that this interface can be easily replaced by a LUT as described in Figure 5-1, significantly increasing the reusability of ECMS and the Series RA.

When the high demand results are examined it can be seen that the penalty weighting shift has little effect on the SOC trace. The maximum power of the CPS is 35kW. This is significanly less than the demand power which often exceeds 75kW. Therefore, given this size of the CPS, it is evident that the vehicle would be unable to maintain high demand cycles for an extended time. The choice of CPS was a legacy constraint from a previous research project, which gave the opportunity for imperical validaiton for this project. However it is an important piece of learning that standard emissions legisaiton based cycles such as NEDC and Artemis may not expose the limitaitons of some component selection. With respect to the Series RA it is encouraging to note that the VSC and system behaves to its limitaiton in the context of poor component sizing with no difficulty. It is argued that the RA also manages a correctly sized CPS.

In summary, the VSC as architected operates in real-time and over a non-deterministic bus sucessfully. This gives strength to the claim that the Series RA is applicable to this series HV variant. A broader set of senarios were demonstated in the HIL environemnt,

[23] *Predictive_Optimisation* functionality was developed as part of LCVTP but not part of this research.

inclusing SOC penalty sensitivity and conponent sizing validaion., but are outside the scope of this reaearch.

6.2.3. In-vehicle demonstration

As an extension of LCVTP the VSC developed in this research was tested on a vehicle demonstrator. It was the view of the project partners that this scope extension provided value for money in terms of research benefit. In the context of this research, this provided the opportunity to retest some key scenarios in an alternate environment, constituting an alternate scenario.

Figure 6-24: LimoGreen demonstrator vehicle at MIRA test facility

Figure 6-24 shows a picture of the LimoGreen demonstrator vehicle used by LCVTP for testing purposes. This vehicle is closely related to the series HV analysed. It is a battery based series HV with centrally mounted drive machine and a simple transmission The VSC software interface was reconfigured to sit within the existing LimoGreen VSC. For expedience and safety concerns, only the VEM was deployed to generate the CPS *power_command* signal. Figure 6-25 presents test data taken form the LimoGreen vehicle from an on-road test on the MIRA test track. The test was conducted over the access roads to the main track hence a significant amount of transient driving is measured. This is presented as vehicle speed in the bottom graph of Figure 6-25.

The top graph shows the power traces, Drive power is in blue. This indicates the positive drive power demand. The ECMS calculates the split (middle graph) as a function of demand and SOC (bottom graph). Hence the demand power is supplied by the PPS power alone (red trace, top graph) or as a combination of PPS and CPS power (green trace, top graph). Globally it can be seen that the ECMS allows the SOC to decrease until an asymptote is reached. This shows how the ECMS can switch from charge depleting to charge sustaining seamlessly. Figure 6-26 presents a detail of the LimoGreen measured data. This shows the compromise between ideal *Instantaneous_Optimisation* and real world *Power_Apportionment.* Initially (to 255 seconds) the ECMS command for CPS when demand is low is ignored. This is followed by a period (to 260 seconds) when the CPS is run at a minimum temperature to build up catalytic converter temperature. From this point until 278 seconds, the CPS follows the split. Note that the split varies to maintain the CPS on a high efficiency power point.

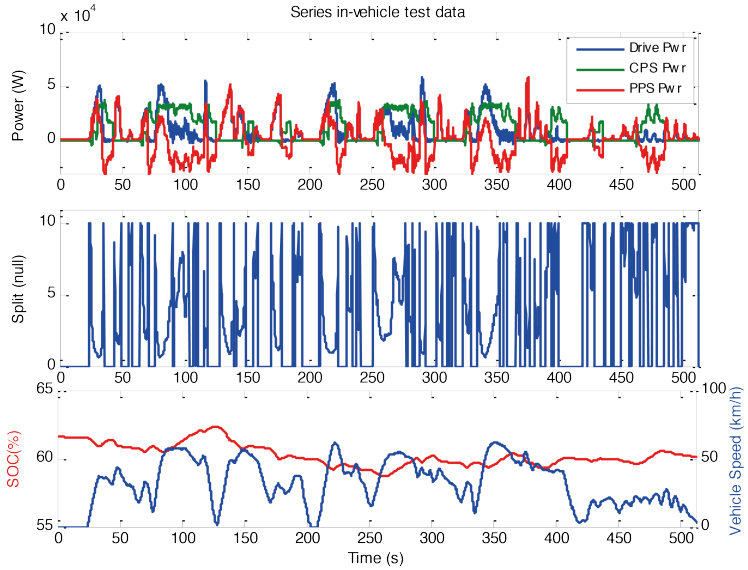

Figure 6-25: On road test data from VSC as deployed onto LimoGreen

At this time, the demand drops and the ideal split is set to zero. In order to avoid repeated engine on and off commands, the *Power_Apportionment* keeps the CPS on. Therefore the CPS does not fully turn off until 300 seconds. Positive drive demand is encountered three times before the end of the trace, but this is either too soon or too low to trigger a full CPS on state,

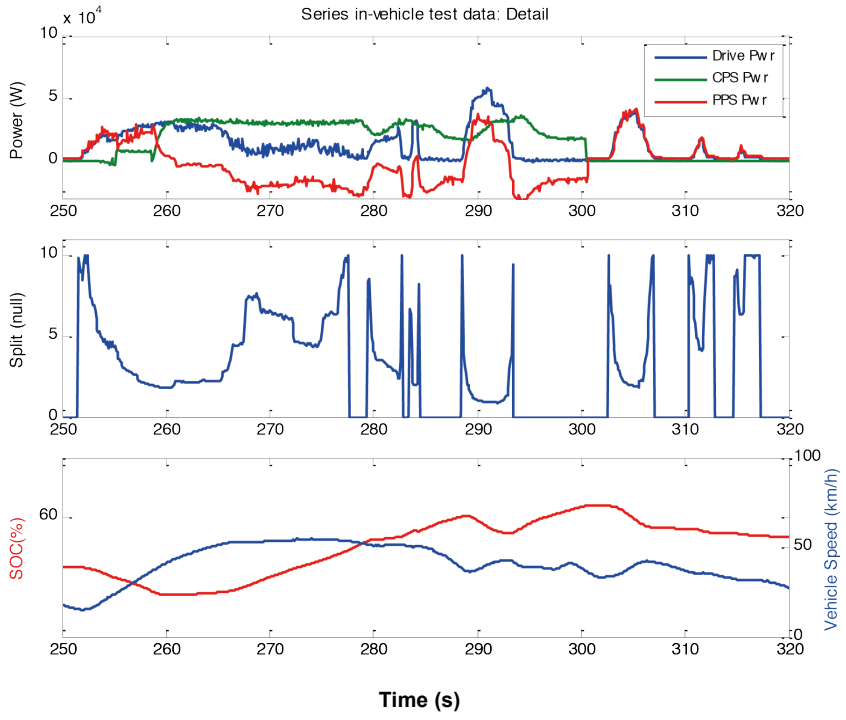

Figure 6-26: Detail of LimoGreen test data

These tests and their results act as scenarios for the series AD which acts as a scenario for the Series RA. Hence they increase confidence in the reusability of the RA, in arguably the most important environment: in-vehicle demonstration.

6.3. Assessment of extendibility of Series RA

This chapter has presented a series AD, one scenario used to test the reusability of the Series RA. This has been further demonstrated as valid in numerical simulation, HIL and on vehicle. Selected functional tests were presented as scenarios for the series AD. Therefore it can be stated that the Series RA is applicable to this instance of Series HV variant. This has not demonstrated that this RA is applicable to other Series HV variants. This section will assess the applicability of the Series RA to the other series variants presented in section 2.4.2.

The three vehicles analysed in the Wren project by Marco and Vaughan centred around a fuel cell based CPS series HVs with a passive, active or compound PPS [16, 46]. The Series RA presented in Chapter 3 is a direct extension of the RA defined by Marco and Vaughan. Therefore by extension, it can be said that the Series RA can be applied to the three vehicles analysed in Wren.

This assertion is valid as the key sub-system boundaries (VEM, VMC, PPS and CPS) and subsequent interfaces (*available, capacity* and *command*) have been carried over from the Wren RA. The extended features of the Series RA are also required in the Wren vehicles also. The fuel cell vehicle will require a 12v system and a HVAC therefore a TPS will exist. All systems defined by Marco and Vaughan can transmit an *actual* signal. None of the vehicle have a transmission therefore the RA transmission placeholder can be omitted. And finally, all vehicles will have some level of powertrain integration with brakes, even if it is a simple as deactivating throttle off regenerative braking.

This brings the demonstrated scenarios in which the Series RA applies to four. However it should be noted that three of these scenarios are very similar. It is in this similarity that the reusability of the RA is founded. The systems are similar because they have been bounded between the storage media and the DC bus and the interfaces are constrained to *available, actual, capacity* and *command*. It is immaterial to the architecture if the CPS *power_available* is from a fuel cell or ICE based CPS. Similarly, the PPS systems to date have mostly been batteries or capacitor system with either passive or active control.

The key question is whether other CPS and PPS variants be bounded and interfaced in the same manner. If so it can be safely asserted that the Series RA is applicable to series HV variants comprising these systems. Finally the drive systems in the three Wren vehicles were similar, with four electrical machines, either inboard or at the hub. The drive system in the series HV presented in Section 6.1, is a single, shaft mounted electrical machine. Therefore it can also be asserted that the RA is robust to drive system configuration. The rest of this section will present architectural models confirming that complex drive systems, gas turbines and flywheels can be encapsulated so that the Series RA is reusable for all series HV variants.

6.3.1. Continuous Power System

The final two CPS options presented in Section **Error! Reference source not found.** not analysed to date are the gas turbine based CPS and the battery based CPS. Firstly the battery based CPS is identical to the PPS version in terms of decomposition, structure

and behaviour. It only exists as a CSP in the context of a high power buffer based PPS such as a capacitor or electric flywheel. Therefore architecturally it does not break the RA.

In terms of response time a gas turbine is much like a fuel cell, but requires a GenSet to convert mechanical power into electrical power, like an ICE. Therefore a gas turbine based CPS will be modelled as the ICE CPS presented in Figure 6-6 and Figure 6-7. Figure 6-27 and Figure 6-28 present the comparable decomposition and context and causality models for a gas turbine based CPS. From the two models it can be seen the CPS is fundamentally different in that it contains a gas turbine as opposed to an ICE. However, careful system bounding has ensured that this difference remains encapsulated within the CPS. This means that the basic interfaces from the CPS manager to VEM of *available*, *actual*, *capacity* and *command* can be retained.

This ensures that the two CPS presented in this chapter can be interchanged which confirms the reusability of the Series RA. It should be noted at this point that the VEM would still need CPS efficiency calibration. As has been discussed in Chapter 5, a running efficiency interface could be mapped from CPS to VEM as part of the Series RA. It is argued that it is considered neither complex nor onerous to expect that VEM needs basic efficiency calibration of the systems under its control.

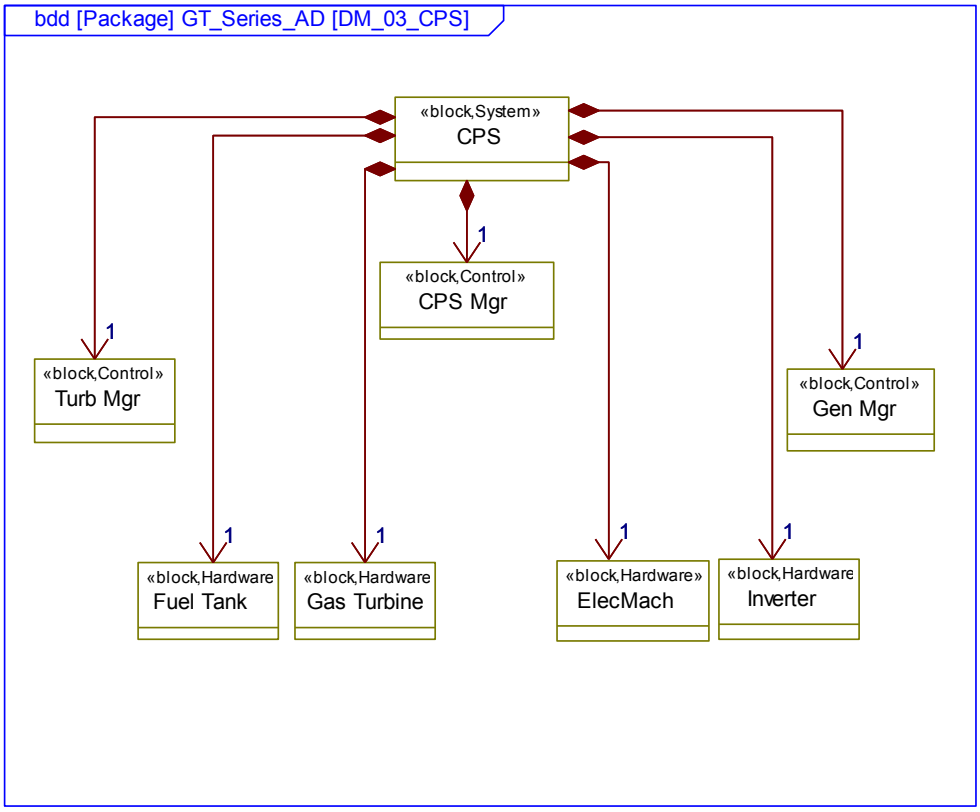

Figure 6-27: AD decomposition model of gas turbine based CPS

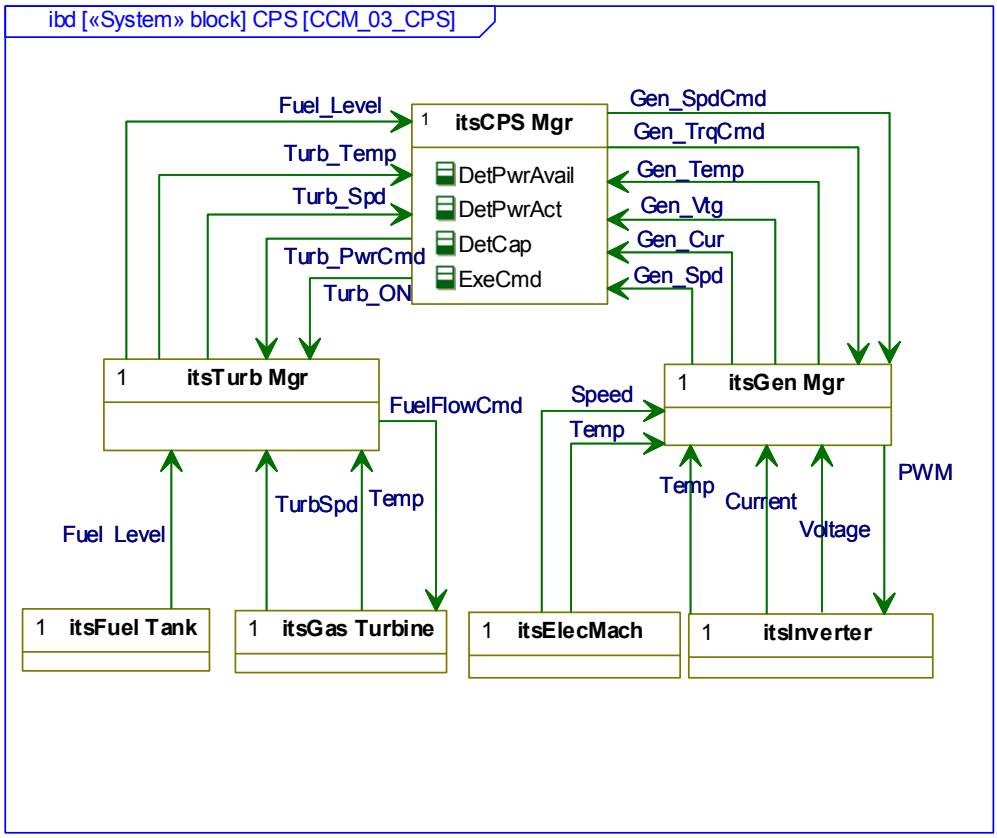

Figure 6-28: AD context and causality Model of gas turbine based CPS

6.3.2. Peak Power System

The final PPS not analysed to date is an electrically mounted flywheel. This system is equivalent to a capacitor in terms of power flow to energy capacity ratio. Also, as it is integrated with an electrical machine, this PPS is an active system. This is similar to the controllable bidirectional converter activated capacitor based PPS presented by Marco and Vaughan in the Wren Project [48].

Figure 6-29 and Figure 6-30 present the decomposition and context and causality models of the electrically mounted flywheel based PPS. As per the battery based PPS earlier in this chapter, the PPS manager must determine total system *power_available*, *power_actual* and *capacity*. The capacity of a flywheel is directly proportional to its speed. However the vacuum level must also be taken into account as it influences the rate of energy leakage. Unlike the battery PPS, this system can be controlled, therefore the PPS *power_command* interface in the Series RA would be retained. The local PPS manager would control the power flow of the PPS by controlling the torque of the electrical machine. This can be done positively to supply power to the DC bus and negatively to draw power from the DC bus

This presents all feasible reversible energy storage systems described in Section **Error! Reference source not found.**. as discussed in Section 2.4.1, other storage systems exist, such as hydraulic accumulators. These types of systems are common on heavy vehicle applications and have been declared outside the scope of this research. However it can

be asserted that applying the same boundary process to a hydraulic storage system results in the same interfaces described in this Thesis.

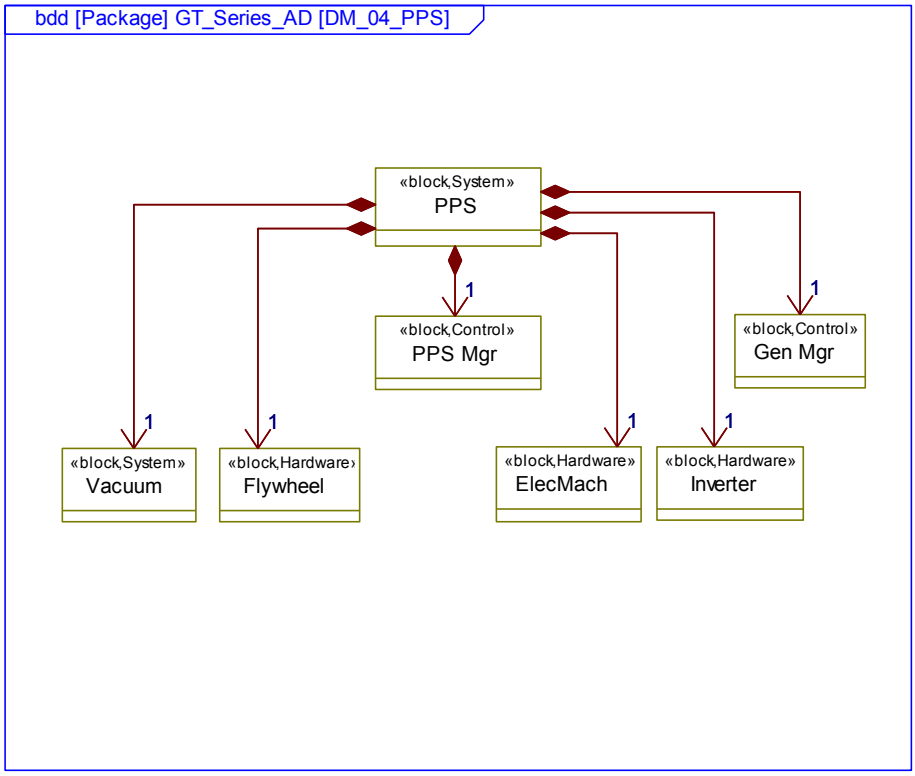

Figure 6-29: AD decomposition model of electric flywheel based PPS

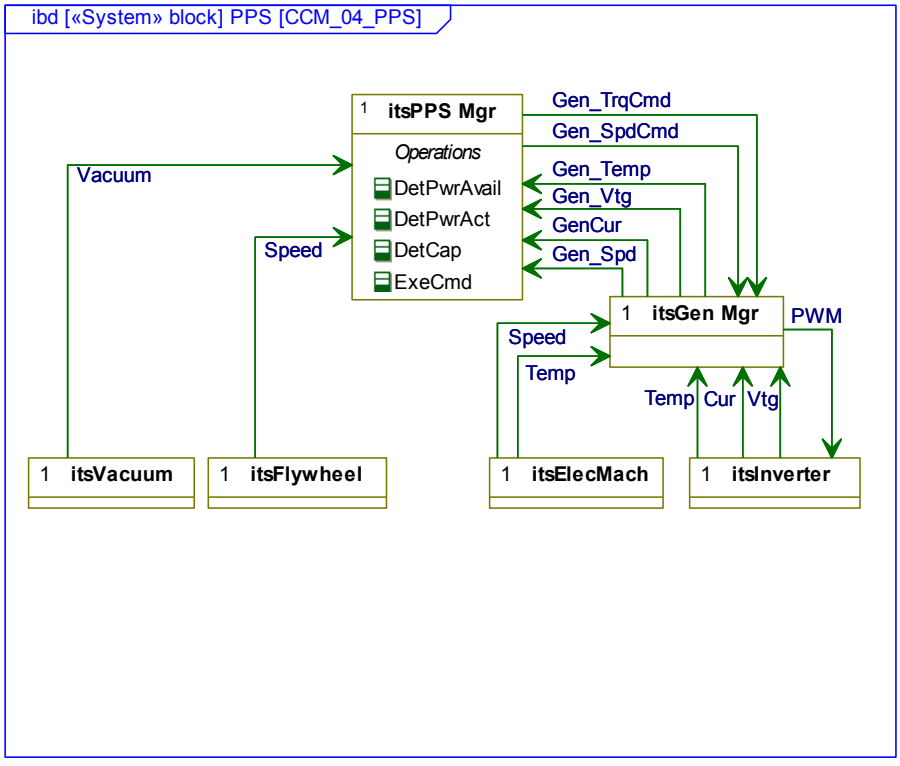

Figure 6-30: AD context and causality Model of electric flywheel based PPS

6.3.3. Drive System

All series HV variants defined in 2.4.2 have an electrical drive system. On a generic level, all defined drive systems must convert DC electrical power to mechanical power, ordinarily through an AC/DC inverter. However drive system may contain more than one electrical machine and this sub-section investigates weather the RA is extendible to multiple drive system configurations, or not.

The series HV presented in Section 6.1 and the vehicles analysed as part of the Wren project (defined in Section 2.4.2) have distinctly different drive systems. The series has a single centrally mounted electrical machine, and the Wren vehicles have four inboard electrical machines or four wheel hub electrical machines [163]. Other Drive systems may contain two or three electrical machines. In some instances it is possible to have more than four electrical machines, such as trailer propulsion or multi axle vehicles.

Figure 6-31 and Figure 6-32 present decomposition and context and causality models of a compounded drive system. The decomposition model defines a new system, the Drive Unit, which comprises an electrical machine, and inverter and a local controller. The drive system is shown to always contain one Drive Unit. However, the drive system may contain more than one Drive Unit, as shown by the multiplicity of the direct composition. In the case of there being only one Drive Unit, an association is shown between the system *Drive_Manager* and the local *Drive_Controller* indicating that they become one in the same. However in the case of multiple Drive Units, a distinct *Drive_Manager* is required to coordinate the torque commands for the multiple instances of the Drive Unit.

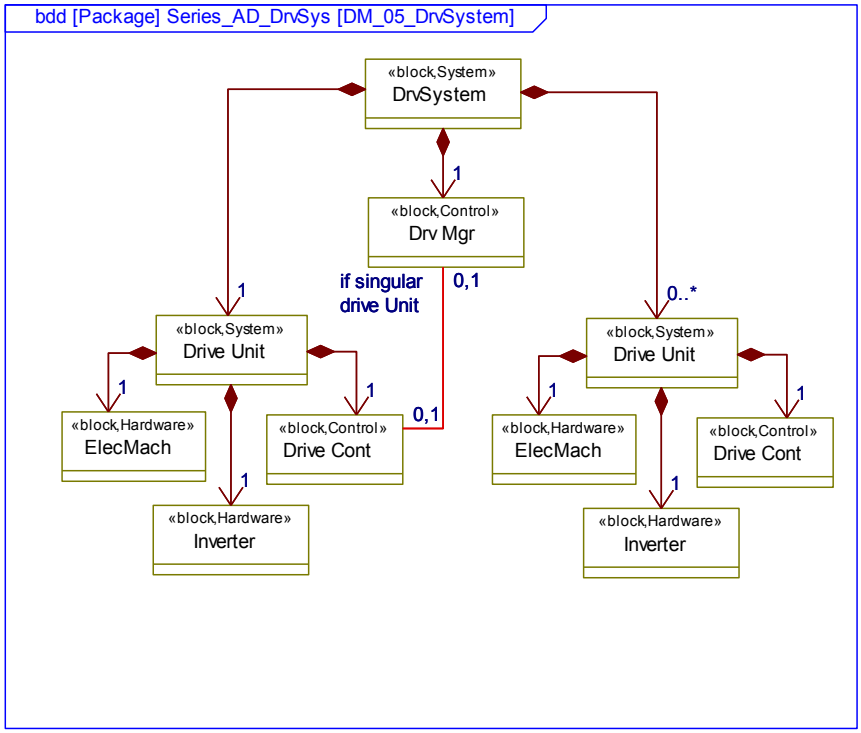

Figure 6-31: AD decomposition model of compound Drive system

Figure 6-32 shows how the local control loop informaiton is contained within the Drive Unit, but key informaiton (possibley at a lower bandwith) is communicated to the *Drive_Manager* to determine the *torque_availabel* and *power_actual*[24]. This enables the *Drive_Manager* to coordinate lonitudinal torque demand and possibly in conjucntion with a chassis dynamics controller lateral attidude control or torque vectoring. This functionality is outside the scope of this Thesis, but it is argued that the architecture is extendible to this important future requriement.

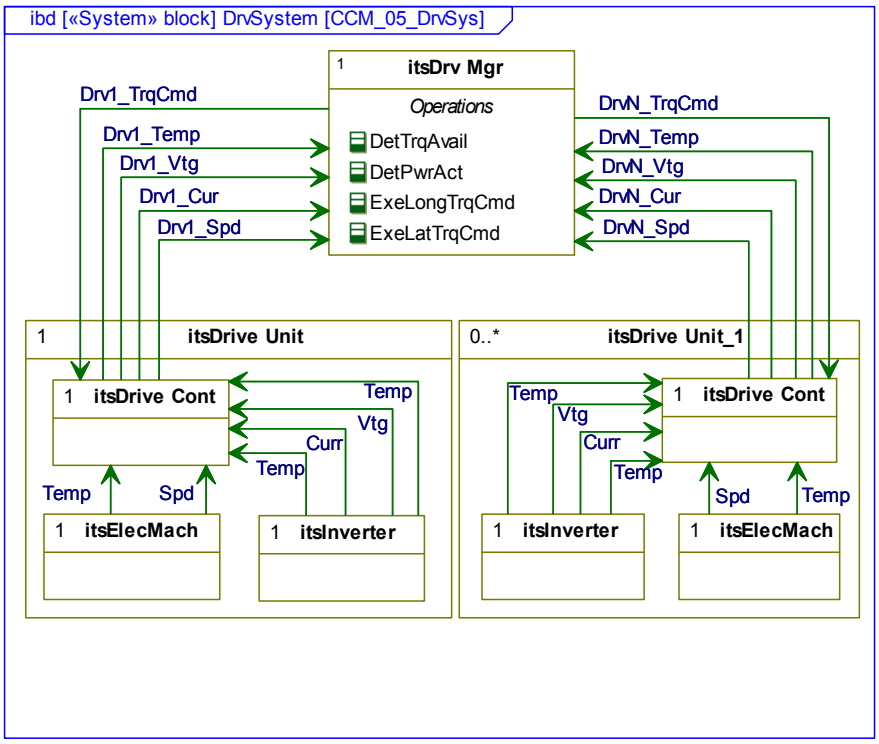

Figure 6-32: AD context and causality model of compound Drive system

6.4. Summary

This chapter has presented work conducted as part of the LCVTP project in the form of a case study. The case study series HV was used to show how an AD could be derived from the Series RA. The issue of CPS system encapsulation was discussed in the context of the LCVTP and the solution proposed here was adopted. The series VSC was developed to a functional level and demonstrated in the simulation, HIL and on-vehicle environments. A selection of functional tests was presented which acts as scenarios for the AD. The selection was targeted to demonstrate key functionality which may have been affected by the architectural partitioning of DD, VEM and VMC.

While the functional tests acted as scenarios for the AD, the AD itself acts as a single scenario for the Series RA. This means that the Series RA has been demonstrated on four scenarios, including the three demonstrated as part of Wren. By inference any series HV

[24] As discussed in Chapter 3, drive *power_actual* is a compound signal comprising *torque_actual* and *speed_actual.*

variant comprising any permutation of the sub-systems presented in the four scenarios is also deemed to be derivable from the Series RA. However, gas turbines flywheels and compound drive systems have not been explicitly demonstrated. These systems were analysed to show that they could be bounded to align with the interfaces of the Series RA. Based on this it can be asserted that all the Series HV permutation defined in Section **Error! Reference source not found.** can be derived from the Series RA. This assertion should be confirmed through demonstration by functional deployment. However, this constitutes future work.

This chapter addresses the first hypothesis presented in Chapter 1. This states that the Wren RA can be extended to an ICE and other Series HV variants and it can be extended to include real world functionality. Chapter 3 and this chapter has addressed this hypothesis. Chapter 3 defined an extension to the Wren RA, referred to as the Series RA. It was asserted in Chapter 3 that all Series HVs could be developed from this RA. This chapter demonstrated the validity of this assertion by designing and developing a series HV VSC using the Series RA as a template. This deployment was demonstrated in simulation, HIL and on-vehicle. A select set of tests was used to ensure that the architected system is functionally sound. The tests were specifically selected to stress functionality which may have been affected by the architectural decisions.

Developing a VSC to deployment for every possible permutation of Series HV is beyond the scope of this research. Therefore it cannot be declared with absolutely certainty that the Series RA is applicable to every variant. However, the act of sub-system encapsulation ensures that the differences between variants can be masked by the generic interfaces. This was demonstrated by architectural analysis. It confirmed that fuel cell, ICE, gas turbine, flywheel battery or capacitor systems can be constrained to a generic set of interfaces. Therefore it is argued that the Series RA is applicable to all series HV variants. The hypothesis has not been disproven.

7. Deployment of Parallel RA

This chapter presents two case studies of parallel HVs deployed as per the Parallel RA guidelines set out in Chapter 4. The first parallel HV is a pre-transmission parallel vehicle, which was studied as part of LCVTP. The second concept vehicle is a hypothetical post-CVT-transmission parallel HV. These two vehicles were chosen as they represent the extremes of parallel HV variants. These two deployments act as scenarios for the Parallel RA. This chapter in part addresses the second hypothesis, that the Series RA is extendable to parallel HVs. Chapter 4 presented analysis that this hypothesis is false. The resulting hypothesis, that a new Parallel RA exists which reuses much of the structure and content of the Series RA, was addressed in Chapter 4. This chapter presents the analytical and numerical evidence which supports that hypothesis.

The first two sections present the architectural deployment analysis and the numerical simulation respectively, for the pre-transmission Parallel HV. The second two sections present the analysis and simulation respectively for the post-transmission parallel HV.

7.1. Case study 2a: Deployment of a pre-transmission AD

This section presents the deployment of a pre-transmission AD of a parallel plug-in HV analysed as part of LCVTP from the Parallel RA. The physical and system domain models are presented here, while the control domain models are presented in Appendix H. The discussion on encapsulation from the last chapter is continued in the context of the PPS.

7.1.1. System schematic

Figure 7-1 presents the system schematic of the pre-transmission parallel plug-in HV. This model extends the simpler version presented in Figure 2-12 by including real-world features. These include a DC/DC converter to the low voltage system, an on-board charger, a low voltage source for an ICE starter motor, a pair of clutches to isolate the ICE and the motor, a discrete transmission and an integrated hydraulic braking system. This vehicle is based on an existing OEM vehicle in the luxury four-wheel-drive class. As mentioned in Chapter 6, the on-board charger is encapsulated within the PPS. The rationale for this will be described in detail later in Section 7.1.3.

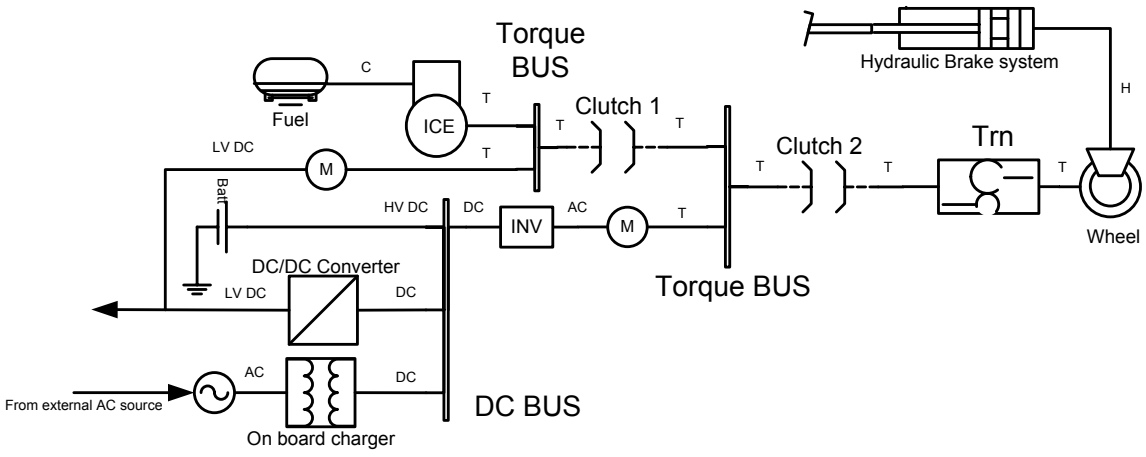

Figure 7-1: System schematic of OEM based pre-transmission parallel HV

7.1.2. System domain models

Figure 7-2 presents the AD decomposition model of the pre-transmission parallel powertrain system. When comparing this to the Parallel RA as defined in Chapter 4 some differences are apparent. Firstly, as this is based on a real vehicle, the non-ideal braking integration is employed, as per the series AD deployment. The association between the driver and BCU represents this integration.

The DriveLine system now shows a multiplicity of two clutch systems an employment of the multiplicity defined in the Parallel RA in Figure 4-3. The transmission is declared in the DriveLine system, therefore its multiplicity is one. Hence the continuous transmission indicated in Figure 4-3 as part of the CPS is omitted. Therefore the CPS is exclusively an ICE in this instance. The possible inclusion of a continuous transmission within the CPS will be addressed in the second half of this chapter.

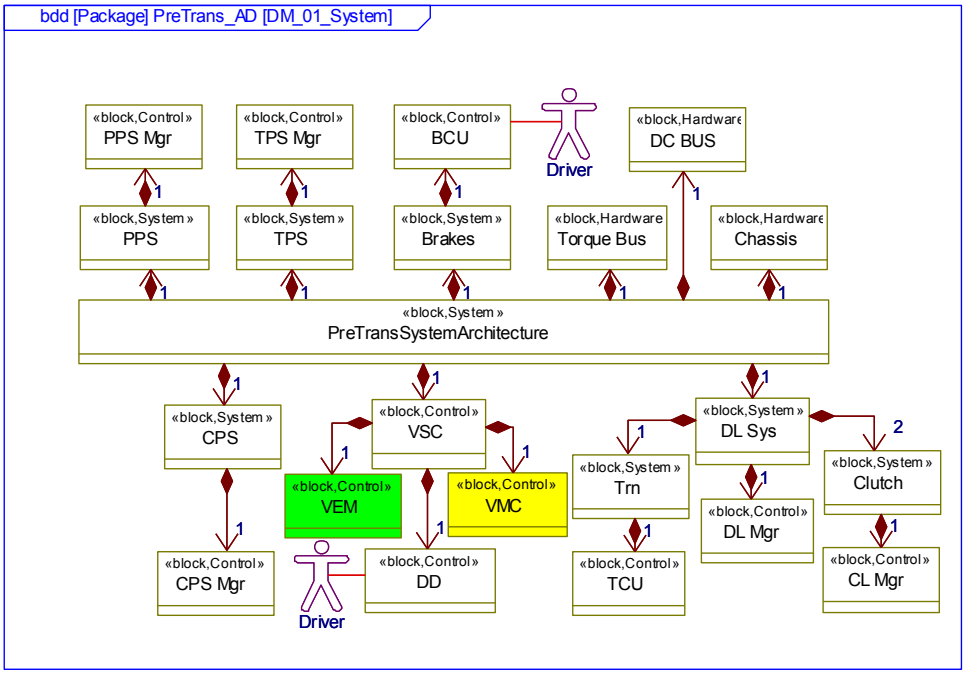

Figure 7-2: AD decomposition model of pre-transmission parallel powertrain system

Figure 7-3 presents the pre-transmission AD context and causality model for the powertrain system. As in previous chapters the VEM and the VMC are highlighted in green and yellow respectively. The obvious difference to the RA is the orientation of the brakes interface where DD receives *regen_torque_demand* from brakes.

The key characteristics of the Parallel RA described in Chapter 4 remain. The driver *torque_demand* is constrained by *torque_available*, which is calculated in the VEM, based on PPS and CPS *power_available* signals. The *torque_command* signals are a function of *torque_demand* from DD and *torque_split* from VEM. The TPS and DriveLine interfaces to the VSC remain as per the RA defined in Chapter 4.

The first new interface in the parallel AD between PPS and VEM is *charge_door*. This is similar to the *charge_status* signal used in the series AD. This *charge_door* signal informs the VSC that the charge door is open, whereas the series AD signal informed that

charging was underway. It is important to note that the PPS *power_available* signal will indicate zero while the system is charging or when the charge door is open. However a redundant path to ensure drive torque prohibition is required for safety. This suggests a requirement for a functional safety architecture layer to complement the functional control architecture layer, part guided by the ISO 26262 process [194]. A detailed discussion on functional safety is beyond the scope of this research. However demonstrating that both options can be deployed within the framework of the RAs is a beneficial learning point from this research.

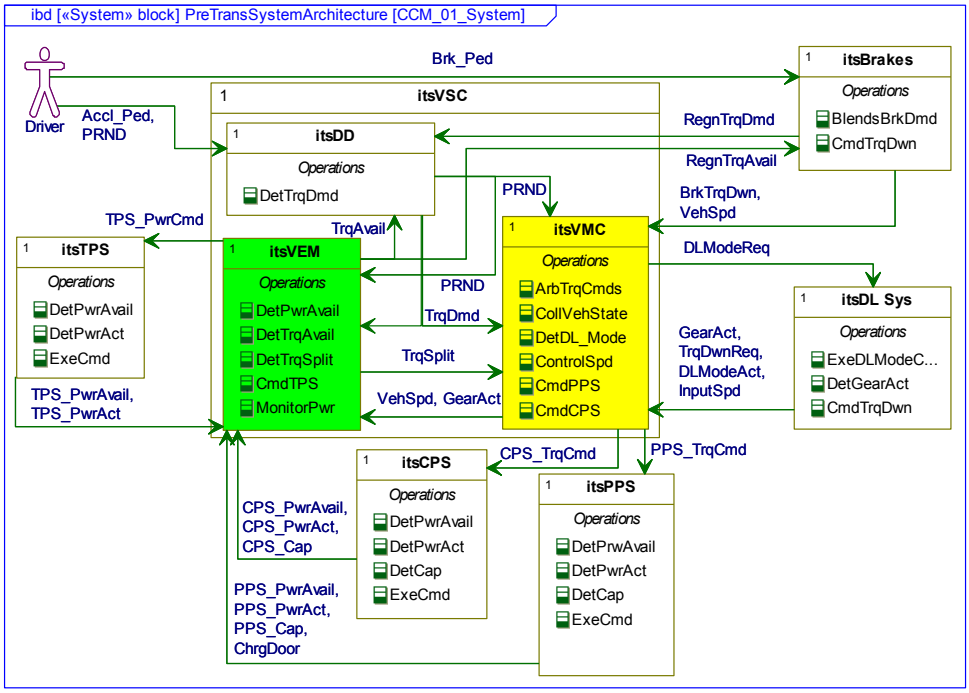

Figure 7-3: AD context and causality model of pre-trans parallel powertrain system

Figure 7-4 presents an example interaction model for the powertrain system of the pre-transmission parallel AD. This model is similar to the Parallel RA model in Figure 4-5. The notable differences are the arrangement of the brakes integration with *regen_torque_available* being communicated to brakes and *regen_torque_demand* returning to DD.

The most striking difference is the inclusion of *charge_door* to the VEM block. This is the second manifestation of this functional safety feature discussed in Chapter 6. This status signal is required to be low otherwise *torque_available* (and *regen_torque_available*) is set to zero. This feature is one of a number of protections against unintended acceleration whilst charging. Others include hard wired, or high voltage interlocks between the battery and the electric machine. This is highlighted here to show the robustness of the interrelationship between *Torque_Available* and the DD. As shown in Figure 4-7, in the Parallel RA this function is housed within the *PowerTorque_Available* block within the VEM, whereas in the Series RA it is a standalone block in the VMC. As discussed in Section 4.3.3, its structural position may have changed between RAs but its functionality remains the same. This is one example of the flexibility of the RA to incorporate functional safety requirements which is an important learning point for

future work. It is important that the functional control layer can be complimented with functional safety and diagnostics requirements. However detailed analysis of this topic is beyond the scope of this research.

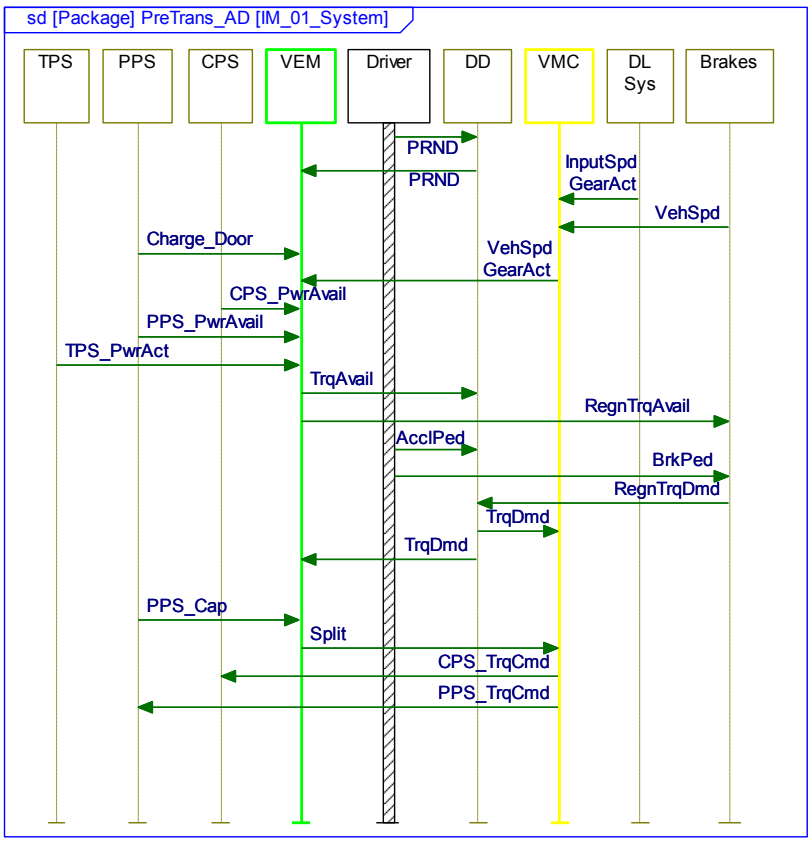

Figure 7-4: AD interaction model of pre-trans parallel powertrain system

7.1.3. Pre-transmission parallel PPS encapsulation discussion

The topic of encapsulation is equally important in the Parallel RA as the Series RA. This section covers two points, the encapsulation of the battery with the drive motor into one universal PPS and the encapsulation of the on-board charger with the PPS, interfacing only with the PPS manager.

Previous patterns of sub-system bounding suggested starting at the storage medium and ending at the point of hybridisation [23]. In keeping with this pattern, the PPS should begin at the battery and end at the mechanical output shaft of the electric machine. Figure 7-5 presents the decomposition model of the PPS. The PPS system comprises the PPS manger, a battery, a charger, and inverter and an electrical machine and if appropriate their local controllers.

Figure 7-6 presents the context and causality model of the PPS showing the interfaces between the PPS components. Firstly it can be seen that the PPS manager acts as a conduit through which the PPS communicates with the VEM how the VMC communicates with it, as shown in Figure 7-3. The presence of this functional block allows the detail of the PPS to be shielded from the VEM and the VMC. A key role of this

block is to determine the total PPS *power_available*. This must be a function of the limits of either the battery or the drive system depending on their limits or de-rating.

Also apparent is that the on-board charger is encapsulated within the PPS. There are a number of considerations which drive this decision, for a parallel plug-in application, as well as series and compound applications. Firstly a charger must be configured for the battery chemistry and is therefore specific to deployment level detail [196]. Secondly chargers must be designed to interface with external grid hardware [197]. Standardisation is being addressed, but at a regional level only, therefore based on the physical interface there may be significant variability to contend with.

Thirdly, the level of functionality of charging capability may differ. LCVTP defined charging options as by Hoke, [198] as:

1. **Passive charging**: where the charger charges the battery at the desired rate as soon as the charger is plugged in.
2. **One-way active charging**: where the charger may partially or fully limit charging depending on grid usage or energy price. This suggests communications integration with the grid infrastructure.
3. **Two-way active charging**: as option 2 but depending on energy price the system may discharge the battery to the grid to generate revenue.

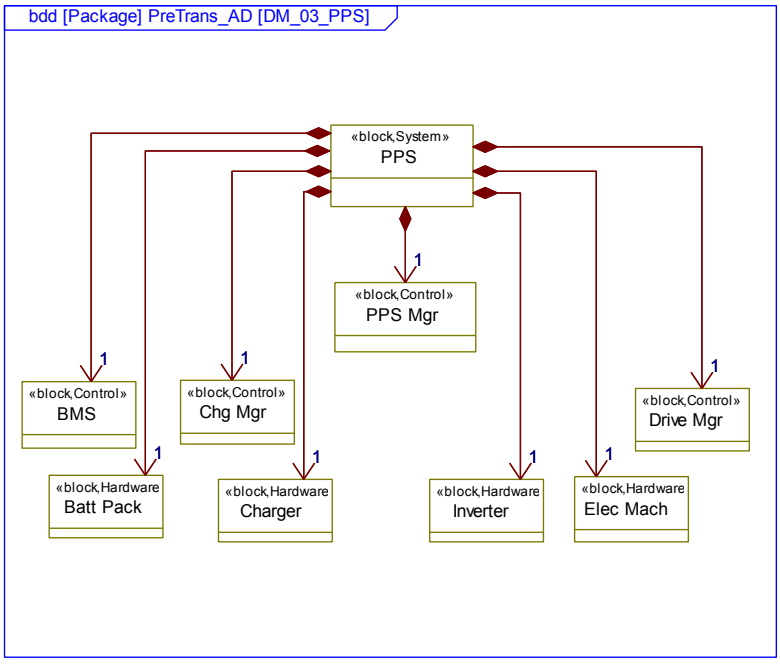

Figure 7-5: Decomposition model of PPS system, including charger

Charging option 1 is presented in this AD but the same encapsulation would apply for all options. Regarding option 2 and 3, there would be a requirement to know the desired time to have the battery fully charged. This information may be driver selectable, would come from HMI, directly or possibly via the VSC. This minimises the VSCs dependency on charger variability.

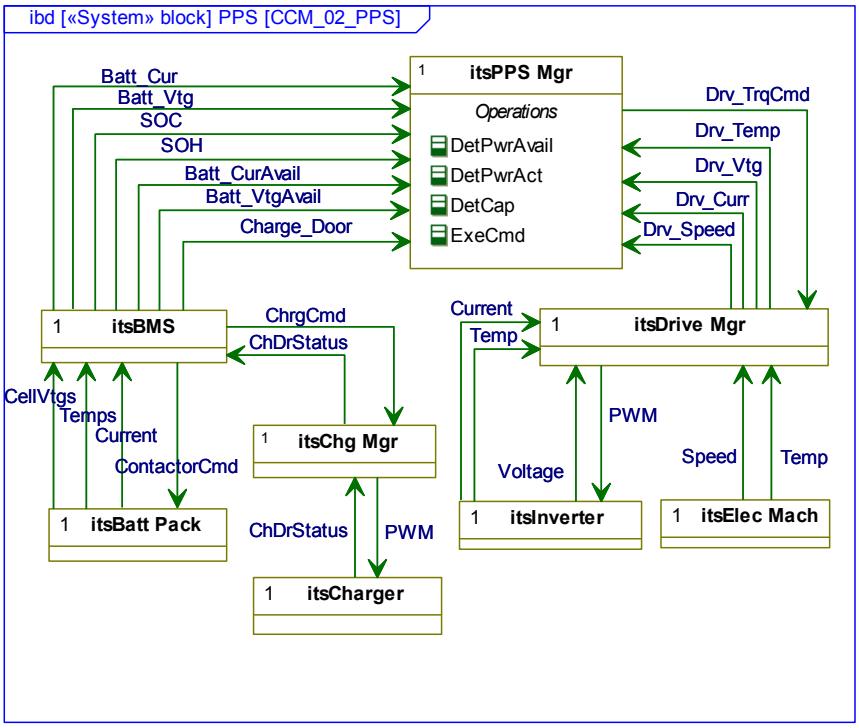

Figure 7-6: Context and causality model of PPS system, including charger

In summary, this section has demonstrated the Parallel RA being developed into a deployment specific AD. For brevity the control level AD views have been presented in Appendix H. It shows that real-world systems do not contravene the RA guidelines. Also the discussion around encapsulation was extended to address the PPS in the context of parallel HVs and the concept of encapsulating on-board chargers.

This deployment has acted as a scenario for the Parallel RA. To build the confidence that this RA is valid, the following section will present outcomes from a numerical simulation developed form the AD presented here. Results of tests are shown which act as scenarios for the AD.

7.2. Case study 2a: Numerical validation of pre-transmission parallel AD

This section presents the deployment and numerical results for the pre-transmission parallel HV studied as an extension to the LCVTP.

7.2.1. Simulation Deployment

Based on the AD described in the last section a VSC for a pre-transmission parallel HV, described in Figure 7-1, was developed. This was developed and deployed within the Simulink based simulation environment. The parameterisation of the plant models was guided by the LCVTP project partners.

Figure 7-7 presents the highest level of abstraction for the pre-transmission parallel VSC. Comparing the second (lower level) view with the corresponding view in Figure 6-12, shows that the key high level functional blocks of DD, VEM and VMC are present. Also the Thermal Management block is retained, as this placeholder is usually needed and will always remain separate to the other three blocks. However the CPS Manager

(shown in Figure 6-12) is now omitted. As has been discussed, the inclusion of the CPS manager was a project specific compromise and is not carried over here. Other than this omission the two VSCs are identical at this level of abstraction.

This observation highlights the importance of abstraction. Attempting to define a universal RA at the levels of abstraction presented in Figure 6-12 or Figure 7-7 would be trivial and valueless. The RA could describe all HVs yet would be unable to define the minimum set of requirements for a full deployment. The RAs set out in Chapters 3 & 4 are defined to a deeper level which differentiates the HV configurations and outlines the key requirements for successful deployment, as will be demonstrated here. The key benefit of this is the ability to crosscut the architecture at multiple levels of abstraction, both vertically and horizontally.

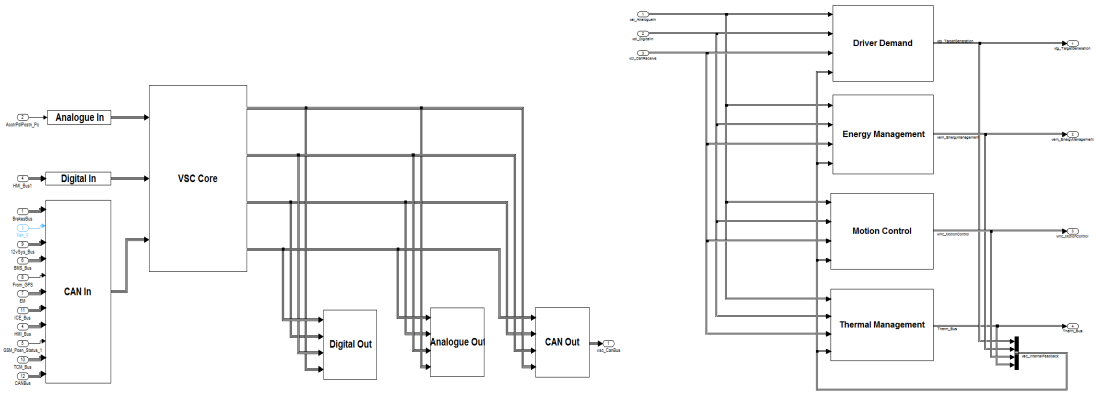

Figure 7-7: Simulink deployment of pre-transmission parallel VSC

The key differences between the series and parallel VSCs reside within the VEM and VMC blocks. As described in Chapters 3 & 4, the VEM block reamins largely the same. However as described in Section 4.3.3, the *Torque_Available* block now resides within *PowerTorque_Available* block, creating a different hierarchical grouping of class, wich lies within the VEM, as shown in Figure 7-8. The *Torque_Available* block is a stand alone block within the VMC in the Series RA.

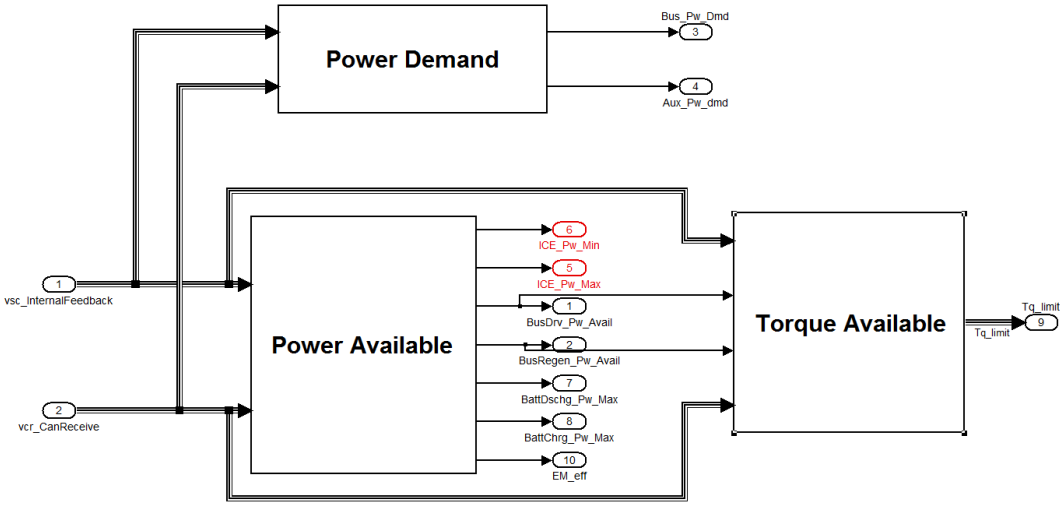

Figure 7-8: Internal view of Parallel *PowerTorque_Available* block

Apart from embedding the *Torque_Available* function within the *PowerTorque_Available* block, the VEM remains largely the same. The *Power_Apporionment* contains less fucntionality as it only comands the TPS. However, as described in Chapter 4, the VMC is distinclty different, as is the interface between VEM and VMC. Figure 7-9 is clearly different to Figure 6-14. This key difference is born out of the requirement to couple two distinct torque sources. Also it is essential that one or both of these torque sources can be decoupled from the drive wheels. This usually requires driveline clutches which are locally controlled but governed by the *Driveline_Mode* block within the VMC. It is the funciton of this block to manage transitions between driveline states such as hybrid mode, EV only mode and charge while stationary mode.

When the driveline mode is set, *Torque_Apportionment* is in full control of the two torque sources. However when states are in transision, the *Speed_Control* will assume control. As per Figure 6-14 The *VMC_Mode* block is retained. This manages the startup sequence across the VSC and the rest of the system. As discussed, this can be deployment specific and therefore is not included in the RA.

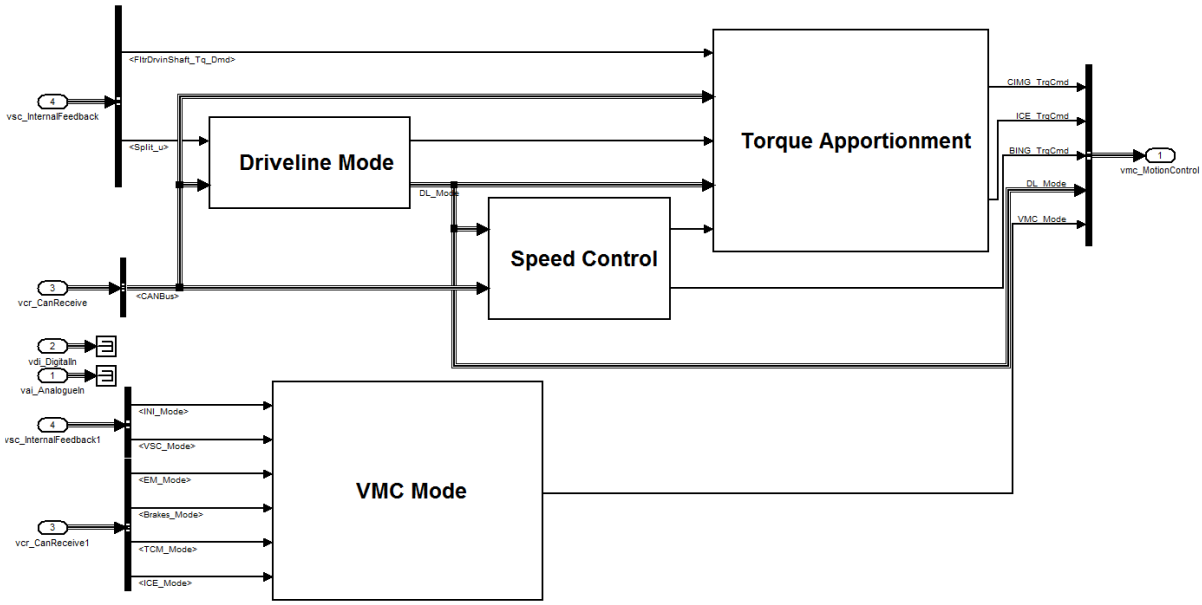

Figure 7-9: Deployment of Parallel VMC

7.2.2. Driveline functionality

Specific to parallel HVs is a complex driveline which is necessary to demarcate the key operating states of the HV system. In a series HV, activating or deactivating the CPS has no direct effect on the driveline of the vehicle as it is decoupled. This is not the case for parallel HVs. The CPS in this case study is an ICE which when deactivated must have a speed of zero. If VEM requires the CPS to be engaged then it must accelerate the CPS to the speed of the clutch before it can be engaged. A pre-transmission parallel driveline can also have a torque converter or a clutch upstream of the transmission. In the case of the vehicle being analysed here, a clutch is chosen as it reflects the project partner target vehicle, therefore it must deliver significant slipping to emulate a torque converter.

Figure 7-10 shows results from an acceleration test conducted on a pre-transmission plant model developed externally to this research. The ICE and drive dynamics are included. The ICE dynamics represent air-path and fuel transport delay as defined by the project partner. The drive dynamics is represented by a first order response, an order of magnitude faster than the ICE dynamics. The gross vehicle dynamics are also included. However, only the impact of the VSC architecture and control, which were developed as part of this research, are discussed here. This test shows how the system transitions between driveline states and manages gear-shifts. Initially the vehicle is at rest and the two clutches are open. The CPS is at rest and the PPS is 'idling' at 30 rad/s. The torque output from the PPS is negligible at this point.

Initially the demand results in the PPS being accelerated to 100rad/s. At this point vehicle motion is being generated by Clutch 2 slip torque input to the transmission. At 2.5 seconds, the demand is high enough to initiate the CPS, reflected as an CPS torque output which is not incorporated into the total transmission torque. At about 3 seconds Clutch 1 is fully engaged and the CPS torque is accounted as part of the total torque.

At 4 seconds Clutch 2 is fully engaged. This represents a deployment specific decision to use a highly slipping clutch to emulate a torque converter. The vehicle in question is an adaptation of an existing ICE only vehicle with an automatic transmission and torque converter. The removal of the torque converter was necessary to allow PPS charging when the vehicle is at rest. However, as much of the system is retained, including a complex transmission with TCU, the replacement clutch needs to slip as much as the original torque converter. From 4 seconds both clutches are closed and the vehicle is operating under full *Torque_Apportionment* control. This is interrupted momentarily for gear shifting. At 18 seconds the vehicle has reached a cruise speed (linearly proportional to transmission speed), which is indicated by a drop in total torque. Throughout the gearshifts the PPS assumes the bulk of the step change in demand. This is based on its superior transient response and increased CPS emissions under transient conditions.

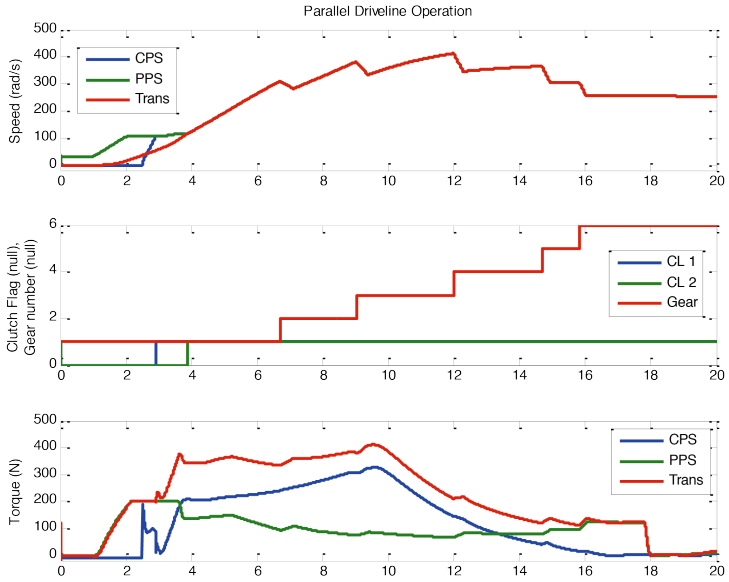

Figure 7-10: Parallel HV driveline functionality analysis

7.2.3. Pre-transmission parallel system testing

As per the series AD testing, the key scenario is one which highlights the cooperation between VEM and VMC. A short drive cycle, (the United Nations Economic Commission for Europe urban cycle ECE-15 (ECE) section of the NEDC) is repeated with the same initial SOC and altered SOC penalty weighting for the ECMS. This has the effect of forcing the ECMS to allow the battery to discharge, maintain the SOC around a fixed point, or to raise the SOC to a higher level. This is referred to as Charge Depleting (CD), Charge Sustaining (CD) and Charge Recovery (CR) respectively. This functionality has been discussed In Section 5.1 and will be addressed in more depth in Section 7.4.2. The system is further tested by running it over the ECE cycle where the speed vector is gained by a factor of 1.4 to show how the system responds to electrical system power saturation.

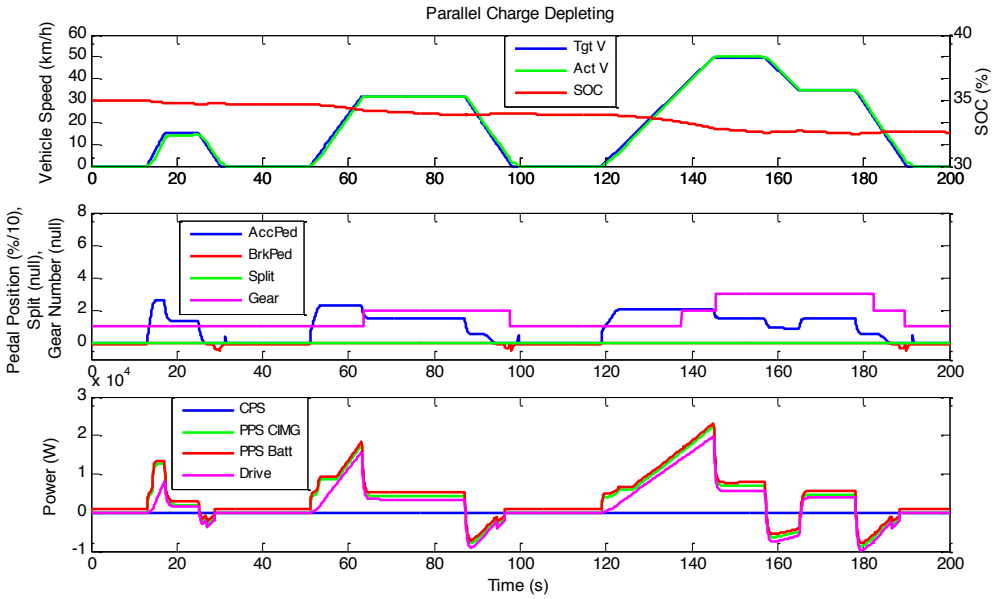

Figure 7-11: Parallel VSC over ECE, CD, a) states, b) inputs c) powers

Figure 7-11 presents the results of the parallel VSC running over one cycle of the ECE. Figure 7-11a shows the target and actual speed traces and is overlaid by the battery SOC. Figure 7-11b comprises the pedal positions, ECMS split and gear number. For clarity the pedal position values have been reduced by one order of magnitude. Figure 7-11c shows the power traces of the CPS, the PPS Battery, and the PPS Crank Integrated Motor Generator (CIMG). The Drive power trace is an artificial signal which reflects the mechanical power at the driven shaft.

It can be seen that the power being drawn for initial pull away differs form the Drive power. This indicates a slipping clutch. Also. There is a constant 800W power draw through the TPS. The remaining difference between the two PPS powers and Drive power is running efficiencies of the PPS Battery and PPS CIMG and is in the order of less than 10% total. There is minimal application of the brake pedal due to the inclusion of a throttle-off negative torque command.

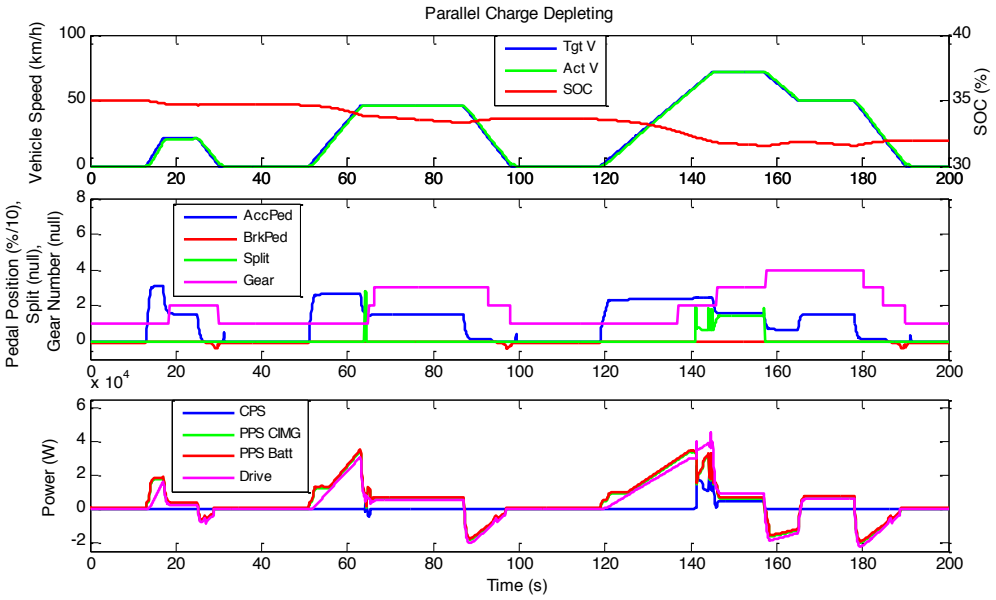

Figure 7-12: Parallel VSC over ECE+40%, CD, a) states, b) inputs c) powers

Figure 7-12 shows an example of the parallel VSC as driven over the ECE cycle which has been multiplied by 40%, resulting in a higher demand on the system. Throughout most of the cycle the split remains zero, which indicates the vehicle is operating as an EV.

On two occasions the split increases, reflecting the PPS CIMG power saturation, which coincides with continued acceleration approaching the higher speeds. In the first case, at about 65 seconds the split command is too short in time to complete an CPS initiation and is ignored. In the second instance, at 140 seconds, the CPS is engaged and the CPS assists the PPS CIMG for the final portion of the acceleration. For drivability the CPS is held on until a braking event is reached.

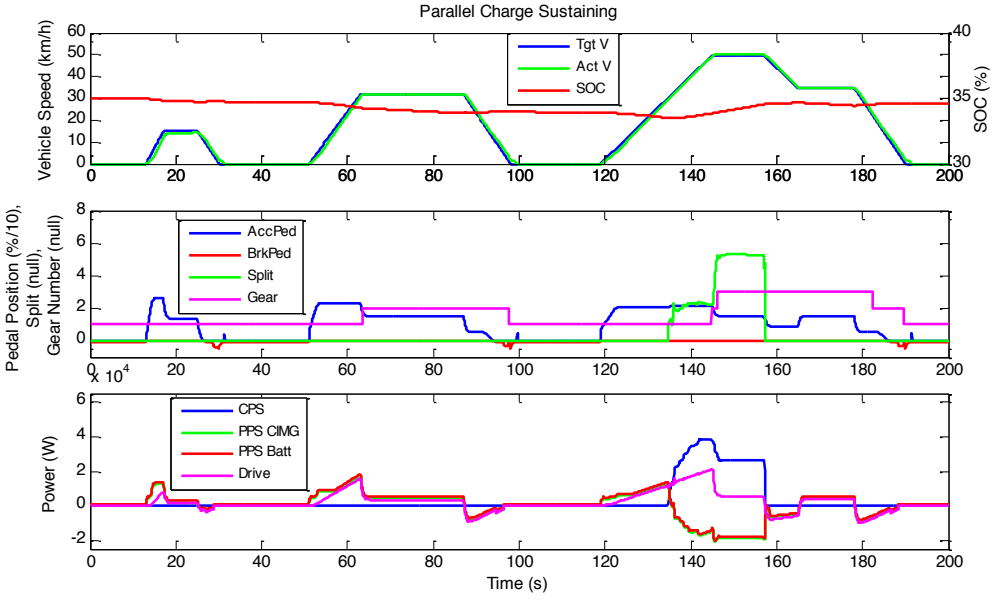

Figure 7-13: Parallel VSC over ECE, CS, a) states, b) inputs c) powers

Figure 7-13 shows the same system tuned to operate as in a CS manner over the ECE cycle. This tuning parameter can be pre-set for a particular minimum SOC level or can be actively controlled by *Predictive_Optimisation*. This functionality will be analysed further in section 7.4.2. The initial and end SOC is about the same. This requires the CPS to be engaged when it is most efficient to do so. The ECMS allows the PPS CIMG to manage most of the acceleration. However when the power demand is high enough for efficient CPS operation, it is engaged. Most of the charging occurs when the vehicle is cruising, this is indicated by a modest Drive power with a high CPS power and a negative PPS CIMG and PPS Battery powers.

Figure 7-14 shows the system operating in a CR manner. It can be seen that the split values are relatively high and the CPS is normally delivering more than the required Drive power. As discussed earlier, this is an unusual but potentially necessary mode in which to operate the system. As a scenario it is useful to demonstrate the cooperation between the two key system requirements of energy management and motion control. When the three scenarios are viewed in context, it can be stated that the system can successfully manage the energy flow as required without affecting the delivery of demanded drive torque.

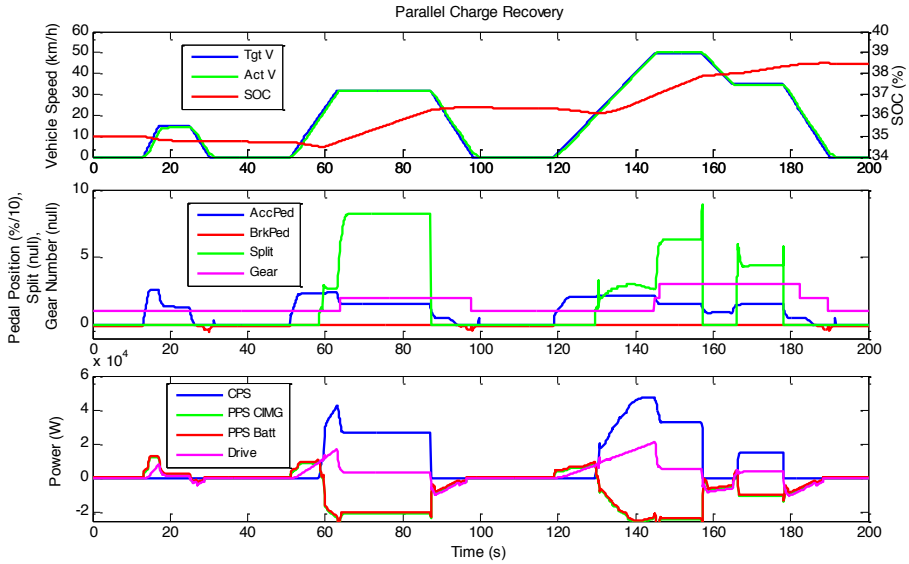

Figure 7-14: Parallel VSC over ECE, CR a) states, b) inputs c) powers

The scenarios presented in this section do not encompass an exhaustive suite which would demonstrate the full functionality of this control system. As per the methodology defined in the Section 2.2.5, it is only necessary to demonstrate the impact of the architecture on the relationship of the high level requirements of the VEM and the VMC for a single deployment. It will require further deployments to build confidence in the broad applicability of the Parallel RA.

The next section directly addresses this point. The system studied so far in this chapter is a discrete ratio pre-transmission parallel HV. The next two sections addresses the architectural and functional issues presented by the inclusion of a variable ratio post-transmission parallel HV.

7.3. Case study 2b Deployment of a post-transmission AD

This section presents the deployment from the Parallel RA of a hypothetical post-transmission parallel HV with a continuous transmission upstream of the torque bus. This type of vehicle is representative of one of the parallel HV variants described by Rahman, [104]. This parallel HV variant is the opposite to the pre-transmission described in the first half of this chapter. This was chosen to demonstrate the flexibility of the Parallel RA across the full scope of parallel HVs.

7.3.1. System schematic

Figure 7-15 presents the system schematic of the hypothetical post-transmission parallel HV with a CVT. Many features of the pre-transmission HV presented in Figure 7-1 are present. There is an on-board charger, a DC/DC converter, a low voltage supply to an ICE starter motor and an integrated hydraulic braking system. However the clear distinction is the location of a continuously variable transmission upstream of the hybridisation torque bus. This enables the ICE speed to be decoupled from the vehicle speed, within the limits of the CVT. This in important distinction as the ICE CVT combination can then be grouped as the CPS and fed with a power command.

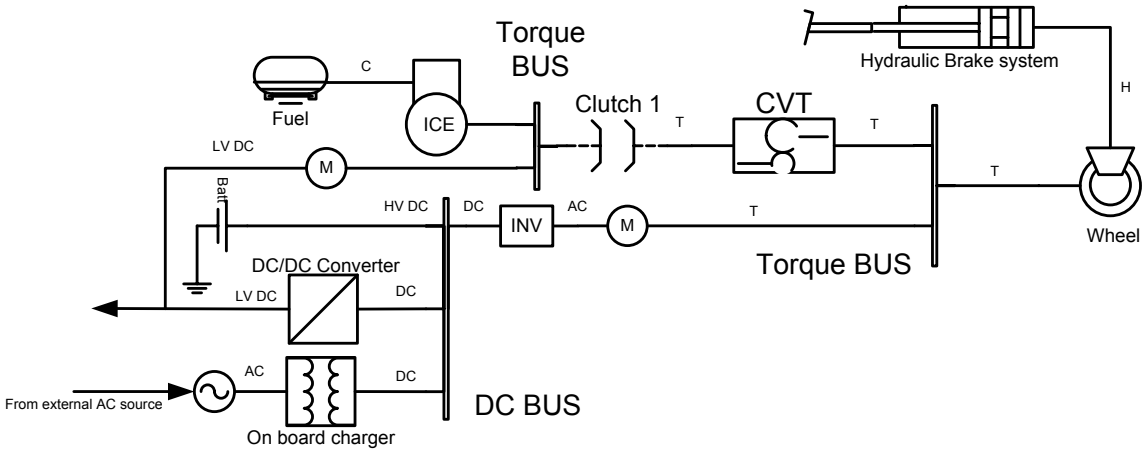

Figure 7-15: System schematic of post-transmission parallel HV with CVT

7.3.2. System domain models

Figure 7-16 presents the system decomposition model for the post-transmission parallel HV deployment. This has been directly derived from the Parallel RA defined in Chapter 4. As this is a hypothetical vehicle, the ideal braking integration is used. Hence the driver is only associated with the DD block. When comparing this to Figure 4-3, it can be seen that the transmission system in the DriveLine system has been omitted and the continuous transmission within CPS has been retained. The multiplicity in Figure 4-3 indicates that these two transmissions are mutually exclusive. The DriveLine system is now reduced to one clutch, and this is indicated by the multiplicity in Figure 7-16. Also it is expected that the DL Manager and the Clutch Manager may be rationalised in this instance as per the drive manager and drive controller in Section 6.3.3. The rest of the decomposition model is an exact redeployment of the Parallel RA.

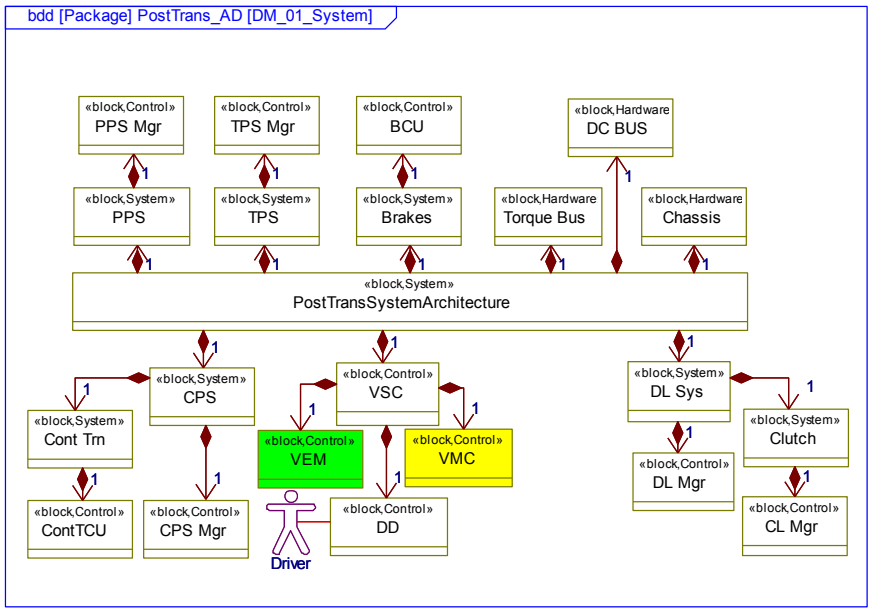

Figure 7-16: AD decomposition model of post-transmission parallel powertrain system

Figure 7-17 presents the context and causality model for the post-tranmsission parallel HV deployment. Firslty, it can be seen that the ideal brakes integraiton is used. The only other difference between this model and the RA model in Figure 4-4 is the CPS and PPS command signals. PPS receives a *torque_command* and CPS receives a *power_command.* This enables the CPS to be operated along the best BSFC curve. In otherwords, the same ECMS methodology utilised in the series application, described in Chapter 6, is used for this application.

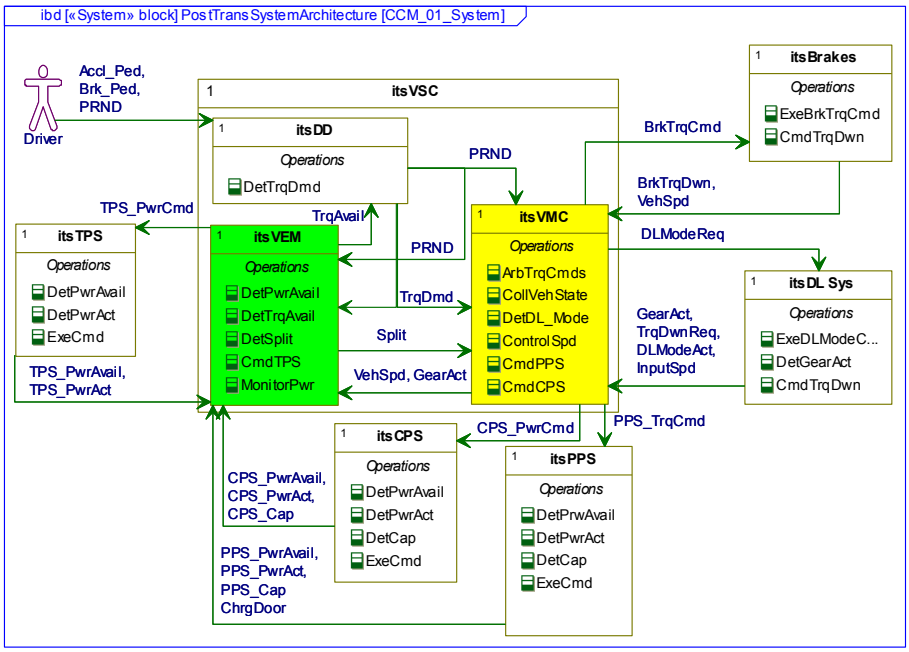

Figure 7-17: AD context and causality model of post-transmission powertrain system

Figure 7-18 presents the interaction model for the same deployment. This model is similar to both the RA and pre-transmission models in Figure 4-5 and Figure 7-4. The

model shows both the ideal brake system integration, and how the charge door status can inhibit motion. However it also shows that the VMC can be used to issue a *power_command* to the CPS.

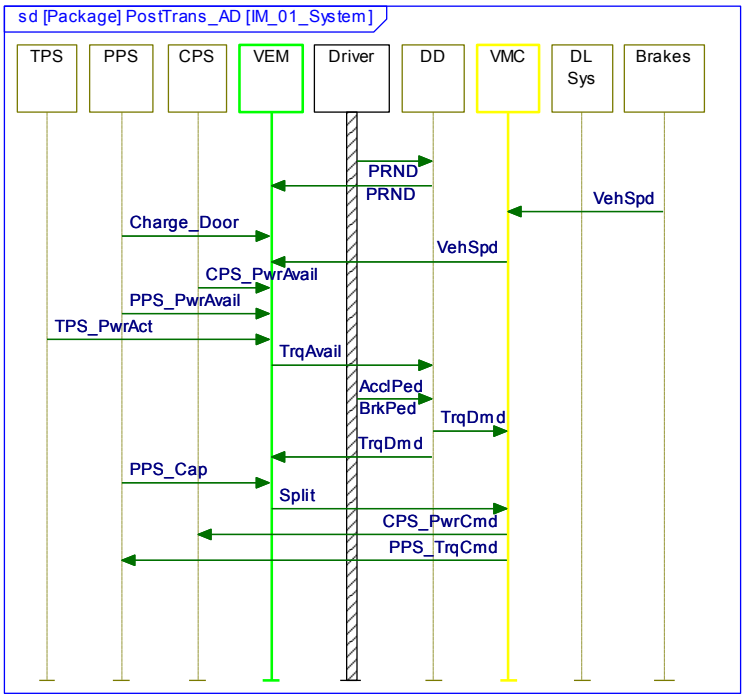

Figure 7-18: AD interaction model of post-transmission parallel powertrain system

As before the control domain models are presented in Appendix H. However it should be noted that the *Instantaneous_Optimisation* functional block has been omitted. This function was developed as part of the LCVTP but outside the bounds of this research activity. The omitting of this function demonstrates the robustness of the RAs and the flexibility of the ECMS approach. As discussed in Section 2.3, the ECMS can act as a standalone EM strategy or it can be controlled in real time by adaptive or predictive control. Separating out the *Instantaneous_Optimisation* and *Predictive_Optimisaiton* blocks ensures that the RAs can incorporate any desired function, or none as basic ECMS is acceptable.

The next section continues the encapsulation discussion specifically focusing on the CPS encapsulation in the context of an upstream continuously variable transmission.

7.3.3. Post-transmission parallel CPS encapsulation Discussion

As mentioned, this deployment contains a CVT upstream of the hybridisation torque bus. This enables the transmission to be encapsulated within the CPS. The advantage of this is the ability to maintain the ICE on the BSFC line, and in doing so utilise the simpler ECMS methodology outlined in Chapter 5 and deployed in Chapter 6. This alteration is allowed as it results in a *power_command* from the VEM to the CPS which has been previously defined in the Parallel RA.

Figure 7-19 presents a decomposition model of the CPS with the encapsulated CVT system. For completeness the fuel tank and the ICE starter motor hve been included. The

continuous transmission system comprises a CVT and a local transmission control unit. As with all other encapsulated systems described previously, there exists the need for a governing CPS manager.

Figure 7-20 shows how the CPS manager acts as a conduit between the CPS and the rest of the powertrain system. The same generic interfaces between CPS and the VSC are retained, (*available*, *actual*, *capacity* and *command* are shown in Figure 7-17). It shields the rest of the system from the detail of the CPS. The CPS manager has the required speed information to determine an ICE *torque_command* and CVT *ratio* for a given CPS *power_command*.

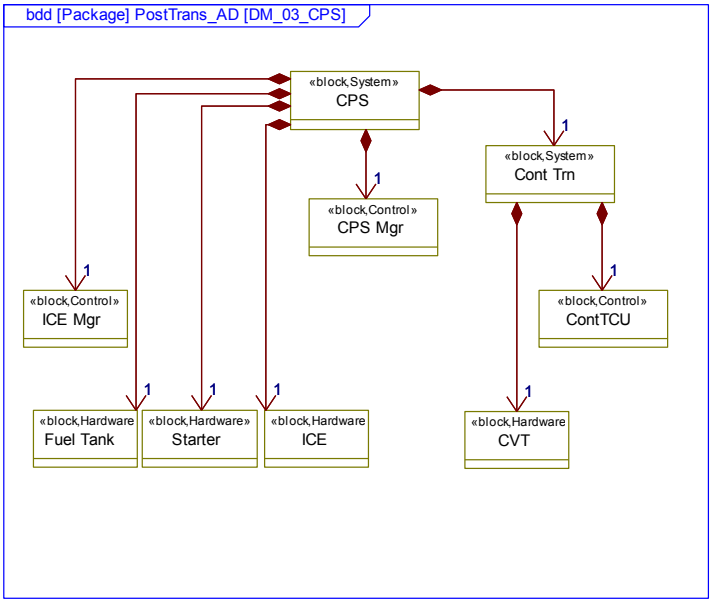

Figure 7-19: Decomposition model of CPS system including CVT

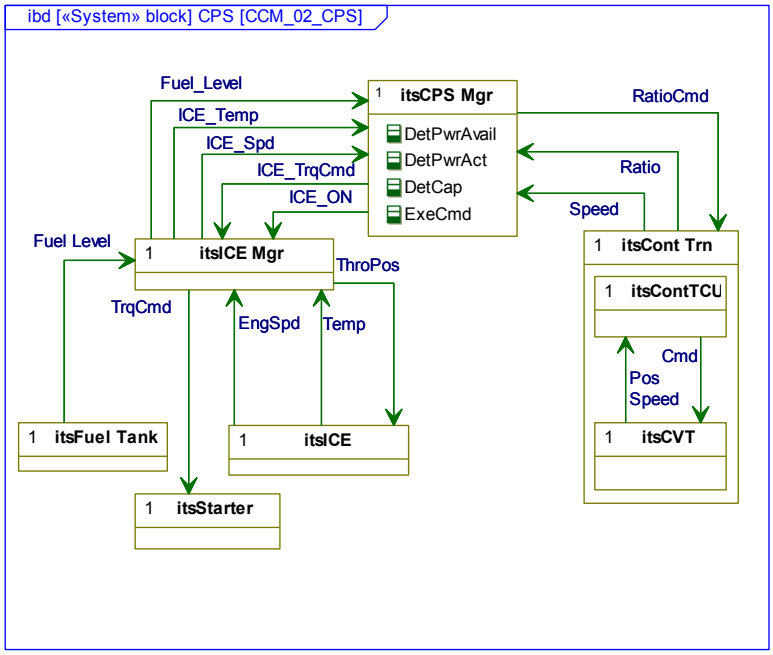

Figure 7-20: Context and causality model of CPS with CVT

7.4. Case study 2b Numerical validation of post-transmission parallel HV

As per previous numerical analyses, a select group of tests are presented to demonstrate that the architected system is valid. In this section the core functionality of the deployed parallel HV is demonstrated by a simulating over a continuously repeated cycle. This shows how the ECMS reacts to degrading SOC and how the ICE operating point is constrained onto the best BSFC line. Secondly the system sensitivity to the SOC penalty function is analysed. This demonstrates the ease with which this system can be changed from a charge depleting to charge sustaining in real time.

For brevity the step showing the architectural deployment in a Simulink environment is omitted. This has been defined previously in Chapter 6 and earlier in this chapter and discussing it here again adds little to this discussion.

7.4.1. Core functionality analysis for post CVT parallel HV

This test was conducted to determine the system response over a continuous cycle. Plug-in hybrids can produce excellent fuel economy results if they are only driven over short distances, largely relying on CD operation [166]. Therefore it is of interest to assess the system functionality in CS mode, beyond the point where the on-board energy storage is exhausted.

Figure 7-21 presents the traces from this test. Figure 7-21a shows the SOC trace, initialising at 1 or full. The test is ended when the SOC has reached an charge sustaining asymptote of 40%. Figure 7-21b shows the split term from the ECMS. Opposite to what was described in Chapter 5, the split in this deployment is targeted to the drive machine. A split of one means all demand is met by the electrical drive. A zero split means all demand is met by the ICE. Negative split indicates charging. Figure 7-21c shows the speed profile, Artimus Urban, being repeated up to 2500 seconds. Examining Figure 7-21b it can be seen that the average split trends negative over time. This shows that ECMS transitions from CD operation to a blended CD operaiton and finally to a CD operation, seamlessly.

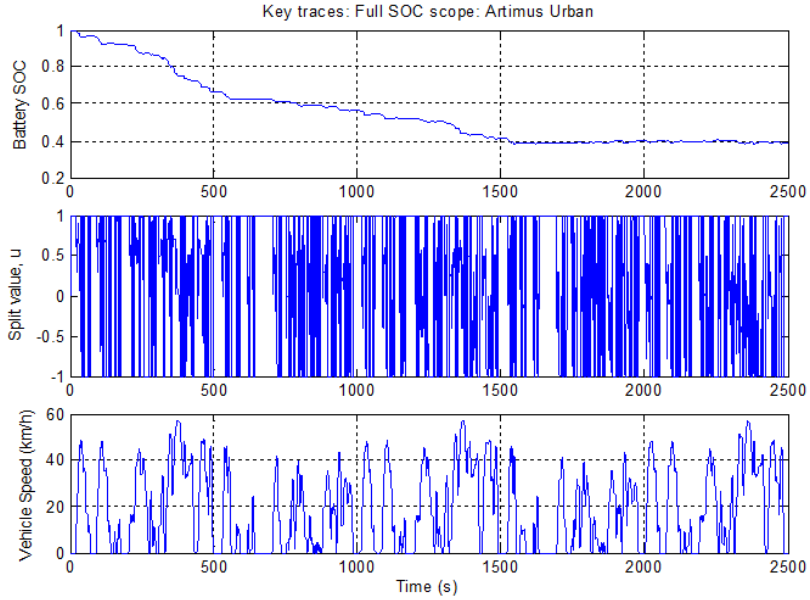

Figure 7-21:Post transmission test ,Artimus Urban, a) SOC, b) split, c) vehicle speed.

Figure 7-22 presents the power traces from the parallel deployment, demand power, CPS power and PPS power. It can be clearly seen that initially the PPS power is following the demand power. As the cycle progresses, the CPS power plays a larger part in meeting the demand power. During the last 1000 seconds, it can be seen that there is a significant amount of negative PPS power. This indicates that the system is operating in CS mode.

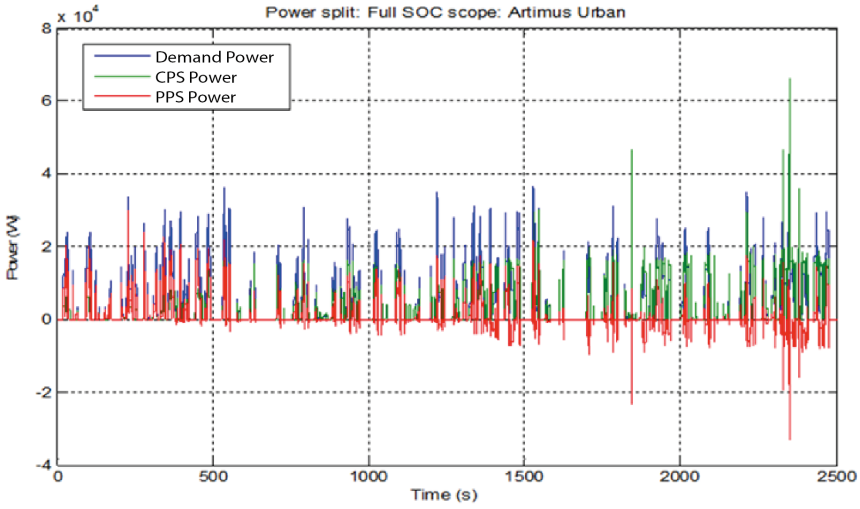

Figure 7-22: Post transmission continuous test power traces

Figure 7-23 presents the engine operating points for this test. The points are overlaid onto the engine efficiency map, shown as contours in percentage. The maximum and minimum torque lines are also shown in continuous blue. The operating points represent the ability of the control system as designed to maintain the ICE on the line of best BSFC. This is made possible by the existence of the CVT. The encapsulation of the CVT into the CPS means that the CPS can follow a power command from the VSC.

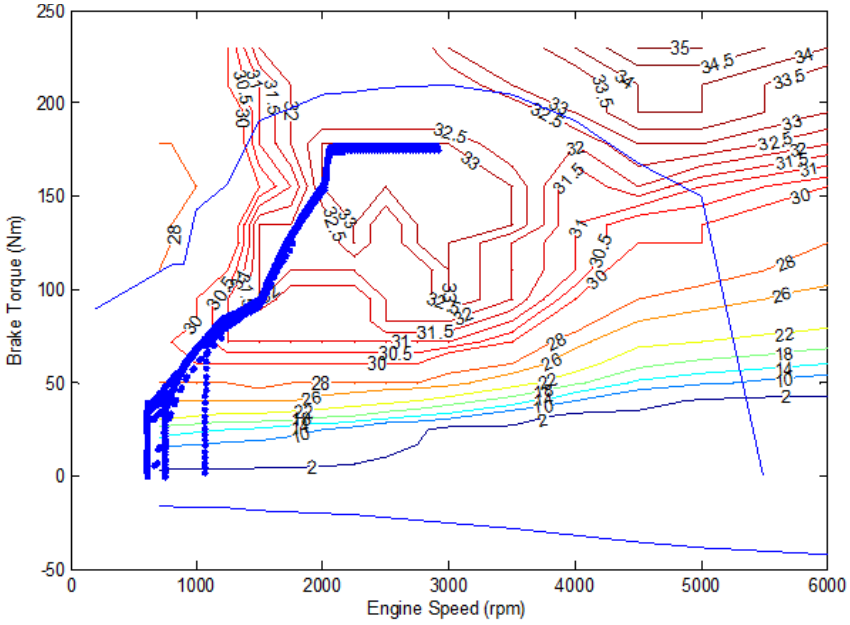

Figure 7-23: Post transmission continuous test ICE operating point

7.4.2. ECMS penalty function sensitivity analysis

This section presents an opportunity to demonstrate the sensitivity of the system to the ECMS SOC penalty function. This penalty function has been described in Chapter 5, and has also been discussed in literature [98, 141, 148]. The power traces in Figure 7-22 show that the CPS was engaged before the charge sustaining point was reached at 1500 seconds. Also Figure 7-21 shows the speed not passing 50km/h. Therefore it can be deduced that the system is not power limited. This suggests that the ECMS is enforcing non-EV operation. This point is confirmed by comparing the SOC swing form t=0 to t=500 and t=1000 and t=1500. Both time periods cover the same speed profile but the SOC swing is 35% in the first section and only 15% in the second section. Further evidence for this can found in Figure 7-22, where the CPS can be seen actively charging the PPS between t=1000 and t=1500.

This is referred to as blended charge depletion [199], where the VSC maximises the time until CS by activating the CPS during CD. Extending CD by using the CPS will result in greater fuel economy over a cycle which is longer than the CS range. If a future repeated route is known (commute to and from work) which is longer than the CD range it may be beneficial to extend the CD mode by blending. It may be possible to avoid CS before arriving home at a known available charge point. This point is discussed in literature [141, 148, 149]. However for the purpose of this research it is sufficient to show that the architecture and the ECMS are robust to the inclusion of this feature.

Figure 7-24 shows the penalty function for blended charge sustaining operation. This is the penalty function utilised in the continuous test presented in the last section. As a reminder from Chapter 5, the penalty function weights the relative cost of using the stored energy versus the fuel energy. In this case the system will favour battery energy from a SOC of 1 to 0.8. From there the system will blend the charge depletion until about 0.45 whereupon it enters charge sustaining. This function is derived from its use in literature, [98, 141, 148] and its shape has been calibrated to generate the transition from CD to blended CD to CS. This calibration process is described here.

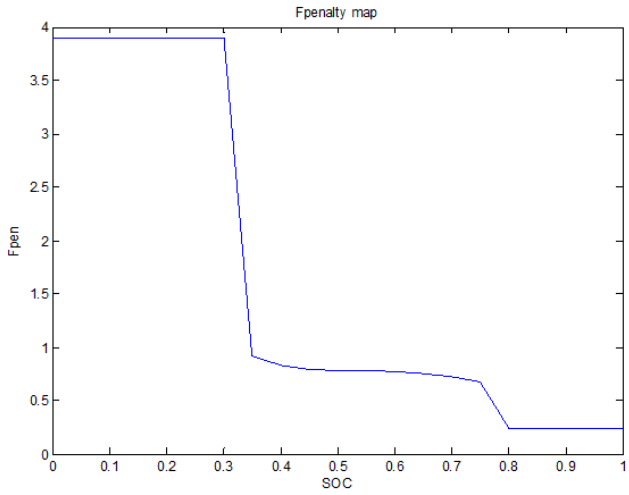

Figure 7-24: Penalty function for blended charge depletion

Figure 7-25 presents a collated set of data which was captured over a series of tests. Each test was conducted over 800 seconds of the ECE cycle, a subdivision of the NEDC cycle. Each cycle is initiated at a different SOC from 1.0 to 0.3 in steps of 0.1. A charge sustaining test, initiating SOC at 0.45 is also included. For context, an equivalent ICE powered vehicle was simulated over the same cycle, using the same engine minus the mass of the hybrid system. The average consumption result for this test is shown as a red line at 4.2L/100km. The Y axis is average consumption and the X axis is SOC. Each test is shown as a set of large points, triangles or circles, tracking the SOC value against the average consumption of that test. If the global track of SOC is down the triangles point left otherwise they point right. The charge sustaining test is shown as a set of circles.

The tests tell a story, when the SOC is high and the penalty is low, the SOC swing is the biggest and the consumption is lowest. As the penalty is increased, the SOC swing drops. This indicates that the demand power is being part met by the ICE therefore the consumption increases. If the SOC was below the charge sustaining point, then the penalty is greater than one, which requires the ICE to charge the battery. This results in increased average consumption.

It can also be seen that the charge sustaining test returns a better consumption that a standard vehicle, 3.9L/100km versus 4.2L/100km. This is an expected result. A non-plug-in HV would expect a greater consumption benefit. However the plug-in HV carries a mass penalty in CS mode, namely the mass of the depleted battery.

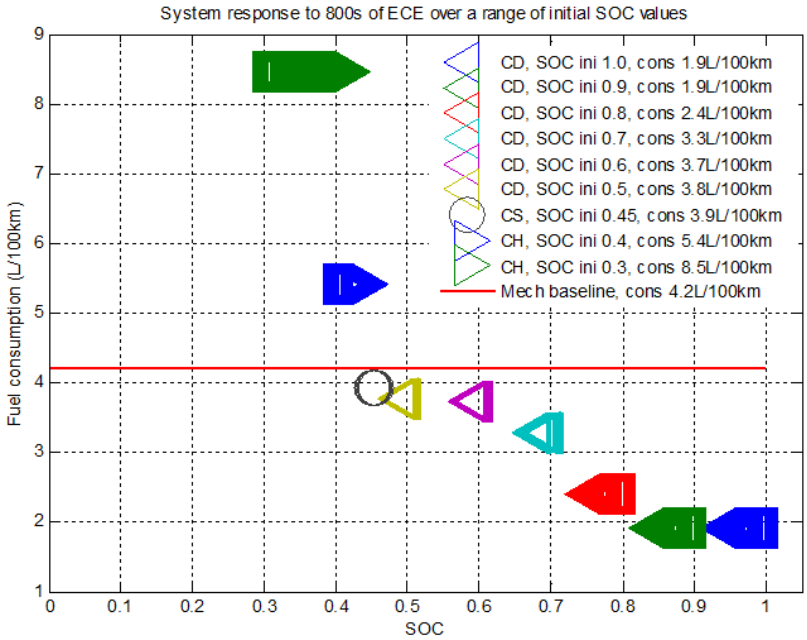

Figure 7-25: Collated test data showing system responses across penalty function

Figure 7-26 presents the penalty function for non-blended charge sustaining operation, or full EV operation until charge sustaining. Figure 7-27 presents the collated results as described earlier. The penalty function lower knee point has been moved from 0.8 to 0.5. This results in the system operating as a full EV until the SOC reaches 0.5. This

subtle change in one LUT can in real time alter the characteristic of the HV from blended charge sustaining to EV operation.

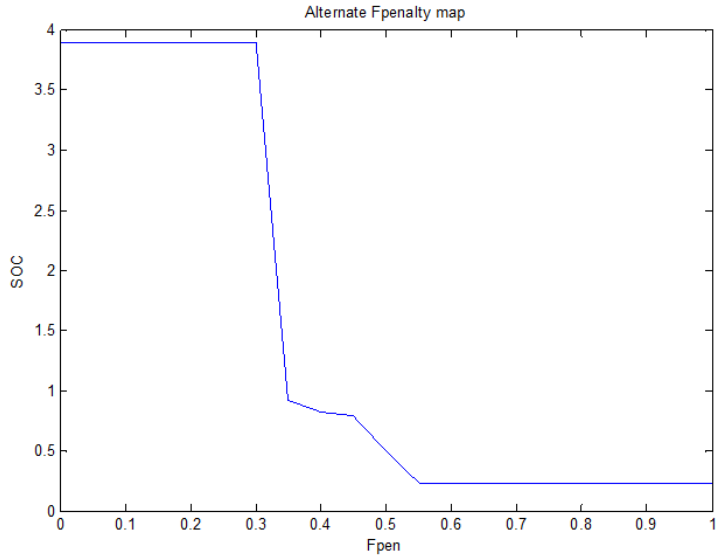

Figure 7-26: penalty function for non-blended charge depletion

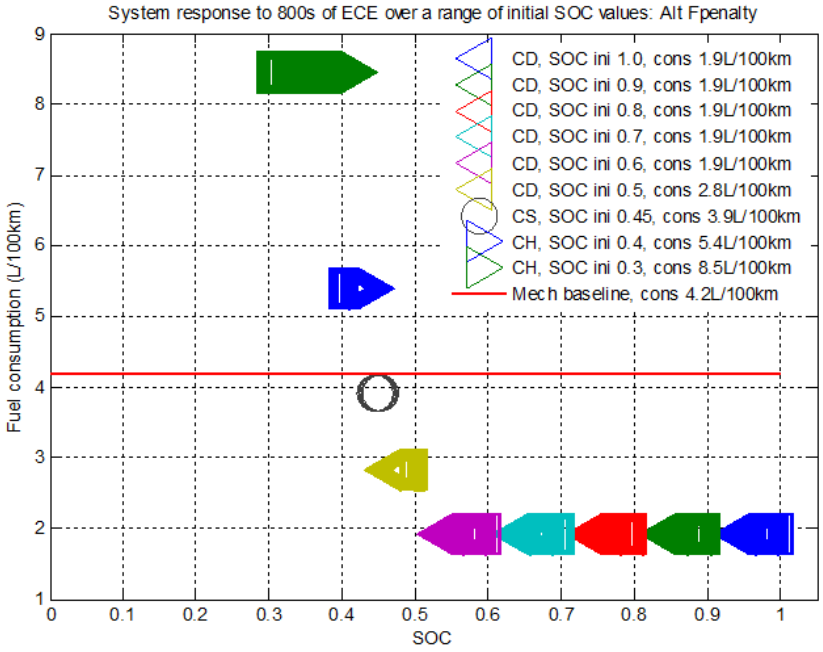

Figure 7-27: Collated test data showing system response across penalty function

The ability to change the characteristic of the HV operation allows developers to include a range of predictive control functionality without upsetting the architecture of the VSC. This LUT can be pre calibrated or updated in real-time. This applies not just to post-transmission parallel HVs but all HV configurations and variants. Much of the literature regarding predictive control assumes that the required information will always be available and accurate. A key learning from this research is that any system developed must be able to operate in the absence of predictive control, either by deployment or during operation in the case of a failure in the predictive control functionality.

7.5. Summary

This chapter has presented two parallel HV case studies. The first is a pre-transmission parallel HV analysed as part of the LCVTP. The second is a hypothetical post-transmission with a CVT. These two variants were chosen as scenarios for the Parallel RA as they represent the extremes of parallel HV powertrain configuration.

ADs for both variants were developed using the Parallel RA as a template. In the first instance the DriveLine system encapsulated the discrete transmission and the two clutches. It is expected that this will represent most instances of parallel powertrain configuration. The second variation analysed the opportunity of having a CVT upstream of the torque bus, thereby enabling it to be encapsulated within the CPS.

The encapsulation discussion was continued in the first instance by a discussion on the PPS in the context of a parallel HV. It is important to coordinate the *power_available* calculation of the battery and the drive machine. The second case study addressed in detail the encapsulation of a CVT within the CPS. In all instances, this generates a requirement for a local CPS or PPS manager. These functional blocks ensure that the generic interfaces are preserved. Both ADs were deployed into the Simulink environment demonstrating core functionality. In the second instance the opportunity was taken to do a detailed sensitivity analysis on the ECMS SOC penalty function. This showed that the system could easily be reconfigured, in real time if necessary. This ensures that the system can operate in the absence of predictive control, by design or in the event of failure.

Several learnt lessons arise from the two deployments presented in this chapter. The RAs must be able accommodate a functional safety layer. Defining the PPS boundary from the battery through the power electronics and electrical machine to the torque bus is essential to maintaining the validity of the RA. This has the added benefit of aggregating the power available signals for the whole PPS, simplifying the VSC interface. The relationship between DD, *Power_Available* and *Torque_Available* must be preserved to ensure system wide limit preservation. In the case of the Parallel RA, the *Torque_Available* is encapsulated within the *PowerTorque_Available* block, but its function and interfaces remain. Multiplicity ensures RA flexibility to cover the wide variety of pre-transmission, post-transmission, and multiple clutch parallel HV variants. Architectural separation of *Instantaneous_Optimisation* and *Predictive_Optimisation* allows future developers to integrate a variety of predictive or adaptive control options.

This chapter tests the second hypothesis set out in Section 1.4. The Parallel RA has been deployed over two scenarios. ADs for two distinct parallel HV variants were deployed, and numerically tested to ensure that the resultant ADs were sensible. Full acceptance of the hypothesis requires deployment of ADs for all parallel HV permutations defined in Table 4-1. However it is argued here that the parallel HV variants chosen represent the extremes of possible deployments. Therefore it can be stated with confidence that the hypothesis will hold for other parallel HV variants.

8. Deployment of Extended Parallel RA

This chapter presents two case studies of compound HVs deployed as per the Extended Parallel RA guidelines set out in Chapter 4. This chapter follows the same format as Chapters 6 and 7. The first compound HV is based on a power-split type vehicle, such as a Toyota Prius or GM Volt. The second is a through-the-road compound HV as described by Morbitzer et al and Koprubasi et al [139, 140]. Also the exhaust gas energy recovery compound HV variants are discussed. Testing of hypotheses so far has revealed that a minimum of two RAs is also required to represent Series and Parallel HVs. This chapter confirms the third hypothesis, that the Extended Parallel RA is deployable onto compound HVs.

Firstly the architectural deployment analysis for the power-split compound HV is presented. This is followed by the results from a numerical simulation of the power-split HV, which acts as a scenario for the compound AD. Then the AD analysis for the through-the-road compound HV is presented. Finally the TurboGen and ThermoGen compound HV variants are discussed in the context of system schematics. These four variants were selected to test the hypothesis as they represent the extremes of compound HVs.

8.1. Case study 3 Deployment of a power-split AD

This section presents the architectural analysis of the power-split compound HV. The physical, system and control domain models are presented here. Adaptations of the Extended Parallel RA for the compound ADs are highlighted.

8.1.1. System schematic

Figure 8-1 presents the system schematic of the power-split compound HV, similar to the Toyota Prius and the GM Volt. This schematic extends the simpler version presented in Figure 2-16, by including real world features. A DC/DC converter and the hydraulic brakes system are shown. However, no on-board charger is included to more closely represent the non-plug-in Toyota Prius as opposed to the GM Volt which is a plug-in HV. It should be noted that the architecture for a plug-in HV would be the same due to charge system encapsulation as shown in Figure 7-5. Torque bus 1 in this instance represents the epicyclic power-split. This divides the power (and torque) from the CPS (an ICE) to either the driven wheels or the Gen which charges the battery. Torque bus 2 represents a direct shaft mounting of the Drv machine to the epicyclic output shaft.

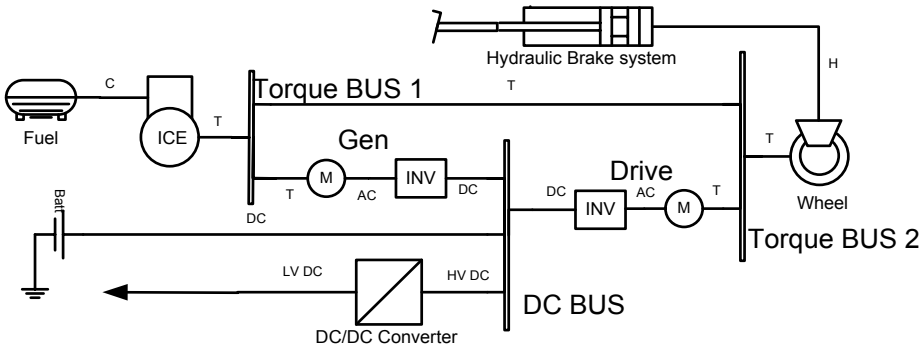

Figure 8-1: System schematic of power-split compound HV

The speed of the Drv machine is directly coupled to the speed of the driven wheels (accounting for the final drive gearing). However, the epicyclic gear decouples the CPS and Gen speeds from the driven wheel speed. This presents the opportunity of confining the CPS operation to the best BSFC line as per the post-transmission CVT parallel HV presented in Section 7.3. The role of the Gen machine is to maintain the CPS at the desired speed for a given power demand, to react the torque across the epicyclic and finally to divert the excess CPS power into the PPS. However, in principle, it is entirely plausible to use the Gen machine to deliver positive drive power. Both the Gen and Drv machines can draw or supply electrical power to the DC bus and the DC/DC converter continuously draws power to run the vehicle loads.

8.1.2. System domain models

Figure 8-2 presents the AD decomposition model of the power-split compound powertrain system. This AD is derived using the extended Parallel RA guidelines discussed in Section 4.5. Unlike the series AD in Section 6.1 and the pre-transmission parallel AD in Section 7.1, this AD employs the ideal brakes integration.

The main difference from the Extended Parallel RA is the absence of a DriveLine system. In this particular case the epicyclic can allow the DriveLine to operate as an EV or a HV without the use of clutches, and it also acts as an infinitely variable transmission whose effective ratio is directly controlled by the torque levels of the three actuators (CPS, Gen and Drv) connected to the three inputs (annulus, sun and ring respectively). Therefore the DriveLine system shown in Figure 4-11 can be deleted entirely. This would not be the case for the GM volt, which used clutches to constrain the epicyclic in some drive modes.

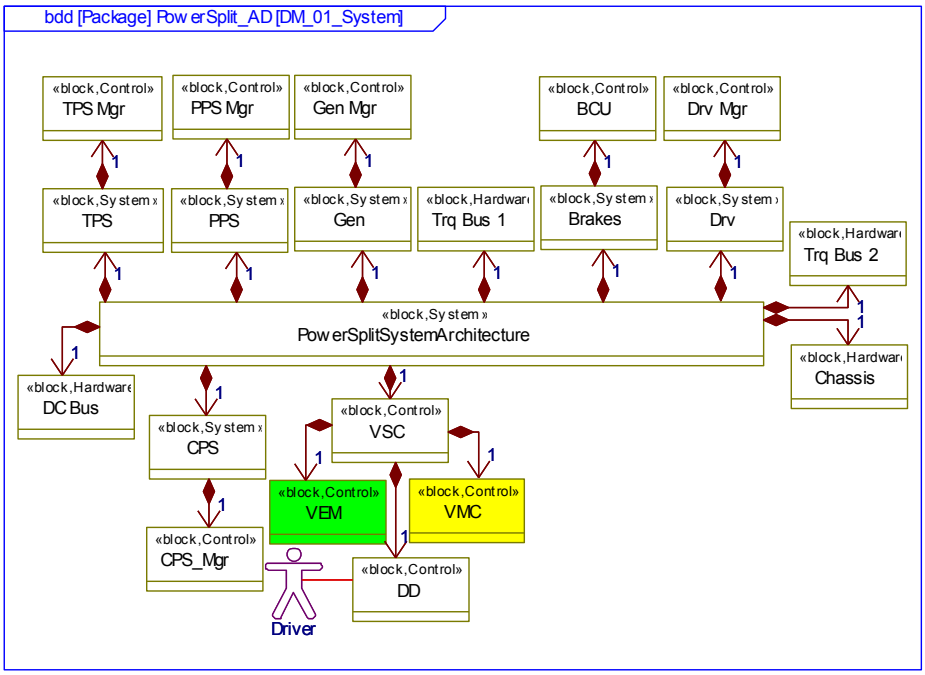

Figure 8-2: AD decomposition model of power-split compound powertrain system

Figure 8-3 presents the power-split compound context and causality model of the powertrain system. This is very similar to the equivalent models shown in Figure 7-3

and Figure 7-17 for the pre and post transmission parallel ADs. The main differences (apart for the brakes integration) are the inclusion of a Gen system, the transmission of two *torque_split* signals from the VEM to the VMC (green and yellow respectively) and the omission of a *gear_actual* signal from the VMC to the VEM. Also absent is the *charge_door* signal as there is no on-board charging system.

As previously discussed, the *torque_demand* is constrained by *torque_available* which is determined in the VEM. This is based on the *power_available* signals from the CPS, Gen, Drv and PPS systems. The three *torque_command* signals are a function of *torque_demand* and the two *torque_split* signals.

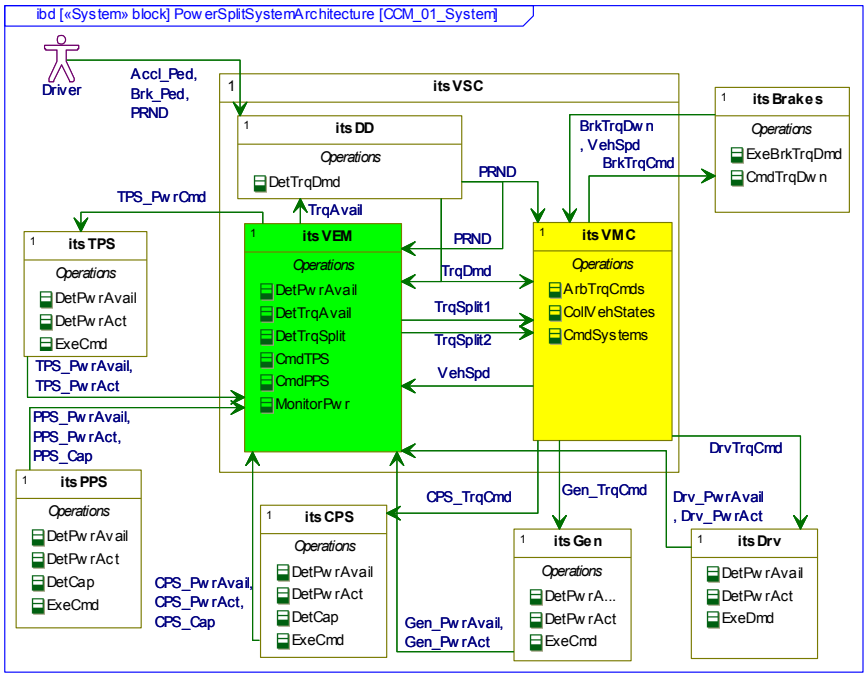

Figure 8-3: AD context and causality model of power-split compound powertrain system

Figure 8-4 presents an example of an interaction model for the power-split compound powertrain system. This interaction model shows the required information before the VSC can deliver a demanded torque. Initially the system must recognise that the drive mode has been selected, as opposed to reverse for example. Then the VEM must collate the *power_available* signals from all five subsystems. Combining this with the *speed*, the VEM determines a *torque_available*. This is communicated to DD which uses these signals (positive and negative) to constrain the *torque_demand* signal. The VEM, using *torque_demand* and PPS *capacity* (meaning SOC) then determines *torque_split1* and *torque_split2*.

Finally the VMC uses the two split signals and the *torque_demand* signal to determine the three *torque_command* signals. This requires a complex driveline-specific dynamic torque control functional block. This is referred to as *Torque_Apportionment* in the next section.

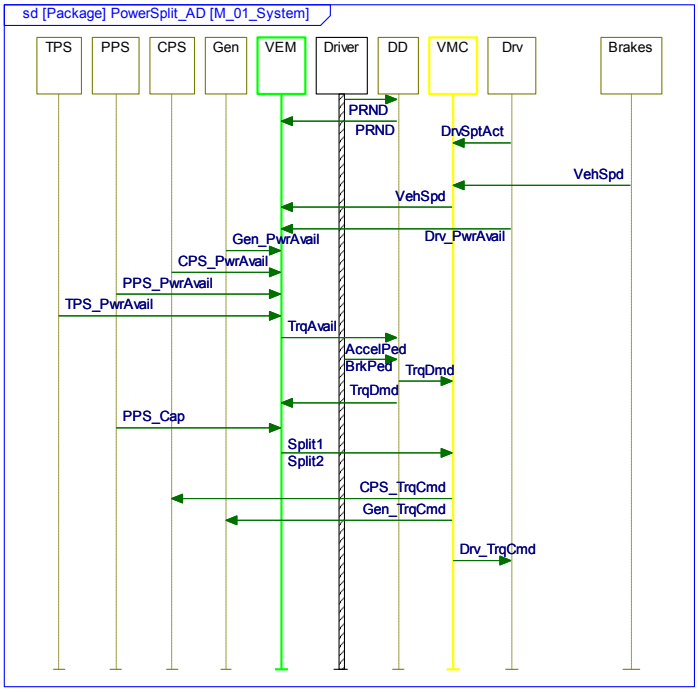

Figure 8-4: AD interaction model of power-split compound powertrain system

8.1.3. Control domain models

This section presents the control domain models for the power-split compound HV as they present significant differences to both the extended Parallel RA and the parallel ADs presented in the last Chapter 7.

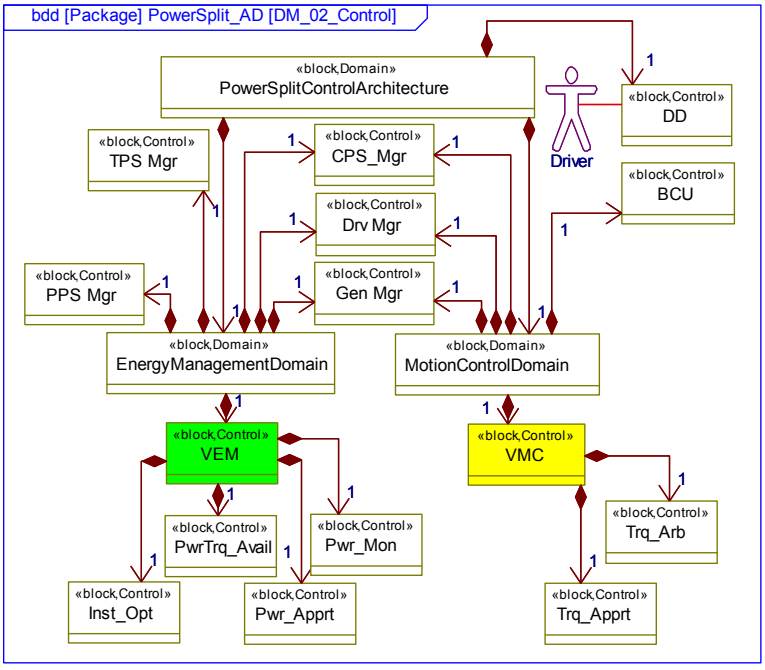

Figure 8-5: AD decomposition model of power-split compound control domain

Figure 8-5 presents the decomposition model of the power-split compound control system. This model is derived directly from Figure 4-14. It shows that the VEM, TPS

Manager and PPS Manager are exclusively in the energy management domain and also that the VMC and BCU are exclusively within the motion control domain. The CPS Manager, Drv Manger and Gen Manager are all shared with both domains. This shows the same characteristic of the Parallel RA. This is reflected in Figure 8-3 by the *available, actual* and *capacity* signals being routed to the VEM and the *command* signals eminating from the VMC. As with all RAs the DD remains outside both domains.

As shown in the Extended Parallel RA in Section 4.5, the VEM comprises *Instantaneous_Optimisation, PowerTorque_Available, Power_Apportionment* and *Power_Monitor*[25], see Figure 8-6. The *Predictive_Optimisation* funcitonal block is omitted, which shows that the RA is capable of capturing variants of differing specification. It can be seen that the *Power_Apportionment* is only required to alter the TPS *power_command* in the case of an excursion of total *power_actual* to the limit, as determined by the *Power_Monitor* functional block. This is common feature to the parallel ADs presented in the last chapter. Also as per the parallel ADs, the *PowerTorque_Available* block calculates *power_available* and *torque_available*. Using *power_available*, *power_demand* and PPS *capacity,* the *Instantenous_Optimisations* block determines two *torque_split* signals, which are broadcast to the VMC. These shared characteristics show the benefit of encapsulation of features and signals, which designs in reusability across dispirate deployments, which, it is argued, will reduce future development cost.

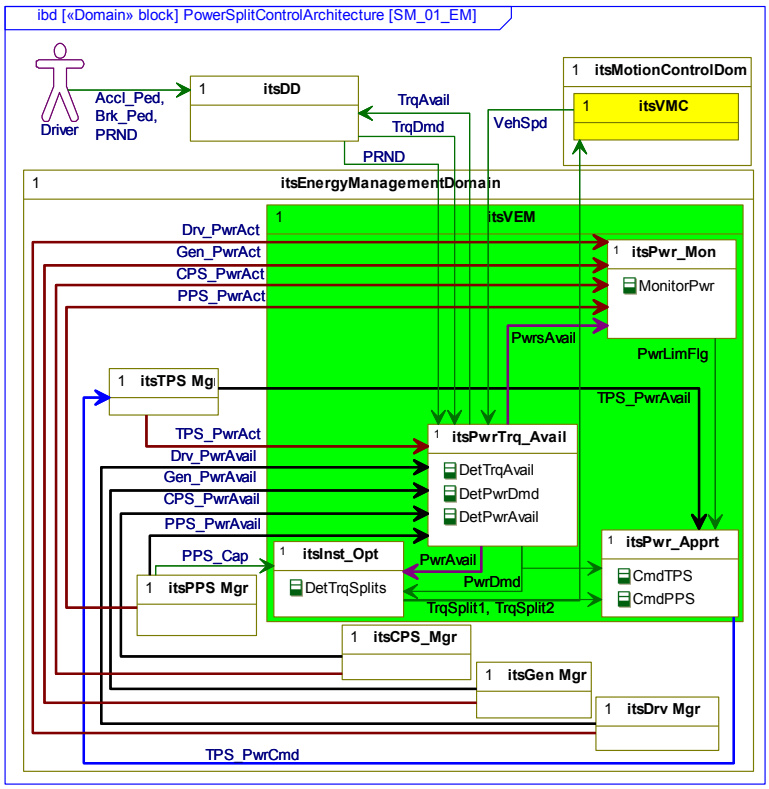

Figure 8-6: AD strategy model of power-split compound energy management domain

[25] Note from earlier, *signal_paths* are italicised, *Functional_Blocks* are italicised with capitals.

The largest difference from the Extended Parallel RA is in the VMC. It is shows in Figure 8-5 that it comprises the *Torque_Arbitration* and *Torque_Apportionment* funcitonal blocks only. As discussed previously, the *Torque_Arbitration* is required to constrain (or increase) *torque_demand* in the event of a brakes intervention, normally associated with a wheel slip (positive or negative) event or a stability event. The *Torque_Apportionment* block converts the *torque_demand* to *torque_command* signals using the two *torque_split* signals.

Unlike the Extended Parallel RA there is no *DriveLine_Mode* or *Speed_Control* blocks. This is due to the presence of the epicyclic, which negates the need for clutches to decouple the PPS from the driven wheels. Therfore there are no clutch states to define distinct deiveline modes, hence the omission of the *DriveLine_Mode* block. Which inturn negates the need to speed match two decoupled systems before clutch engagement, hence the omission of the *Speed_Control* block.

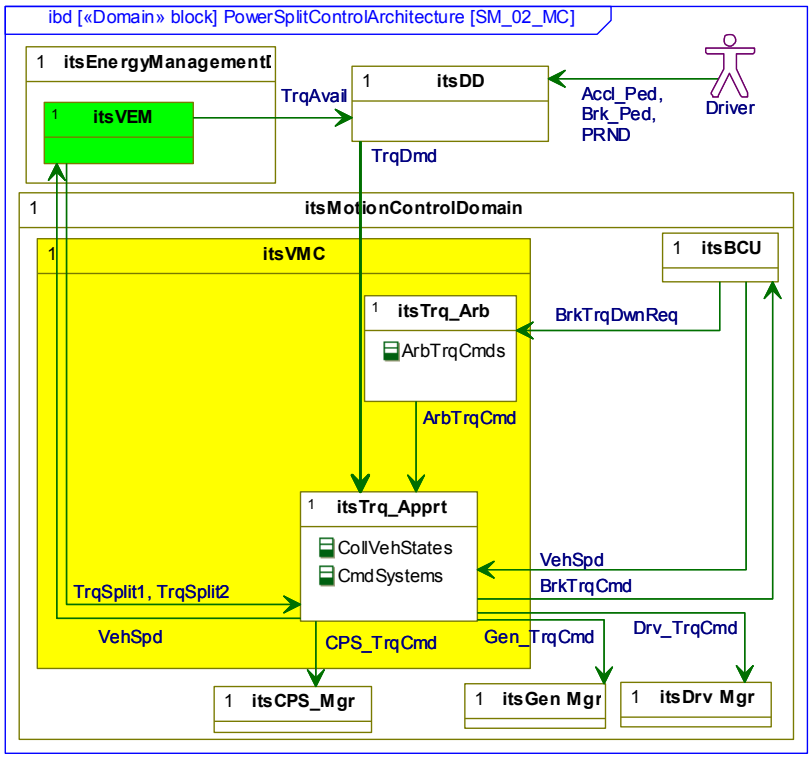

Figure 8-7: AD strategy model of power-split compound motion control domain

The clutches used in the GM Volt constrain the motion of one part of the epicyclic, this would require the reinstatment of the *DriveLine_Mode* block. While the determination of this point is outside the scope of this research, it can be stated with confidence that the Extended Parallel RA is applicable to both types of power-split compound HVs, as the inclusion or omission of a funcitonal block is a normal procedure when using an RA to a guide a deployment. An added advantage of this set of models is the ability to assess the impact of physical and control requirements concurrently.

8.2. Case study 3 Numerical verification of power-split compound AD

This section presents the deployment and numerical results for the power-split compound HV as derived from the Extended Parallel RA presented in Section 4.5.

8.2.1. Simulation deployment

This section only presents the differences between the deployment of a parallel HV and a compound HV. Section 7.2.1 presented, in detail, the deployment of a functional VSC from the parallel AD presented in Section 7.1. Most of the detail presented in Figure 7-7, Figure 7-8 and Figure 7-9 is identical for the compound deployment. The exception is the VMC. The parallel VMC presented in Figure 7-9 includes a *DriveLine_Mode* and a *Speed_Control* functional block. As shown in Figure 8-8, the compound VMC no longer requires these functional blocks.

As per Figure 6-14 and Figure 7-9 the *VMC_Mode* block is retained. This manages start-up processes. This block is in place as this compound VSC was extended from the parallel VSC from Section 7.2. As the underlying architecture for both are identical this is possible. It is also a demonstration of the ease with which alternate deployments can reuse existing knowledge. As mentioned before, this VMC_Mode block is not included in the RA as this can be deployment or enterprise specific.

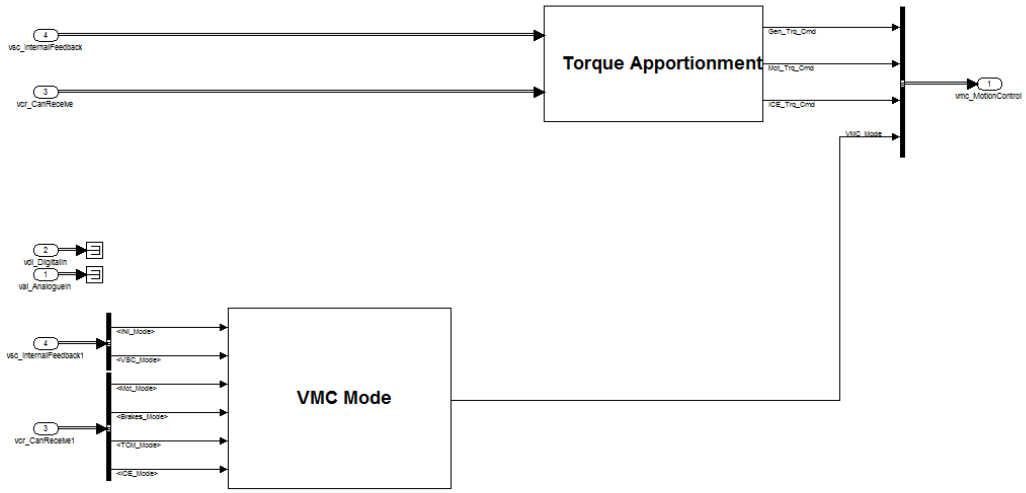

Figure 8-8: Deployment of power-split compound VMC

In Figure 8-8, only the *Torque_Apportionment* is shown. This functional block takes the *torque_demand* and the two *torque_split* signals to determine the *torque_command* signals for the Gen, Drv and CPS sub-systems. It is conceivable that the *DriveLine_Mode* and *Speed_Control* functional blocks would be required if the power-split system included a series of clutches. This would be expected in an AD representing the GM Volt powertrain. It is argued that this deployment demonstrates the flexibility of the RA. The encapsulation of DriveLine and speed functionality allows these to be omitted as the system requirements allow, without any undue impact on the control system development.

The next section presents the results for the simulation tests on the power-split compound HV.

8.2.2. Power-split compound system testing

This section presents a sub-set of the results from the power-split simulation tests. The tests conducted represent scenarios for the power-split compound AD, which is itself one scenario for the Parallel RA.

As with previous numerical verifications the tests focus on the relationship between VEM and VMC functionality. Specifically this means that the separation of both VEM and VMC, as defined in the RA, does not affect their functionality. With this in mind, similar tests to those in Sections 6.2 and 7.2 have been conducted. These tests are designed to show that VEM functionality can operate without affecting the VMC functionality. Hence the system is tested under charge depletion and charge recovery modes.

The first test presented here is a low power test using the first 200 seconds of the NEDC drive cycle, which is referred to as ECE. In this case the battery SOC (PPS *capacity*) was set high to allow the system to operate in charge depletion mode. Although this simulation is based on the parameters of a Toyota Prius, which is not a plug-in HV, it still would be required to operate in CD or CR modes.

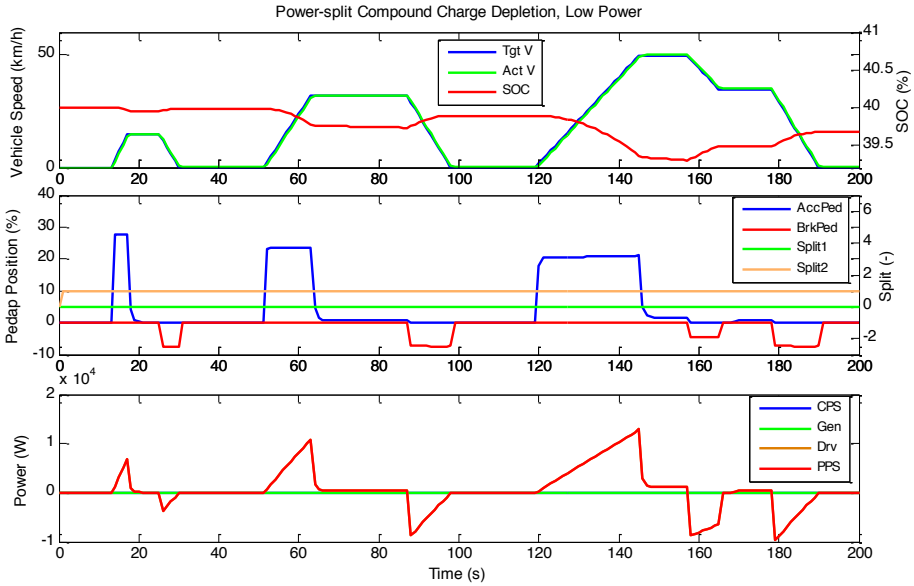

Figure 8-9 : Power-split system, ECE, CD, a) states, b) inputs c) powers

Figure 8-9 presents the system data from the ECE charge depletion test. Figure 8-9a shows the target and actual speeds overlaid with the SOC. Figure 8-9b shows the accelerator and brake pedal traces overlaid with the two split signals. Figure 8-9c presents the four power traces, CPS, Gen, Drv and PPS[26]. This format is identical to that used in Section 7.2 and for consistency will be used throughout this section also. Figure

[26] The Gen, Drv and CPS powers are all zero, but the Gen trace is overlaid on the other two.

8-10a and Figure 8-10b present the DriveLine torque and speed traces respectively, for the three subsystems connected to torque busses; CPS, Gen and Drv.

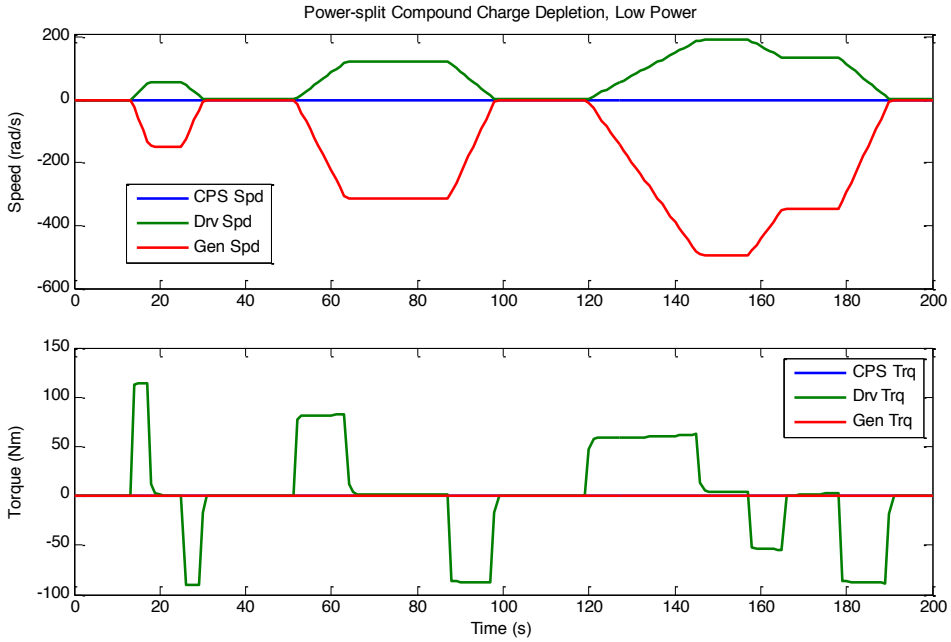

Figure 8-10: Power-split driveline, ECE, CD, a) speeds, b) torques

In this test, the system operates in EV mode. split 1 is zero and split 2 is one, hence all demand power and torque is derived from the Drv machine, as defined in Section 5.4. The bottom graph shows the four powers but some are overlaid. The Drv and PPS powers are aligned, and the CPS and Gen powers are both zero throughout the test. This is better demonstrated in Figure 8-10. It can be seen that the Drv speed is proportional to the vehicle speed, a function of final drive ratio. As the power demand for the CPS is zero, it is beneficial to set the CPS speed to zero to avoid friction and pumping losses and any NVH issues. Therefore the Gen speed must compensate by rotating in the opposite direction. The rate at which it must rotate is defined by the epicyclic ratio of 1:2.1 as [193]. Finally it can be seen in Figure 8-10 that only the Drv machine is generating the required torque, and both the CPS and Gen torque traces are set to zero.

This first test is relatively trivial. The ECMS confines the split values to ensure EV operation and the VMC functional block must only demand the total torque from the Drv machine and allow the Gen to rotate freely to ensure zero CPS speed. However the second test presented in Figure 8-11 and Figure 8-12 tests the system, from the same initial SOC condition over a higher power cycle, in this case the Extra Urban Drive Cycle (EUDC) section of the NEDC.

For most of the test the system operates as an EV with the split values of zero and one respectively. However, at about 320 seconds, the high power demand combined with the drop in SOC triggers the ECMS to alter the split values, which requires the CPS to be activated. Figure 8-12 shows how the Gen speed must change to set the engine speed, however as the vehicle speed (and hence Drv speed) is already very high, the Gen speed will still be negative, resulting in negative power.

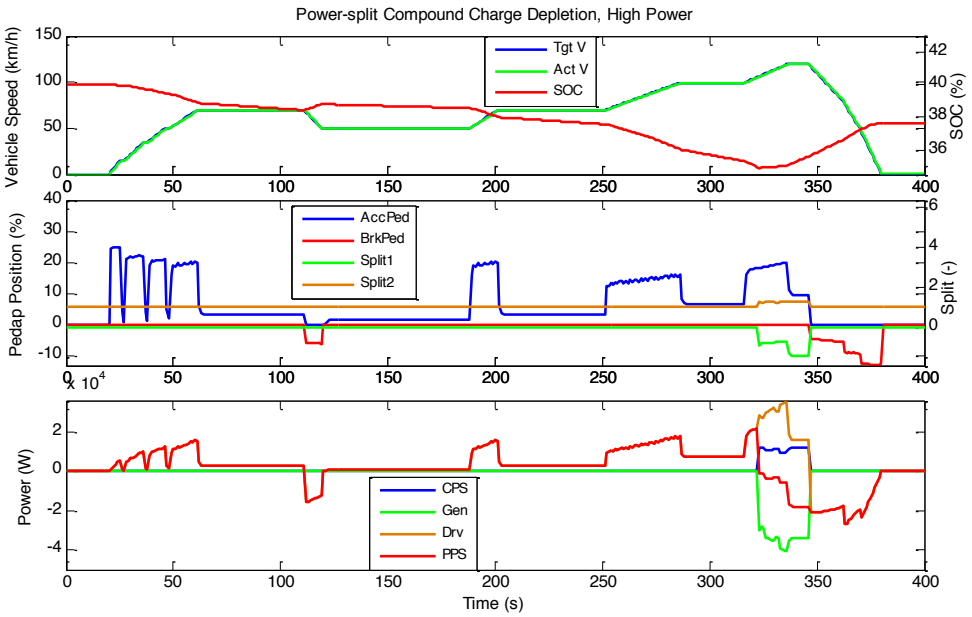

Figure 8-11: Power-split system, EUDC, CD, a) states, b) inputs c) powers

On close examination it can be seen that the PPS power is close to zero meaning that the Drv machine directly uses the power generated by the Gen machine. Clearly this is not an optimal energy path, as this converts mechanical power, to electrical power and back to mechanical power again, including all inverter and electric machine efficiencies. It will be seen later in this section that given the opportunity the ECMS will not allow power to be looped in this way unless in extreme demand situation such as this one.

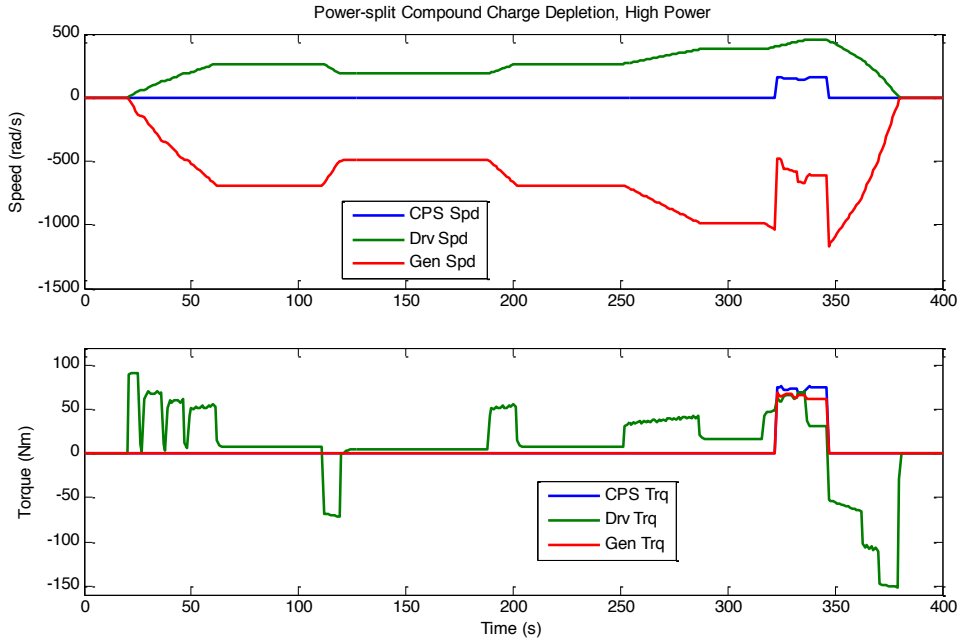

Figure 8-12: Power-split driveline, EUDC, CD, a) speeds, b) torques

Figure 7-13 and Figure 7-14 present an ECE test where the initial SOC has been artificially lowered, which results in CR mode. This low power test demonstrates the flexibility of the ECMS approach and the RA to the extremes of operation, in this case, an

excessively low SOC. As soon as demand is detected Split 2 and hence the Drv torque is set to zero and the engine is initiated. As before the Drv speed must be proportional to the vehicle speed as it is directly coupled to the output shaft of the epicyclic. Therefore the Gen speeds up to allow the CPS to operate at its desired power. As defined by the best BSFC curve. In all points of this test the PPS is being charged by the excess CPS power, via the Gen, or the PPS is being slightly depleted when the Gen is assisting the CPS. The Drv is not used to deliver accelerative torque, nor is it used to assist the CPS.

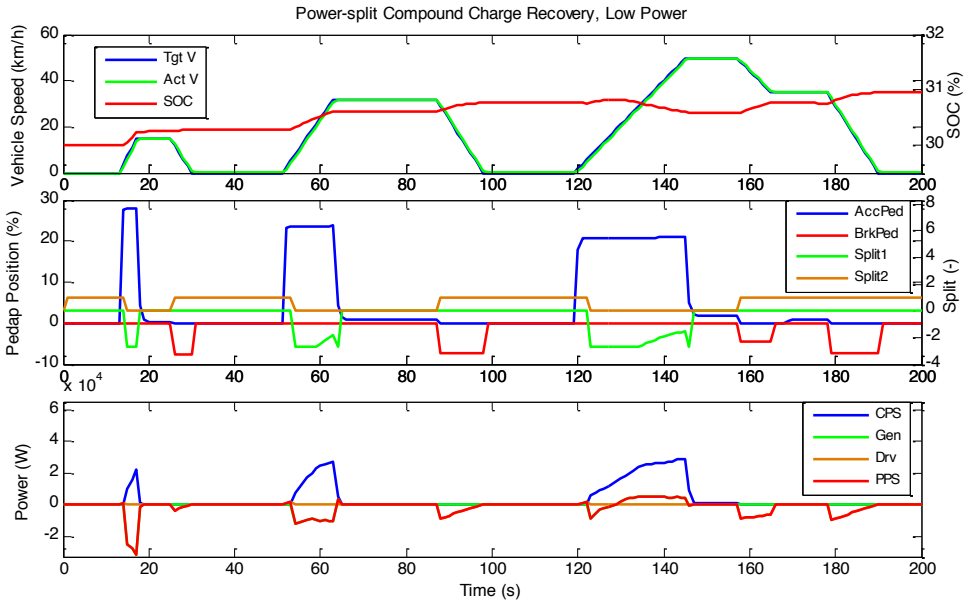

Figure 8-13: Power-split system, ECE, CR, a) states, b) inputs c) powers

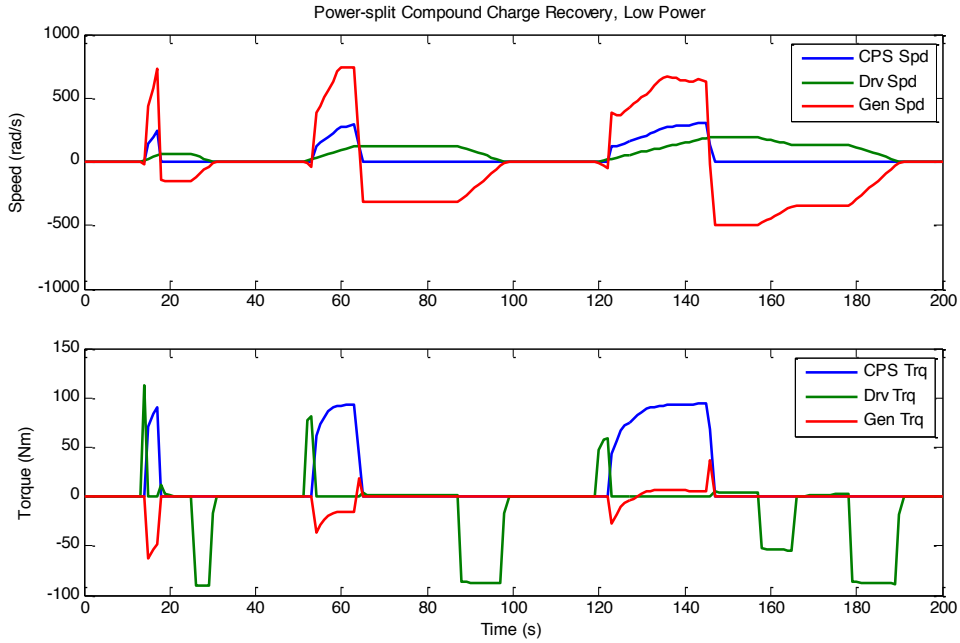

Figure 8-14: Power-split driveline, ECE, CR, a) speeds, b) torques

Finally Figure 8-15 and Figure 8-16 present the results from a charge recovery test with a higher power demand, EUDC. The traces show similar characteristics to the ECE CR

test. Normally the Drv machine is unused, unless in the case of initial pull away, braking and low speed cruise. However as the power (and speed) demand is higher than the last test, the split values do not necessarily result in battery charging. This is driven by the speed required by the Gen and the torque it must apply to react the CPS torque. This results in the Gen assisting the CPS in many occasions throughout the cycle. The PPS and Gen power are often overlapping in Figure 8-15.

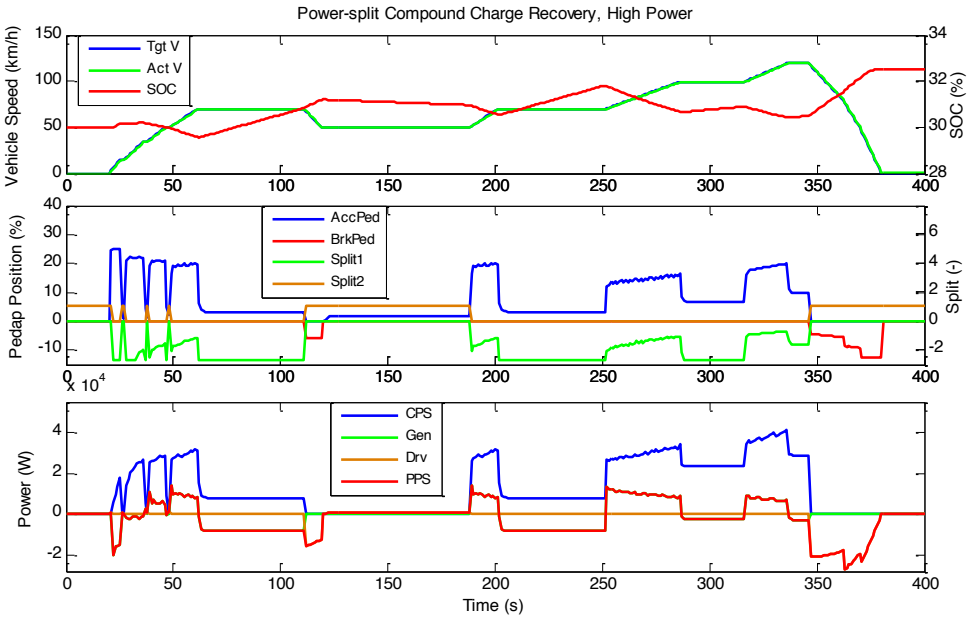

Figure 8-15: Power-split system, EUDC, CR, a) states, b) inputs c) powers

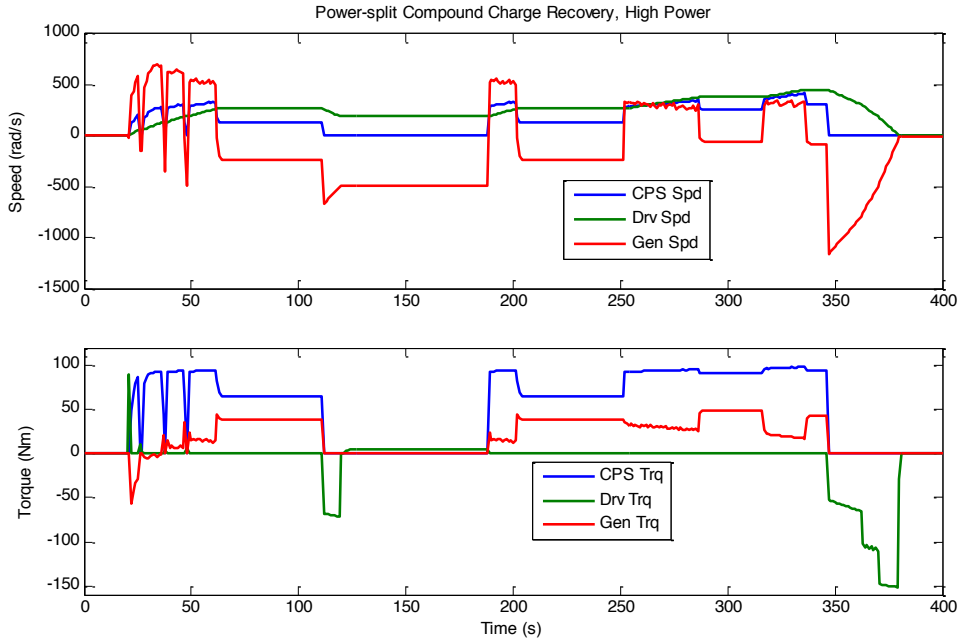

Figure 8-16: Power-split driveline, EUDC, CR, a) speeds, b) torques

Some interesting points can be taken from these tests. The existing Toyota Prius energy management algorithm would not normally allow the Gen to assist the CPS. It is interesting that the ECMS determines that this mode is both allowed and beneficial.

There exist limitations with this simulation, most notably the efficiencies of the electric machines and power electronics have been fixed, and the real world Gen system may exhibit poor efficiency when motoring. Given more scope, the power-split simulation would be validated against real-world data, the existing Toyota energy management algorithm reverse engineered and the two systems compared.

Also, given the limited research scope, the driveline has been simplified by omitting the driveline dynamics and converting it into a partial backwards model. This manifests as Gen and CPS speeds changing instantaneously, but avoided the requirement of a comprehensive dynamic torque controller for the *Torque_Apportionment* functional block. However, given the time and resources, a functional dynamic controller would be built, and inserted into the *Torque_Apportionment* functional block with in the AD, and the correct dynamic driveline described by Jinming and Heui would be used, [144]. This means that the AD as derived from the RA will not be affected by the omission of a fully functional dynamic torque controller, or its later insertion. Therefore these tests demonstrate that the encapsulation of *Torque_Apportionment* functional block adds robustness to the AD and by inference the RA.

The next section presents the architectural analysis for a distinctly different type of compound HV, showing that the extended Parallel RA still applies.

8.3. Deployment of through-the-road AD from the extended Parallel RA

This section presents the architectural analysis of the through-the-road compound HV. The physical, system and control domain models are presented here. Adaptions of the Extended Parallel RA for the through-the-road compound AD are highlighted and compared to the power-split AD. This AD is not verified by numerical simulation due to both scope limitations and that the encapsulation in the AD observably encompasses the altered drivetrain.

8.3.1. System schematic

Figure 8-17 presents the system schematic of the through-the-road compound HV as described by Morbitzer et al and Koprubasi et al [139, 140]. This type of vehicle contains an electrical machine directly connected to the output shaft of the ICE (CPS) both of which directly drive one axle of the vehicle via a transmission, the front axle in this case study. A second electrical machine drives the other (or rear) axle independently. In Figure 8-17 the first electrical machine is referred to as the Gen and the second is referred to as the Drv. This is for consistency in terminology. As seen in the previous section the Gen may assist the CPS and the Drv acts as a generator under braking.

The system schematic still contains two torque busses, the second of which is actually represents the road itself. However the definition of compound HV still applies as the Gen and Drv are both connected to the same DC bus. As the front of the vehicle is very similar to a parallel HV (pre-transmission in this case) then it is expected that the *DriveLine_Mode* and *Speed_Control* functional blocks will be retained in this deployment of the extended Parallel RA, distinguishing the through-the-road from the power-split ADs.

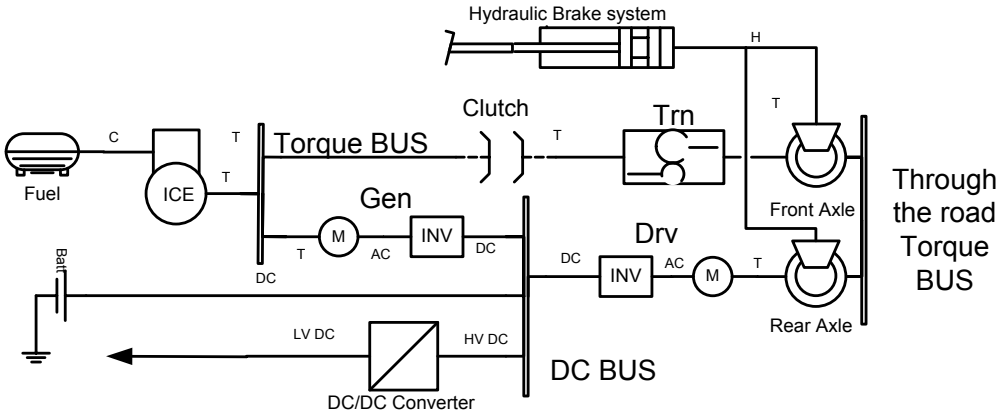

Figure 8-17: System schematic of through-the-road compound HV

8.3.2. System domain models

Figure 8-18 presents the AD decomposition model of the power-split through-the-road compound powertrain system. This AD is derived using the Extended Parallel RA guidelines set out in Section 4.5. As with the power-split compound AD and unlike the series deployment in Section 6.1 and the pre-transmission parallel deployment in Section 7.1, this AD employs the ideal brakes integration.

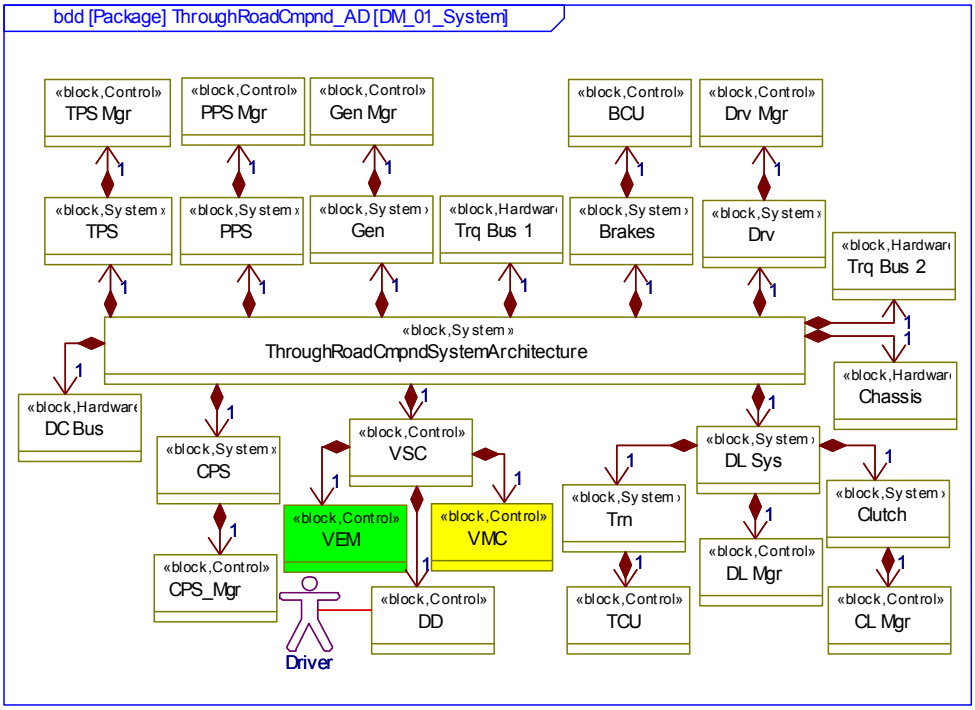

Figure 8-18: AD decomposition model of rough-the-road compound powertrain system

The main difference between this AD and the power-split AD is the presence of a DriveLine system. This DriveLine system comprises a transmission, a single clutch with local Clutch Manager and a coordinating DriveLine Manager. In principle, it is preferable for these two systems to be controllable but this is not always possible. If this was a manual transmission and a pedal operated clutch (like the DriveLine of the original

Honda Insight) the VSC cannot control the DriveLine operation but would still need to be aware of the states of the DriveLine such as gear number and clutch status. This would have minimal effect on the RA. Only the *command* signals would be omitted, reducing the VSC to a reactive rather than a proactive interface with the DriveLine.

As such the AD presented in Figure 8-18 contains all the blocks shown in the Extended Parallel RA system domain decomposition model shown in Figure 4-11 [27]. This may seem counterintuitive, as the through-the-road seems like a very different physical vehicle. However this can be overcome once it is accepts that the through-the-road torque bus in Figure 8-17 is treated as a normal torque bus described in Section 2.4.2.

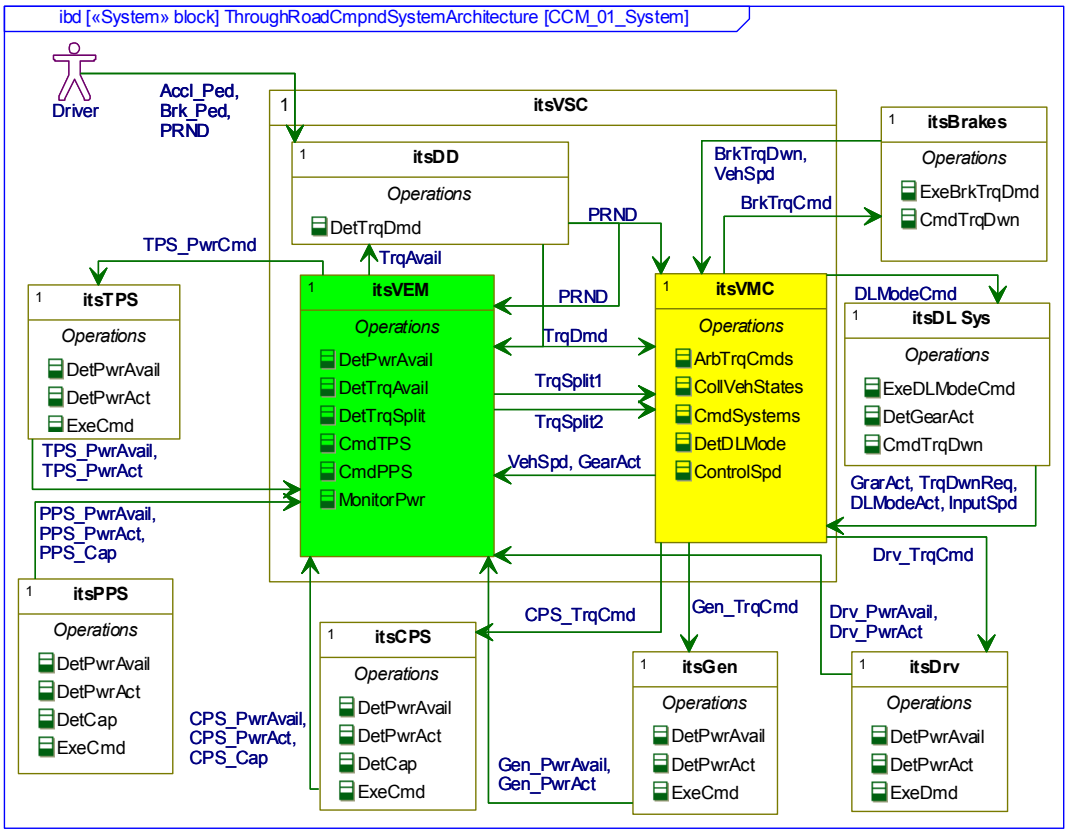

Figure 8-19: AD context and causality model of TTR compound powertrain system

Figure 8-19 presents the AD context and causality model of the through-the-road compound powertrain system. For consistency, the VEM and VMC are highlighted in green and yellow respectively. This model closely reflects its Extended Parallel RA counterpart in Figure 4-12. This model differs from the power-split context and causality model in Figure 8-3 by the inclusion of the DriveLine system discussed earlier.

The context and causality model shows the ideal brakes integration. The communication of *available*, *actual* and *capacity* signals to the VEM and *command* signals from the VMC is also shown clearly. As previously stated the role of the VEM is to determine the torque

[27] Omitted is the CVT transmission which is encapsulated within the ICE system, as the CVT transmission and the DriveLine transmission (included here), are mutually exclusive.

splits required to deliver driver demand most efficiently. Unlike the power-split AD the VMC communicates *gear_actual* to the VEM.

Figure 8-20 shows an example AD interaction model of the through-the-road compound powertrain system. This interaction model simply shows the required information for a non-zero torque demand. The only difference between this and the power-split interaction model in Figure 8-4 is the presence of *gear_actual* from the DriveLine System. This interaction model does not display the sequence of events required for a DriveLine System mode change, such as a gear shift. However, it should be noted that this would be exactly the same as that presented in

Figure 4-9. This shows how the control level functional blocks interact to allow a gear change or clutch engagement.

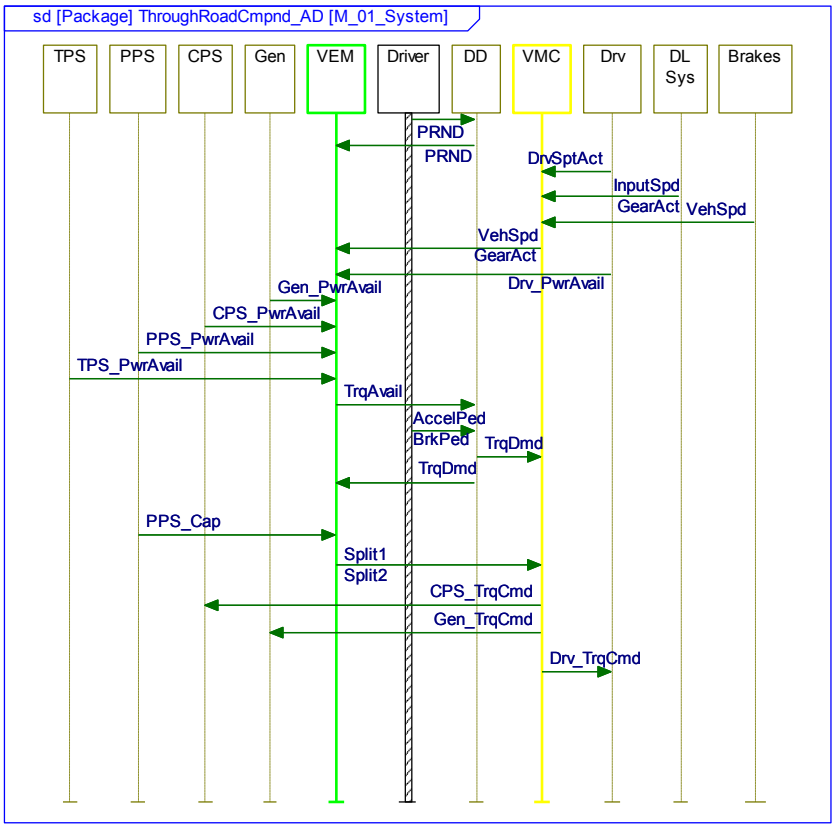

Figure 8-20: AD interaction model of rough-the-road compound powertrain system

In each presentation of an AD one interaction model has been included. As discussed previously each AD deployment would requires many interaction models to represent all scenarios that would be expected of the system. The interaction model represents the behavioural aspect of the systems engineering process, and would form the basis of future system level testing. It is not feasible to present all interaction models which would be necessary for a full vehicle deployment, but one is included as an example.

The next section presents the control domain models for the through-the-road compound AD, focusing on the differences to the RA and the power-split AD

8.3.3. Control domain models

Figure 8-21 presents the AD decomposition model of the through-the-road compound control domain. Comparing this to Figure 4-14 it can be seen that the *CVT_Manager* and the *Instantaneous_Optimisation* control blocks are omitted. The omission of the *CVT_Manager* is due to the presence of a transmission in the DriveLine System. However, encapsulation ensures no redundant interfaces. The *Instantaneous_Optimisation* functional block, as discussed earlier, is an optional function. Finally the multiplicity variables shown in Figure 4-14, have been aligned to the vehicle in Figure 8-17, as there is only one clutch.

Figure 8-21 differs from the power-split control domain decomposition model shown in Figure 8-5 in that the DriveLine system controllers are retained, the DriveLine Manager, the Clutch Manager and the *TCU*. Also the VMC retains the *DriveLine_Mode* and *Speed_Control* functional blocks. Figure 8-23 and Figure 8-23 show this decomposition in control strategy model detail.

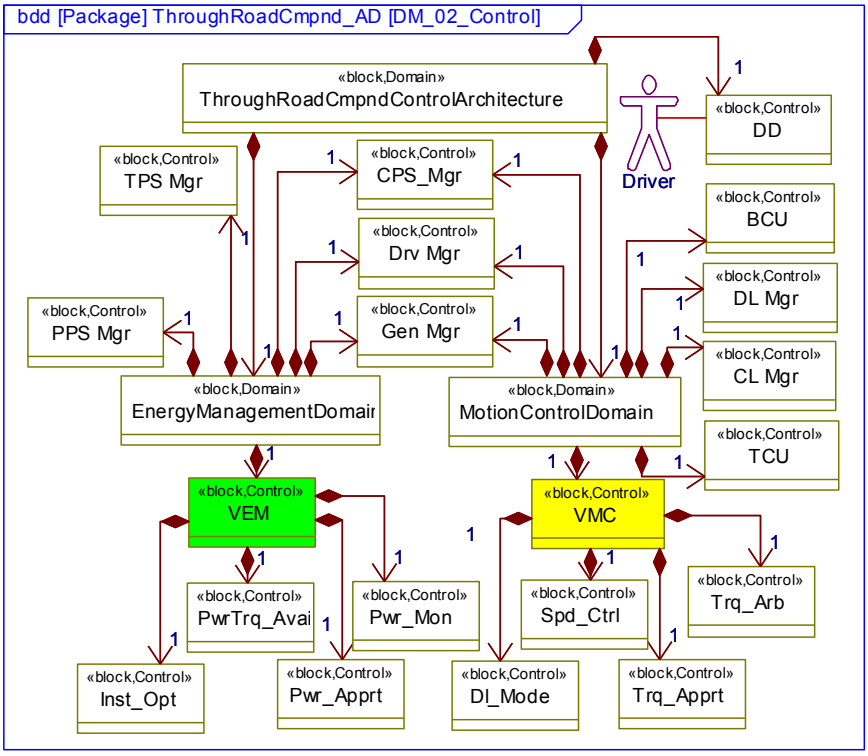

Figure 8-21: AD decomposition model of rough-the-road compound control domain

Figure 8-23 presents the AD strategy model of the through-the-road compound energy management domain. This model is almost identical to the equivalent power-split mode shown in Figure 8-6. The only difference here is the inclusion of the *gear_actual* signal. The salient point here is that the encapsulation defined in the Extended Parallel RA has ensured minimal change between the VEM for the power-split and through-the-road compound HV variants. Moreover, this energy management domain model is closely related to the equivalent parallel AD energy management domain models in Figure H-2 and Figure H-5 (the control domain strategy models of the pre and post transmission parallel ADs in Appendix H). This confirms the reusability of the Parallel and Extended

Parallel RAs as significant changes to the vehicle powertrain have minimal impact on the energy management domain.

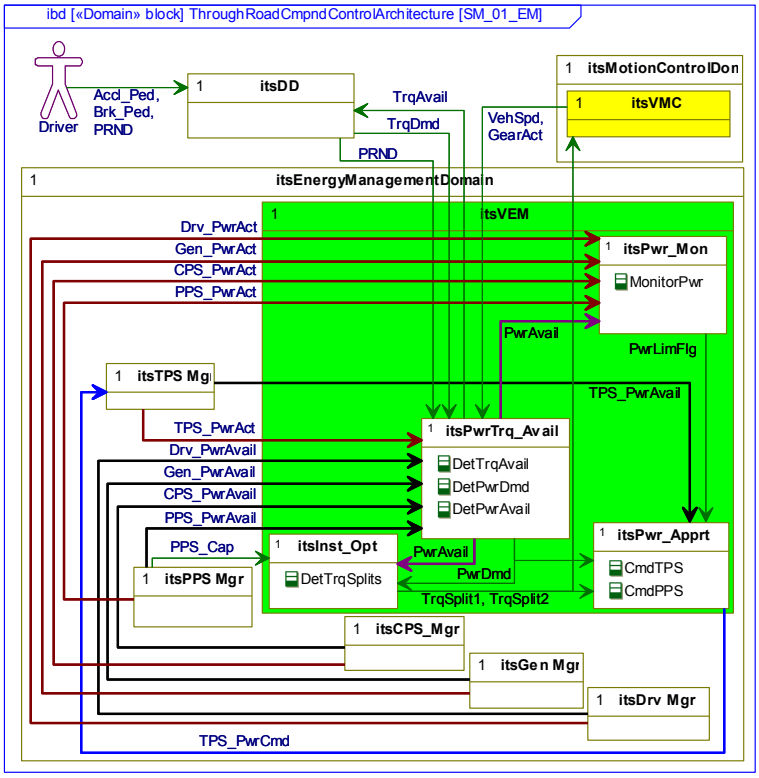

Figure 8-22: AD strategy model of through-the-road compound EM domain

Figure 8-23 presents the AD strategy model for the through-the-road compound motion control domain. This model is derived from the Extended Parallel RA model in Figure 4-16, and is closely related to the Parallel RA model in Figure 4-8. Unlike the power-split AD the *DriveLine_Mode* and *Speed_Control* functional blocks are included. In the case of this AD it is assumed that the DriveLine components are controllable (either directly by the VSC or independently). Therefore as a DriveLine mode changes the system must be arbitrated for driveability purposes and in some cases the speed of the engine and Gen will need to be aligned with the transmission input speed.

This DriveLine configuration may also not be directly controlled by the VSC. In that case, the driver has direct control over the clutch and transmission. However the system still needs information such as DriveLine *mode_actual* (which comprises *gear_actual* and *clutch_status*). The system may still be required to arbitrate torque during DriveLine mode changes.

As before, *Torque_Apportionment* is the key functional block of the VMC. This block determines the three *torque_command* signals from the *torque_demand*, *torque_split1* and *torque_split2* setpoints. This must incorporate the dynamic characteristics of the three actuators and the driveline through which these torques must be transmitted. It is clear that this block will always be deployment specific therefore it is essential that the encapsulation shown here must always be respected.

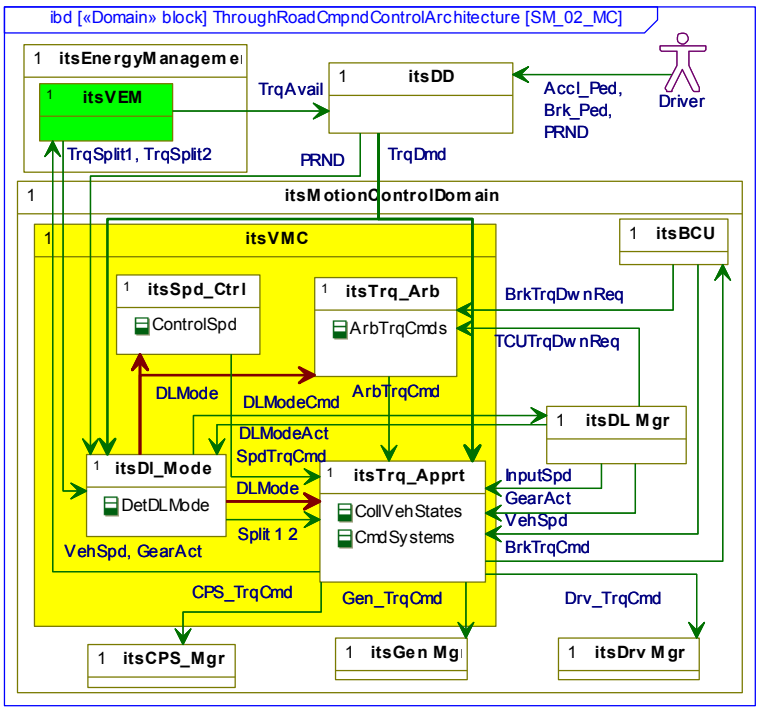

Figure 8-23: AD strategy model of through-the-road compound motion control domain

As discussed previously this AD will not be verified by means of a numerical simulation. The purpose of a simulation in the context of this research is to show by demonstration that the through-the-road AD as derived from the extended Parallel RA is valid. This activity is outside the scope of this research. However the through-the-road AD has been shown to have significant commonality with the power-split AD and where it differs (the inclusion of a DriveLine System) it has been shown to have commonality with the two Parallel ADs.

Therefore it can be asserted with confidence that the Extended Parallel RA correctly represents the through-the-road compound HV variant. This therefore, does not disprove the hypothesis that the Extended Parallel RA is sufficient for all compound HV variants. It would be unexpected if a numerical deployment of a through-the-road compound AD contradicted this assertion.

The next section will briefly discuss some alternate compound HV variants.

8.4. Deployment of other compound ADs from the Extended Parallel RA

In Section 2.4.2 some unusual types of HVs were discussed. These included the TurboGenerator variants as described by Algrain and Bumby et al where a small electrical machine integrated onto the shaft of a turbocharger which can draw some power from the ICE to charge the battery [184, 185], as shown in Figure 2-18. Other methods of capturing exhaust gas energy such as the ThermoGen have been analysed [186] and presented in Figure 2-19. It is proposed here that both systems are similar in architecture and both can be described by the Extended Parallel RA. The system schematics of the TurboGen and ThermoGen compound HVs are reiterated in Figure 8-24 and Figure 8-25.

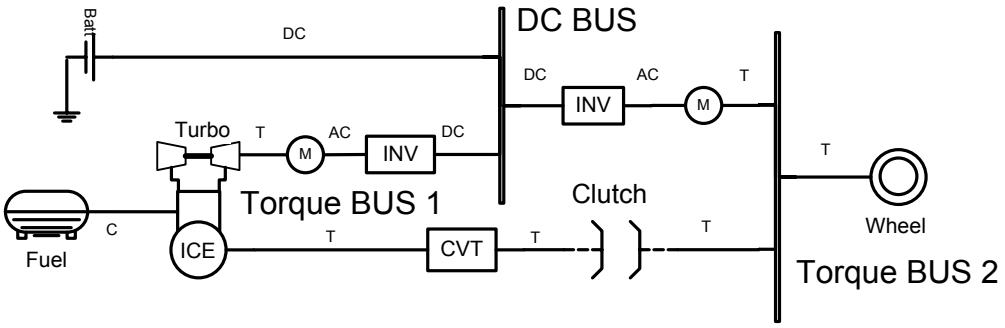

Figure 8-24: System schematic of TurboGen compound HV

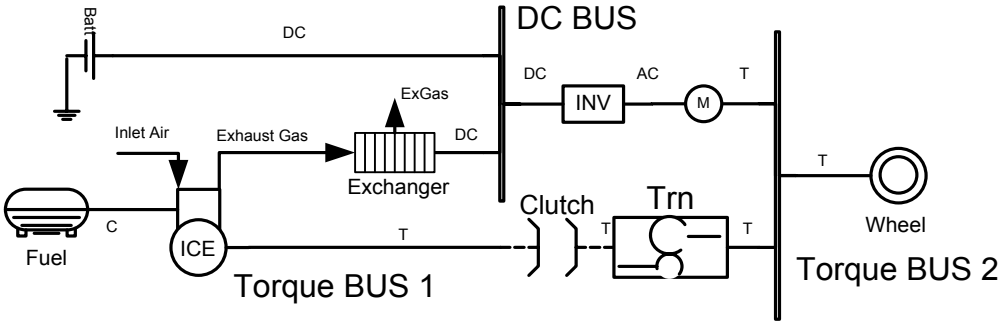

Figure 8-25: System schematic of ThermoGen compound HV

Both systems are designed to capture exhaust gas energy. The TurboGen operates by mechanically driving an electrical machine using the shaft of the turbocharger. The ThermoGen uses the heat of the gas to generate electricity, either directly or through a medium such as a refrigerate gas.

Both of these systems are distinctly different from the previously discussed compound HVs. In both cases the alternate means of generating electrical power is by exhaust gas energy recovery. Neither system is directly coupled with the mechanical output shaft of the vehicle. However in both cases, excessive energy recover may affect the engines ability to generate torque. This is due to the back-pressure which can be created by either the TorboGen or ThermoGen systems. Increased exhaust manifold pressure directly reduces indicated mean effective pressure. Therefore it can be argued that there exist a weak torque coupling between the ICE torque and the DC power generated.

Figure 8-27 presents an alternate system schematic of the TurboGen compound HV and Figure 8-27 shows the same alternate view for the ThermoGen compound HV. In both these models the Gen system is shown to directly connect torque bus 1 with the DC bus. In reality this coupling is via the air path. However this configuration is exactly as described by previous compound HV system schematics (power-split and through-the-road) in Figure 8-1 and Figure 8-17. It can therefore be inferred that the TurboGen and ThermoGen compound HV variants can be described by the same Extended Parallel RA.

It can be seen that the two variants described here contained different transmission types and clutch locations. As described in Chapter 6, this variability is managed by

encapsulation of the DriveLine system or encapsulating the CVT with in the ICE system. It has no bearing on the determination that these two systems can be treated as compound HVs and by extension can be described by the Extended Parallel RA.

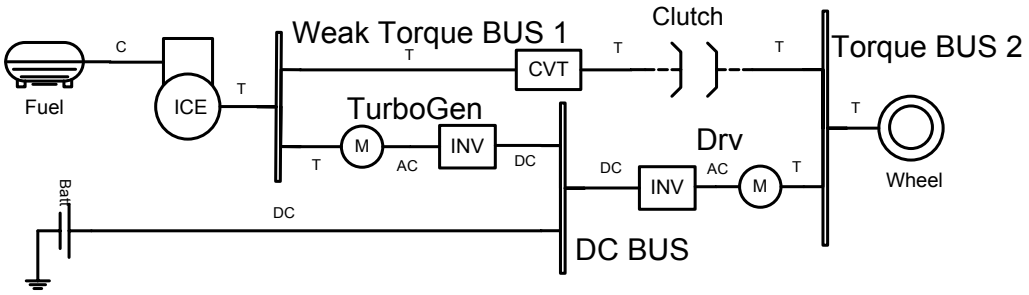

Figure 8-26: Alternate system schematic of TurboGen compound HV

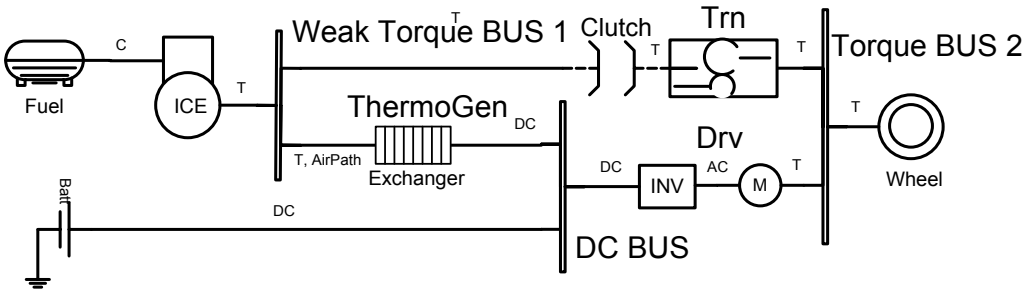

Figure 8-27: Alternate system schematic of ThermoGen compound HV

This discussion does not claim to present a full architectural analysis of the two variants presented. However it is asserted here that to do so would involve excessive repetition once the alternate system schematics are presented. Therefore it can be stated with confidence that the Extended Parallel RA covers the exhaust gas recovery HV variants, which have been classed here as compound HVs.

8.5. Summary

The purpose of this chapter is to test the hypothesis that the Extended Parallel RA can be used to describe the set of compound HV variants. The scope of variants was chosen to encompass the full spectrum of compound HVs. Each variant acts as a scenario to test the reusability of the Extended Parallel RA by demonstration. Failure of one of these scenarios would prove that the hypothesis fails, and that another RA would be required.

The first variant is the power-split compound HV, representing vehicles such as the Toyota Prius and the GM Volt. This was analysed architecturally by deploying it to an AD using the Extended Parallel RA as a template. This was further analysed by deploying a functional controller within a vehicle and driveline plant model. The numerical tests conducted here acted as scenarios for the power-split compound AD, which gives confidence that the RA, as used to design the AD, correctly encompasses the characteristics of the power-split compound HV.

The second variant, the through-the-road compound HV was analysed architecturally by deploying an AD using the Extended Parallel RA as a template. It is immediately apparent that this AD shared much commonality with the power-split compound AD and the pre and post transmission parallel ADs. Therefore it could be asserted that the numerical simulation confirming that the AD is sensible is not required. The similarity of the ADs is due to sensible encapsulation, especially in the motion control domain. Therefore, significant differences in driveline configuration do not affect the architecture.

The two exhaust gas energy recovery compound HV variants seem at first glance very different to the other compound HVs. However it was shown that incorporating a weakly coupled torque bus, both the TurboGen and ThermoGen could be represented as per traditional compound system schematics. It is from this system schematic that the architectural deployment to an AD would begin. Therefore this ensured that both variants would be developed using the same Extended Parallel RA as the earlier compound HV variants. This architectural analysis was not presented here, as it would represent much repetition. This level of repetition would be undesired in a Thesis, however this repetition is exactly what would be desired and expected in industry, resulting in reduced future development costs.

Other compound HV variants can be composed by combining the components in Table 4-2 in the permutations available in the generic system schematic presented in Figure 4-10. This may include capacitors or electrically driven flywheels. However as has been shown in previous chapters, the encapsulation and generic interfaces ensures that these variants do not break the RAs. Similarly, it is expected that the Extended Parallel RA can encompass the alternate component permutations, as described in Chapter 4,

The hypothesis tested by this chapter is whether or not the Extended Parallel RA encompasses the key characteristic for the full set of compound HVs. Only four compound HV variants were analysed, to a varying degree of depth. For these four variants, it has been shown that the hypothesis holds. It needs to be declared that there may be other variants which have not been presented and are not described as potential component permutations, as described in Chapter 4. At this stage of the research it is unclear if such a vehicle exists, or could be developed and sold at a sensible cost. Therefore it can be stated with confidence that the Extended Parallel RA does encompass, based on the analysis conducted in this chapter and given the full scope of compound HVs defined in Section 2.4.2.

The next chapter concludes the Thesis by bringing together the key hypotheses and learning points, recommendations for applying the RAs, limitations of this research and recommendations for future work.

9. Discussion and Conclusions

This chapter presents the discussion and conclusions from this research comprising a review of the research and lessons learnt, limitations of the research and proposed areas of future work.

9.1. Critical review of the research undertaken

The aim of this research is to determine the minimum set of RAs which describe the key functionality of all feasible HV configurations. The rationale for this research stems from the disparate nature of the possible HV configurations. It is argued that an RA used as a template for design, can simplify and reduce development time and cost.

9.1.1. Methodology

As described in Chapter 2 it is common to use quantitative methods to assess system implementations such as number of interface, functions and code line count. However, abstraction can weaken the value of such quantitative methods. An RA is the most abstracted expression of a system. Generic enough to represent a broad set of disparate applications while specific enough to include the key functional characteristics of each. Section 2.2.4 presented several examples of the objectivity of numerical analysis of non-functional attributes of abstracted RAs and how they can be contaminated by the subjectivity of the architect. If, as is the case in industrial settings, this subjectivity can be normalised and benchmarked through extensive application, then the numerical analysis has merit. However, for the purposes of this research, there has been no opportunity to build sufficient experience to normalise a potential quantitative process. It is argued that, to do so would result in numerical backed assertions which would be difficult to defend in the absence of a background data set to normalise or validate against.

To overcome this difficulty, with respect to RAs, the author has opted for a scenario based method. The reusability of an RA is demonstrated by its reuse. In addition, to answer the research question, whether there exists one RA which is applicable to all HV configurations, a set of hypotheses were formed (see section 1.4). A twin layer scenario methodology has been deployed to assess the validity of the hypotheses, as described in Figure 1-1. An AD acts as a scenario for a RA and a numerical deployment acts as a scenario for the AD. Therefore, if an RA is used as a template for the development of an AD, which is in turn numerically tested to ensure the RA does not interfere with the functional relationship between EM and MC, then the hypothesis holds true for this scenario. Then it can be argued that the RA correctly reflects the key functional requirements of the HV variant in question.

This does not automatically mean that the RA is applicable to all other variants of that HV configuration. It is beyond the scope of this research to deploy and numerically test all possible variant permutations within each HV configuration group. However a detailed discussion on encapsulation and interfaces increases the confidence that the RA will be applicable to other variants. Also, careful scenario selection of the most disparate variants within a configuration group, adds further confidence to the reusability of the proposed RA.

9.1.2. Scope

As suggested in the previous section, a detailed scope definition of the potential HV configuration and their potential variants is essential. Section 2.4.2 presents the variety of HVs within three configuration groups; series, parallel and compound HVs. Sections **Error! Reference source not found.**, 4.3.1 and 4.5.1 present the component based variants of each configuration group. It is possible to have more complex configurations or additional components not included in the above sections, but these were considered not to be feasible. Hence the RAs are designed to represent the set of HVs defined within this boundary.

Scenario selection for deployment analysis within each configuration group was guided by the principle of testing the RAs to the limits of the HV scope described in Section 2.4.2. Previous research on the Wren project presented architectural analysis on a set of series HVs with a fuel cell based CPS. The three vehicles analysed had a passive capacitor PPS, a controllable capacitor PPS and a compound PPS with a passive battery and a controllable capacitor. They all had multiple machine drive systems, comprising four wheel or inboard machines. Therefore the series HV chosen for analysis in this research, (to extend the Wren research) comprised an ICE and GenSet CPS with a passive battery PPS and a Drv system comprising a single centrally mounted electrical machine with a transmission. As has been shown, the Series RA encompasses all four variants from the Wren project and from case study 1. Therefore it is argued that the Series RA can be used to develop other series HV variants.

With respect to Parallel HVs there exist two distinct variant groups; pre-transmission and post transmission. Therefore one of each was chosen for deployment and analysis, with the post-transmission including a CVT which decouples the CPS speed from the vehicle speed. Similarly, two distinct types of compound HV variants were chosen. The first is a traditional compound, reflecting the Toyota Prius and GM Volt type HVs. The second is a through the road compound HV. Demonstrating the applicability of the Extended Parallel RA to these disparate compound HV variants, increases the confidence that the Extended Parallel RA is holds for intermediate compound HV variants.

9.1.3. Key findings & lessons learnt

All HVs must realise one overarching requirement: “deliver driver demand efficiently”. This requirement can be resolved into three sub-requirements; driver demand determination, energy management and motion control. These form the basic functional groups of all RAs pertaining to the VSC. However, the non-functional requirement of reusability forces the RAs to incorporate the full HV system, as opposed to the VSC in isolation. The reusability of the VSC architecture is dependent on its interfaces to the wider system. Careful sub-system bounding ensures a simple set of generic interfaces can be retained across all deployments. Throughout this research all HV configurations and variants have been defined by these sub-system boundaries. This is essential to the reusability of the RAs.

Hypothesis 1

This research finds that the first hypothesis holds true. In that the Wren RA is extendable to other series HV variants, including real world consideration, such as integrated hybrid braking systems, transmissions and on-board chargers. The separation of energy management and motion control is still valid as all series HVs share the characteristics of a dedicated drive system. Therefore the PPS and CPS remain under the control of the VEM. The RA was extended to incorporate brakes, transmissions, on-board-chargers and other vehicle loads referred to as the TPS. The key interface between the VEM and the VMC is *power_available.* The VMC does not need to be aware of the detail within the energy management domain.

An important relationship between Driver Demand, *power_available* and *torque_available* was highlighted. The *torque_available* signal ensures that the system cannot exceed either its total limit or the individual sub-system limits. This is done by selecting the minimum between the *torque_available* from the Drive system with the *power_available* from the VMC. The resultant *torque_avaialable* constrains *torque_demand* from the Driver Demand. This structure is essential to systems which draw power from more than one sub-system, as the total system power, by definition exceeds the individual sub-system limits.

The previous point raises another issue. Traditionally vehicle speed and engine speed are unsigned broadcast variables, and engine control operates in a single quadrant in the speed torque plane. However in the case of electric drive vehicles, it is possible to operate in four quadrants of that plane. A typical use case is commanding positive torque while rolling backwards. Initially positive torque and negative speed results in negative PPS power (charging). As more torque is applied the speed will increase (negative speed reduces), until the PPS is delivering positive power (discharging). In both these conditions, different PPS limits will apply. The *torque_available* signal must reflect this *power_available* transition. The *Torque_Available* functional block was defined in detail and it is argued that this should be applied to all series HV variants.

Encapsulation has been used to protect the RAs from sub-system variability. This ensures that the CPS can represent a fuel cell or an ICE and GenSet type systems as demonstrated. By inference it is also argued that this may apply to other un deployed CPS variants, such as a gas turbine. The theme of encapsulation is also applied to the series drive system to show how it can incorporate a single machine or a complex four-machine system. This point counters the standard industry approach to system development, in that enterprises are segmented along component based lines. This creates a difficulty with the CPS which combines and ICE with a GenSet. The traditional approach would see the VSC interfacing directly with the two CPS sub-systems directly, which would impair reusability. However the Series RA presented here ensures that this does not happen and highlights the benefits of encapsulation.

Hypothesis 2

With respect to the second hypothesis, parallel HVs do not have a dedicated drive system. More specifically, both the CPS and PPS share a torque coupling to the vehicle inertia. Therefore the Series RA cannot be applied nor extended to be applicable to

parallel HV configurations. Therefore a second RA is defined which allows the VEM to manage the demand efficiently by means of *split* command to the VMC. The VMC uses this *split* to allocate the correct level of *torque_command* to both the CPS and the PPS, based on the *torque_demand* from the DD block. The characteristic of sharing subsystems between the energy management and motion control domains is a distinguishing feature of the Parallel RA. As is the *split* interface between the VEM and the VMC.

Hypothesis 3

The third hypothesis is addressed by demonstrating that the Parallel RA can be extended to incorporate the compound HV configuration. The key characteristics are preserved. However, now three sub-systems are shared between the energy management and motion control domains; the CPS, Drive and Gen systems. Also the compound VMC require two *split* signals from the VEM. It has been shown that the Parallel RA and the extended Parallel RA can be used to deploy a wider variety of variants.

The final three chapters present scenario analyses which testes the hypotheses. Since none of the hypotheses failed, it can be stated that the RAs are applicable to the scenarios chosen. It is argued that through encapsulation and careful selection of the scenarios, the RAs are applicable to a wider set of scenarios than demonstrated here. It is conceded that a HV variant may exist within the scope boundary which may require slight extension to the one or both of the RAs. However it is argued that this extension will be limited and the RA will still present a valuable template to initiate development. This research has presented strong evidence that the two RAs will aid future HV development for a wide variety of HV variants.

The numerical deployments act as scenarios for the ADs and hence add confidence to the above assertions. The numerical tests presented have been selected to highlight the relationship between energy management and motion control. The demarcation of these two functions is the key characteristic of both RAs. While the numerical tests are not comprehensive they do demonstrate how the RA structure does not adversely affect the relationship between these two functional groups.

9.1.4. Contribution and novelty

This Thesis has presented two novel RAs which can be used as design templates for HV system development. As discussed in Chapter 2, RAs have been developed before, but none were comprehensive enough to encompass all HV variants. Also, it is argued that key features such as sub-system boundary definitions and encapsulation ensures the RAs ensure reusability of the RAs for future HVs, yet to be defined. With respect to series HV CPS systems, encapsulation highlighted the need for industry players to alter how their structures their enterprises. Different departments will be required to understand each other's requirements and work more closely together.

In addition, a novel implementation of the ECMS approach for series HVs and parallel HVs where the CPS speed is decoupled form the vehicle speed was developed and implemented. This new method is based on a polynomial function of the power to

efficiency relationship of the CPS. This is easier to calibrate and will generate a continuous split signal.

9.1.5. Conclusion

Based on a set of hypothesis, it has been determined that two RAs are required. By using ADs as scenarios for RAs it has been demonstrated that the RAs are applicable to the HVs variants analysed. The numerical simulations, HIL and in-vehicle tests act as scenarios for the ADs giving confidence to the findings on the hypotheses. Therefore the aim of this research has been achieved.

The next section addresses acknowledged weaknesses in the research undertaken and areas for future work.

9.2. Research limitations and future work

9.2.1. Scenario analysis versus quantitative analysis

The choice to employ the scenario based analysis methodology to test the hypotheses is a controversial one. It is argued with respect to subjectivity and abstraction, that employing published quantitative methods would be difficult to defend without significant validation data; a resource not available to this research. However, a comprehensive scenario analysis would require each scenario to be tested before full confidence in the reusability of the RA is established. It is beyond the scope of this research to deploy and numerically test every HV variant as a scenario.

To combat this contradiction, key variants have been selected which, it is argued, test the RAs to the extremes of their potential deployments. Arguments on encapsulation, generic interfaces, sub-system bounding and HV configuration grouping have been presented which infers RA reusability beyond the scenario deployments. However, due to the number of ADs analysed, the resultant Thesis is quite broad. Given the limitation of access to industry based metric data for reusability of RAs, it is argued that the trade-off between methodology defendibility and research depth is appropriate given the research aim and resultant hypotheses.

9.2.2. Model based analysis (UML/SysML)

As presented in Section 2.2.1, model based design using the SysML is the standard approach within in the systems engineering field. The main goal of model based design is to move away from a document based system for capturing and communicating system architectures. However, given the constraint of a Thesis, all the SysML models presented here have been designed to be viewable in a document format.

Furthermore, the SysML has minimal penetration within the automotive powertrain system development field. When presenting this work to a broader audience, simplified diagrams based on the SysML models were designed for ease of communication, as shown in Harrington et al [23]. These simplified models loose the semantic detail of the SySML but retain the key characteristics of the RAs.

A final limitation of employing the SysML tool is its poor navigability. With automotive software developers who are used to environments such as Simulink, the inability to

navigate horizontally between models and vertically through the hierarchy is a significant barrier to industry wide adoption. The SySML was used in this research to present the RAs in a semantically formal environment, which is the preferred method in the wider systems engineering field.

9.2.3. Industry opinion surveys

While industry participants encountered throughout this research have responded positively to the RAs and their reusability, no formal survey was conducted. Therefore, any anecdotal suggestion that the RAs are being employed presently in industry cannot be relied upon as evidence of RA reusability within this research. Such a survey would increase confidence in the assertions of RA reusability. However, it is argued that demonstrating the deployed ADs for a meaningfully large set of HVs was a priority with respect to RA reusability.

9.2.4. Terminology

The terms series and parallel, when referred to HVs, has a well understood meaning within the low carbon vehicle industry. As presented in this research, the Wren fuel cell vehicles and the LCVTP vehicle, discussed in Chapter 6, were defined as series HVs. However, these types of vehicle are commonly referred to as EVs or 'EVs with range extenders'. None of these vehicles are true EVs. These terms point to one defining characteristic of series HVs, in that they all have dedicated electric drive systems. However, they are all series HVs, as power is drawn from one or more power sources and hybridised by means of an electrical DC bus. Moreover, if an electrical circuit of these vehicles were drawn, it would be seen that they are electrically in parallel. A true series HV which is electrically in series, would be very difficult to engineer and control and it is argued that no such vehicle exists.

It is suggested in Harrington et al that these vehicles should be termed electrical HVs [23], as they are hybridised electrically. Conversely the 'parallel" vehicles should be referred to as mechanical HVs, as their point of hybridisation is a mechanical torque bus. However, as the terms series and parallel are embedded in the HV industry, they have been used here. Compound HVs are sometimes referred to as series-parallel HVs. As this term refers to some potential operating modes of this type of vehicle, and not the characteristics of its architecture, the term compound HV is used throughout this research.

9.2.5. Future work

Under the scenario methodology, it is desired to demonstrate the reusability of the RAs on all possible HV variants. This would require that all HV variants (including every component permutation) be deployed using the RAs as a template to functional testing. This is a significant task which would confirm the reusability of the RAs for the full scope of HVs as defined in Section 2.4.2. However, it is argued that high confidence in the RAs reusability across the full scope would be reached long before all deployments were completed. The principle of diminishing returns suggests that this task would provide little value to the argument of reusability beyond a certain stage.

Of more interest is the scope to conduct a more comprehensive set of functional tests on the deployed control systems. Due to time and space constraints, functional tests in this research focused on the relationship between energy management and motion control and the potential impact of the RAs on that relationship. More detailed tests on drivability, incorporating dynamic plant models and dynamic *Torque_Apportionment* functional blocks would be desirable. This was done for the pre-transmission parallel HV in Section 7.2, but should be extended to all HVs deployed for testing.

True and comprehensive validation would require full deployment to a production ready HV using the RA as a template, followed by a second (or more) production ready deployment. The multiple production level deployments of HVs using the RAs would generate the data required to validate the usability of the RAs. This would require close partnership with a vehicle manufacturer.

Functional safety and functional diagnostics have been mentioned briefly in this research. Functional safety analysis methods, such as ISO 26262, highlight issues such as charge door interlock and functional diagnostics, namely the *Power_Monitor* functional block [194]. These are included in this Thesis as they represent an overlap between functionality, safety and diagnostics. These attributes are particularly important for HVs which may have electric drives directly coupled to the wheels and draw power from several sources. It is expected that a full architectural investigation on these topics would result in functional safety and functional diagnostics RAs which would complement the main functional RAs defined in this Thesis. These functional and diagnostic RAs would add significant value to the research presented here.

As mentioned in the previous section, industry surveys assessing the opinions of system developers regarding the reusability of the RAs would be beneficial. However, it is argued that giving guidance on how the RAs can be deployed and then their reusability measured quantitatively in an industrial setting is more important. In such a setting it is foreseeable that development teams will have more than one HV development program at a given time, and more again over time. A quantitative methodology for measuring RA reusability would be appropriate in this environment. This would require the architects and developers to agree a set of weighted metrics. Not all interfaces or functions are of equal importance and they must be weighted accordingly [200]. The assignment and magnitude of such weightings must be the responsibility of the system owner, with reference to the desired system attributes. This may present further opportunities in formal optimisation of a cost function of these weighted metrics.

Once the metrics have been decided, the data from each deployment must be captured and bookshelved. As a history of deployments is completed, reusability of the RAs can be measured. It is expected that as experience is built up the system architects and owners will update the weightings and priorities of their metrics, but as the historical data has been recorded, this can be done retrospectively. Hence the natural subjectivity of such metrics can be normalised, and the true reusability value of the RAs can be determined. This may manifest as development cost savings or flexibility to enter market quickly with new HV vehicles. However, It should be pointed out that this quantitative approach will be relative and not absolute, and specific to the enterprise in question, the

experience of its architects and developers and its desired product attributes with respect to its target market. While it would be desired that this activity should be conducted with academic rigour, it is unlikely that any vehicle manufacturer would share such a commercially sensitive activity with a third party.

9.2.6. Concluding remarks

This Thesis addressed the problem of vehicle to vehicle system and VSC development waste due to a lack of architectural reusability. RAs, which takes advantage of shared system characteristics and encapsulates variances, have been shown to reduce development time and cost. Two RAs have been proposed which, it is argued, represent the full scope of feasible HVs (series, parallel and compound) for the light vehicle market. The reusability of these RAs has been demonstrated using the scenario method to test a set of hypothesis. The scenarios chosen represent the extremes of the HV variants. This generates confidence that the RAs represent the characteristics of the full scope of HVs. It is argued that the proposed RAs can be used as design templates for future HV development programs.

References

[1] Anon, "IPCC First Assessment Report," IPCC, Geneva, Switzerland1990.

[2] Anon, "Climate Change 2007: Synthesis Report. Contribution of Working Groups I, II and III to the Fourth Assessment Report of the Intergovernmental Panel on Climate Change," IPCC, Geneva, Switzerland2007.

[3] N. Stern, "Stern Review on the Economics of Climate Change," HM Treasury, London2006.

[4] J. King, "The King Review of low-carbon cars. Part 1: the potential for CO2 reduction," HM Treasury, London 978-1-84532-335-6, 2007.

[5] J. Annema, "Effectiveness of the EU White Paper: 'European transport policy for 2010'," Netherlands Environmental Assessment Agency., Bilthoven, Neatherlands2005.

[6] D. A. Hensher and S. M. Puckett, "Road user charging: The global relevance of recent developments in the United Kingdom," *Road User Charging: Theory and Practices,* vol. 12, pp. 377-383, 2005.

[7] Anon, "Congestion Charging Impacts Monitoring - Fifth Annual Report," Transport for London2007.

[8] Anon, "Congestion Charging Impacts Monitoring - Sixth Annual Report," Transport for London2008.

[9] D. MacKay, *Sustainable Energy : without the hot air*. Cambridge: UIT Cambridge, 2008.

[10] Naigt, "An Independent Report on the Future of the Automotive Industry in the UK," BERR2009.

[11] X. Nuo, C. Huiyan, H. Yuhui, and L. Haiou, "The Integrated Control System in Automatic Transmission," in *Mechatronics and Automation, 2007. ICMA 2007. International Conference on*, Harbin, Heilongjiang, China, 2007, pp. 1655-1659.

[12] R. N. Charette. (2009) This car runs on code. *IEEE Spectrum*.

[13] R. Cloutier, G. Muller, D. Verma, R. Nilchiani, E. Hole, and M. Bone, "The Concept of Reference Architectures," *Systems Engineering,* vol. 13, pp. 14-27, 2010.

[14] J. Nzisabira, Y. Louvigny, and P. Duysinx, "Comparison of ultra capacitors, hydraulic accumulators and batteries technologies to optimize hybrid vehicle ecoefficiency," in *Power Engineering, Energy and Electrical Drives, 2009. POWERENG '09. International Conference on*, ed, 2009, pp. 353-358.

[15] R. J. Cloutier and D. Verma, "Applying the concept of patterns to systems architecture," *Systems Engineering,* vol. 10, pp. 138-154, 2007.

[16] J. Marco and N. D. Vaughan, "Design of a Reference Control Architecture foe the Energy Management of Electric Vehicles," *International Journal of Vehicle Design,* 2011.

[17] Anon, *Systems Engineering Handbook* vol. 3.2. San Diego, CA, USA: INCOSE International Council on Systems Engineering, 2010.

[18] M. W. Maier and E. Rechtin, *The Art of Systems Architecting* vol. 2. USA: CRC Press, 2000.

[19] E. Rechtin, *Systems Architecting: Creating and Building Complex Systems*. New Jersey, USA: Prentice Hall, 1991.

[20] P. Thoma, "Automotive electronics-a challenge for systems engineering," in *Design, Automation and Test in Europe Conference and Exhibition 1999. Proceedings*, 1999, p. 4.

[21] G. Leen and D. Heffernan, "Expanding automotive electronic systems," *Computer,* vol. 35, pp. 88-93, 2002.

[22] J. Marco and N. D. Vaughan, "Architectural Modelling of an Energy Management Control System Using The UML," *International Journal of Vehicle Design,* 2010.

[23] C. M. Harrington, J. Marco, and N. D. Vaughan, "The Design of a Reference Control Architecture to Support Vehicle Hybridisation," *International Journal of Vehicle Design,* 2011.

[24] C. Del Rosso, "Continuous evolution through software architecture evaluation: a case study," *Journal of Software Maintenance and Evolution: Research and Practice,* vol. 18, pp. 351-383, 2006.

[25] C. Alexander, S. Ishikawa, M. Silverstein, M. Jacobson, I. Fiksdahl-King, and S. Angel, *A Pattern Language*. New York, USA: Oxford University Press, 1977.

[26] A. E. Hickey, "The Systems Approach: Can Engineers Use the Scientific Method?," *Engineering Management, IRE Transactions on,* vol. EM-7, pp. 72-80, 1960.

[27] Anon, "What is Systems Engineering," vol. 2010, ed: International Council on Systems Engineering, 2004.

[28] S. Bennett, S. McRobb, and R. Farmer, *Object-Orineted Systems Analysis and Design using UML*. England: MCGraw-Hill, 1999.

[29] D. Truscan, J. M. Fernandes, and J. Lilius, "Tool support for DFD-UML model-based transformations," in *Engineering of Computer-Based Systems, 2004. Proceedings. 11th IEEE International Conference and Workshop on the*, 2004, pp. 388-397.

[30] V. Symons, "Evaluation of information systems: IS development in the Processing Company," *Journal of Information Technology,* vol. 5, pp. 194-204, 1990.

[31] R. C. Booton and S. Ramo, "The Development of Systems Engineering," *Aerospace and Electronic Systems, IEEE Transactions on,* vol. AES-20, pp. 306-310, 1984.

[32] C. Barker. (1998) London Ambulance Service gets IT right. Available: **http://www.computing.co.uk/computing/news/2064653/london-ambulance-service-gets-right**

[33] A. P. Sage and J. E. Armstrong, Jr., "Introduction to Systems Engineering," ed: John Wiley & Sons, 2000.

[34] M. V. Linhares, A. J. da Silva, and R. S. de Oliveira, "Empirical Evaluation of SysML through the Modeling of an Industrial Automation Unit," in *Emerging Technologies and Factory Automation, 2006. ETFA '06. IEEE Conference on*, 2006, pp. 145-152.

[35] J. H. Brill, "Systems engineering? A retrospective view," *Systems Engineering,* vol. 1, pp. 258-266, 1998.

[36] Anon, "Introduction to OMG's Unified Modeling Language,Ñ¢ (UML¬Æ)," vol. 2010, ed: OMG, 2009.

[37] Y. Grobshtein, V. Perelman, E. Safra, and D. Dori, "Systems Modeling Languages: OPM Versus SysML," in *Systems Engineering and Modeling, 2007. ICSEM '07. International Conference on*, 2007, pp. 102-109.

[38] J. M. Fernandes and J. Lilius, "Functional and object-oriented views in embedded software modeling," in *Engineering of Computer-Based Systems, 2004. Proceedings. 11th IEEE International Conference and Workshop on the*, 2004, pp. 378-387.

[39] X. Gao and Z. Li, "Business process modelling and analysis using UML and polychromatic sets," *Production Planning & Control: The Management of Operations,* vol. 17, p. 780, 2006.

[40] Y. Vanderperren, W. Mueller, and W. Dehaene, "UML for electronic systems design: a comprehensive overview," *Design Automation for Embedded Systems,* vol. 12, pp. 261-292, 2008.

[41] Anon, "The Systems Modelling Language, OMG SysML, Specification 1.1," OMG2008.

[42] M. Hause, F. Thom, and A. Moore, "Inside SysML," *Electronics Systems and Software,* vol. 3, pp. 20-25, 2005.

[43] M. Hause, F. Thom, and A. Moore, "Inside SysML," *Computing & Control Engineering Journal,* vol. 16, pp. 10-15, 2005.

[44] Y. Grobshtein and D. Dori, "Creating SysML views from an OPM model," in *Model-Based Systems Engineering, 2009. MBSE '09. International Conference on*, 2009, pp. 36-45.

[45] G. Yue and R. P. Jones, "A study of approaches for model based development of an automotive driver information system," in *Systems Conference, 2009 3rd Annual IEEE*, 2009, pp. 267-272.

[46] J. Marco and N. D. Vaughan, "Integration of Architectural Modeling Using the SysML within the Traditional Automotive CACSD Process," in *Proceedings of the International Conference on Control*, 2010.

[47] Y. Vanderperren and W. Dehaene, "From UML/SysML to Matlab/Simulink: Current State and Future Perspectives," in *Design, Automation and Test in Europe, 2006. DATE '06. Proceedings*, 2006, pp. 1-1.

[48] J. Marco and N. D. Vaughan, "Architectural modelling of an energy management control system using the SysML," *International Journal of Vehicle Design,* vol. 55, pp. 1-22, 2011.

[49] Anon, "Recommended practice for architectural description of software-intensive systems," in *IEEE Std 1471-2000*, ed, 2007, pp. i-23.

[50] M. Richards, N. Shah, D. Hastings, and D. Rhodes, "Architecture Frameworks in System Design: Motivation, Theory, and Implementation," 2007.

[51] J. Van Gurp, R. Smedinga, and J. Bosch, "Architectural Design Support for Composition \& Superimposition," *HICSS '02: Proceedings of the 35th Annual Hawaii International Conference on System Sciences (HICSS'02)-Volume 9,* p. 287, 2002.

[52] M. Termeer, C. F. J. Lange, A. Telea, and M. R. V. Chaudron, "Visual Exploration of Combined Architectural and Metric Information," in *Visualizing Software for Understanding and Analysis, 2005. VISSOFT 2005. 3rd IEEE International Workshop on*, 2005, pp. 1-6.

[53] M. Sghairi, J. J. Aubert, P. Brot, A. de Bonneval, Y. Crouzet, and Y. Laarouchi, "Distributed and reconfigurable architecture for flight control system," in *Digital Avionics Systems Conference, 2009. DASC '09. IEEE/AIAA 28th*, 2009, pp. 6.B.2-1-6.B.2-10.

[54] M. J. Marco, P. Leitao, A. W. Colombo, and F. Restivo, "Service-oriented control architecture for reconfigurable production systems," in *Industrial Informatics, 2008. INDIN 2008. 6th IEEE International Conference on*, 2008, pp. 744-749.

[55] R. Stenzel, "A behavior-based control architecture," in *Systems, Man, and Cybernetics, 2000 IEEE International Conference on*, 2000, pp. 3235-3240 vol.5.

[56] J. Ullberg, R. Lagerstrom, and P. Johnson, "A Framework for Service Interoperability Analysis using Enterprise Architecture Models," in *Services Computing, 2008. SCC '08. IEEE International Conference on*, 2008, pp. 99-107.

[57] D. Ahrens, A. Pfeiffer, and T. Bertram, "Comparison of ASCET and UML - Preparations for an abstract software architecture," in *Specification, Verification and Design Languages, 2008. FDL 2008. Forum on*, 2008, pp. 233-234.

[58] J. Yunho, P. Jungmin, S. Insub, C. Young-Jo, and O. Sang-Rok, "An object-oriented implementation of behavior-based control architecture," in *Robotics and Automation, 1996. Proceedings., 1996 IEEE International Conference on*, 1996, pp. 706-711 vol.1.

[59] P. Ridao, J. Yuh, J. Batlle, and K. Sugihara, "On AUV control architecture," in *Intelligent Robots and Systems, 2000. (IROS 2000). Proceedings. 2000 IEEE/RSJ International Conference on*, 2000, pp. 855-860 vol.2.

[60] J. K. Rosenblatt and J. A. Hendler, "Architectures for Mobile Robot Control," in *Advances in Computers*. vol. Volume 48, V. Z. Marvin, Ed., ed: Elsevier, 1999, pp. 315-353.

[61] X. Li and l. Jiang, "Study on control system architecture of modular robot," in *Robotics and Biomimetics, 2007. ROBIO 2007. IEEE International Conference on*, 2007, pp. 508-512.

[62] H. Yavuz and A. Bradshaw, "A new conceptual approach to the design of hybrid control architecture for autonomous mobile robots," *Journal of Intelligent and Robotic Systems: Theory and Applications,* vol. 34, pp. 1-26, 2002.

[63] G. Reichart and M. Haneberg, "Key Drivers for a Future System Architecture in Vehicles," *SAE Technical Paper Series,* vol. 2004-21-0025, 2004.

[64] F. Santos, J. Trovao, A. Marques, P. Pedreiras, J. Ferreira, L. Almeida, and M. Santos, "A Modular Control Architecture for a Small Electric Vehicle," in *Emerging Technologies and Factory Automation, 2006. ETFA '06. IEEE Conference on*, 2006, pp. 139-144.

[65] E. Ibarra, R. Stobart, and R. Lutz, "System Safety Analysis: SysML and UML in the Automotive Context," in *European Systems Engineering Conference*, Edinburgh, UK, 2006, pp. 440-448.

[66] D. Wild, A. Fleischmann, J. Hartmann, C. Pfaller, M. Rappi, and S. Rittman, "An Architecture-Centric Approach towards the Construction of Dependable Automotive Software," *SAE,* vol. 2006-01-1222, 2006.

[67] L. Rosario, P. C. K. Luk, J. T. Economou, and B. A. White, "A Modular Power and Energy Management Structure for Dual-Energy Source Electric Vehicles," in *Vehicle Power and Propulsion Conference, 2006. VPPC '06. IEEE*, 2006, pp. 1-6.

[68] U. Beher and K. Werthschulte, "Energy Management as Configurable System Software Function," *SAE,* vol. 2009-01-0516, 2009.

[69] A. M. Phillips, "Functional decomposition in a vehicle control system," in *American Control Conference, 2002. Proceedings of the 2002*, 2002, pp. 3713-3718 vol.5.

[70] M. Ceraolo, A. di Donato, and G. Franceschi, "A General Approach to Energy Optimization of Hybrid Electric Vehicles," *Vehicular Technology, IEEE Transactions on,* vol. 57, pp. 1433-1441, 2008.

[71] E. Gamma, R. Helm, J. Johnson, and J. Vlissides, *Elements of Reusable Object Orientated Software*. Reading, Ma, USA: Addison-Wesley, 1995.

[72] J. O. Coplien, "Idioms and patterns as architectural literature," *Software, IEEE,* vol. 14, pp. 36-42, 1997.

[73] M. W. Maier, "Architecting principles for systems-of-systems," *Systems Engineering,* vol. 1, pp. 267-284, 1998.

[74] P. Avgeriou and U. Zdun, "Architectural patterns revisited-a pattern language," in *10th European Conference on Pattern Languages of Programs*, 2005.

[75] A. Engel and T. R. Browning, "Designing systems for adaptability by means of architecture options," *Systems Engineering,* vol. 11, pp. 125-146, 2008.

[76] R. Sanz and J. Zalewski, "Pattern-based control systems engineering," *Control Systems Magazine, IEEE,* vol. 23, pp. 43-60, 2003.

[77] A. Howard, A. Kochhar, and J. Dilworth, "Application of a generic manufacturing planning and control system reference architecture to different manufacturing environments," *Proceedings of the Institution of Mechanical Engineers, Part B: Journal of Engineering Manufacture,* vol. 213, pp. 381-396, 1999.

[78] R. Boulanger and D. Overland, "Control System Architectures, Technologies, and Concepts for Near Term and Future Human Exploration of Space," *SAE,* vol. 2004-01-2478, 2004.

[79] M. Larsen, S. W. De La Salle, and D. Reuter, "A reusable Control System Architecture for Hybrud Powertrains," *SAE,* vol. 2002-01-2808, 2002.

[80] F. Vanek, P. Jackson, and R. Grzybowski, "Systems engineering metrics and applications in product development: A critical literature review and agenda for further research," *Systems Engineering,* vol. 11, pp. 107-124, 2008.

[81] J. Muskens, M. Chaudron, and C. Lange, "Investigations in Applying Metrics to Multi-View Architecture Models," *EUROMICRO Conference,* vol. 0, pp. 372-379, 2004.

[82] C.-h. Lung and K. Kalaichelvan, "An Approach to Quantitative Software Architecture Sensitivity Analysis," in *International Journal of Software Engineering and Knowledge Engineering*, 1998, pp. 185-192.

[83] D. Ahrens, A. Frey, A. Pfeiffer, and T. Bertram, "Restructuring and Optimization of Software Architectures for Longitudinal Driver Assistance Systems," in *FISITA*, Hungary, 2010.

[84] X.-l. Bai, X.-s. Luo, X.-h. Bai, X.-q. Yi, H.-h. Chen, and D.-k. Guo, "Study of DoD Architecture Simulation Validation based on UML and Extended Colored Petri Nets," in *Networking, Sensing and Control, 2008. ICNSC 2008. IEEE International Conference on*, 2008, pp. 61-66.

[85] L. W. Wagenhals, S. Haider, and A. H. Levis, "Synthesizing executable models of object oriented architectures," *Systems Engineering,* vol. 6, pp. 266-300, 2003.

[86] T. R. Browning, "Applying the design structure matrix to system decomposition and integration problems: a review and new directions," *Engineering Management, IEEE Transactions on,* vol. 48, pp. 292-306, 2001.

[87] A. Yassine, "An Introduction to Modeling and Analyzing Complex Product Development Processes Using the Design Structure Matrix (DSM) Method," *Quaderni di Management (Italian Management Review),* vol. 9, 2004.

[88] D. M. Sharman and A. A. Yassine, "Characterizing complex product architectures," *Systems Engineering,* vol. 7, pp. 35-60, 2004.

[89] T. R. Browning and S. D. Eppinger, "Modeling impacts of process architecture on cost and schedule risk in product development," *Engineering Management, IEEE Transactions on,* vol. 49, pp. 428-442, 2002.

[90] W. Abdelmoez, M. Shereshevsky, R. Gunnalan, H. H. Ammar, Y. Bo, S. Bogazzi, M. Korkmaz, and A. Mili, "Quantifying software architectures: an analysis of change propagation probabilities," in *Computer Systems and Applications, 2005. The 3rd ACS/IEEE International Conference on*, 2005, p. 124.

[91] P. Popic, D. Desovski, W. Abdelmoez, and B. Cukic, "Error propagation in the reliability analysis of component based systems," in *Software Reliability Engineering, 2005. ISSRE 2005. 16th IEEE International Symposium on*, 2005, pp. 10 pp.-62.

[92] I. Shaik, W. Abdelmoez, R. Gunnalan, A. Mili, C. Fuhrman, M. Shereshevsky, A. Zeid, and H. H. Ammar, "Using Change Propagation Probabilities to Assess Quality Attributes of Software Architectures 1," in *Computer Systems and Applications, 2006. IEEE International Conference on.*, 2006, pp. 704-711.

[93] I. Shaik, W. Abdelmoez, R. Gunnalan, M. Shereshevsky, A. Zeid, H. H. Ammar, A. Mili, and C. Fuhrman, "Change Propagation for Assessing Design Quality of Software Architectures," in *Software Architecture, 2005. WICSA 2005. 5th Working IEEE/IFIP Conference on*, Pittsburgh, PA, USA, 2005, pp. 205-208.

[94] J. Muskens, M. R. V. Chaudron, and R. Westgeest, "Software Architecture Analysis Tool -Software Architecture Metrics Collection," *Proceedings of the 3rd Progress workshop on embedded systems, Utrecht, Neatherlands. ,* pp. 128- 139, 2002.

[95] M. Eriksson, K. Borg, and J. r. B√∂rstler, "Use Cases for Systems Engineering?An Approach and Empirical Evaluation," *Systems Engineering,* vol. 11, pp. 39-60, 2008.

[96] A. P. Sage and C. L. Lynch, "Systems integration and architecting: An overview of principles, practices, and perspectives," *Systems Engineering,* vol. 1, pp. 176-227, 1998.

[97] E. Cacciatori, N. D. Vaughan, and J. Marco, "Energy management strategies for a parallel hybrid electric powertrain: Fuel economy optimisation with driveability requirements," in *Hybrid Vehicle Conference, IET The Institution of Engineering and Technology, 2006*, 2006, pp. 157-172.

[98] L. Serrao, S. Onori, and G. Rizzoni, "ECMS as a realization of Pontryagin's minimum principle for HEV control," in *American Control Conference, 2009. ACC '09.*, ed. St. Louis, Missouri, USA., 2009, pp. 3964-3969.

[99] M. Ehsani, Y. Gao, S. E. Gay, and A. Emadi, *Modern Electric, Hybrid Electric, and Fuel Cell Vehicles: Fundametals, Theory and Design*. Boca Raton, FL, USA.: CRC, 2004.

[100] M. Ross and W. Wu, "Fuel economy analysis for a hybrid concept car based on a buffered fuel-engine operating at an optimal point," *SAE International Congress and Exposition,* vol. Detroit, Michigan, USA, 1995.

[101] M. Mohammadian and M. T. Bathaee, "Motion control for hybrid electric vehicle," in *Power Electronics and Motion Control Conference, 2004. IPEMC 2004. The 4th International* vol. 3; 3, ed, 2004, pp. 1490-1494 Vol.3.

[102] J. R. Bumby and I. Forster, "Optimisation and control of a hybrid electric car," *Control Theory and Applications, IEE Proceedings D,* vol. 134; 134, pp. 373-387, 1987.

[103] N. Jalil, N. A. Kheir, and M. Salman, "A rule-based energy management strategy for a series hybrid vehicle," in *American Control Conference, 1997. Proceedings of the 1997* vol. 1; 1, ed, 1997, pp. 689-693 vol.1.

[104] Z. Rahman, K. L. Butler, and M. Ehsani, "A Comparison Study Between Two Parallel Hybrid Control Concepts," *SAE,* vol. 2000-01-0994, 2000.

[105] D. L. Buntin and J. W. Howze, "A switching logic controller for a hybrid electric/ICE vehicle," in *American Control Conference, 1995. Proceedings of the* vol. 2; 2, ed, 1995, pp. 1169-1175 vol.2.

[106] L. Jinming, P. Huei, and Z. Filipi, "Modeling and Control Analysis of Toyota Hybrid System," in *Advanced Intelligent Mechatronics. Proceedings, 2005 IEEE/ASME International Conference on*, 2005, pp. 134-139.

[107] B. Wu, C.-C. Lin, Z. Filipi, H. Peng, and D. Assanis, "Optimal Power Management for a Hydraulic Hybrid Delivery Truck," *Vehicle System Dynamics: International Journal of Vehicle Mechanics and Mobility,* vol. 42, p. 23, 2004.

[108] L. Chan-Chiao, P. Huei, and J. W. Grizzle, "A stochastic control strategy for hybrid electric vehicles," in *American Control Conference, 2004. Proceedings of the 2004* vol. 5; 5, ed, 2004, pp. 4710-4715 vol.5.

[109] L. Chan-Chiao, P. Huei, J. W. Grizzle, and K. Jun-Mo, "Power management strategy for a parallel hybrid electric truck," *Control Systems Technology, IEEE Transactions on,* vol. 11; 11, pp. 839-849, 2003.

[110] F. R. Salmasi, "Control Strategies for Hybrid Electric Vehicles: Evolution, Classification, Comparison, and Future Trends," *Vehicular Technology, IEEE Transactions on,* vol. 56; 56, pp. 2393-2404, 2007.

[111] L. Hyeoun-Dong and S. Seung-Ki, "Fuzzy-logic-based torque control strategy for parallel-type hybrid electric vehicle," *Industrial Electronics, IEEE Transactions on,* vol. 45; 45, pp. 625-632, 1998.

[112] L. Hyeoun-Dong, K. Euh-Suh, S. Seung-Ki, K. Joohn-Sheok, M. Kamiya, H. Ikeda, S. Shinohara, and H. Yoshida, "Torque control strategy for a parallel-hybrid vehicle using fuzzy logic," *Industry Applications Magazine, IEEE,* vol. 6; 6, pp. 33-38, 2000.

[113] S. M. T. Bathaee, A. H. Gastaj, S. R. Emami, and M. Mohammadian, "A fuzzy-based supervisory robust control for parallel hybrid electric vehicles," in *Vehicle Power and Propulsion, 2005 IEEE Conference*, ed, 2005, p. 7 pp.

[114] L. Weimin, X. Guoqing, W. Zhancheng, and X. Yangsheng, "A Hybrid Controller Design For Parallel Hybrid Electric Vehicle," in *Integration Technology, 2007. ICIT '07. IEEE International Conference on*, ed, 2007, pp. 450-454.

[115] B. Glenn, G. Washington, and G. Rizzoni, "Operation and Control Strategies for Hybrid Electric Automobiles," *SAE,* vol. 2000-01-1537, 2000.

[116] B. M. Baumann, G. Washington, and G. Rizzoni, "Intelligent Control of Hybrid Vehicles Using Neural Networks and Fuzzy Logic," *SAE,* vol. 981061, 1998.

[117] N. J. Schouten, M. A. Salman, and N. A. Kheir, "Fuzzy logic control for parallel hybrid vehicles," *Control Systems Technology, IEEE Transactions on,* vol. 10; 10, pp. 460-468, 2002.

[118] W. Jong-Seon and R. Langari, "Intelligent energy management agent for a parallel hybrid vehicle," in *American Control Conference, 2003. Proceedings of the 2003* vol. 3; 3, ed, 2003, pp. 2560-2565 vol.3.

[119] R. Langari and W. Jong-Seob, "Intelligent energy management agent for a parallel hybrid vehicle-part I: system architecture and design of the driving situation identification process," *Vehicular Technology, IEEE Transactions on,* vol. 54; 54, pp. 925-934, 2005.

[120] R. Langari and W. Jong-Seob, "Integrated drive cycle analysis for fuzzy logic based energy management in hybrid vehicles," in *Fuzzy Systems, 2003. FUZZ '03. The 12th IEEE International Conference on* vol. 1; 1, ed, 2003, pp. 290-295 vol.1.

[121] W. Jong-Seob and R. Langari, "Intelligent energy management agent for a parallel hybrid vehicle-part II: torque distribution, charge sustenance strategies, and performance results," *Vehicular Technology, IEEE Transactions on,* vol. 54; 54, pp. 935-953, 2005.

[122] S. Ichikawa, Y. Yokoi, S. Doki, S. Okuma, T. Naitou, T. Shiimado, and N. Miki, "Novel energy management system for hybrid electric vehicles utilizing car navigation over a commuting route," in *Intelligent Vehicles Symposium, 2004 IEEE*, ed, 2004, pp. 161-166.

[123] A. Rajagopalan, G. Washington, G. Rizzoni, and Y. Guezennec, "Development of Fuzzy Logic and Neural Network Control and Advanced Emissions Modeling for Parallel Hybrid Vehicles," NREL2003.

[124] L. Yao-Lun, T. Chia-Chang, J. Wu-Shun, and L. Shuen-Jeng, "Design an Intelligent Neural-Fuzzy Controller for Hybrid Motorcycle," in *Fuzzy Information Processing Society, 2007. NAFIPS '07. Annual Meeting of the North American*, ed, 2007, pp. 283-288.

[125] G. Paganelli, T. M. Guerra, S. Delprat, J. J. Santin, M. Delhom, and E. Combes, "Simulation and Assessment of Power Control Strategies for a Parallel Hybrid Car," *Proceedings of the I MECH E Part D Journal of Automobile Engineering,* vol. 214, pp. 705-717, 2000.

[126] L. Serrao and G. Rizzoni, "Optimal control of power split for a hybrid electric refuse vehicle," in *American Control Conference, 2008*, ed, 2008, pp. 4498-4503.

[127] Y. Huang, C. Yin, and J. Zhang, "Design of an energy management strategy for parallel hybrid electric vehicles using a logic threshold and instantaneous optimization method," *International Journal of Automotive Technology,* vol. 10, pp. 513-521, 2009.

[128] L. Guzzella and A. Sciarretta, *Vehicle Propulsiton Systems: Introduction to Modeling and Optmization*. Berlin: Springer-Verlag, 2005.

[129] G. Paganelli, S. Delprat, T. M. Guerra, J. Rimaux, and J. J. Santin, "Equivalent consumption minimization strategy for parallel hybrid powertrains," in *Vehicular Technology Conference, 2002. VTC Spring 2002. IEEE 55th* vol. 4; 4, ed, 2002, pp. 2076-2081 vol.4.

[130] G. Paganelli, G. Ercole, A. Brahma, Y. Guezennec, and G. Rizzoni, "General supervisory control policy for the energy optimization of charge-sustaining hybrid electric vehicles," *JSAE Review,* vol. 22, pp. 511-518, 2001.

[131] G. Paganelli, M. Tateno, A. Brahma, G. Rizzoni, and Y. Guezennec, "Control development for a hybrid-electric sport-utility vehicle: strategy, implementation and field test results," in *American Control Conference, 2001. Proceedings of the 2001* vol. 6, ed, 2001, pp. 5064-5069 vol.6.

[132] Y. Guezennec, C. Ta-Young, G. Paganelli, and G. Rizzoni, "Supervisory control of fuel cell vehicles and its link to overall system efficiency and low-level control requirements," in *American Control Conference, 2003. Proceedings of the 2003* vol. 3; 3, ed. Denver Colorado, USA, 2003, pp. 2055-2061 vol.3.

[133] G. Rizzoni, L. Guzzella, and B. M. Baumann, "Unified modeling of hybrid electric vehicle drivetrains," *Mechatronics, IEEE/ASME Transactions on,* vol. 4, pp. 246-257, 1999.

[134] G. Rizzoni, "Vp-Sim: a Unified Approach to Energy and Power Flow Modeling Simulation and Analysis of Hybrid Vehicles," *SAE Transactions,* vol. 2000-01-1565, 2000.

[135] M. Hopka, A. Brahma, S. Dilmi, G. Ercole, C. Hubert, S. Huseman, H. Kim, G. Paganelli, M. Tateno, Y. Guezennec, G. Rizzoni, and G. Washington, "The 2000 Ohio State University FutureTruck," *SAE Journal,* vol. SAE SP-1617, 2001.

[136] P. Pisu and G. Rizzoni, "A supervisory control strategy for series hybrid electric vehicles with two energy storage systems," in *Vehicle Power and Propulsion, 2005 IEEE Conference*, ed. Chicago, Il USA, 2005, p. 8 pp.

[137] P. Pisu, K. Koprubasi, and G. Rizzoni, "Energy Management and Drivability Control Problems for Hybrid Electric Vehicles," in *Decision and Control, 2005 and 2005 European Control Conference. CDC-ECC '05. 44th IEEE Conference on*, ed, 2005, pp. 1824-1830.

[138] J. M. Morbitzer, S. Yurkovich, and G. Rizzoni, "Advanced Propulsion Systems Education and Applications at The Ohio State University," in *Decision and Control, 2005 and 2005 European Control Conference. CDC-ECC '05. 44th IEEE Conference on*, ed, 2005, pp. 1831-1836.

[139] J. M. Morbitzer, G. Rizzoni, and E. R. Westervelt, "Dynamic analysis and control development for a cross-over vehicle with a dual hybrid-electric system," in *Vehicle Power and Propulsion, 2005 IEEE Conference*, ed, 2005, pp. 152-159.

[140] K. Koprubasi, J. M. Morbitzer, E. R. Westervelt, and G. Rizzoni, "Toward a framework for the hybrid control of a multi-mode hybrid-electric driveline," in *American Control Conference, 2006*, ed, 2006, p. 6 pp.

[141] P. Pisu and G. Rizzoni, "A Comparative Study Of Supervisory Control Strategies for Hybrid Electric Vehicles," *Control Systems Technology, IEEE Transactions on,* vol. 15, pp. 506-518, 2007.

[142] K. Koprubasi, E. R. Westervelt, and G. Rizzoni, "Toward the Systematic Design of Controllers for Smooth Hybrid Electric Vehicle Mode Changes," in *American Control Conference, 2007. ACC '07*, ed, 2007, pp. 2985-2990.

[143] P. Tulpule, V. Marano, and G. Rizzoni, "Effects of different PHEV control strategies on vehicle performance," in *American Control Conference, 2009. ACC '09.*, ed, 2009, pp. 3950-3955.

[144] L. Jinming and P. Huei, "Modeling and Control of a Power-Split Hybrid Vehicle," *Control Systems Technology, IEEE Transactions on,* vol. 16, pp. 1242-1251, 2008.

[145] R. Cipollone and A. Sciarretta, "Analysis of the potential performance of a combined hybrid vehicle with optimal supervisory control," in *Computer Aided Control System Design, 2006 IEEE International Conference on Control Applications, 2006 IEEE International Symposium on Intelligent Control, 2006 IEEE*, ed, 2006, pp. 2802-2807.

[146] A. Sciarretta, M. Back, and L. Guzzella, "Optimal control of parallel hybrid electric vehicles," *Control Systems Technology, IEEE Transactions on,* vol. 12; 12, pp. 352-363, 2004.

[147] P. Rodatz, G. Paganelli, A. Sciarretta, and L. Guzzella, "Optimal power management of an experimental fuel cell/supercapacitor-powered hybrid vehicle," *Control Engineering Practice,* vol. 13, pp. 41-53, 2005.

[148] C. Musardo, G. Rizzoni, and B. Staccia, "A-ECMS: An Adaptive Algorithm for Hybrid Electric Vehicle Energy Management," in *Decision and Control, 2005 and 2005 European Control Conference. CDC-ECC '05. 44th IEEE Conference on*, ed. Seville, Spain, 2005, pp. 1816-1823.

[149] C. Musardo, B. Staccia, S. Midlam-Mohler, Y. Guezennec, and G. Rizzoni, "Supervisory control for NOx reduction of an HEV with a mixed-mode HCCI/CIDI engine," in *American Control Conference, 2005. Proceedings of the 2005*, ed, 2005, pp. 3877-3881 vol. 6.

[150] C. Zhang, A. Vahidi, P. Pisu, X. Li, and K. Tennent, "Role of Terrain Preview in Energy Management of Hybrid Electric Vehicles," *Vehicular Technology, IEEE Transactions on,* 2009.

[151] J. S. Chen and M. Salman, "Learning energy management strategy for hybrid electric vehicles," in *Vehicle Power and Propulsion, 2005 IEEE Conference*, ed, 2005, pp. 68-73.

[152] A. Sciarretta and L. Guzzella, "Control of hybrid electric vehicles," *Control Systems Magazine, IEEE,* vol. 27; 27, pp. 60-70, 2007.

[153] W. Di and S. S. Williamson, "Performance Characterization and Comparison of Power Control Strategies for Fuel Cell Based Hybrid Electric Vehicles," in *Vehicle Power and Propulsion Conference, 2007. VPPC 2007. IEEE*, ed, 2007, pp. 55-61.

[154] G. Jianping, S. Fengchun, H. Hongwen, G. G. Zhu, and E. G. Strangas, "A Comparative Study of Supervisory Control Strategies for a Series Hybrid Electric Vehicle," in *Power and Energy Engineering Conference, 2009. APPEEC 2009. Asia-Pacific*, ed, 2009, pp. 1-7.

[155] S. Kim and B. E. Dale, "Environmental aspects of ethanol derived from no-tilled corn grain: nonrenewable energy consumption and greenhouse gas emissions," *Biomass and Bioenergy,* vol. 28, pp. 475-489, 2005.

[156] K. G. H√∏yer, "The history of alternative fuels in transportation: The case of electric and hybrid cars," *Sustainable Energy and Transportation Systems,* vol. 16, pp. 63-71, 2008.

[157] U. Bossel, "Does a Hydrogen Economy Make Sense?," *Proceedings of the IEEE,* vol. 94, pp. 1826-1837, 2006.

[158] C. M. Harrington, J. Marco, N. D. Vaughan, M. Kellaway, A. Cooper, and A. Eastlake, "Affordable Hybrid Electric System for Urban Commercial Vehicle Applications, Using Advanced VRLA Battery," in *Hybrid and Eco-Friendly Vehicle Conference, 2008. IET HEVC 2008*, 2008, pp. 1-8.

[159] P. Van den Bossche, F. d. r. Vergels, J. Van Mierlo, J. Matheys, and W. Van Autenboer, "SUBAT: An assessment of sustainable battery technology," *Special issue*

including selected papers from the International Power Sources Symposium 2005 together with regular papers, vol. 162, pp. 913-919, 2006.

[160] F. Kalhammer, B. Kopf, D. Swan, V. Roan, and M. Walsh, "Status and Prospects for Zero Emissions Vehicle Technology Report of the ARB Independent Expert Panel 2007," California Air Resources Board, Sacramento, CA. USA.2007.

[161] A. F. Burke, "Batteries and Ultracapacitors for Electric, Hybrid, and Fuel Cell Vehicles," *Proceedings of the IEEE,* vol. 95, pp. 806-820, 2007.

[162] C. M. Harrington, J. Marco, N. D. Vaughan, J. Allan, B. D. Smither, and G. Farmer, "Low Cost Hybrid Motorcycle Optimisation Model," *SAE Technical Paper Series,* vol. 2010-32-0131, 2010.

[163] J. Marco, N. Vaughan, H. Spowers, and M. McCulloch, "Modelling the acceleration and braking characteristics of a fuel-cell electric sports vehicle equipped with an ultracapacitor," *Proceedings of the Institution of Mechanical Engineers, Part D: Journal of Automobile Engineering,* vol. 221, pp. 67-81, 2007.

[164] H. Liu and J. Jiang, "Flywheel energy storage,ÄîAn upswing technology for energy sustainability," *Energy and Buildings,* vol. 39, pp. 599-604, 2007.

[165] Y.-c. Yan, G.-q. Liu, and J. Chen, "Parameter design strategies of a parallel hydraulic hybrid bus," in *Vehicle Power and Propulsion Conference, 2008. VPPC '08. IEEE*, 2008, pp. 1-6.

[166] Anon, "Proposal for a regulation of the European Parliament and of the European Council setting emission performance standards for new passenger cars as part of the Community's integrated approach to reduce CO2 emissions from light duty vehicles," vol. COM(2007) 856 final, ed: EC, 2007.

[167] J. W. G. Turner, D. Blake, J. Moore, P. Burke, R. J. Pearson, R. Patel, D. W. Blundell, R. B. Chandrashekar, L. Matteucci, and P. C. C. A. Barker, "The Lotus Range Extender Engine," *SAE,* vol. 2010-01-2208, 2010.

[168] J. Bernard, S. Delprat, N. Buchi, and M. Guerra, "Fuel Cell Hybrid Powertrain: Towards Minimization of Hydrogen Consumption," *Vehicular Technology, IEEE Transactions on,* 2009.

[169] B. K. Bose, M. H. Kim, and M. D. Kankam, "Power and energy storage devices for next generation hybrid electric vehicle," in *Energy Conversion Engineering Conference, 1996. IECEC 96. Proceedings of the 31st Intersociety*, pp. 1893-1898 vol.3.

[170] T. J. Woolmer, "Analysis of the Yokeless And Segmented Armature Machine," in *Electric Machines & Drives Conference, 2007. IEMDC '07. IEEE International* vol. 1, M. D. McCulloch, Ed., ed, 2007, pp. 704-708.

[171] J. R. Bumby, E. Spooner, and M. Jagiela, "Solid Rotor Induction Machines for use in Electrically-Assisted Turbochargers," in *Power Electronics, Machines and Drives, 2006. The 3rd IET International Conference on*, 2006, pp. 341-345.

[172] Y. Chuang, Z. Xiaodong, G. Shuang, and W. Diyun, "Comparison of permanent magnet brushless motors for electric vehicles," in *Vehicle Power and Propulsion Conference (VPPC), 2010 IEEE*, 2010, pp. 1-5.

[173] M. Ehsani, G. Yimin, and S. Gay, "Characterization of electric motor drives for traction applications," in *Industrial Electronics Society, 2003. IECON '03. The 29th Annual Conference of the IEEE*, 2003, pp. 891-896 vol.1.

[174] M. Ceraolo, A. Caleo, P. Capozzella, M. Marcacci, L. Carmignani, and A. Pallottini, "A parallel-hybrid drive-train for propulsion of a small scooter," *Power Electronics, IEEE Transactions on,* vol. 21, pp. 768-778, 2006.

[175] S. Cho, K. Ahn, and J. Lee, "Efficiency of the planetary gear hybrid powertrain," *Proceedings of the Institution of Mechanical Engineers, Part D: Journal of Automobile Engineering,* vol. 220, pp. 1445-1454, 2006.

[176] G. H. Gelb, N. A. Richardson, T. C. Wang, and B. Berman, "An Electromechanical Transmission for Hybrid Vehicle Power Trains - Design and Dynamometer Testing," *SAE Technical Paper Series,* vol. 710235, 1971.

[177] J. Voelcker, "Chevy Volt sparks a series of plug-in hybrids [Update]," *Spectrum, IEEE,* vol. 48, pp. 16-18, 2011.

[178] X. Lin-Shi, F. Morel, A. M. Llor, B. Allard, and J. M. Retif, "Implementation of Hybrid Control for Motor Drives," *Industrial Electronics, IEEE Transactions on,* vol. 54, pp. 1946-1952, 2007.

[179] D. W. Gao, "Modeling and Simulation of Electric and Hybrid Vehicles," in *Proceedings of the IEEE* vol. 95, C. Mi, Ed., ed, 2007, pp. 729-745.

[180] D. Cross and J. Hilton, "High Speed Flywheel Based Hybrid Systems for Low Carbon Vehicles," in *Hybrid and Eco-Friendly Vehicle Conference, 2008. IET HEVC 2008*, 2008, pp. 1-5.

[181] R. Cogan, "Volvo Hybrid Environmental Concept Car," vol. Accessed 2011, ed, 2007.

[182] A. Cooper, "Development of a high-performance lead,Äìacid battery for new-generation vehicles," *Selected papers from the Ninth European Lead Battery Conference,* vol. 144, pp. 385-394, 2005.

[183] W. Jong-Seob, R. Langari, and M. Ehsani, "An energy management and charge sustaining strategy for a parallel hybrid vehicle with CVT," *Control Systems Technology, IEEE Transactions on,* vol. 13; 13, pp. 313-320, 2005.

[184] M. Algrain, "Controlling an electric turbo compound system for exhaust gas energy recovery in a diesel engine," in *Electro Information Technology, 2005 IEEE International Conference on*, ed, 2005, p. 6 pp.

[185] J. R. Bumby, S. Crossland, and J. Carter, "Electrically assisted turbochargers: Their potential for energy recovery," in *Hybrid Vehicle Conference, IET The Institution of Engineering and Technology, 2006*, 2006, pp. 43-52.

[186] R. Stobart, "An availability approach to thermal energy recovery in vehicles," *Proccedings IMechE,* vol. 221, pp. 1107-1124, 2007.

[187] J. Marco and E. Cacciatori, "The Use of Model Based Design Techniques in the Design of Hybrid Electric Vehicles," in *Automotive Electronics, 2007 3rd Institution of Engineering and Technology Conference on*, 2007, pp. 1-10.

[188] J. O. Grady, "Universal Architecture Description Framework," *Syst.Eng.,* vol. 12, pp. 91-116, 2009.

[189] Anon, "ECE 13-h, Braking of Passenger Cars," ed. **http://live.unece.org/trans/main/wp29/wp29regs1-20.html:** UNECE, 2008.

[190] G. Paganelli, Y. Guezennec, and G. Rizzoni, "Optimizing Control Strategy for Hybrid Fuel Cell Vehicle," *SAE Journal,* vol. 2002-01-0102, 2002.

[191] J. Heywood, *Internal Combustion Engine Fundamentals*. Singapre: McGraw-Hill Book Co., 1988.

[192] C. Mansour and D. Clodic, "Dynamic Modeling of the Electri-Mechanical Confuguration of the Toyota Hybrid System Series/Parallel Power Train," *International Journal of Automotive Technology,* vol. 13, pp. 143-166, 2012.

[193] C. W. Ayers, J. S. Hsu, L. D. Marlino, C. W. Miller, J. G. W. Ott, and C. B. Oland, "Evaluation of 2004 Toyota Prius Hybrid Drive System interim report," Oak Ridge National Laboratory, Tennessee2004.

[194] Anon, "ISO 26262 Road vehicles -- Functional safety," ed. Switzerland: ISO, 2011.

[195] E. Cacciatori, Bonnet, B., Vaughan, N.D., Burke, M., Price, D., and Wejrzanowski, K., "Launch and Driveability Performance Enhancement for a Parallel Hybrid With a Torque-Controlled IVT," presented at the Powertrain and Fluid Systems Conference and Exhibition, San Antonio, Texas, USA, 2005.

[196] T. Ikeya, N. Sawada, S. Takagi, J.-i. Murakami, K. Kobayashi, T. Sakabe, E. Kousaka, H. Yoshioka, S. Kato, M. Yamashita, H. Narisoko, Y. Mita, K. Nishiyama, K. Adachi, and K. Ishihara, "Multi-step constant-current charging method for electric vehicle, valve-regulated, lead/acid batteries during night time for load-levelling," *Journal of Power Sources,* vol. 75, pp. 101-107, 1998.

[197] Z. Chengke, Q. Kejun, M. Allan, and Z. Wenjun, "Modeling of the Cost of EV Battery Wear Due to V2G Application in Power Systems," *Energy Conversion, IEEE Transactions on,* vol. 26, pp. 1041-1050, 2011.

[198] A. Hoke, A. Brissette, D. Maksimovic, A. Pratt, and K. Smith, "Electric vehicle charge optimization including effects of lithium-ion battery degradation," in *Vehicle Power and Propulsion Conference (VPPC), 2011 IEEE*, 2011, pp. 1-8.

[199] J. Gonder and A. Simpson, "MEASURING AND REPORTING FUEL ECONOMY OF PLUG-IN HYBRID ELECTRIC VEHICLES," *World Electric Vehicle Association,* vol. 1, 2007.

[200] D. M. Sharman and A. A. Yassine, "Architectural Valuation using the Design Structure Matrix and Real Options Theory," *Concurrent Engineering,* vol. 15, pp. 157-173, 2007.

Appendix A: Vehicular technology development

The early years: up to 1905

The first recorded example of an 'automobile' or self-propelling vehicle was built by Ferdinand Verbiest, a Jesuit priest, for the Chinese Emperor between 1665 and 1680 [201]. The vehicle was far too small to support, much less transport a human. A century later, the Frenchman Cugnot demonstrated his steam tractor. While it was not very effective, it heralded the nascent automotive steam era and was the dominant technology until the late 19th century [201]. The steam car was feasibly demonstrated over an 85 mile round trip by Goldsworthy Gurney in 1825 [202]. In 1828 Ányos Jedlik demonstrated the first electrically powered vehicle, although it was very small [203] and Robert Anderson demonstrated a full size electric vehicle in 1839 [204]. Lenoir is credited with demonstrating the first coal gas internal combustion engine in 1860 [201]. However it was Karl Benz who in 1878 was granted a patent for his four-stroke gasoline internal combustion engine and in 1885 he built his first 'motorwagon', which was patented the following year. By 1888 Benz had begun selling his production vehicles. This series of events is widely credited as the beginning of the automotive sector as a commercial industry [204]. Over the following 20 years, attempts were made to develop and productionise a variety of self propelled motorised vehicle formats. These included steam, gasoline, diesel, electric and hybrid electric vehicles, i.e. a combination of chemical and electrical energy on-board storage [99]. In 1899, Camille Jénatzy, a Belgian, designed and drove his 200V battery electric car beyond 100km/h [201].

As mentioned, steam significantly preceded the ICE and electric cars outperformed ICE vehicles. In the early years, gasoline propelled vehicles were just one among several propulsion technologies. In 1900 1,681 steam, 1,575 electric and 936 gasoline vehicles were manufactured in the US [203]. In the same year Ferdinand Porsche produced the first electric hybrid vehicle, see Figure A-1, on behalf of Hofwagenfabrik Ludwig Lohner & Co, the Viennese coachmakers. This vehicle combined two gasoline engines powering two generators which could supply electrical power to two wheel hub motors or the onboard battery: making it the first series hybrid [205]. This was quickly followed with the Lohner Porsche 'Mixed' which replaced the two 2.6kW ICEs with one 18kW ICE, which sold 11 units.

Figure A-2 shows the Pieper patent for a parallel hybrid [206]. This is the first patent for a parallel hybrid configuration. This vehicle was capable of several modes of operation, including electric only, engine assist, charge and regenerative braking, although the mode selection was controlled by manual input from the driver [207].

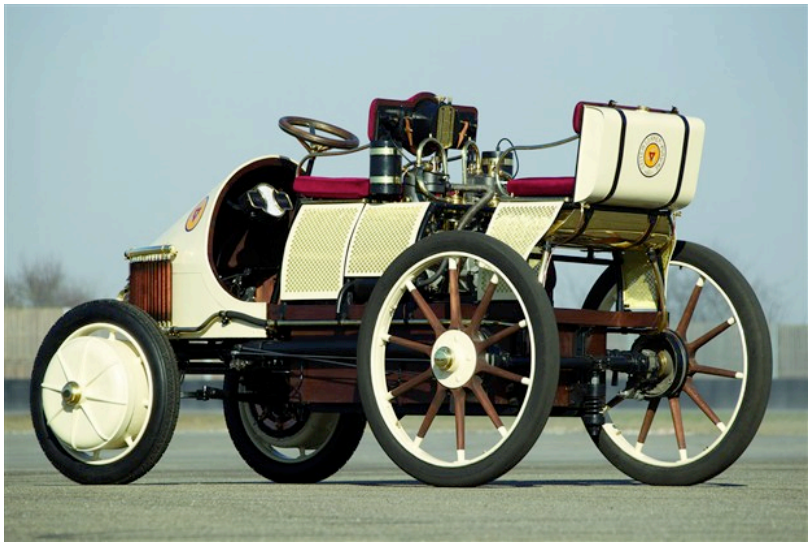

Figure A-1: The Lohner Porsche 'Semper Vivus" (replica): the first hybrid vehicle

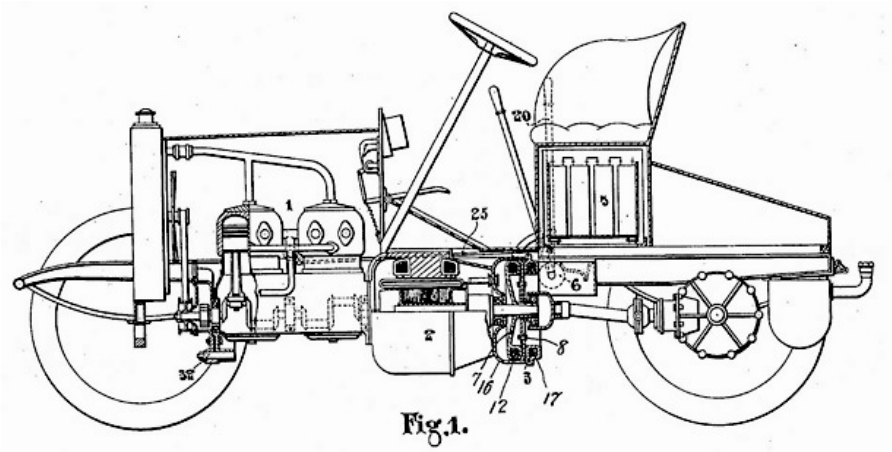

Figure A-2: Henri Pieper's patent for the first parallel hybrid, submitted 1905 [206]

The Edwardian years: 1905 to 1914

During this period of invention, steam powered cars were breaking speed records [208] however this period also quickly saw the rationalisation of vehicle technologies. By 1910, gasoline powered ICE driven vehicles had come to dominate, with diesel maintaining a significant minority share of the market [201]. 1914 saw the development of the production line at Ford, thereby making an automobile affordable to the mass market whereupon the car began to have a significant impact on human transport patterns [201]. Significant technological developments in this era include electric ignition, independent suspension, multivalve engines and throttle control [209]. The Model T Ford has a detachable engine head for ease of maintenance [203].

The vintage years: 1918 to 1929

As the front engine, rear wheel drive vehicle layout became standard, engine size and power began to climb with V12 and V16 engines being made available for high end luxury cars such as the Caddilac V16 [201]. Hydraulic brakes were first deployed on the Dusenberg Model A [209]. The modern automatic transmission - comprising a two

speed planetary gear set with lock up clutches and a torque converter - was developed by Vulcan, but was not yet deployed [209]. Lancia unveiled the first productionised monocoque body on its Lambda, which incorporated the coach and chassis [201]. The first instance of minimising mass for performance was demonstrated by the Bugatti 35; the axles were hollowed out to minimise unsprung weight [209].

1917 saw the development of the Woods Motor Company Dual Power hybrid, Figure A-3. They claimed a top speed of 35mph and a consumption of 45mpg [203]. This was to be the last hybrid for over half a century. By 1920, the swiftly reducing cost of gasoline cars and the new availability of inexpensive fuel for the developing Texas oil fields ensured fossil fuel motive power would dominate road transport for at least a century [201].

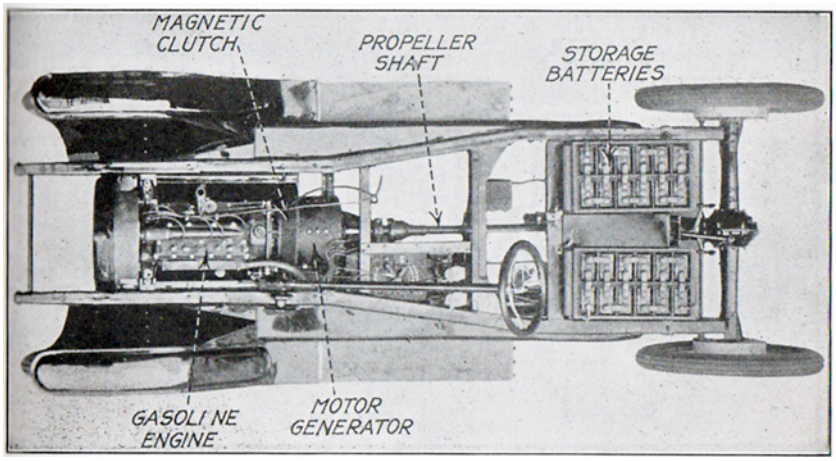

Figure A-3: The Woods Dual Power parallel Hybrid [203]

The pre-war years: 1930 to 1948

The Great Depression drove significant market consolidation resulting in a step decrease in vehicle manufacture numbers and an overall reduction in vehicle size [201]. The front engine, front wheel drive layout re-emerged for its packaging benefits [201]. In principle most of the mechanical technology available today, had been invented by this stage and was being refined. Synchromesh appeared on manual gearboxes, and by the 1940s was available for all ratios [201]. High-end vehicles were experimenting with alternate materials - such as the Rolls Royce Phanton's aluminium engine block. However the enduring vehicle design from this period was the VW Beetle, an exemplar of form, function, efficiency and affordability.

The post-war years: 1949 to circa 1970

Three distinct industrial regions were established in this time, the US, Europe and Japan. The post-war Japanese government stipulated the Kai Car standard. These standards defined the type of small car (engine and foot print) which would avoid tax and insurance penalties with a view to promoting industry and producing, in bulk, a fleet of affordable vehicles [201]. Europe was progressing with small cars, carrying strong technology aimed at providing cheap, functional transport. The Beetle went into full production after the war - and was soon followed by the Citreon 2CV, the SAAB 92 and

the Morris Minor [201]. Each was inexpensive, yet, had its own contribution to the advancement of the technology. The 2CV, the most efficient car of its day, came with fully independent suspension - which was horizontally integrated into the floor of the vehicle - and rack and pinion steering. The SAAB 92 set a drag coefficient record of 0.3, unbeaten until the 1980s. The Morris Minor, which included torsion bar suspension, was measured to give 35 mpg [209].

The US on the other hand experimented with economy cars in the expectation of a post-war depression - which never materialised. GM developed, but never sold, the Chevy Cadet. The lead developer for the Cadet was Earl McPherson and the car featured his eponymous independent coil over damper strut. However the McPherson strut was first deployed onto European cars [201] because the Cadet program was cancelled in the face of US customer rejection of the small car. In the mean time the US discovered the high compression V8 and growing demand for the automatic transmission.

Through the 1960s the European brands pushed further with technology and packaging, for example, the Jaguar E-type and the Mini. Also distinct markets began to overlap and US manufactures began to react to the importation of low cost, nimble and efficient Japanese and European competitors. This brought about captive marketing and badge engineering; the precursor to shared platform engineering [209]. Towards the end of this decade raw performance became the dominant marketing tool for American manufactures selling to an American market in the face of increased Japanese imports. The high torque Mustang, Charger and Camero offered American customers high power with emphasis on styling at an affordable price [201]. Areas of technology which became mature during this period include the rotary Wankle engine, the turbocharger and mechanical fuel injection [201].

The modern years: circa 1970 to present

In the early 70s two distinct pressures were effecting vehicle development. The California Air Resources Board (CARB) enacted state legislation to minimise tailpipe pollutant emissions Carbon Monoxide (CO), Oxides of Nitrogen (NOx) and un-burnt HydroCarbons (HC's) [210]. These tailpipe emissions combined with some topographical peculiarities in the Los Angeles basin resulted in significant air quality (smog) issues [160]. Catalytic converters were introduced to limit emissions which required closed loop lambda engine control using electronic fuel injection [160, 210]. Simultaneously, crash safety was being researched, particularly wheel lock-up under braking [211]. Hence ABS (from the German AntiBlockierSystem) systems were developed which could limit or reduce the individual brake pressure to minimise wheel slip, resulting in significantly shorter braking distances and controllable stability throughout [211]. The era of electronic automotive control systems had arrived.

The defining component in this period is the electronic control system using the microchip. Automotive electronics expanded quickly to the point where there could be more than 100 micro processors on each high-end vehicle [12]. The area of automotive electronics is usually divided into five sub groups (often reflecting the operational structure of automotive companies) [63, 211].

- Body (electric windows, doors locking, alarm, immobiliser)
- Chassis (brakes, active suspension)
- Powertrain (engine transmission)
- Active Safety (airbags, occupant protection)
- Infotainment (audio, video, navigation, telecommunications)

Early electronic systems were standalone and were usually dedicated to a particular component on the vehicle; for example the ABS controller managed the hydraulic brake modulator. Some systems became heavily coupled such as the engine management systems and their counterpart transmission controllers (automatic variants) [211]. Other systems became integrated heavily with a large number of other systems. Infotainment systems can have many formats and communication protocols and it was quickly desirable to formally coordinate the development and integration of these systems [21]. It was at this point that systems engineering appeared in the automotive industry. Appendix B will discuss systems engineering in more detail.

Non-conventional powertrains were also being investigated again, after a hiatus of 50 years. The late 1960s clean air legislation and the early 1970s oil crisis fostered an initial interest into research of alternative powertrain technologies. Between 1968 and 1971, a team of scientists from TRW (an automotive supplier) developed, demonstrated and patented a compound hybrid which used two electric machines and an ICE all driving the separate parts of an epicyclic gear-set [176], see Figure A-4.

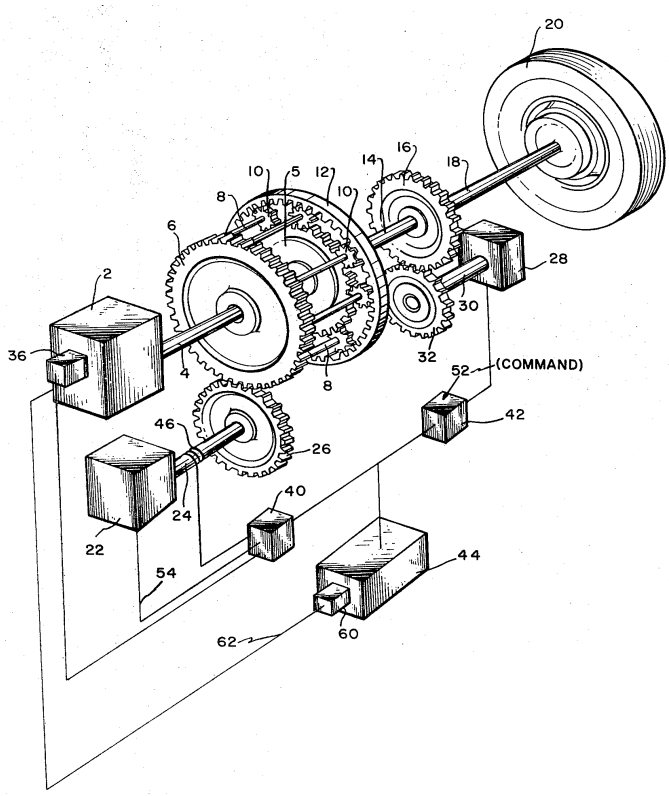

Figure A-4: The first Compound HV patent, TRW epicyclic hybrid transmission [212]

In Figure A-4, *2* refers to the IC engine, *22* is the 'generator' and *28* is the 'motor'. Both electric machines can charge or discharge the same electrical storage device, hence the

compound nature of this hybrid [176, 212]. This term will be discussed in detail in Chapter 3. In 1969 GM developed a gasoline hybrid demonstrator [203]. However three years earlier GM had also built and demonstrated the first recorded Fuel Cell road vehicle, the 'ElecroVan', (see Figure A-5). This vehicle carried both Hydrogen and Oxygen in cryogenic liquid form. This vehicle achieved a range of 120 miles, with a top speed of about 70 mph. However the acceleration was limited: 0-60 mph in 30 seconds and the system had safety concerns, excessive mass and a prohibitive cost [203].

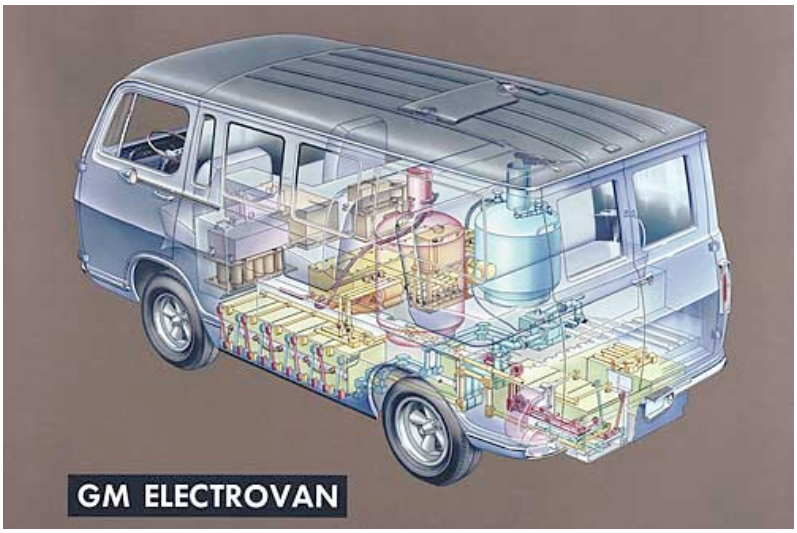

Figure A-5: 1966 GM ElectroVan Fuel Cell vehicle [213].

However the 1970 oil spike was relatively short lived, and pollutant emissions legislation required correct combustion, not necessarily less combustion. Therefore alternative powertrain research was largely dormant until the 1990s. The most famous vehicles of this era are the GM EV1, the Honda Insight, and the Toyota Prius. While the EV1 was a pure electric drive vehicle the latter two were parallel and compound hybrid variants respectively. True series hybrids are uncommon unless in Bus application or concepts such as the 1992 Volvo ECC, which used a gas turbine [181].

With the arrival of the millennium, several production HVs became commercially available. This emerged from the growing awareness of, and concern for the influence of CO_2 emissions on the planets climate. Pressure for highly efficient vehicles increased further with the onset of the recent increase in oil price and CO_2 based legislation (Europe is legislating fleet CO_2 averages of 130g/km [5, 166]. Most vehicle manufacturers are now producing at least one hybrid variant (excluding micro hybrids, which employ stop-start technology only). Most hybrids still fall into either the parallel variant or compound variant, although there exist several concept demonstrators with the series configuration.

Appendix B: Systems Architecting & Engineering

Systems engineering and architecting overview

The terms used in systems architecting and engineering are commonly interchangeable or have overlapping meaning depending on literature source, [13, 17, 19, 214]. Table B-1 presents a summary of the common terms used. The terms used for *the process* and *the person* are the most often conflicting and interchanged. Consider a process of activity starting with user requirements for a product and ending with the detailed development activity of the final product. Sage defines systems engineering as the totality of process steps between the user requirements capture and detailed system development [33]. Sages defined the person who carries out these system engineering steps as the systems engineer. Whereas Rechtin defines systems architecting as a number of the process steps, mostly related to the user requirements, and arising early in the process [18, 19]. Rechtin defines the person who carries out this activity as the systems architect.

The process	Systems engineering	Systems architecting	
The person	Systems engineer	Systems architect	
Attribute of a system		System architecture, Architectural Description	Reference architecture

Table B-1: Summary of systems terminology

The attribute terms are distinct and easier to define. IEEE guidelines first define a system as a collection of sub-systems or parts interrelated by interfaces to each other and external stakeholders [49]. The IEEE then declares that every system has an architecture. However the IEEE guidelines define the AD as the collection of artefacts (models, drawing and documents) which describe facets of that architecture [49]. A RA is abstracted from several ADs capturing reusable learning which can be applied to new systems. Thereby the RA can become a template for future systems development [13, 16, 19]. The rest of this section will give a general overview of systems engineering, systems architecting and the reference architecture

Systems engineering overview

Systems engineering, as a profession, is relatively young in the context of traditional engineering sectors such as civil or mechanical. The first record reference to this activity as "Systems Engineering" is Bell Labs during their development of the US national telephone network [215]. Schlager states that (at that time) it was too early to attempt to define systems engineering. His study was an empirical review of existing work practices in a number of companies working on complex systems. He goes on to describe the five definitive activities of systems engineering: *planning, analysis, optimisation, integration* and *evaluation* [215].

The jet age required a surface to air defence system beyond the capabilities of traditional anti-aircraft weapons. The US army and Bell Labs defined a system which utilised a computer to guide (in real time) missiles to an air-born target using ground radar. This system involves many interdisciplinary sub-systems, multiple stakeholders

with a wide range of requirements and a clearly verifiable objective. The Nike Ajax missile was successfully demonstrated in 1951 [17, 214]. The launch by the USSR of the satellite 'Sputnik' in 1957 was in fact an international demonstration of their Inter-Continental Ballistic Missile (ICBM) system, capable of delivering nuclear payloads around the world. This pushed the surface to air missile defence by creating new requirements for missile speed and altitude, and resultant system tracking and computing performance. The Nike Hercules missile system was deployed by 1958, capable of tracking and destroying ICBMs [33]. The ability to define and deliver a complex systems engineering project and repeat the process efficiently against more challenging requirements demonstrated the benefit of systems engineering. This is considered to be the formal beginnings of systems engineering, as a defined profession [17].

A natural extension of the defence orientated systems engineering processes is the aerospace industry. Military aircraft and space vehicles were developed using the systems engineering approach, most notably the Apollo program [17]. Civil aviation soon adopted systems engineering as industry standard [18, 75]. The software industry [71], telecommunications [72], and control [76] all adopted the systems engineering process [17, 18]. A key development from the software industry was a formulisation of the UML for object orientated software development [36]. UML is a standard language for specifying, visualizing, constructing, and documenting the artefacts of software systems [36]. The systems engineering community took advantage of the flexibility of the UML profile feature and the SysML was developed [41]. The SysML is a general purpose modelling language for systems engineering applications [41, 42].

Electronic control of distinct sub-systems appeared on vehicles in the early 1970s. As in-vehicle systems became more complex and coupled, systems engineering became a necessary tool for the automotive industry [20]. More recently, infotainment, chassis and body system complexity grew and systems engineering has been successfully applied in the automotive industry [12, 21]. The powertrain systems have been historically integrated as per deployment, mainly between engine management and transmission (automatic) [11].

There are a wide range of definitions of systems engineering published; these are presented in Appendix D However a short summary is presented here. There is significant overlap between the published definitions. They all describe a series of coordinated activities which embodies a Systems Engineering Process. Key themes are universal:

- System definition with stakeholder acceptance
- System creation along the lines set out by the definition
- System evaluation against stakeholder concerns

The styles of *definition*, types of *stakeholders*, manifestations of *creation* and methods of *evaluation* will be entirely dependent on the system or industry context. Hence any definition of systems engineering must be, by necessity, robust to the link between the system and the process required to engineer it. Hence the list of definitions (presented

in Appendix D), share one critical attribute: the creation of models of aspects of the system by means of abstraction. Abstraction is key a theme of this research.

The most common representations of the Systems Engineering Process are the Waterfall Model, Figure B-1, and the V model, Figure B-2. Both models represent the transition from definition to creation to evaluation. The V model is the more modern representation of the Systems Engineering process, showing the ability to tie upstream definition activity with downstream testing and validation [17].

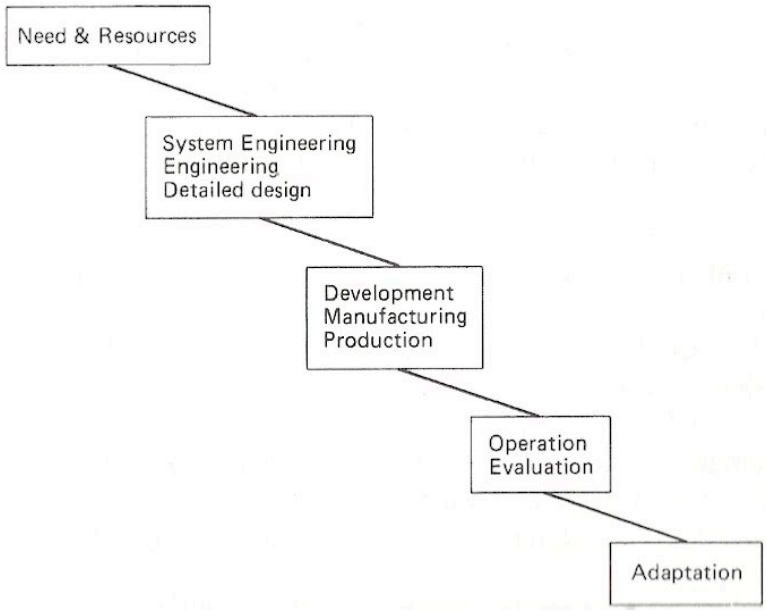

Figure B-1: Systems Engineering Waterfall process model [19]

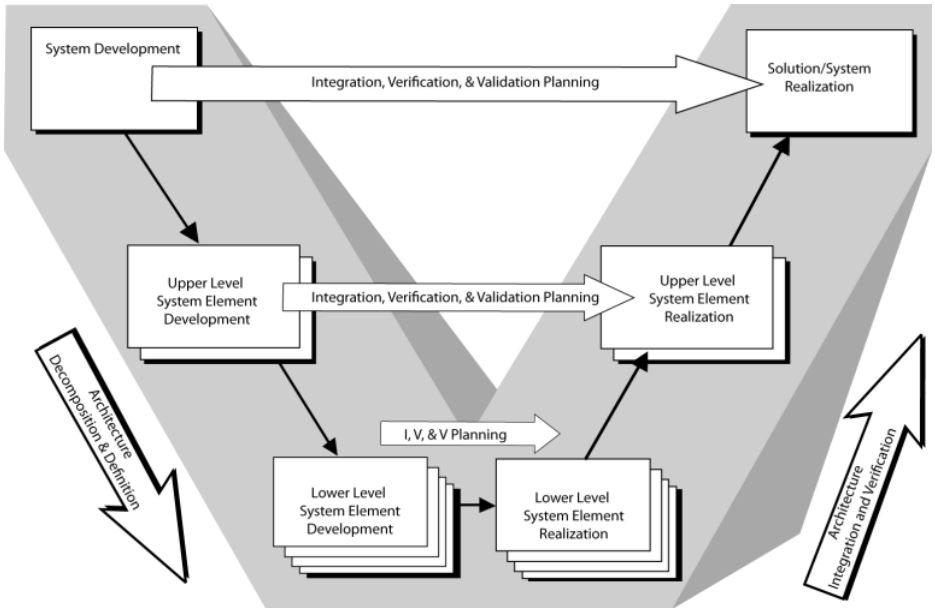

Figure B-2: Systems Engineering V process model [17]

A key feature of both these processes is their cyclical or iterative nature in practice. This is a result of learning through development and feeding that learning back to the definition stage. One goal of this Thesis is to present a RA which can act as a design

template for HV control system, thereby reducing the iteration and resultant development cost [13, 15, 216].

System architecting overview

The seminal work on systems architecting was published by Eberhardt Rechtin in 1991 [15, 19]. The previous section described the systems engineering process as a collection of activities required to bring about a successful systems solution to a complex problem. Rechtin defines systems architecting as a sub-group of the activities in the systems engineering process. Usually systems architecting focuses on high level system definition (usually in conjunction with system owner/user/client) and system evaluation or validation [18]. The systems architect is the person who carries out or supervises these activities. Figure B-3 shows a more detailed waterfall model with the role of the architect and the key architecting activities highlighted.

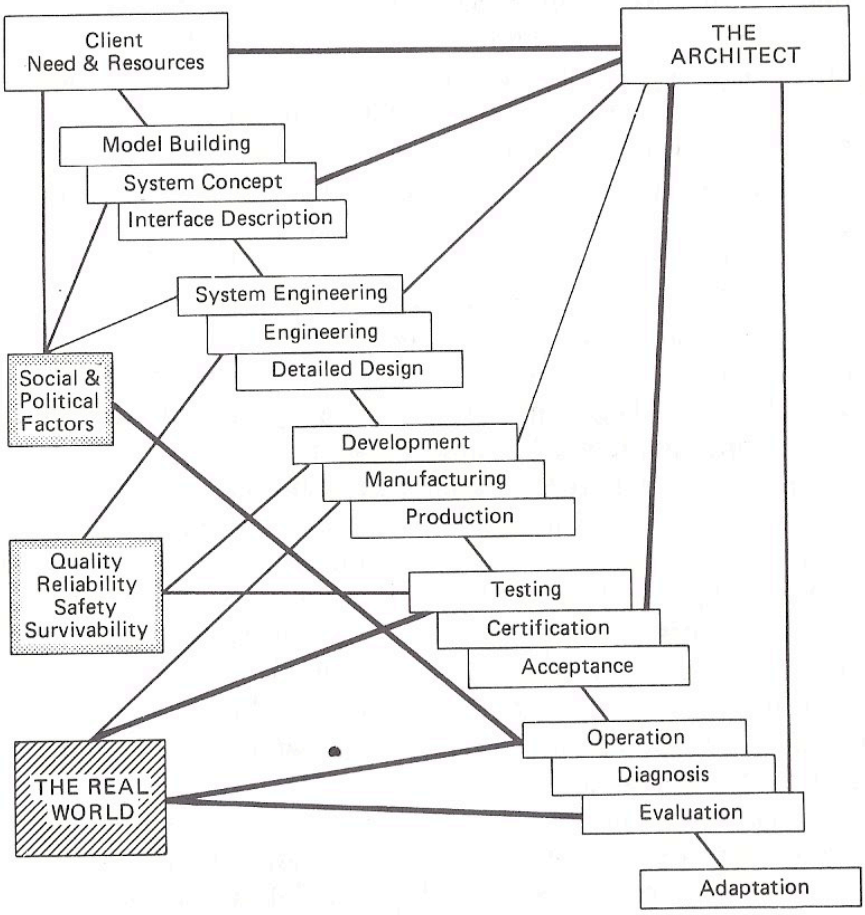

Figure B-3: Detailed systems engineering waterfall model, showing architects role [19]

The history of the systems architecture, system architecting and the systems architect is heavily intertwined with systems engineering but has only formally been defined relatively recently. Systems architecture is first mentioned in the context of software development in 1984. However Rechtin asserts that, by definition, architecture, architecting and the architect has inherently been part of systems engineering from the beginning [19]. Often these concepts have existed without formal definition or by

another name. Rechtin claims that the titles chief engineer, chief designer, design team leader, configurator and advanced-system engineer all com under the term 'The Architect' [18, 19].

Moreover, Rechtin points out that the concepts of Architecture, Architecting and the Architect have existed since classical times. He defines the architect as the interface between the client and the builder. This terminology comes from civil engineering. The role of the Architect is to mediate between the client and the builder. Therefore the architect must possess enough technical knowledge to communicate the client's requirements for the builder or engineer to develop a detailed technical specification, and further to execute the build from the technical specifications. The Architect must also use this technical knowledge or experience to manage the client's expectations in the context of engineering constraints. Table B-2 shows an equivalency between different industries with regards to the Architect and their relationship to other stakeholders.

Civil engineering	Software engineering	Systems Engineering
Client	Client/User	Client/end user
Architect	Architect	Systems Architect
Builder	Developer	Systems Engineer

Table B-2: Relationship between key stakeholders [19]

The deliverables of the architect reflect this relationship, abstract enough to view the 'whole' picture, but detailed enough to initiate an engineering discussion. Importantly the deliverables of the architect are not detailed enough for implementation, this required another step.

The IEEE defines the terms 'systems architecture' and AD in the context of systems (specifically software-intensive systems) in their 2007 guidelines [49]. They state that every system embodies a systems architecture. Whereas the collection of artefacts (models, documents etc) which capture and communicate facets of that architecture are collectively called the AD of the system. From the ADs of several similar systems which contain repeated patterns, a RA can be derived. The next section will present an overview of the RA.

Reference architecture overview

There is evidence of human beings applying patterns to their endeavours dating back several thousand years. Figure B-4 shows a pair of Dolmen (Neolithic tombs) situated in Ireland about 280km apart. While the two examples are clearly different, the underlying pattern is the same. The concept of a reusable pattern was first formalised by Christopher Alexander, a civil architect, through the '60s and 70's [25].

Figure B-4: Pulnabrone and Kilcooney dolmen (tombs). circa 2000 to 3000 BCE

Alexander defines patterns as follows: "Each pattern is a three-part rule, which expresses a relation between a certain context, a problem and solution....." [25]. Figure B-5 shows an example of an Alexandrian pattern, "A house for a small family" [25]. The pattern presented is a high level abstraction of what a house should, at a minimum, contain for a small family. It contains no detail on the finished house but contains the key requirements that it must satisfy. This is an important feature as the same finished 'house' could be a rural bungalow or an urban apartment, both of which adhere to the pattern.

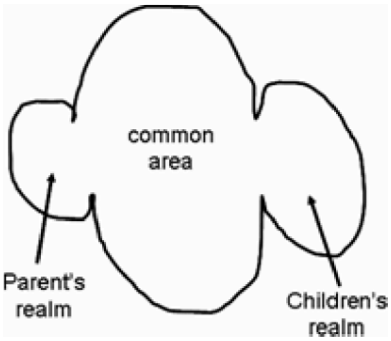

Figure B-5: Alexandrian pattern for 'a house for a small family' [15]

The software industry adopted the concept of the design pattern by the late 1980s for reoccurring functions or solutions [15, 71]. In the context of the telecommunications industry, Bell Laboratories mined their embedded systems for patterns [72]. Systems engineering involves capturing requirements, often in a structure which can be analysed over time to identify patterns; an area explored in detail by Kaffenberger [217]. Kaffenberger showed that applying patterns to requirements capture and definition could reduce the problem of misleading, ambiguous or missing requirements.

The term "reference architecture" became the systems engineering and architecting term for design pattern [13]. The paper describes the output of a Systems Architecting Forum on the concept of the reference architecture, held at the Stevens Institute in the US. They define it as follows:

"Reference Architectures capture the essence of existing architectures, and the vision of future needs and evolution to provide guidance to assist in developing new system architectures." [13].

It can be seen from this definition that the very nature of a reference architecture is future reuse. Figure B-6 describes a process of continuous product development. It can be seen that the reference architecture is referred to form the basis of the systems architecture. Then any learning from existing activities is driven back into the RA repository to be book-shelved for future reuse.

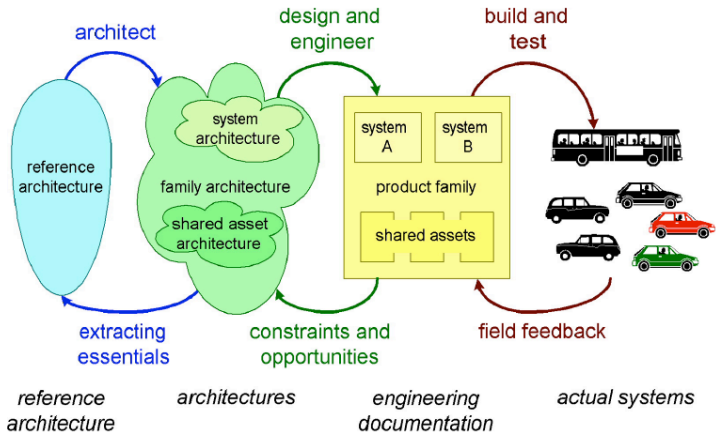

Figure B-6: Reference architecture in the loop [13]

Future reuse is a key theme of this research. It is proposed that any RA defined can be demonstrated as reusable to a distinctly different application. However the only evidence of application of RA methodology to maximise reusability in hybrid powertrain systems development is by Marco and Vaughan [16]. Marco and Vaughan derived a RA from the analysis of a subset of series hybrid vehicles. This presents the starting point of this Thesis.

Appendix C: Associated projects

Project Wren

In order to satisfy the requirements of increasingly stringent environmental legislation, the international automotive industry is attempting to make a step-change in the level of vehicle technology with the market introduction of HVs and the proposed introduction of fuel cell vehicles. However, the global automotive market is characterised by very high levels of competition in which manufacturers must continually introduce new products while concurrently reducing development time and costs. As a result, the long term viability of these technologies will be largely dependent on the ability of the automotive industry to design, integrate and test the different powertrain concepts at a cost and within a time frame that is comparable to that associated with conventional vehicles.

Such advanced vehicles can be generically thought of as being complex systems, the design of which crosses functional boundaries and combines traditional technology disciplines. It can be argued that the complexity associated such vehicles stems from two main sources;

- the need to take an overall systems view with respect to the integration and optimisation of multiple different powertrain architectures, control algorithms and subsystem technologies, and

- the need to integrate new levels of supervisory control, energy management and propulsion control algorithms with the already highly complex and distributed control architecture in modern vehicles.

The need for complex energy management and supervisory control functions, coupled with such vehicles inherent dependency on "by-wire" technology will further increase the software and control system content of future hybrid and fuel cell vehicles. The ability to cope with high levels of system complexity has therefore become and will continue to be one of the critical success factors within the automotive industry.

One means of reducing the level of system complexity and therefore programme risk would be the ability to easily interchange control and software functions between the different vehicle platforms and derivatives. The primary aim of the Wren project is the design of a novel, generic, control architecture for HVs and fuel cell vehicles that supports the easy integration and evaluation of different powertrain concepts.

A major recent technological development within the automotive research domain is the study of service–based control architectures and the use of whole system modelling and simulation environments such as the UML and the SysML. As part of the Wren project, the system requirements, the vehicle's control structure and the controller behaviour will be modelled and analysed independently of the physical partitioning and deployment of the system functionality. In order to facilitate the most efficient use of design resources, the use of co-simulation between different modelling and simulation environments will be investigated.

As part of the verification process for the new control architecture, the control system will be deployed and tested on Hyrban; a fuel cell hybrid commuter vehicle using ultracapacitors as the energy storage medium and independent wheel control via four electrical machines.

The design and validation of the proposed new control and systems integration architecture will be used as the basis for demonstrating how a systematic design process, based on model driven systems engineering, can be employed to progress the state-of-the-art beyond the current prototype control architectures that are often associated with many FCV and HEV research programmes.

In addition to delivering a flexible development environment for control and systems integration, the Wren project will also address the fundamental issues of reliability, robustness and safety that are of critical importance to the automotive industry and to the future productionisation of these vehicles.

Low Carbon Vehicle Technology Project

'Reducing our carbon footprint' is a phrase that is becoming more and more familiar. As the debates rage on over global warming, renewable energy sources, the carbon cost of international supply chains, product lifecycles, and personal energy consumption, what can really be achieved and how can UK firms stay ahead in the new economy that is already emerging?

With both the UK government and the European Union setting arguably ambitious targets for a competitive low carbon economy in Europe by 2050, the area that many believe will create the most rapid effect is transport. Already there is a certain amount of technology for introducing behavioural change, and it is an area that will have less impact on the less well off than other government target sectors such as domestic heat and power. More than this, there are huge opportunities for long term technological advances which are stimulating some of the biggest changes the automotive industry has ever seen.

TheLCVTP, based in the West Midlands, is addressing these changes head on and aims to revolutionise the way vehicles are powered and manufactured. It was also pivotal to the Government's decision in in 2010 to declare the West Midlands a Low Carbon Economic Area for advanced automotive engineering and make the West Midlands a global centre of excellence in low carbon vehicle engineering.

A multi-million pound project, funded by Advantage West Midlands, the European Regional Development Fund and contribution from industry partners, it is a major collaboration between leading automotive companies and research partners aimed at revolutionising the way low carbon vehicles, including fully electric and hybrid vehicles, are designed and developed in order to significantly reduce carbon emissions. Already, a study has shown that if several key technologies developed by the project were to be incorporated into a large luxury saloon car, CO_2 emissions would be cut by up to 40%. LCVTP has brought together world class UK OEMs, consultancies, suppliers and

academic institutions into a focused collaborative programme to create the required R&D capability and capacity for the development of the key low and ultra-low carbon vehicle technologies of the future.

The project partners, Jaguar Land Rover, MIRA, Ricardo, Tata Motors European Technical Centre, Zytek Automotive, Coventry University, Cranfield Univeristy and WMG at the University of Warwick, have also worked with a significant number of local Small & Medium Enterprises (SME's) in the West Midlands in order to deliver socio-economic improvements such as improved technical skills, business capability and new products and processes. The project aims to accelerate the research and development of the first low carbon vehicles by four years and to safeguard over 2,000 jobs in the region's automotive supply chain as businesses embrace low carbon opportunities.

With 15 R&D streams investigating everything from high performance battery modules and auxiliary power units, low cost electric drive motors and flexible high voltage distribution systems, to waste energy recovery and storage systems, new control software, lightweight structures, aerodynamics, and next generation braking systems, the project has already created 41 new products and processes for the design and manufacture of automotive vehicles and by 2014 will have created over £36m in value added.

Appendix D: A list of definitions of Systems Engineering

The International Council on Systems Engineering (INCOSE) [17, 27]:
"An interdisciplinary approach and means to enable the realisation of successful systems"
The Institute of Electrical and Electronic Engineering (IEEE) IEEE 1220 standard [218]
"An interdisciplinary collaborative approach to derive, evolve and verify a life-cycle-balanced system solution that satisfies customer expectations and meets public acceptability" [218]
Sage, an acclaimed practitioner and disseminator of systems engineering **[33, 96, 214]**
"The definition, design, development, production and maintenance of functional, reliable and trustworthy systems within cost and time constraints"
The Electronic Industries (EIA) EIA/IS-632 standard [219]
"An interdisciplinary approach encompassing the entire technical effort to evolve and verify an integrated and life-cycle-balanced set of system people, product and process solutions that satisfy customer needs It encompasses: • The technical efforts related to the development, manufacturing, verification, deployment, operations, support, disposal of and user training for, system products and processes. • The definition and management of the system configuration • The translation of the system definition into work breakdown structures • The development of information for management decision making"
US DOD defined systems engineering as follows [220]:
"Involves design and management of a total system which includes hardware and software, as well as other system life-cycle elements. The systems engineering process is a structured, disciplined, and documented technical effort through which systems products and processes are simultaneously defined, developed and integrated. Systems Engineering is most effectively implemented as part of an overall integrated product and process development effort using multidisciplinary teamwork"
Eisner, a early practitioner of systems engineering defines systems engineering as [221]:
"Iterative process of top-down synthesis, development, and operation of a realworld system that satisfies, in a near-optimal manner, the full range of requirements for the system".
The Defence Systems Management College defines it as [222]:
"An interdisciplinary engineering management process that evolves and verifies an integrated, life-cycle balanced set of system solutions that satisfy customer needs"
NASA **[223]** :
"A robust approach to the design, creation and operation of systems". elaborated with: • Identification and quantification of goals • Creation of alternative system design concepts • Performance of design trades • Selection and implementation of the best design • Verification that the design is properly built and integrated • Post-implementation assessment of how well the system meets the stated goals

Appendix E: SysML Model Acronyms

The following list of abbreviation or acronyms are combined in the SysML RA and AD models to create block, signal flow and function names

accl (accel)	Accelerator (Wren)
Act	Actual
Apprt	Apportionment
Arb	Arbitrate/Arbitration
Avail (avail)	Available (Wren)
BCU	Brakes Control Unit
Brk	Brake
Calc	Calculate
Cap	Capacity
Chg	Change
Chrg	Charge
CL	Clutch
Cmd	Command
Coll	Collate
Cont	Continuous
CPS (cps)	Continuous Power System (Wren)
Ctrl	Control
Cur	Current
CVT	Continuously Variable Transmission
DD	Driver Demand
Det	Determine
DL	Driveline
Dmd (dmd)	Demand (Wren)

Drv	Drive
Drv	Drive
Dwn	Down
Elec	Electrical
esc	energy system control
Exe	Execute
Flg	Flag
Fut	Future
Gen	Generator
Gr	Gear
Inst	Instantaneous
Lim	Limit
Mach	Machine
Max	Maximum
Mgr	Manager
Min	Minimum
Mon	Monitor
Neg	Negative
NW	North West
Opt	Optimisation
Ped	Pedal
Pen	Penalty
Pos	Position
PPS (pps)	Peak Power System (PPS)
Pred	Predictive
PRND	Park Reverse Neutral Drive
PWM	Pulse Width Modulation

Pwr (pow)	Power (Wren)
Quad/Q	Quadrant
regen	regeneration
Req (req)	Request (Wren)
Sat	Saturation
SE	South East
Shft	Shaft
SOC (soc)	State Of Charge (Wren)
SOH	State of Health
Spd	Speed
SW	South West
SW	South West
TCU	Transmission Control Unit
Temp	Temperature
TPS	Tertiary Power System
Trans/Trn	Transmission
Trq	Torque
Turb	Turbine
Veh	Vehicle
VEM	Vehicle Energy Manager
VSC	Vehicle Supervisory Controller
Vtg	Voltage

Appendix F: Reference Architecture

This appendix presents additional material to assist the understanding of the proposed RAs from Chapters 3 and 4.

Series RA

The RAs as defined only show the ideal braking integration strategy. Figure F-1 shows the context and causality model of the series RA with the legacy Brakes-master and VSC-slave configuration. It is expected that this structure will be employed for the foreseeable future, doe to supplier legacy constraints. However, as can bee seen the total torque 9including regenerative braking torque) is still collated and coordinated by the DD block. This ensures that a future transition to an ideal VSC to brakes stricture will be seamless.

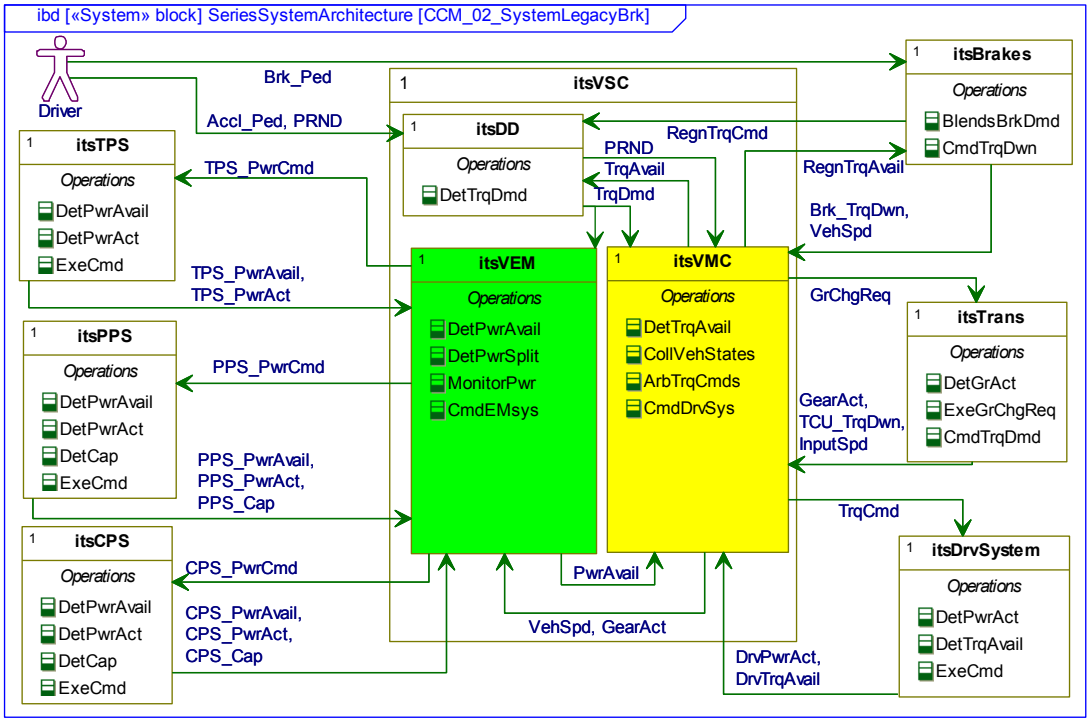

Figure F-1: Context and Causality Model of Series RA: Legacy brakes integration

Series RA tables

This section presents an interaction matrix and a tabular system description for the Series RA. These can be used to ease understanding of the RA for those with little exposure to the SysML.

	PPS, PPS Manager	CPS, CPS Manager	TPS, TPS Manager	Driver	VSC, Driver Demand	VSC, Vehicle Energy Management	VSC, Vehicle Motion Control	Transmission System, TCU	BrakesSystem, BCU	Drive System, Drive Manager
PPS, PPS Manager						PPSPwrAvail PPSPwrAct PPSCap				
CPS, CPS Manager						CPSPwrAvail CPSPwrAct CPSCap				
TPS, TPS Manager						TPSPw Avail TPSPwrAct				
Driver					PRND AcclPed BrkPed					
VSC, Driver Demand						TrqDmd	TrqDmd PRND			
VSC, Vehicle Energy Management	PPSPwrCmd	CPSPwrCmd	TPSPwrCmd				PwrAvail			
VSC, Vehicle Motion Control					TrqAvail	VehSpd GearAct		GearChgReq	BrkTrqCmd	TrqCmd
Transmission System, TCU							GearAct TrnTrqDwnReq InputSpeed			
BrakesSystem, BCU							BrkTrqDwnReq VehicleSpeed			
Drive System, Drive Manager							DrvPwrAct DrvTrqAvail			

Table F-1: Series integration matrix

System block	Function block	Sub-function block	Inputs	Operations	Outputs
Peak Power System					
	PPS Manager		PPS power command	Determine power available Determine power actual Determine capacity Execute power command	PPS power available PPS power actual PPS capacity
Continuous Power System					
	CPS Manager		CPS power command	Determine power available Determine power actual Determine capacity Execute power command	CPS power available CPS power actual CPS capacity
Tertiary Power System					
	TPS Manager		TPS power command	Determine power available Determine power actual Execute power command	TPS power available TPS power actual
Vehicle Supervisory Controller					
	Driver Demand		PRND Accelerator pedal position Brake pedal position Torque available	Interface with driver to determine total torque demand	Torque demand PRND Future data (GPS)
	Vehicle Energy Management				
		Power Available	PPS power available CPS power available TPS power actual Torque demand Vehicle speed Gear actual	Determines power available Determines power demand	Power available Powers available Power demand
		Predictive Optimisation	Future data (GPS)	Determines weighted SOC penalty function	Future penalty
		Instantaneous Optimisation	Future penalty Power demand Powers available PPS capacity CPS capacity	Determines instantaneous optimal power split	Power split
		Power Monitor	Powers available PPS power actual CPS power actual	Monitors subsystem power limits	Power limit flag
		Power Apportionment	Power demand Power split Power limit flag TPS power available	Apportions power command as a function of split and real world considerations (on/off limitation) and limit flag status	CPS power command PPS power command TPS power command

	Vehicle Motion Control				
		Torque Available	Power available Drive torque available Drive speed actual PRND	Determines total torque available	Torque available
		Torque Arbitration	Torque demand Brake torque down request TCU torque down request	Arbitrates between torque commands	Arbitrated torque command
		Torque Apportionment	Arbitrated torque command Gear actual Input speed Vehicle speed Drive speed actual Drive torque actual	Apportions torque command allowing for system dynamics Determines vehicle states (speed, gear)	Brake torque command Torque command Vehicle speed Gear change request Gear actual
Transmission System					
	TCU		Gear change request	Execute gear change request or Command torque down	TCU torque down request Gear actual Input speed
Brakes System					
	BCU		Brake torque command	Execute brake torque command Command brake torque down	Brake torque down request Vehicle speed
Drive System					
	Drive Manager		Torque command	Execute torque command Determine torque available Determine torque actual Determine speed actual	Drive speed actual Drive torque actual Drive torque available
DC Bus				Arithmetically sums DC power flows	
Vehicle Chassis				Transmits torque output to vehicle inertia	

Table F-2: Series system description

Parallel RA tables

This section presents an interaction matrix and a tabular system description for the Parallel RA. These can be used to ease understanding of the RA for those with little exposure to the SysML.

	PPS, PPS Manager	CPS, CPS Manager	TPS, TPS Manager	Driver	VSC, Driver Demand	VSC, Vehicle Energy Management	VSC, Vehicle Motion Control	Drivleline System, Mgr	BrakesSystem, BCU
PPS, PPS Manager						PPSPwrAvail PPSPwrAct PPSCap			
CPS, CPS Manager						CPSPwrAvail CPSPwrAct CPSCap			
TPS, TPS Manager						TPSPw Avail TPSPwrAct			
Driver					PRND AcclPed BrkPed				
VSC, Driver Demand						TrqDmd PRND	TrqDmd PRND		
VSC, Vehicle Energy Management			TPSPwrCmd		TrqAvail		Split		
VSC, Vehicle Motion Control	PPSTrqCmd	CPSTrqCmd				VehSpd GearAct		DLModeCmd	BrkTrqCmd
Drivleline System, Mgr							GearAct TrnTrqDwnReq DLModeAct InputSpeed		
BrakesSystem, BCU							BrkTrqDwnReq VehicleSpeed		

Table F-3: Parallel interaction matrix

System block	Funciton block	Sub-function block	Inputs	Operations	Outputs
Peak Power System					
	PPS Manager		PPS torque command	Determine power available Determine power actual Determine capacity Execute torque command	PPS power available PPS power actual PPS capacity
Continuous Power System					
	CPS Manager		CPS torque command (CPS power command) (Continuous ratio actual)	Determine power available Determine power actual Determine capacity Execute torque command	CPS power available CPS power actual CPS capacity (Continuous ratio cmd)
Continuous Transmission		Continuous TCU	Continuous ratio cmd		Continuous ratio actual
Tertiary Power System					
	TPS Manager		TPS power command	Determine power available Determine power actual Execute power command	TPS power available TPS power actual
Vehicle Supervisory Controller					
	Driver Demand		PRND Accelerator pedal position Brake pedal position Torque available	Interface with driver to determine total torque demand	Torque demand PRND Future data (GPS)
	Vehicle Energy Management				
		Power Available	PPS power available CPS power available TPS power actual Torque demand Vehicle speed Gear actual PRND	Determines torque available Determines power available Determines power demand	Torque available Power available Powers available Power demand
		Predictive Optimisation	Future data (GPS)	Determines weighted SOC penalty function	Future penalty
		Instantaneous Optimisation	Future penalty Power demand Powers available PPS capacity CPS capacity	Determines instantaneous optimal split	Split
		Power Monitor	Powers available PPS power actual CPS power actual	Monitors subsystem power limits	Power limit flag

		Power Apportionment	Power limit flag TPS power available	Commands TPS as a function of limit flag status	TPS power command
	Vehicle Motion Control				
		Driveline mode	Split PRND Torque demand Driveline mode actual	Determines best driveline mode	Driveline mode command Driveline mode
		Speed control	CPS speed Input speed Driveline mode	Manages mode transition through speed control	Speed torque command
		Torque Arbitration	Torque demand Speed torque command Driveline mode Brake torque down request TCU torque down request	Arbitrates between torque commands	Arbitrated torque command
		Torque Apportionment	Arbitrated torque command Split Driveline mode Gear actual Input speed Vehicle speed	Apportions torque command to CPS and PPS allowing for system dynamics Determines vehicle states (speed, gear)	Brake torque command PPS torque command CPS torque command Vehicle speed Gear actual
Driveline System					
	Driveline Manager		Driveline mode command Clutch status Torque down request	Manages driveline systems	Driveline mode actual Clutch command Gear change request TCU torque down request Gear actual Input speed
Transmission		TCU	Gear change request	Execute gear change request or Command torque down	Torque down request Gear actual Input speed
Clutch		Clutch manager	Clutch command	Local control for driveline clutch	Clutch status
Brakes System					
	BCU		Brake torque command	Execute brake torque command Command brake torque down	Brake torque down request Vehicle speed
DC Bus				Arithmetically sums DC power flows	
Torque Bus				Arithmetically sums torques	
Vehicle Chassis				Transmits torque output to vehicle inertia	

Table F-4: Parallel system description

Extended Parallel or Compound RA tables

This section presents an interaction matrix and a tabular system description for the Extended Parallel RA. This can be referred to as the Compound RA, but this must not be taken to suggest that it is distinct from the Parallel RA. These can be used to ease understanding of the RA for those with little exposure to the SysML.

	PPS, PPS Manager	CPS, CPS Manager	TPS, TPS Manager	Driver	VSC, Driver Demand	VSC, Vehicle Energy Management	VSC, Vehicle Motion Control	Drive System, Drive Manage	Generator System, Gen Manager	Drivleline System, Mgr	BrakesSystem, BCU
PPS, PPS Manager						PPSPwrAvail PPSPwrAct PPSCap					
CPS, CPS Manager						CPSPwrAvail CPSPwrAct CPSCap					
TPS, TPS Manager						TPSPw Avail TPSPwrAct					
Driver					PRND AcclPed BrkPed						
VSC, Driver Demand						TrqDmd PRND	TrqDmd PRND				
VSC, Vehicle Energy Management	PPSPwrCmd		TPSPwrCmd		TrqAvail		Split 1 Split 2				
VSC, Vehicle Motion Control		CPSTrqCmd				VehSpd GearAct		DrvTrqCmd	GenTrqCmd	DLModeCmd	BrkTrqCmd
Drive System, Drive Manager						DrvPwrAct DrvTrqAvail					
Generator System, Gen Manager						DrvPwrAct DrvTrqAvail					
Drivleline System, Mgr							GearAct TrnTrqDwn DLModeAct InputSpeed				
Brakes System, BCU							BrkTrqDwnReq VehicleSpeed				

Table F-5: Compound interaction matrix

System block	Function block	Sub-function block	Inputs	Operations	Outputs
Peak Power System					
	PPS Manager		PPS power command	Determine power available Determine power actual Determine capacity Execute power command	PPS power available PPS power actual PPS capacity
Continuous Power System					
	CPS Manager		CPS torque command (CPS power command) (Continuous ratio actual)	Determine power available Determine power actual Determine capacity Execute torque command	CPS power available CPS power actual CPS capacity (Continuous ratio cmd)
Continuous Transmission		Continuous TCU	Continuous ratio cmd		Continuous ratio actual
Tertiary Power System					
	TPS Manager		TPS power command	Determine power available Determine power actual Execute power command	TPS power available TPS power actual
Vehicle Supervisory Controller					
	Driver Demand		PRND Accelerator pedal position Brake pedal position Torque available	Interface with driver to determine total torque demand	Torque demand PRND Future data (GPS)
	Vehicle Energy Management				
		Power Available	PPS power available CPS power available Drive power available Generator power available TPS power actual Torque demand Vehicle speed Gear actual PRND	Determines torque available Determines power available Determines power demand	Torque available Power available Powers available Power demand
		Predictive Optimisation	Future data (GPS)	Determines weighted SOC penalty function	Future penalty
		Instantaneous Optimisation	Future penalty Power demand Powers available PPS capacity CPS capacity	Determines instantaneous optimal splits	Split 1 Split 2

		Power Monitor	Powers available PPS power actual CPS power actual Drive power actual Generator power actual	Monitors subsystem power limits	Power limit flag
		Power Apportionment	Power limit flag TPS power available	Commands TPS as a function of limit flag status	TPS power command
	Vehicle Motion Control				
		Driveline mode	Split 1 Split 2 PRND Torque demand Driveline mode actual	Determines best driveline mode	Driveline mode command Driveline mode
		Speed control	CPS speed Input speed Driveline mode	Manages mode transition through speed control	Speed torque command
		Torque Arbitration	Torque demand Speed torque command Driveline mode Brake torque down request TCU torque down request	Arbitrates between torque commands	Arbitrated torque command
		Torque Apportionment	Arbitrated torque command Split 1 Split 2 Driveline mode Gear actual Input speed Vehicle speed	Apportions torque command to CPS, Drive and Generator allowing for system dynamics Determines vehicle states (speed, gear)	Brake torque command CPS torque command Drive torque command Generator torque command Vehicle speed Gear actual
Generator System					
	Generator Manager		Generator torque command	Execute torque command Determine torque available Determine torque actual Determine speed actual	Drive power actual Drive power available
Drive System					
	Drive Manager		Drive torque command	Execute torque command Determine torque available Determine torque actual Determine speed actual	Generator power actual Generator power available
Driveline System					
	Driveline Manager		Driveline mode command Clutch status Torque down request	Manages driveline systems	Driveline mode actual Clutch command Gear change request TCU torque down request Gear actual Input speed

Transmission		TCU	Gear change request	Execute gear change request or Command torque down	Torque down request Gear actual Input speed
Clutch		Clutch manager	Clutch command	Local control for driveline clutch	Clutch status
Brakes System					
	BCU		Brake torque command	Execute brake torque command Command brake torque down	Brake torque down request Vehicle speed
DC Bus				Arithmetically sums DC power flows	
TorqueBus 1				Arithmetically sums torques	
TorqueBus 2				Arithmetically sums torques	
Vehicle Chassis				Transmits torque output to vehicle inertia	

Table F-6: Compound system description

Additional system schematics for the Parallel RA

This section presents two alternate system schematics for the Parallel RA. These system schematics show the alternate methods for integrating the TPS.

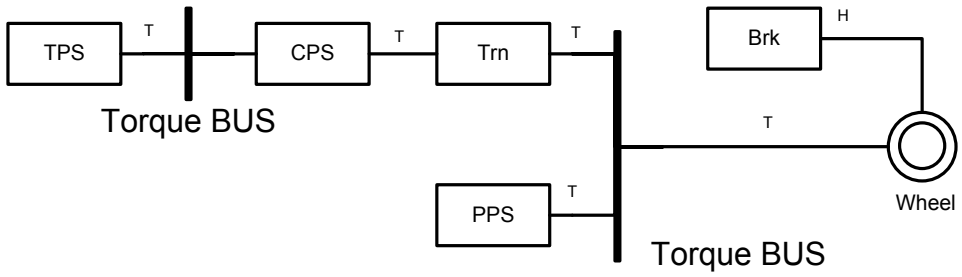

Figure F-2: Post-transmission parallel HV with TPS mechanically powered by CPS

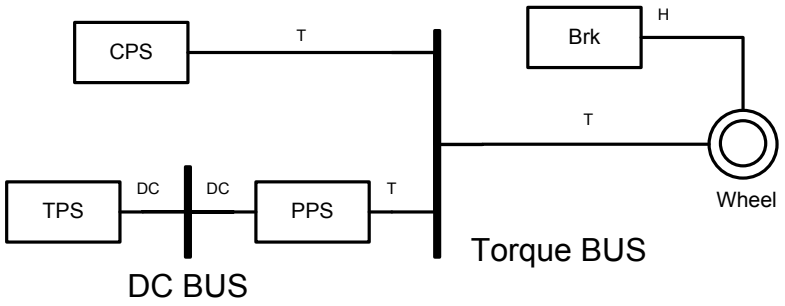

Figure F-3: Parallel HV with CVT incorporated into the CPS

Appendix G: Series HV Case study

This section presents the control domain models of the series AD from the first case study presented in Chapter 6. They are presented here as there is minimal difference between these and the Series RA control domain models from Chapter 3.

Figure G-1, Figure G-2 and Figure G-3 present the decomposition and two strategy models of the control domain of the series deployment. When comparing these models to the corresponding models in Chapter 3, it can be seen that there is very little change to the control architecture.

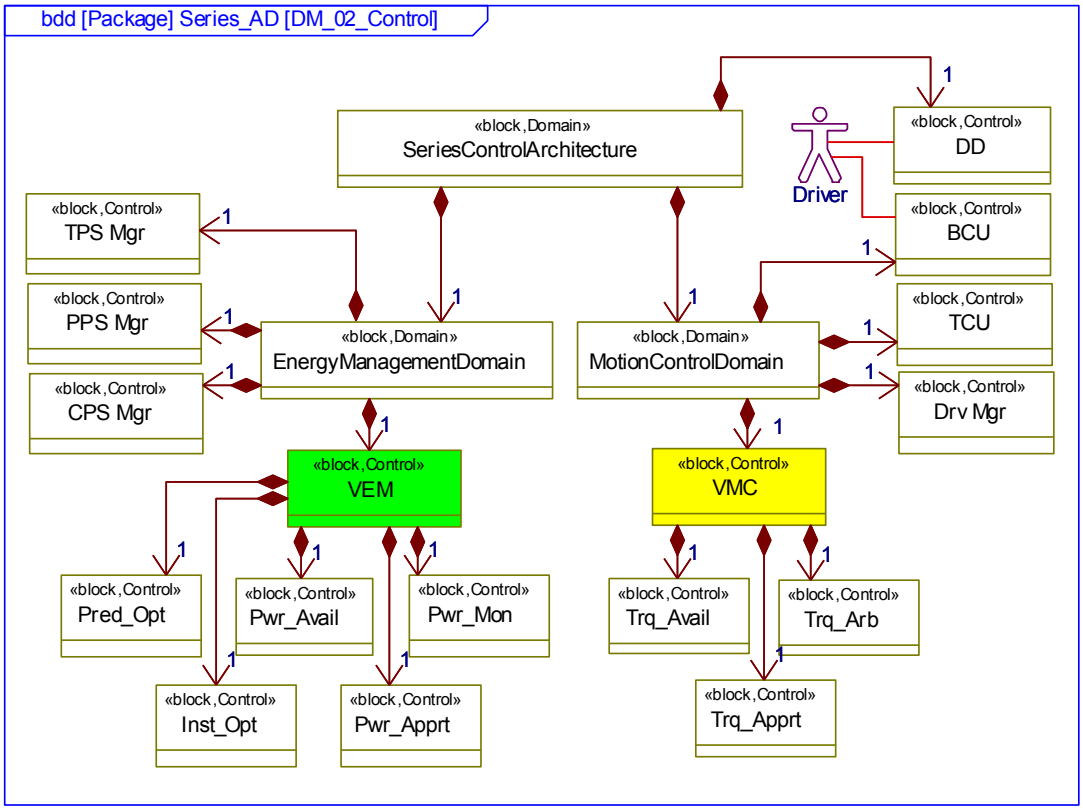

Figure G-1: AD decomposition model of series control domain

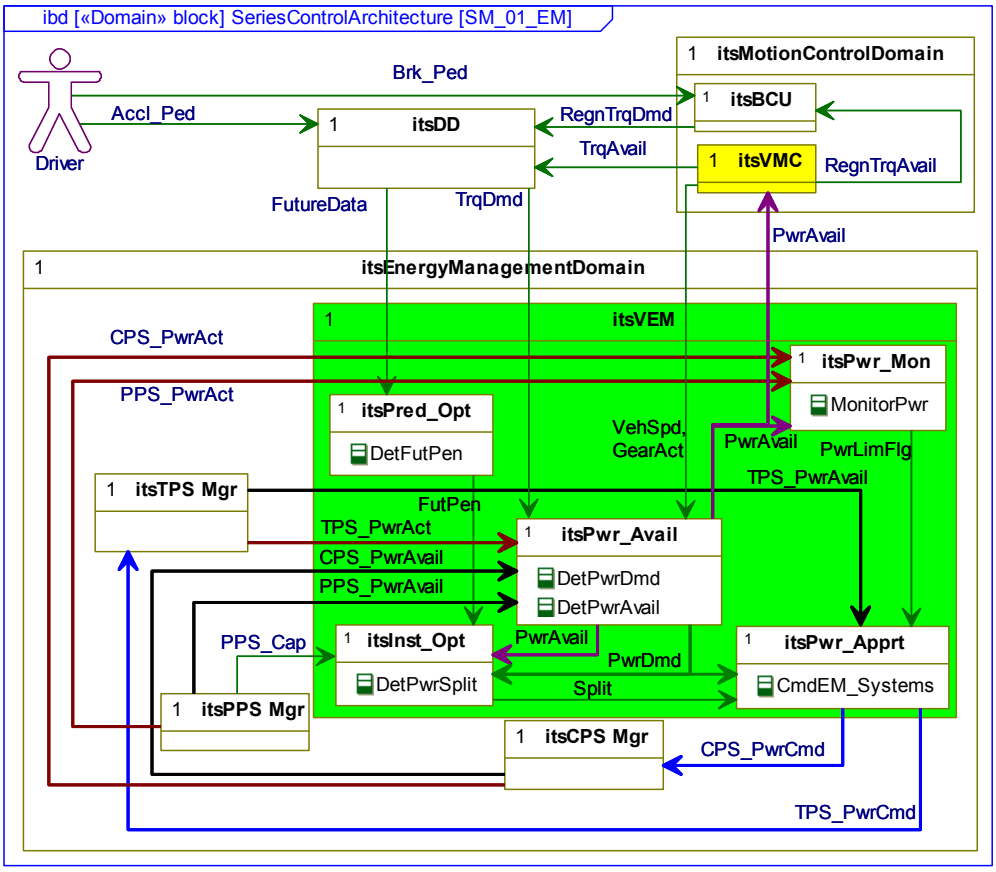

Figure G-2: AD strategy model of series energy management domain

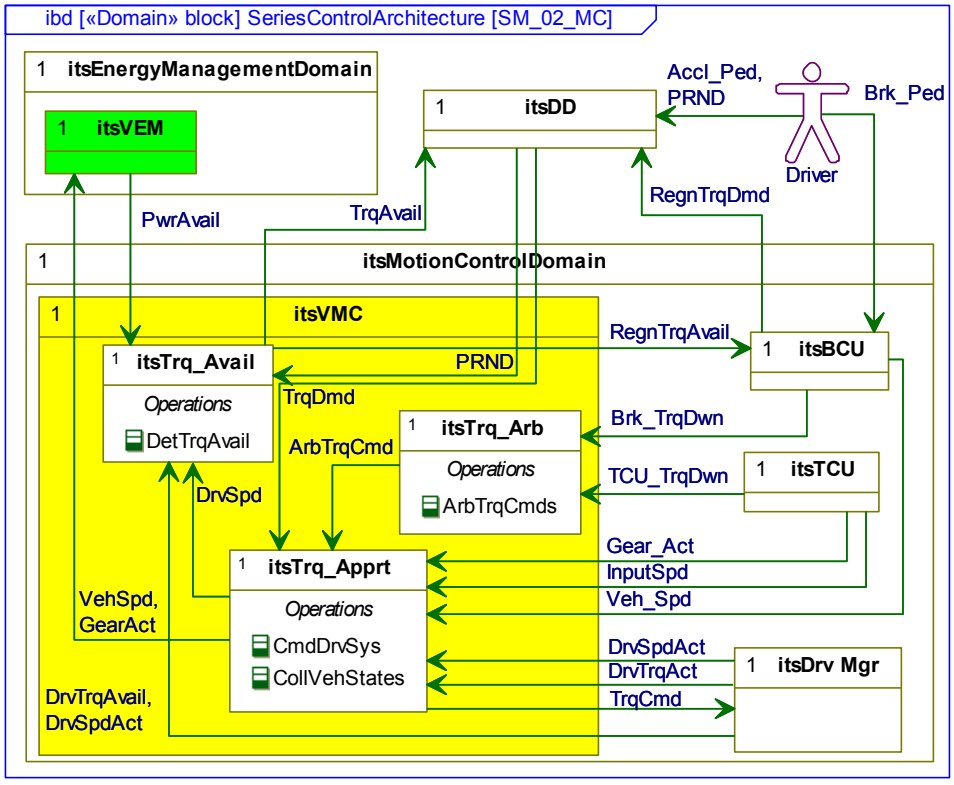

Figure G-3: AD strategy model of series motion control domain

Appendix H: Pre and post transmission Case Studies

This section presents the control domain models of the pre-transmission and post-transmission parallel ADs from the second case study presented in Chapter 7. They are presented here as there is minimal difference between these and the Parallel RA control domain models from Chapter 4.

Pre-transmission control domain models

Figure H-1, Figure H-2 and Figure H-3 present the decomposition and two strategy models of the control domain of the pre-transmission AD. When comparing these models to the corresponding models in Chapter 4, it can be seen that there is very little change to the control architecture.

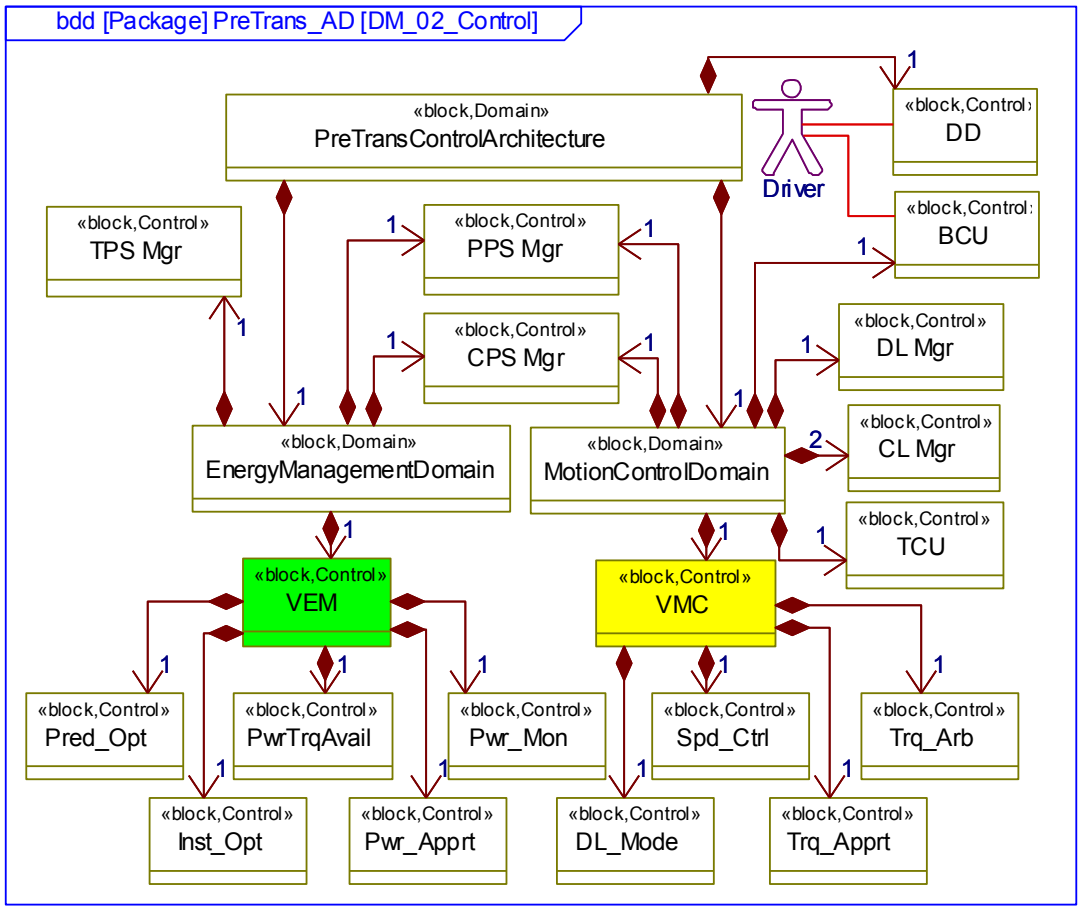

Figure H-1: AD decomposition model of pre-transmission Parallel control domain

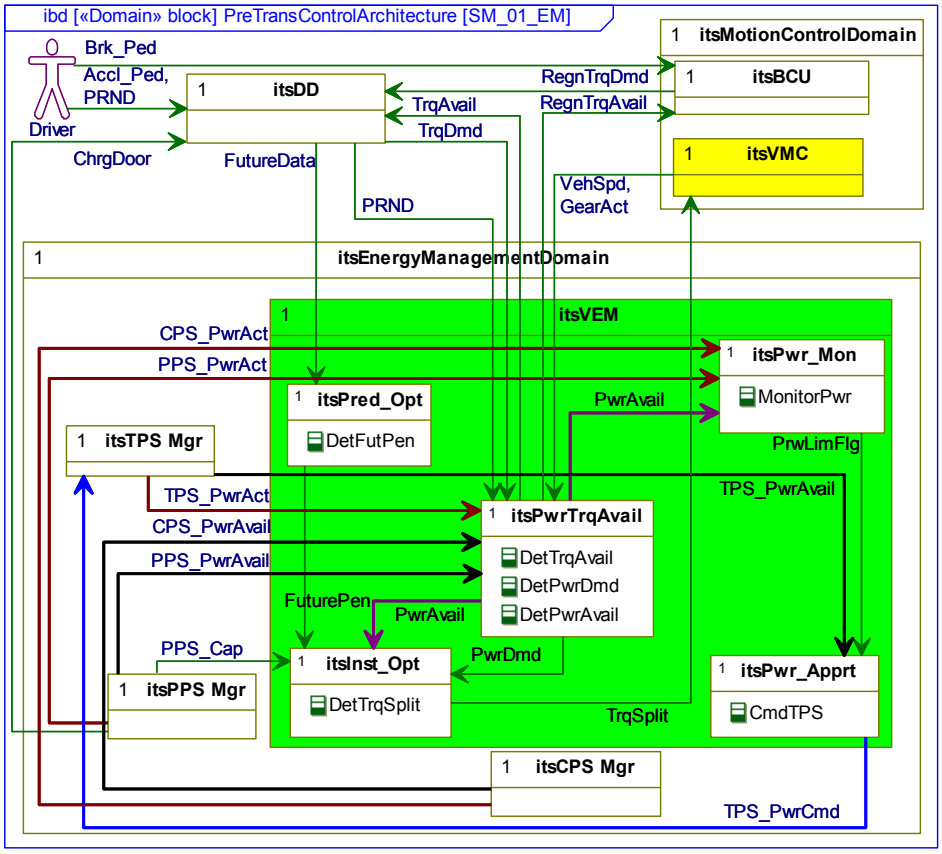

Figure H-2: AD strategy model of pre-trans Parallel energy management domain

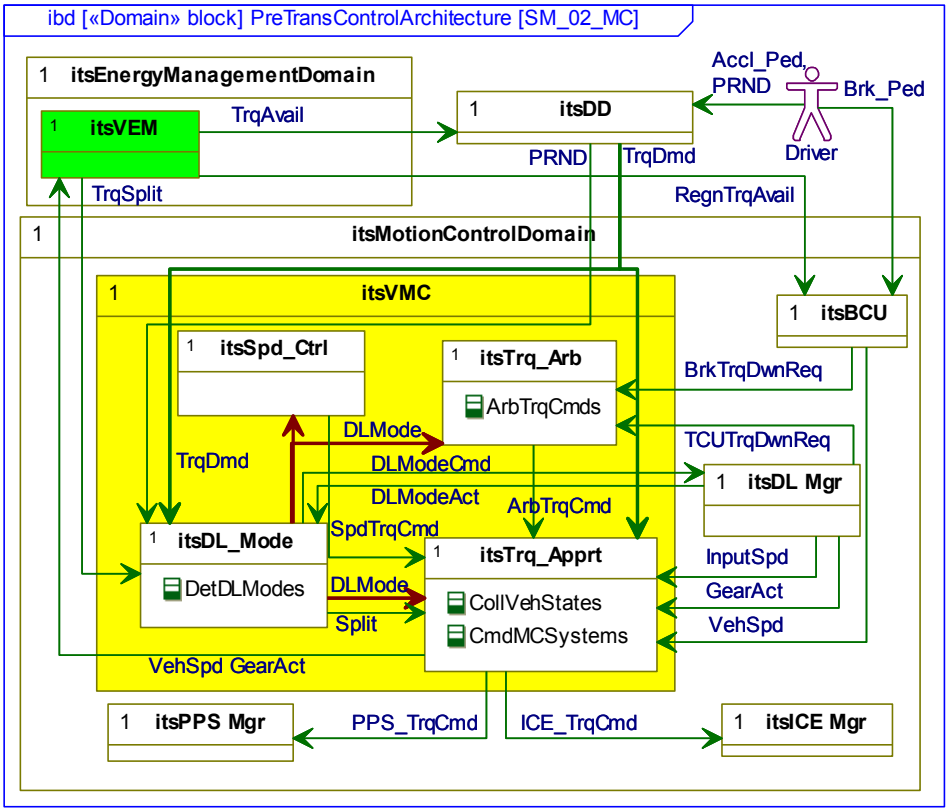

Figure H-3: AD strategy model of pre-trans Parallel motion control domain

Post transmission control domain models

Figure H-,4 Figure H-5 and Figure H-6 present the decomposition and two strategy models of the control domain of the post-transmission AD. When comparing these models to the corresponding models in Chapter 4, it can be seen that there is very little change to the control architecture.

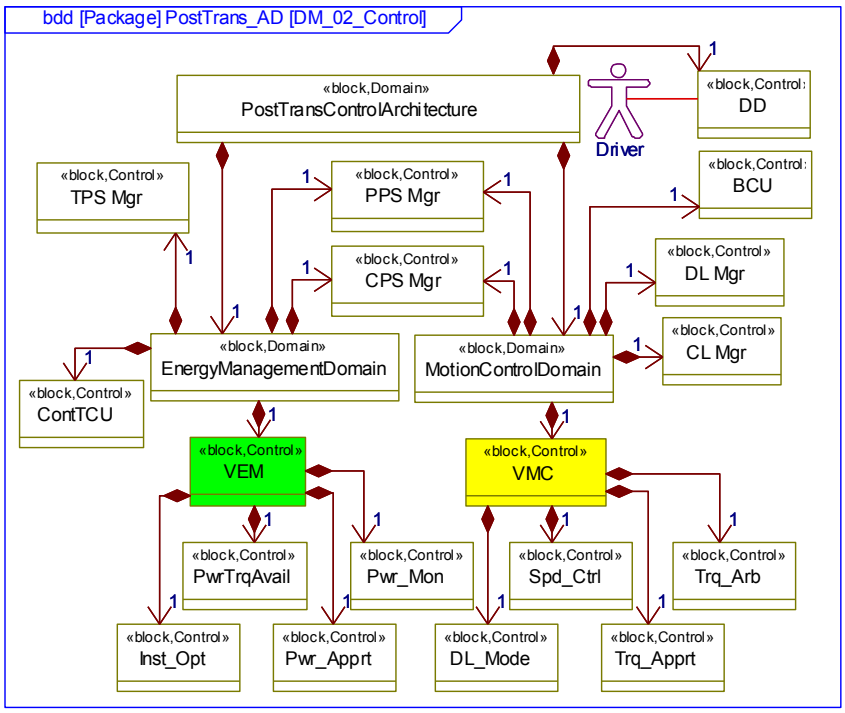

Figure H-4: AD decomposition model of post-transmission parallel control domain

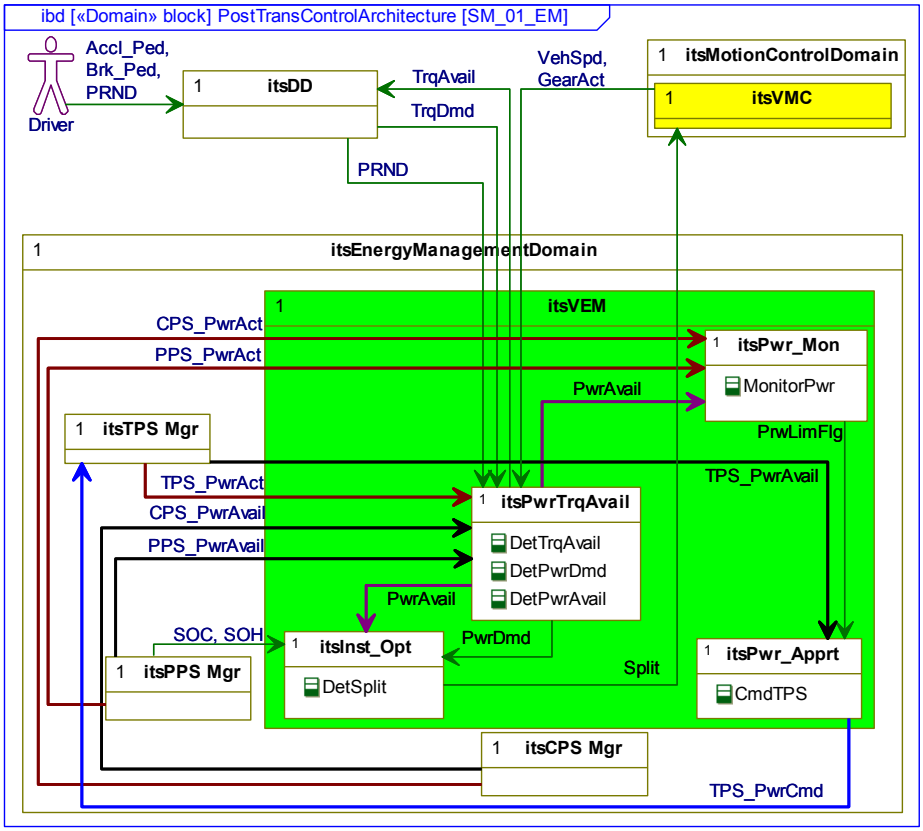

Figure H-5: AD strategy model of post-trans parallel energy management domain

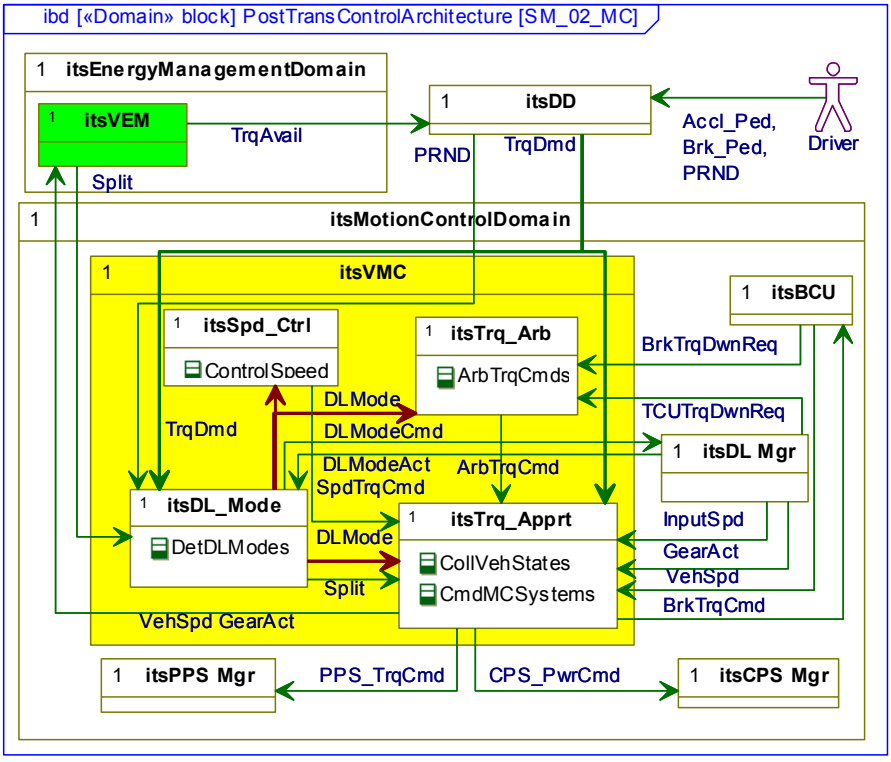

Figure H-6: AD strategy model of post-trans parallel motion control domain

References from the Appendices

[201] L. J. K. Setright, *Drive On!: A Social History of the Motor Car*. UK: Granta, 2003.

[202] D. West, "Goldsworthy Gurney and the Steam Drag: Iron Horse or Fable?," vol. Accessed 2011, ed, 1998.

[203] Anon, "History of hybrid vehicles," vol. Accessed 2011, ed, 2011.

[204] K. Benz, "Automobile fuelled by gas," Germany Patent DRP-37435, 1886.

[205] Anon, "Porsche history: milestones," vol. Accessed 2011, ed, 2011.

[206] H. Pieper, "Mixed drive for autovehicles," US 913846, 1909.

[207] Anon, "100th Anniversary of first US hybrid car patent," vol. Accessed 2011, ed, 2009.

[208] M. Glaskin, "Steam-powered car breaks century-old speed record," vol. Accessed 2011, ed: Newscientist, 2009.

[209] Anon, "Automobile history," vol. Accessed 2011, ed, 2010.

[210] A. C. Waltner, "Paradise delayed - the continuing sage of the Los Angeles Basin Federal Clean Air Implementation Plan," *UCLA Journal of Environmental Law & Policy,* pp. 247-283, 1996.

[211] K. H. Dietsche and M. Klingebiel, *Bosch Automotive Handbook* vol. 7th. Plochengen, Germany: Robert Bosch GnbH, 2007.

[212] B. Berman, G. Gelb, N. A. Richardson, and T. C. Wang, "Powertrain using multiple power sources," US Patent 3566717, 1971.

[213] Anon, "Hydrogen cars now: 1966 GM Electrovan," vol. Acessed 2011, ed, 2011.

[214] A. P. Sage and W. B. Rouse, "Handbook of Systems Engineering and Management (2nd Edition)," ed: John Wiley & Sons, 2009.

[215] K. J. Schlager, "Systems engineering-key to modern development," *Engineering Management, IRE Transactions on,* vol. EM-3, pp. 64-66, 1956.

[216] D. Verma, J. Boardman, and R. Cloutier, "Application of Patterns to Systems Engineering and Architecting," 2006.

[217] R. Kaffenberger, "The Difference - On the Use of Pattern-Based Requirements," 2004.

[218] Anon, "Standard for Application and Management of the Systems Engineering Process," in *IEEE Std 1220-1998*, ed: IEEE, 1998.

[219] Anon, "Process fo Systems Engineering," ed: EIA ANSI/GEIA, 2003.

[220] H. Eisner, "Systems engineering: Building successful systems," vol. 14, ed, 2011, pp. 1-141.

[221] H. Eisner, "Essentials of Project and Systems Engineering Management (2nd Edition)," ed: John Wiley & Sons, 2002.

[222] Anon, *Systems Engineering Fundamentals*. Ft. Belvoir, VA, USA.: Defense Systems Management, College Press, 1999.

[223] R. Shishko, *NASA Systems Engineering Handbook*. Linthicum Heights, MD, USA.: NASA Scientific and Technical Information Porgram Oddice, 1995.